UNIVERSIDAD AUTÓNOMA DE MADRID

FACULTAD DE CIENCIAS

DEPARTAMENTO DE BIOLOGÍA MOLECULAR

CARACTERIZACIÓN MOLECULAR DE CNVs, MUTACIONES SIN SENTIDO Y DE *SPLICING* EN ENFERMEDADES METABÓLICAS HEREDITARIAS. INVESTIGACIÓN EN TERAPIAS PERSONALIZADAS

ROCíO SÁNCHEZ ALCUDIA

TESIS DOCTORAL

Madrid, 2012

UNIVERSIDAD AUTÓNOMA DE MADRID

FACULTAD DE CIENCIAS

DEPARTAMENTO DE BIOLOGÍA MOLECULAR

CARACTERIZACIÓN MOLECULAR DE CNVs, MUTACIONES SIN SENTIDO Y DE *SPLICING* EN ENFERMEDADES METABÓLICAS HEREDITARIAS. INVESTIGACIÓN EN TERAPIAS PERSONALIZADAS

Directora de tesis:

Dra. Lourdes Ruiz-Desviat

Memoria presentada por la Licenciada Rocío Sánchez Alcudia para optar al grado de Doctor en Bioquímica

El presente trabajo ha sido realizado en el laboratorio de la Prof. Magdalena Ugarte, Catedrática del Departamento de Biología Molecular, en el Centro de Biología Molecular "Severo Ochoa" de la Universidad Autónoma de Madrid, con la ayuda de una beca predoctoral concedida por el ministerio de Educación y Ciencia (2008-2012).

AGRADECIMIENTOS

Parece increíble cómo pasa el tiempo, recuerdo el primer día que entré en el laboratorio siendo la nueva estudiante, y cómo un día de repente eres la más veterana de la "U" de becarios. Sólo tengo palabras de agradecimiento para todas las personas que habéis compartido conmigo todo este tiempo, la verdad es que ha sido una suerte haberos conocido.

En primer lugar, quiero agradecer a la Dra. Magdalena Ugarte por darme la oportunidad de realizar la tesis doctoral en su laboratorio y de formar parte de este magnífico grupo.

A Lourdes, muchísimas gracias por su ayuda prestada tanto personal como profesionalmente, por confiar en mí y darme ánimos cuando las cosas se atascaban, gracias por hacerme pensar que era posible, por enseñarme tantas cosas, por confiar en mí y transmitir siempre tranquilidad.

A Belén, por toda la ayuda prestada, por enseñarme tantas cosas, muchas gracias por ayudarme especialmente durante mi primer año de tesis. A Pilar, por su apoyo, por prestarme su ayuda siempre que la he necesitado.

A Eva y Álex, por ser un gran apoyo en el laboratorio, por ser tan cercanas. A Eva, por su confianza, por su ayuda, por las conversaciones. A Álex por contestar siempre con una sonrisa, por proponer siempre una solución, por sus consejos.

A Rosa y Fátima, no tendría suficiente papel para agradecerles, ni expresar todo lo que me han aportado durante este tiempo. A Rosa, por ser mi *propi*, mi profe cuando entré en el laboratorio, por compartir tantos buenos momentos, por tantas conversaciones. A Fátima, "*vida*", por ser tan cariñosa, por tener siempre palabras de ánimo y darme un abrazo siempre que lo he necesitado. Muchas gracias de verdad por enseñarme tantas cosas, por todos vuestros consejos y complicidad, por darme todo vuestro apoyo y confiar siempre en mí. A Ascen, por enseñarme tantas cosas, especialmente en cultivos, por explicarme todo lo que curiosamente le preguntaba, por trasmitir tanta paz.

A toda la gente del CEDEM, a Bego y Celia por recibirme siempre que bajaba con una sonrisa, a las "biosecres", a Isa, Julia y Eva, por ayudarme siempre con los temas burocráticos, a Julia por tantos momentos divertidos, a Eva por compartir risas en las comidas de Navidad. A los más recientes Susana, Ana y Paco. A Gonzalo, por prestarme su ayuda siempre que la he necesitado, por temas informáticos, algún percance con el coche…, gracias por los buenos y divertidos momentos dentro y fuera del laboratorio. A Marga, gracias por acordarse siempre de nosotros para compartir roscón en Reyes; a María Jesús, por enseñarme a medir carboxilasas; a Pedro, por su interés, por tener siempre algo que enseñarte. A Marisé, Paloma, Fernando, Isaac, Charo, Manu, Marina y Leticia. Muy especialmente a Carmen, por enseñarme a trabajar con respeto en cultivos, por ser tan entrañable.

A las ya doctoras con las que empecé mi andadura en el laboratorio, por enseñarme tantas cosas y por toda vuestra ayuda, a Cris, Ana Vega, Ana R., Ana Jorge y Patri. A Cris, muy especialmente por ser mi profe cuando empecé, por transmitir tanto entusiasmo, por explicarme y enseñarme tantas cosas. A Patri, por ser tan buena amiga, por tener siempre

una palabra de consuelo, por todo el apoyo y los buenos momentos compartidos a lo largo de estos años, gracias por estar siempre ahí y tener la suerte de tenerte aún cerquita.

A la "U" de becarios del 204, ¡qué deciros! Que sois una gente estupenda, me alegro de tener la suerte de haberos conocido, de teneros además de como compañeros, como amigos y que podamos haber compartido tantos buenos momentos juntos:

A Sandra, por ser de gran apoyo, por poner siempre el toque de respeto en el laboratorio, muchas gracias por tu ayuda con el inglés. A Lore, por tantos momentos entrañables y divertidos compartidos desde la carrera, por ser un apoyo tan importante, por compartir conocimientos y por estar siempre dispuesta a echar una mano. A Alfonso, por su ayuda en cada momento, por ser tan perfeccionista, por preocuparse por mí, por tener esa lengua viperina que tanto nos hace reir. A Pachu, por su ayuda, por tantos buenos y divertidos momentos, por ser tan perseverante. A Cristina, por su entusiasmo y su energía, por su apoyo y consejos. A Raquel, por ser tan divertida, por aportar ese toque fresco al laboratorio, por tantos buenos momentos. A Celia Medrano, por compartir experiencias desde la carrera, por haberte integrado tan bien en el 204. Al recién incorporado Pablo, por ser ya uno más, por ser tan amable y educado.

¡¡Esos lokis como molan se merecen una olaaaaa!! ¡Sois los mejores!

A Sven, por la ayuda prestada. A todos los que han pasado por el laboratorio en distintos momentos: A Paula, por compartir tantos TNTs, por creer tanto en lo que haces y por toda la ayuda prestada. A Esther, por toda su ayuda, a Virginia y a Elena, a todas gracias por aportar aire nuevo al laboratorio, por ser tan divertidas y haber compartido tantos momentos, por seguir todavía en contacto. A Laura y a Jonay, por las conversaciones, por ser tan trabajadores. A Borja, por su ayuda. A Liliana, por aportar tanta alegría en su visita, por enseñarnos dichos portugueses. A Maja, por tener siempre una sonrisa, por seguir compartiendo momentos en congresos y alguna visita.

A los bioquímicos, a Abel, Roci, Eli y Lorena, por mantenernos unidos durante todo este tiempo a pesar de la distancia, por todo vuestro apoyo, consejos, por todos los momentos compartidos. "Vivimos siempre juntos y seguiremos juntos….". A David, por aportar ese toque de corrección al grupo, por seguir estando en contacto.

A las *Maris:* Silvia, Sara, Mayte, Mari, Alicia, Anita y Anuska, gracias por estar siempre ahí, por todo vuestro apoyo y confianza a lo largo de todos estos años, por tantos momentos, risas y confidencias compartidas.

A mi familia, a Marisol, Nuria, Alfonso y los "peques", Inés, Carlos, Yaiza y Javier, por estar siempre a mi lado, especialmente a mis abuelos por confiar siempre en mí.

A mi hermano Carlos, por estar a mi lado, por su apoyo, a Noelia por interesarse tanto por lo que hago, a *Nito* por haber estado a mi lado, por ser de gran apoyo y por la complicidad. Gracias a todos por haber ensayado conmigo las presentaciones y darme tantos buenos consejos.

A mis padres, por haberme apoyado siempre en todo lo que he hecho, por su confianza y su cariño, por preocuparse tanto por mí, por estar incondicionalmente a mi lado. Gracias por todo lo que me habéis enseñado, porque sin vosotros no hubiera llegado hasta aquí.

"El sabio no se sienta para lamentarse,
sino que se pone alegremente a su tarea de
reparar el daño hecho"

William Shakespeare (1564-1616).

A mis padres.

César y Rafi

ÍNDICE

ABREVIATURAS

5HIAA:	5-hidroxindolacético
AdoCbl:	Adenosilcobalamina
AMM:	Acidemia metilmalónica aislada
AON:	Oligonucleótiodo antisentido
AP:	Acidemia propiónica
AR:	Aldolasa reductasa
***Array* CGH:**	*Array* de hibridación genómica comparativa (*Comparative genomic hibridization*)
AST:	Analyzer Splice Tool
ATR:	ATP:adenosil cob(I)lamina transferasa
BAC:	Cromosoma artificial bacteriano
BC:	Dominio biotina carboxilasa
BCCP:	Dominio de biotinilización
BDGP:	Berkeley Drosophila Genome Project
BH4:	(6R)-L-eritro-5,6,7,8-tetrahidrobiopterina
BSA:	Albúmina de suero bovino
Cbl:	Cobalamina
CNV:	Variaciones en el número de copias (*Copy number variation*)
CR:	Carbonil reductasa
CT:	Dominio carboxiltransferasa
DHFR:	Dihidrofolato reductasa
DHPR:	Dihidropterina reductasa
DMD:	Distrofia muscular de Duchenne
DMSO:	Dimetil sulfóxido.
DTT:	1,4-ditio-L-treitol
EJC:	Complejo de la unión de exones (*Exon junction complex*)
EMH:	Enfermedades metabólicas hereditarias
ESE:	Secuencia exónica potenciadora de *splicing* (*exonic splicing enhancer*)
ESS:	secuencia silenciadora de *splicing* (*exonic splicing silencer*)
EURORDIS:	Organización Europea para las enfermedades raras (*European Organisation for Rare Diseases*)
FBS:	Suero fetal bovino.
GAPDH:	Gliceraldehído-fosfato deshidrogenasa
GCS:	Complejo de ruptura de la glicina
GTPCH:	GTP ciclohidrolasa I
HCS:	Holocarboxilasa sintetasa
HGMD:	Base de datos de mutaciones genéticas (*Human gene mutation database*)
HGVS:	Sociedad de variaciones genómicas humanas (*Human genome variation society*)
hnRNP:	Ribonucleoproteína heterogénea nuclear
HVA:	Ácido homovalínico
ISE:	Secuencia intrónica potenciadora de *splicing* (*intronic splicing enhancer*)
ISS:	Secuencia intrónica silenciadora de *splicing* (*intronic splicing silencer*)
IVS:	Intrón (*Intervening sequence*)
MCC:	3-metilcrotonil-CoA carboxilasa
MEM:	Medio mínimo esencial de Eagle
MLPA:	Multiplex ligation probe amplification
MUT:	Metilmalonil-CoA mutasa

NMD: Mecanismo de decaimiento del mRNA (*nonsense mediated mRNA decay*)
OH-Cbl : Hidroxicobalamina
ORF: Marcos abiertos de lectura (*open reading frame*)
PBS: Tampón fosfato salino
PCC: Propionil-CoA carboxilasa.
PCD: pterin-4a-carbinolamina dehidratasa
PDB: Banco de datos de proteínas (*Protein Data Bank*).
PTC: Codón de parada prematuro (*Premature termination codon*)
PTPS: 6-piruvoil-tetrahidropterina sintasa
PVDF: Fluoruro de polivinilo
SC35: Componente 35 del *splicing* (*splicing component 35*)
SDS: Dodecilsulfato sódico
SDS-PAGE: Electroforesis en geles de poliacrilamida en presencia de SDS
SF2/ASF: Factor de *splicing* 2/factor alternativo de *splicing* (*splicing factor 2/alternative splicing factor*)
siRNA: RNA de interferencia pequeño (*small interfering RNA*)
snRNAU1: RNAU1 nuclear pequeño (*small nuclear RNAU1*)
snRNP: ribonucleoproteínas nucleares pequeñas
SR: Sepiapterina reductasa
SRp: Proteína rica en serina y arginina (*serine-arginine protein*)
SURF: Complejo SMG-1–Upf1–eRF1–eRF3
TH: Tirosina hidroxilasa
Tm: Temperatura de semidesnaturalización
TNT: Sistema transcripción-traducción acoplada
TPH: Triptófano hidroxilasa
U2AF: Factor auxiliar de U2
wt: Salvaje o normal

Algunos términos ingleses, ampliamente utilizados en Biología Molecular y sin clara traducción en castellano, se presentan en cursiva.

SUMMARY

In this work, we have characterized copy number variations (CNVs) and nonsense mutations identified in patients diagnosed with propionic acidemia (PA), one of the most frequent organic acidemias inherited in autosomal recessive fashion as well as diverse splicing mutations identified in different genes involved in several inherited metabolic diseases (IMD). Our findings lead to the investigation in specific mutation therapeutic approaches.

We have employed multiplex ligation probe amplification (MLPA) and long PCR in some cases to screen for genomic deletions in the PCCA gene in 20 patients in whom standard mutation detection techniques had failed to complete genotype analysis. We have identified eight different exonic deletions corresponding to a frequency of 21.3% of the total PCCA alleles genotyped in the laboratory. Two of them were frequent, one involving exons 3 and 4 where two different chromosomal breakpoints were identified and another one involving exon 23. The high frequency of large genomic deletions in the PCCA gene could be due to the characteristics of the gene structure and its abundance in intronic repetitive elements. These data underscore the need of using MLPA analysis to complete routine genetic analysis in PCCA patients.

We have also identified 12 different nonsense mutations in a cohort of 190 PA patients, seven of them novel, accounting for 10% of the total mutant alleles. We have established the proof of principle that nonsense mutations in PA can be partially suppressed *in vitro* by aminoglycosides with different efficiencies depending on the nonsense mutation and the sequence context. To correct the metabolic defect, the incorporated aminoacid should support protein function, most of them retaining partial activity as was evaluated by *in silico* and *in vitro* expression analysis of the predicted missense changes. In patient´s fibroblasts treated with readthrough compounds we observed a 40-50 fold increase in enzymatic activity, reaching up to 10-15% levels of treated control cells. These results point to readthrough therapy as a potential or supplementary treatment for a number of PA patients encouraging further clinical trials with newly developed readthrough compounds without toxic effects.

Several splicing defects that overall account for 15-30% of the mutant alleles in most IMD were also analyzed. We have characterized mutations found at the conserved splice sites and at deep intronic sequences that activate or create new splice sites resulting in the aberrant inclusion of pseudoexons in the mRNA. We have performed *in silico* and functional analysis using minigenes to analyze the individual effect of mutations on the splicing process to understand the precise molecular mechanism involved in the splicing defect and in the patient´s phenotypic expression, as well as to investigate in splicing-directed therapies. In this work we have employed the overexpression of splicing factors and U1snRNAs with extended base-pairing with the mutated 5´ splice site to modulate the aberrant pre-mRNA splicing resulting from different mutations. The antisense therapy has efficiently restored normal splicing affected by pseudoexon activation due to deep intronic mutations with a functional recovery close to normal levels even for a heterozygous mutation.

1. INTRODUCCIÓN

1.1. ENFERMEDADES METABÓLICAS HEREDITARIAS. ASPECTOS GENERALES.

Las Enfermedades Metabólicas Hereditarias (EMH) se definen como alteraciones bioquímicas de origen genético causadas por la alteración de un gen que codifica para una enzima implicada en una de las muchas reacciones químicas que intervienen en el metabolismo celular; lo que conlleva la alteración del funcionamiento fisiológico de la célula.

El primer error metabólico congénito fue identificado por *Archibald Garrod* a principios del siglo XX con sus estudios sobre la alcaptonuria, una deficiencia en la enzima homogentisato dioxigenasa implicada en el metabolismo de la tirosina. *Garrod* describió también la cistinuria, la pentosuria y el albinismo (Garrod, 1975). Posteriormente, el conocimiento de este tipo de enfermedades ha ido aumentando progresivamente y, así como en el primer libro de *Garrod* se describieron estos cuatro trastornos mencionados, en 1983 *Stanbury* y colaboradores describían 200, *Scriver* y colaboradores en 1995 hablan de 459 patologías y actualmente hay alrededor de 700 trastornos definidos (Ruiz Pons et al., 2004) (Pampols, 2010). La posibilidad actual de realizar el diagnostico genético de estas enfermedades ha influido en gran medida en este avance.

Estas enfermedades son consideradas enfermedades raras (definidas por la EURORDIS (*European Organisation for Rare Diseases*) como aquellas que afectan a menos de 1 de cada 2000 personas en Europa). La incidencia acumulada para el conjunto de todas ellas es de alrededor de 1/800 recién nacidos vivos (Pampols, 2010).

Dependiendo de cuál sea la función alterada puede producirse bien un acumulo del sustrato no metabolizado, la aparición de sustancias producidas al metabolizarse dicho sustrato por vías alternativas, o bien, fenómenos derivados de la menor formación del producto final o de su ausencia. Los efectos fisiopatológicos del acumulo de sustancias no metabolizadas dependen del grado de acumulación y de su posible toxicidad; la utilización de vías metabólicas inusuales o alternativas, puede producir nuevas sustancias potencialmente tóxicas; y las consecuencias derivadas de la deficiencia de determinados compuestos dependen del grado de su esencialidad.

Las manifestaciones clínicas pueden ser muy variadas apareciendo fundamentalmente en el período neonatal, aunque también pueden manifestarse en épocas más tardías (Sanjurjo et al., 2001).

La mayoría de las EMH son monogénicas, el 60% se heredan de forma autosómica recesiva, el 20% autosómica dominante y el 12% ligada al X. Alrededor de un 8% están relacionadas con alteraciones en el genoma mitocondrial. En general, hay una gran heterogeneidad alélica y las diferentes mutaciones suelen estar ligadas al tipo y a la intensidad de las manifestaciones clínicas de las EMH (Desviat et al., 2001).

Los estudios moleculares en individuos afectados son clave para llegar a definir la naturaleza de la mutación en sí, caracterizando las alteraciones producidas a nivel

genómico y proteico, siendo fundamental para entender la base de las enfermedades genéticas, permitir un diagnóstico certero y en muchos casos, predecir el pronóstico de la enfermedad y adecuar un mejor tratamiento a cada individuo.

De hecho, en los últimos años han surgido una gran variedad de terapias genéticas y farmacológicas basadas en el mecanismo molecular específico del tipo de mutación de cada paciente.

1.2. ACIDURIAS ORGÁNICAS

En este trabajo se han estudiado las mutaciones de pacientes con **acidemia propiónica** (**AP;** MIM 606054) y **aciduria metilmalónica aislada** (**AMM; tipo *mut:*** MIM 251000*,* **tipo *cblA*:** MIM 251100, **tipo *cblB*:** MIM: 251110**, tipo *cblD* variante 2:** MIM 277410), dos de las formas más frecuentes de acidurias orgánicas, causadas por defectos en el catabolismo de aminoácidos ramificados, ácidos grasos de cadena larga y de la cadena lateral del colesterol, concretamente en los pasos de degradación de propionil-CoA a succinil-CoA. Estas acidurias orgánicas son enfermedades genéticas que se heredan de forma autosómica recesiva. Pertenecen al grupo de enfermedades metabólicas que cursan con intoxicación aguda debido al acumulo de metabolitos tóxicos de la vía de oxidación del propionato.

Las acidurias orgánicas se caracterizan por una gran heterogeneidad fenotípica, de manera que la presentación clínica puede ir desde una forma más severa de aparición neonatal, hasta una forma de aparición más tardía. La mayoría de los pacientes con síntomas en el período neonatal presentan acidosis metabólica severa, rechazo a la alimentación, vómitos, letargia e hipotonía siendo la mortalidad elevada y las secuelas neurológicas frecuentes.

El tratamiento está dirigido, principalmente, a prevenir el acumulo de metabolitos tóxicos y el catabolismo endógeno de proteínas, por lo que la principal medida consiste en una dieta con restricción proteica (Fenton et al., 2001).

1.2.1. Acidemia propiónica

La academia propiónica fue descrita por primera vez en un paciente por *Childs* y colaboradores en 1961. Afecta aproximadamente a uno de cada 30.000 nacidos vivos en todo el mundo (Hofherr et al., 2009), aunque en áreas de mayor incidencia como Arabia Saudí puede afectar a 1/2000 (Al Essa et al., 1998; Ugarte et al., 1999). Está causada por la deficiencia de la enzima mitocondrial propionil-CoA carboxilasa (**PCC**; E.C. 6.4.1.3) que cataliza la carboxilación dependiente de biotina del propionil-CoA hasta D-metilmalonil-CoA (Figura 1). El propionil-CoA proviene del catabolismo de los aminoácidos valina, isoleucina, metionina y treonina, de los ácidos grasos de cadena impar y de la cadena lateral del colesterol. Además, una fuente importante de propionato en humanos proviene de la fermentación realizada por bacterias de la flora intestinal (Bain et al., 1988; Thompson et al., 1990).

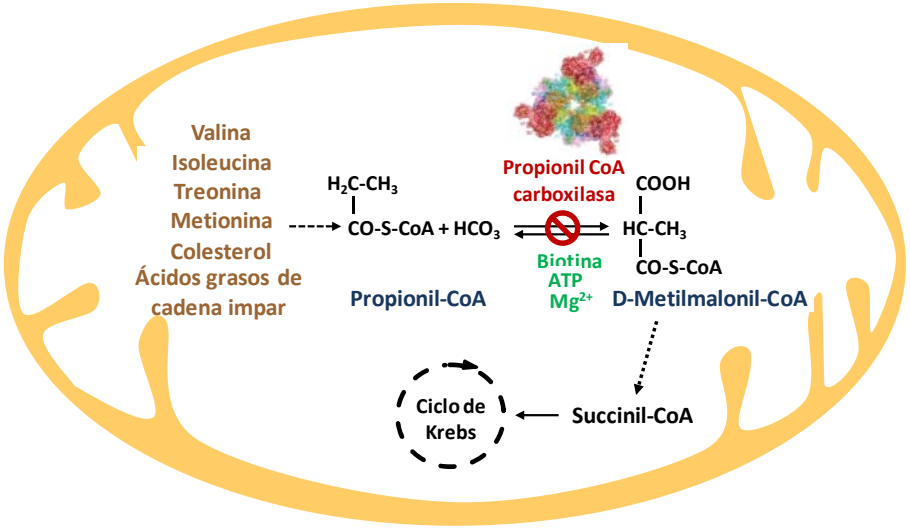

Figura 1. Ruta catabólica del propionil-CoA. La enzima mitocondrial propionil-CoA carboxilasa cataliza la carboxilación dependiente de biotina del propionil-CoA hasta D-metilmalonil-CoA.

La reacción catalizada por esta enzima tiene lugar en dos etapas. En la primera etapa, la cual requiere ATP y Mg^{2+}, el bicarbonato (fuente del grupo carboxilo) se une al nitrógeno N1 de la biotina, formando un intermediario carboxibiotina-enzima. En la segunda etapa, este complejo reacciona con un carbono del sustrato propionil-CoA transfiriendo el grupo carboxilo de la biotina:

1. Enzima-biotina + ATP + HCO^-_3 $\rightleftharpoons$ Enzima-biotina-CO_2 + ATP +Pi + H^+

2. Enzima-biotina-CO_2 + propionil-CoA $\rightleftharpoons$ Enzima-biotina + D-metilmalonil-CoA

La proteína PCC, al igual que el resto de carboxilasas dependientes de biotina, se sintetiza en forma de apoenzima y es después biotinilada por la enzima holocarboxilasa sintetasa (HCS). La liberación del la biotina se lleva a cabo por la enzima biotinidasa.

La PCC es un dodecámero compuesto por 6 unidades α y 6 unidades β. Se localiza en la matriz mitocondrial y tiene un peso aproximado de 750 kDa (Huang et al., 2010). La subunidad α de mayor tamaño (72KDa) contiene el dominio biotina carboxilasa (BC) y el dominio de biotinilización (BCCP) con el motivo conservado A-M-K-M (localizado en el exón 23); la subunidad β (56 KDa) proporciona la actividad carboxiltransferasa (CT).

Recientemente, se ha cristalizado el dodecámero de una proteína quimérica PCC bacteriana (PDB 3N6R) demostrándose que tiene una estructura muy similar a la humana, siendo de gran ayuda para el entendimiento del mecanismo molecular de un gran número de mutaciones asociadas con AP (Huang et al., 2010) (Figura 2).

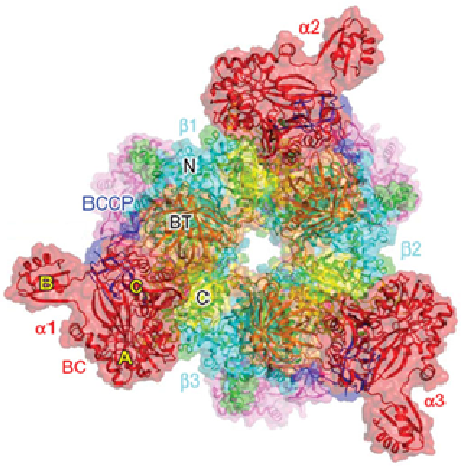

Figura 2. Dibujo esquemático de la estructura cristalográfica de la propionil-CoA carboxilasa (α6β6) bacteriana descrita por Huang et al., 2010. Se muestra la estructura de la holoenzima, dispuesta en un núcleo central hexamérico β_6 en forma de cilindro corto con un pequeño hueco a lo largo de su eje. Las subunidades α se disponen en los extremos del núcleo. **BCCP**: dominio de biotinilización, **BC:** biotina carboxilasa, **N**: dominio N-terminal, **C:** dominio C-terminal, **BT**: dominio de la subunidad α (formado por residuos de BC y BCCP), crucial para las interacciones con la subunidad β. Imagen modificada de Huang et al., 2010.

Los dos genes codificantes para cada una de las subunidades de la PCC son los genes *PCCA* y *PCCB*:

- El **gen *PCCA*** (MIM 232000) que codifica para la subunidad α está localizado en el cromosoma 13q32 (Kennerknecht et al., 1992) y está constituido por 24 exones de 37 a 335 pb de longitud (Campeau et al., 2001). El mRNA codificante tiene una fase abierta de lectura de 2184 nucleótidos codificando para una proteína de 728 aminoácidos (Campeau et al., 2001).

- El **gen *PCCB*** (MIM 232050) codifica para la subunidad β, está localizado en el cromosoma 3q13.3-q22 (Kraus et al., 1986; Lamhonwah et al., 1986) y está constituido por 15 exones de 57-183 pb de longitud (Rodriguez-Pombo et al., 1998). El mRNA codificante tiene una fase abierta de lectura de 1617 nucleótidos codificando para una proteína de 539 aminoácidos (Ohura et al., 1993).

Mutaciones en cualquiera de estos dos genes puede causar AP con un espectro muy amplio de fenotipos (Desviat et al., 2004; Perez-Cerda et al., 2000). En el momento de comenzar este trabajo la mayoría de las mutaciones descritas correspondían a cambios de aminoácido, seguidas de pequeñas inserciones o deleciones, mutaciones que afectan al procesamiento del mRNA (*splicing*) y mutaciones sin sentido.

El diagnóstico de la enfermedad se realiza reuniendo datos bioquímicos, enzimáticos y genéticos:

Los **datos bioquímicos** característicos son fundamentalmente debidos al acumulo intramitocondrial de propionil-CoA que se metaboliza por vías secundarias, por lo que la AP se caracteriza por la presencia de altas concentraciones de ácido propiónico libre además de sus metabolitos derivados: metilcitrato, 3-OH propiónico, propionilglicina y tiglilglicina en sangre y orina además de propionilcarnitina en plasma. Estos pacientes también presentan hiperamonemia (debido a la formación de N-propionilglutamato, inhibidor competitivo del enzima N-acetilglutamato sintetasa

(Coude et al., 1979; Stewart and Walser, 1980) e hiperglicinemia (debido a una disminución secundaria de la actividad enzimática del complejo de ruptura de la glicina (GCS) por el acumulo de propionil-CoA intracelular (Kolvraa, 1979; Hayasaka et al., 1982). Por otra parte, el propionil-CoA puede actuar como sustrato, en lugar del acetil-CoA, en la síntesis de ácidos grasos, dando lugar a un aumento relativo de los ácidos grasos de cadena impar (OLCFA) (Sperl et al., 2000).

La comprobación de la deficiencia de la enzima PCC se realiza por **determinación enzimática** en leucocitos de sangre periférica o en fibroblastos de piel (Fenton et al., 2001), así como por **análisis genético** de mutaciones en los genes *PCCA* o *PCCB*. Es posible el **diagnóstico prenatal** de la enfermedad mediante cuantificación enzimática de PCC y medida de metabolitos específicos en vello coriónico y/o líquido amniótico, y asimismo, el análisis genético prenatal se realiza por extracción de DNA de cualquier tejido fetal y análisis de las mutaciones en los genes *PCCA* o *PCCB* presentes en la familia (Perez-Cerda et al., 2004).

Actualmente, no hay cura para la acidemia propiónica. El **tratamiento** principal de la enfermedad está dirigido a restablecer el equilibrio bioquímico, previniendo el acumulo de metabolitos tóxicos y el catabolismo endógeno de proteínas, además de evitar el ayuno prolongado, ya que se ha comprobado que propicia el acumulo de metabolitos tóxicos (Thompson and Chalmers, 1990). Para ello, la principal medida es la limitación de la ingesta proteica, en combinación con la administración de suplementos especiales exentos de aminoácidos precursores de ácido propiónico, la suplementación con L-carnitina, que puede atenuar los síntomas al actuar como transportador para retirar la acumulación de propionil-CoA de las células (Roe et al., 1984), la suplementación de biotina (Wolf et al., 1981; Lehnert et al., 1994), o el tratamiento con antibióticos como el metronidazol para disminuir la producción bacteriana de propionato intestinal (Mellon et al., 2000). Adicionalmente, también se ha descrito que la administración de N-carbamilglutamato puede reducir la hiperamonemia al eludir la inhibición de la N-acetilglutamato sintasa.

En algunos casos, niños con frecuentes descompensaciones metabólicas han sido sometidos a trasplante hepático (Yorifuji et al., 2000; Kayler et al., 2002), observándose una corrección de la hiperamonemia, un control de la descompensación metabólica (Yorifuji et al., 2000) y, sobre todo, una mejora significativa respecto al retraso mental y del crecimiento; aunque en contrapartida, los efectos sobre los niveles de los metabolitos del propionil-CoA en sangre, son mínimos. No obstante, ésta es una intervención invasiva que, además requiere un tratamiento inmunosupresor de por vida, por lo que es necesario la búsqueda de tratamientos alternativos para la AP.

1.2.2. Aciduria metilmalónica

Otra de las acidurias orgánicas estudiadas es la aciduria metilmalónica aislada, caracterizada por defectos en el paso de L-metilmalonil-CoA a succinil-CoA. Esta reacción está catalizada por la enzima mitocondrial metilmalonil-CoA mutasa (**MUT**; E.C. 5.4.99.2), dependiente del cofactor adenosilcobalamina (AdoCbl); por lo cual,

defectos tanto en la enzima MUT como en alguna de las enzimas **MMAA**, ATP: cob(I)alamina adenosiltransferasa (**ATR**; EC 2.5.1.17) o **MMADHC**, implicadas en el metabolismo mitocondrial de la forma activa del cofactor, producen **aciduria metilmalónica aislada** (Merinero et al., 2008) (Figura 3). Estos defectos son responsables de los grupos de complementación *mut*, *cblA*, *cblB* y *cblD* variante 2, respectivamente, definidos por estudios con líneas celulares de pacientes con defectos en el metabolismo de las cobalaminas.

La vitamina B_{12} (cobalamina) es absorbida de la dieta y entra en la célula a través de un receptor específico, pasa a través del lisosoma, sigue su procesamiento en el citosol y prosigue bien por vía citosólica, o bien por vía mitocondrial. En la vía mitocondrial sintetiza, mediante la enzima ATR, adenosilcobalamina (AdoCbl), cofactor de la metilmalonil-CoA mutasa (MUT) que cataliza el paso de L-metilmalonil-CoA a succinil-CoA (Figura 3).

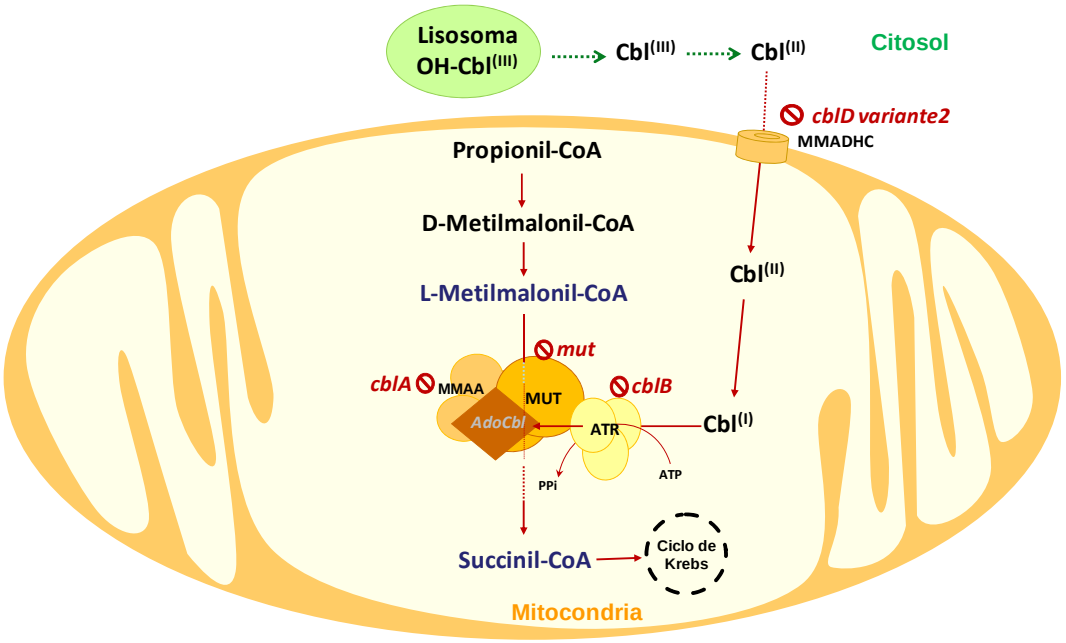

Figura 3. Metabolismo mitocondrial de las cobalaminas y enzimas implicadas en aciduria metilmalónica aislada. En rojo se muestran los grupos de complementación asociados a defectos en cada una de las proteínas.

La incidencia de la acidemia metilmalónica aislada es de 1/50.000 nacidos vivos (Fenton et al., 2001), en la cual están implicados los genes *MUT, MMAA, MMAB* y *MMADHC*:

- El **gen *MUT*** (MIM 609058), localizado en el cromosoma 6q21, codifica para la metilmalonil CoA mutasa (MUT) deficiente en el grupo de complementación ***mut*.**

- Defectos en el **gen *MMAA*** (MIM 607481), localizado en el cromosoma 4q31.1-2, son responsables del grupo ***cblA*.** Este gen codifica para la proteína MMAA con

actividad GTPasa que se cree que interviene en la "reactivación" de la enzima MUT (Padovani and Banerjee, 2006).

- El **gen *MMAB*** (MIM 607568), localizado en el cromosoma 12q24, codifica para la enzima **ATR** que cataliza la transferencia de un grupo adenosilo desde el ATP a la cobalamina para generar la adenosilcobalamina (AdoCbl). Defectos en este gen son responsables del grupo de complementación ***cblB.***

- Mutaciones en distintas regiones del **gen *MMADHC*** (MIM 611935), localizado en el cromosoma 2q23.2, se han asociado a la coexistencia de tres variantes fenotípicas diferentes. El análisis del gen *MMADHC* de pacientes *cblD* con aciduria metilmalónica aislada indica que mutaciones de parada prematura de la traducción en la región N-terminal de la proteína causan aciduria metimalónica (*cblD* variante 2), mientras que si se localizan en la región C-terminal causan aciduria metilmalónica combinada con homocistinuria (*cblD* combinada). Por último, pacientes con homocistinuria aislada (*cblD variante 1*) presentan mutaciones de cambio de aminoácido en el extremo C-terminal. Para explicar la coexistencia de tres fenotipos, todos con mutaciones en el mismo gen, se ha postulado que puede haber una segunda metionina iniciadora, o dos dominios funcionales distintos. También, se ha postulado que sería posible la existencia de dos transcritos, aunque no hay indicios experimentales para esta hipótesis (Coelho et al., 2008; Miousse et al., 2009; Suormala et al., 2004).

Las **características bioquímicas** de la AMM incluyen altos niveles de ácido metilmalónico, así como de los metabolitos derivados: 2-metilcitrato, 3-OH propionato, propionilcarnitina y propionilglicina en fluidos fisiológicos, junto con la presentación de cetoacidosis, hiperamonemia e hiperglicinemia.

El principal **tratamiento** para paliar los síntomas de estos pacientes es la limitación de la ingesta proteica con suplementación dietética especial exenta de aminoácidos precursores de ácido propiónico. Según el caso, se administra además L-carnitina, folato o betaína, así como metronidazol (Fenton et al., 2001; Zwickler et al., 2008). Otros tratamientos incluyen también la administración de N-carbamilglutamato para reducir la hiperamonemia o en algún caso el trasplante hepático.

1.3. DEFICIENCIA DE SEPIAPTERINA REDUCTASA

La deficiencia de sepiapterina reductasa (SRD), de herencia autosómica recesiva, pertenece al grupo de enfermedades del metabolismo de la tetrahidrobiopterina **(BH_4)** que cursan sin hiperfenilalaninemia. Hasta la fecha, han sido incluidos 31 pacientes con esta enfermedad en la base de datos de deficiencias en BH_4, BIODEF (http://www.biopku.org).

La BH_4 es un cofactor esencial para tres enzimas implicadas en la hidroxilación de aminoácidos aromáticos: la fenilalanina, triptófano y tirosina hidroxilasas (PAH, TPH,

TH, respectivamente), estas dos últimas claves en la biosíntesis de los neurotransmisores serotonina y dopamina, respectivamente (Figura 4), lo cual explica que los pacientes con defectos en BH_4 presenten deterioro neurológico (Blau et al., 2001). Además, la BH_4 actúa de cofactor de la óxido nítrico sintasa y la gliceril eter monooxigenasa (Thony et al., 2000).

La BH_4 es sintetizada de *novo* a partir de GTP en 3 pasos catalizados por las enzimas GTP ciclohidrolasa I (GTPCH), 6-piruvoil-tetrahidropterina sintasa (PTPS) y la enzima sepiapterina reductasa (**SR**; E.C. 1.1.1.153), codificada por el **gen *SPR*** (MIM 182125) de localización cromosómica 2p14-p12, que cataliza el paso final de reducción de 6-piruvoil-tetrahidropterina a BH_4. Otras tres enzimas adicionales pueden reemplazar a la SR: la aldosa reductasa (AR), carbonil reductasa (CR) y dihidrofolato reductasa (DHFR), en una ruta activa en tejidos periféricos pero no en cerebro, lo que explica por qué los pacientes con deficiencia de SR no presentan hiperfenilalaninemia, aunque sí síntomas neurológicos (Bonafe et al., 2001b) (Figura 4).

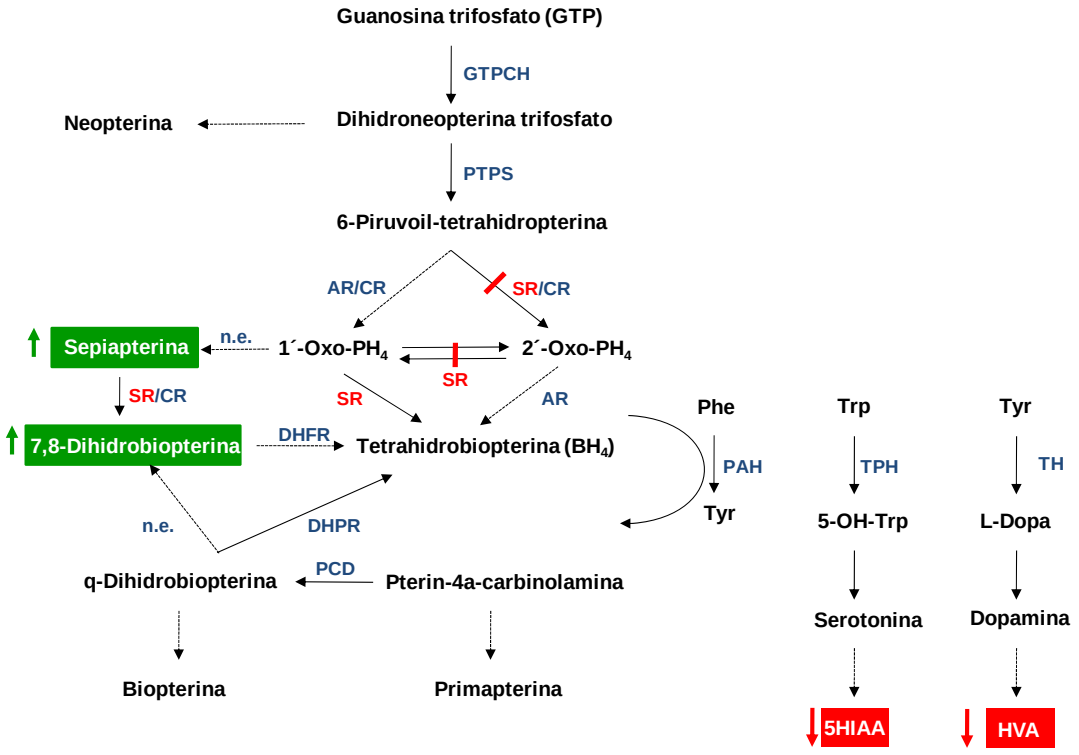

Figura 4. Biosíntesis y regeneración de tetrahidrobiopterina (BH_4) y su implicación en la deficiencia de sepiapterina reductasa (SR). Se muestran en verde los metabolitos aumentados en la deficiencia de sepiapterina reductasa y en rojo los disminuidos ***HVA:*** ácido homovalínico, ***5HIAA:*** 5-hidroxindolácetico. ***GTPCH:*** GTP ciclohidrolasa I, ***PTPS:*** 6-piruvoil-tetrahidropterina sintasa, ***AR:*** aldosa reductasa, ***CR:*** carbonil reductasa, ***DHFR:*** dihidrofolato reductasa, ***DHPR:*** dihidropteridina reductasa ***PCD:*** pterin-4a-carbinolamina dehidratasa, ***PAH, TPH y TH:*** fenilalanina, triptófano y tirosina hidroxilasas respectivamente, ***n.e:*** no enzimático.

Las **manifestaciones clínicas** en la mayoría de los pacientes aparecen en los primeros años de vida, siendo, principalmente, retraso psicomotor progresivo y diferentes defectos neurológicos, como temblor de tipo Parkinson, distonías

fluctuantes, opsoclonus, hipotonía central con hipertonía periférica y respuesta positiva a L-dopa (Echenne et al., 2006; Neville et al., 2005).

Al no presentar hiperfenilalaninemia, esta enfermedad no se detecta en los análisis rutinarios de cribado neonatal. El **diagnóstico bioquímico** de esta enfermedad se basa en el análisis de pterinas y aminas biógenas en líquido cefalorraquídeo, encontrándose niveles disminuidos de ácido homovalínico (HVA) y 5-hidroxindolácetico (5-HIAA), y aumentados de 7, 8-dihidrobiopterina y sepiapterina. El diagnóstico se completa con el análisis genético, confirmando la presencia de mutaciones en el gen SPR, y/o la disminución en la medida de actividad SR en fibroblastos (Bonafe et al., 2001a; Thony and Blau, 2006).

En la mayoría de los casos, la respuesta al **tratamiento** con L-dopa es excelente, aunque el retraso cognitivo puede persistir, de ahí la importancia de un diagnóstico precoz de la enfermedad.

1.4. REORDENAMIENTOS GENÓMICOS Y ENFERMEDADES METABÓLICAS HEREDITARIAS

Desde el punto de vista genético, las mutaciones en los genes descritos son mayoritariamente de cambio de aminoácido, mutaciones que afectan al procesamiento del mRNA *(splicing*), mutaciones sin sentido y pequeñas deleciones e inserciones. La metodología habitual para realizar el análisis genético, basada en la amplificación por PCR de las regiones codificantes del gen, seguida de secuenciación, no permite identificar reordenamientos genómicos como grandes deleciones, duplicaciones, inversiones, etc.

Se han descrito variaciones genómicas en el número de copias (CNVs) que conllevan la implicación de grandes segmentos de DNA como causa de muchas enfermedades genéticas, siendo asimismo, una fuente de diversidad genética entre humanos. La extensión de estos reordenamientos puede variar desde una duplicación de un cromosoma entero hasta variaciones en el número de copias de un solo exón (Saillour et al., 2008). Se ha sugerido que las CNVs pueden estar implicadas en la expresión fenotípica y penetrancia variable de las enfermedades mendelianas, así como en la etiología de enfermedades complejas (Beckmann et al., 2007) siendo varios los mecanismos moleculares propuestos incluyendo variaciones en la dosis génica, disrupción o fusión génica, efectos de posición, etc. (Zhang et al., 2009). Las CNVs, especialmente la duplicación génica y la reestructuración de exones, son los principales mecanismos de evolución génica y genómica.

Según la base de datos de mutaciones patogénicas humanas (HGMD-www.hgmd.cf.ac.uk), aproximadamente un 6% de las mutaciones corresponden a grandes deleciones genómicas y duplicaciones; aunque, teniendo en cuenta que los métodos diagnósticos estándar no detectan dichos reordenamientos genómicos, esta frecuencia podría ser menor que la real.

En algunas enfermedades como la distrofia muscular de Duchenne (DMD), el porcentaje de alelos con grandes deleciones es de hasta el 65%. En EMH, se ha descrito una alta frecuencia (15-25%) de este tipo de defectos en hiperglicinemia no cetósica (gen *GLDC*) (Kanno et al., 2007), en defectos de ornitina transcarbamilasa (gen *OTC*) (Shchelochkov et al., 2009) y en intolerancia proteica con lisinuria (gen *SLC7A7*) (Font-Llitjos et al., 2009). En fenilcetonuria, se han descrito por MLPA deleciones exónicas en el gen *PAH* (Desviat et al., 2006b), aunque la frecuencia es en general baja. En pacientes coreanos se ha descrito que la frecuencia alélica de deleción exónica o duplicación es del 9% (Lee et al., 2008).

En los últimos años, han ido surgiendo distintas técnicas que permiten analizar la dosis génica en cualquier región del genoma, gracias a las cuales se han identificado numerosos CNVs. Entre estas técnicas se incluyen aquellas basadas en *arrays* bien de SNPs (Stanczak et al., 2007), de BACs u oligos como es la hibridación genómica comparativa en *array* o *array* CGH (Saillour et al., 2008; Shchelochkov et al., 2009; Wong et al., 2008), otros métodos por PCR, entre los que está el MLPA (*Multiplex Ligation Probe Amplification*) basado en la hibridación y ligación de sondas, seguida de PCR y electroforesis capilar (Schouten et al., 2002), y las últimas técnicas de secuenciación masiva o *next generation sequencing*.

1.5. MUTACIONES SIN SENTIDO Y TERAPIAS SUPRESORAS DE LA TERMINACIÓN DE LA TRADUCCIÓN

Las mutaciones sin sentido o *nonsense* están presentes en un 10-15% de los pacientes con distintas enfermedades genéticas. La introducción de un codón de parada prematuro (PTC) conlleva la producción de proteínas truncadas que generalmente no son funcionales ni incluso estables, además, de que los mRNAs que contienen PTCs son en sí mismos frecuentemente inestables y degradados por el mecanismo de decaimiento del mRNA o *nonsense mediated decay* (NMD). Todo esto, tiene como consecuencia una reducción importante en la producción de proteína funcional de forma patogénica (Keeling and Bedwell, 2011).

Durante la fase de elongación en la traducción, el ribosoma avanza sobre el mRNA asociándose en cada caso el aminoacil tRNA complementario para cada uno de los codones codificantes. En raras ocasiones, cuando el ribosoma se encuentra un PTC, en lugar de originar la terminación prematura de la síntesis proteica, un aminoacil tRNA con un anticodón complementario en 2 de los 3 nucleótidos con el codón de parada, puede asociarse a la subunidad mayor (sitio A), siendo su aminoácido incorporado en la cadena polipeptídica naciente (Fearon et al., 1994) (Figura 5). De manera que, sobre el PTC se originaría una mutación de cambio de aminoácido, cuya actividad resultante tendría que ser evaluada posteriormente en cada caso. Este proceso es conocido como **supresión de la terminación de la traducción** y ocurre de manera natural en menos del 1% de los casos sobre PTCs (Manuvakhova et al., 2000), siendo de menos del 0,1% para codones de parada originales (McCaughan et al., 1995; Tate et al., 1995). Son varios los factores que previenen que esta supresión ocurra en

codones de parada originales, ya que se ha descrito que las secuencias de terminación más eficientes se encuentran, con mayor frecuencia, al final de los marcos abiertos de lectura u ORFs (*open reading frames*) (McCaughan et al., 1995), además, de que al final de muchos de los ORFs se encuentran múltiples codones de parada, reduciendo la posibilidad de que la traducción continúe en la región 3´UTR (Dalphin et al., 1999). Finalmente, si la traducción continuase en esta región, mecanismos de supervivencia, que incluyen el decaimiento del mRNA que ha continuado la traducción, bien hasta la cola de poli(A) (Frischmeyer and Dietz, 1999), o bien hasta un codón de parada en la región 3´UTR (Kong and Liebhaber, 2007), degradarían estos mRNAs que pudieran generarse (Keeling and Bedwell, 2011).

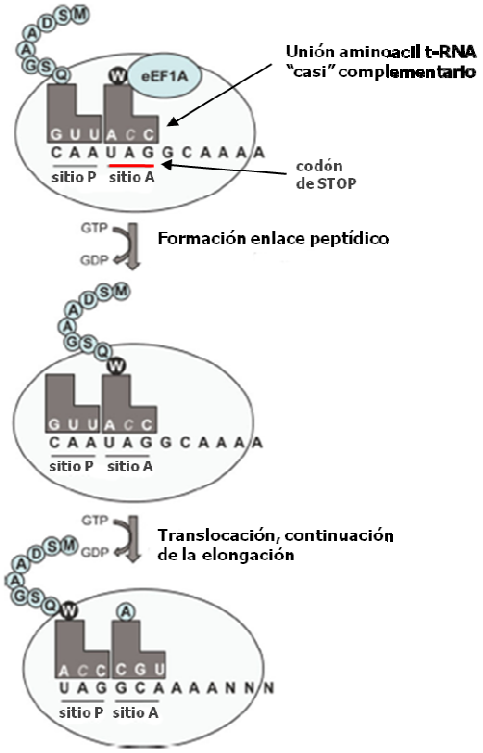

Figura 5. Supresión de la terminación de la traducción. Durante la supresión de un PTC un aminoacil tRNA cuyo anticodón es complementario con 2 de las 3 bases del codón de parada se asocia al sitio A de la subunidad grande del ribosoma siendo su aminoácido incorporado a la cadena polipeptídica de manera que la traducción continúa en fase hasta alcanzarse el codón de parada original. Figura modificada de Keeling and Bedwell, 2011.

Se han identificado un gran número de compuestos de bajo peso molecular que incrementan la frecuencia de supresión de la terminación, de manera que podrían utilizarse como una prometedora terapia específica para mutaciones sin sentido. En concreto, la propiedad de los antibióticos aminoglucósidos como supresores de PTCs se ha estado estudiando desde hace varios años. La primera enfermedad genética estudiada fue la fibrosis cística, donde se demostró la recuperación de proteína funcional para mutaciones sin sentido tras el tratamiento con los aminoglucósidos gentamicina y geneticina (G418) (Bedwell et al., 1997; Howard et al., 1996).

Diferentes aminoglucósidos más, incluyendo amikacina, paromomicina, lividomicina, tobramicina y estreptomicina, han demostrado ser eficientes en la supresión de la terminación y recuperación de proteína funcional para más de 20 modelos de enfermedad *in vitro* y 8 modelos *in vivo* (Dietz, 2011; Linde and Kerem, 2008; Keeling and Bedwell 2010). Varios ensayos clínicos pilotos con gentamicina han

resultado efectivos, en diferente medida, en fibrosis cística (Clancy et al., 2001; Wilschanski et al., 2003), distrofia muscular de Duchenne (Dunant et al., 2003; Politano et al., 2003), hemofilia A y B (James et al., 2005) y la enfermedad de Hailey-Hailey (Kellermayer et al., 2006).

En la eficiencia de la supresión mediada por los aminoglucósidos influye en gran medida la identidad del codón de parada, así como la secuencia del mRNA alrededor de éste. En concreto, se ha descrito la importancia del nucleótido siguiente al codón de parada, por lo que se habla de tetranucleótido como señal de la terminación (McCaughan et al., 1995). Tras ser ensayadas distintas construcciones con los 12 posibles tetranucleótidos, mediante un sistema de transcripción-traducción *in vitro* en reticulocitos de conejo, se ha observado que el codón de parada UGA seguido prioritariamente por una pirimidina, en concreto una citosina, es el más susceptible a la supresión de la terminación con aminoglucósidos (Manuvakhova et al., 2000).

Además de esta última consideración, previa a la administración de los aminoglucósidos como terapia supresora para mutaciones sin sentido, otra importante a tener en cuenta es que el uso prolongado de éstos es limitado debido a su nefro y ototoxicidad. Por lo que, ante la necesidad de encontrar compuestos sin efectos adversos y capaces de suprimir la terminación de PTCs, se han realizado varios estudios mediante un rastreo de alto rendimiento en librerías de compuestos de bajo peso molecular. De esta manera, se identificó el compuesto PTC124 por su capacidad de producir selectivamente la supresión de la terminación de PTCs, pero no de los codones originales de parada, con una mayor potencia que los aminoglucósidos, a concentraciones de tipo nanomolar y sin producir efectos tóxicos (Welch et al., 2007). Inicialmente, el compuesto PTC124 fue ensayado con éxito, suprimiendo de manera efectiva mutaciones sin sentido asociadas con DMD y fibrosis cística en modelos de ratón (Du et al., 2008; Welch et al., 2007). En el modelo de ratón para DMD se recuperó aproximadamente un 20-25% de los niveles de proteína normal tras el tratamiento con PTC124. Actualmente, este compuesto comercializado como *Ataluren® (PTC Therapeutics®)* está en fase 3 en ensayos clínicos para pacientes con fibrosis cística (http://www.ptcbio.com). Asimismo, se han identificado otros compuestos con capacidades similares (Du et al., 2009), así como, derivados de aminoglucósidos, específicamente diseñados para suprimir la terminación de PTCs sin producir efectos tóxicos (Hainrichson et al., 2008).

1.6. DEFECTOS DE *SPLICING* Y TERAPIAS ESPECÍFICAS

1.6.1. *Splicing* y enfermedades genéticas

Aproximadamente, un 15% de las mutaciones puntuales asociadas a enfermedades genéticas humanas afectan al procesamiento del mRNA o *splicing* (Cooper et al., 2006; Krawczak et al., 1992; Wang et al., 2005). Se conoce como *splicing* al proceso mediante el cual, el mRNA sufre el procesamiento de eliminación de sus intrones previamente a la traducción de la secuencia codificante. Se lleva a cabo por

un complejo macromolecular denominado ”spliceosoma”, compuesto por 5 partículas ribonucleoproteicas -snRNPs- (U1, U2, U4, U5 y U6) y más de 100 proteínas, entre las que se incluyen proteínas de unión a RNA y enzimas (helicasas/RNPasas, quinasas, fosfatasas…). Cada snRNP está compuesto por un RNA pequeño nuclear (snRNA), rico en uridinas, y múltiples proteínas asociadas.

Se han descrito tres **secuencias conservadas de *splicing*,** localizadas en las uniones exón-intrón, que contienen gran parte de la información requerida para el procesamiento correcto de los distintos exones: las secuencias 5´ y 3´ de *splicing* y la secuencia de ramificación localizada 30-50 nucleótidos aguas arriba del sitio 3´ de *splicing* (Cooper et al., 2009) (Figura 6). Estas secuencias son reconocidas a través de interacciones RNA-RNA y RNA-proteínas por los diferentes componentes del “spliceosoma”. En concreto, el proceso de *splicing* comienza en el sitio 5´ de *splicing* al que se une, por complementariedad de bases, U1snRNP como primer paso de la formación del “spliceosoma”; a su vez, el sitio 3´ de *splicing* es reconocido por el factor auxiliar heterodímero de U2 (U2AF), formado por una subunidad pequeña (U2AF35) y una grande (U2AF65), que reclutan a U2snRNP. Posteriormente, se reclutan las tres snRNPs (U4, U5 y U6), ensambladas en un complejo trimérico, y, tras interacciones específicas y modificaciones conformacionales queda formado el complejo de la maquinaria de *splicing* catalíticamente activo (Tazi et al., 2005).

La variabilidad en el reconocimiento de las secuencias conservadas de *splicing* por los diferentes componentes del “spliceosoma” contribuye a la diferente eficiencia y fidelidad del *splicing*. Mutaciones puntuales localizadas en cualquiera de estas secuencias, que interrumpan estas interacciones, son responsables de ~10% de las enfermedades genéticas (Cartegni et al., 2002; Wang and Cooper, 2007).

El resto de la información requerida para el procesamiento del mRNA se dispone en las **secuencias reguladoras auxiliares** menos conservadas, relativamente cortas (~6 nucleótidos), como son los potenciadores o *enhancers* y los silenciadores de *splicing* que pueden estar localizados en secuencias exónicas (ESE –*exonic splicing enhancers*-, ESS -*exonic splicing silencers*-) o intrónicas (ISE –*intronic splicing enhancers*-, ISS –*intronic splicing silencers*-). Estas secuencias ejercen su acción a través de factores proteicos. En concreto, los ESEs realizan su función activadora gracias a las proteínas SR, compuestas por uno o dos dominios de reconocimiento de RNA (RRM) en su extremo N-terminal y un dominio C-terminal rico en arginina y serina de distinta longitud (dominio RS). Los silenciadores interaccionan con una serie de reguladores negativos que pertenecen frecuentemente a la familia de las ribonucleoproteínas heterogéneas nucleares (hnRNPs) (Figura 6).

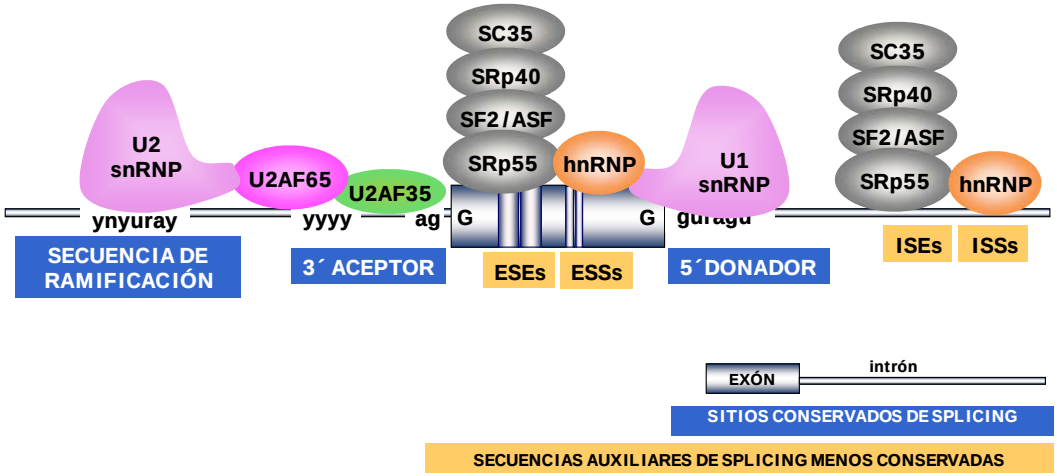

Figura 6. Representación esquemática de los distintos factores implicados en el procesamiento del mRNA y las distintas zonas de reconocimiento de los mismos. ESEs: *exonic splicing enhancers*, ESSs: *exonic splicing silencers*, ISEs: *intronic splicing enhancers*, ISSs: *intronic splicing silencers*. Proteínas SR: SC35 (*splicing component 35*), SRp40, SF2/ASF (*splicing factor 2/alternative splicing factor*), SRp55), hnRNP: proteína heterogénea nuclear.

Clásicamente, las mutaciones de *splicing* han sido descritas por interrumpir secuencias conservadas de *splicing*, la mayoría de ellas afectando a los dinucleótidos invariables *ag* o *gt* en los sitios 3´ y 5´ de *splicing,* respectivamente (Krawczak et al., 2007). Pero en los últimos años se han descrito numerosas mutaciones localizadas lejos de estos sitios, en secuencias intrónicas o exónicas, que causan un defecto en el *splicing*. Estas mutaciones, bien activan nuevos sitios crípticos de *splicing,* o bien afectan a elementos exónicos e intrónicos activadores o silenciadores, reconocidos específicamente por proteínas SR o hnRNPs, respectivamente. En concreto, las mutaciones localizadas en secuencias exónicas deben ser evaluadas cuidadosamente ya que normalmente suelen interpretarse por su efecto en la secuencia codificante de la proteína resultante, sin tener en cuenta su papel en la implicación en el procesamiento del mRNA (Cartegni et al., 2002).

Muchas de las proteínas SR y hnRNPs fluctúan continuamente entre el núcleo y el citoplasma (Caceres et al., 1998; Pinol-Roma and Dreyfuss, 1992), pudiendo variar su distribución subcelular en respuesta a señales de estrés. Los cambios resultantes en la estequiometria de los factores de *splicing* en el núcleo pueden tener efectos significativos en la modulación del *splicing*. Se han descrito varias enfermedades asociadas a cambios en la expresión de proteínas de unión a RNA implicadas en el *splicing* y su regulación, como la artritis reumatoide, la esquizofrenia, el síndrome de Leigh o la distrofia muscular de Duchenne y la de Becker (Gabut et al., 2008; Lukong et al., 2008; Ule, 2008).

Los dos efectos más comunes de las mutaciones de *splicing* son la exclusión de algún exón en el mRNA (*exon skipping*), o la activación de nuevos sitios crípticos de *splicing* produciendo la exclusión de secuencias codificantes o la inclusión de secuencias aberrantes.

En ocasiones, más que interrumpir secuencias conservadas de *splicing,* ciertas mutaciones pueden crear nuevos sitios utilizados erróneamente por la maquinaria de *splicing* dando lugar a transcritos aberrantes. La presencia de secuencias similares a las consenso de *splicing* en secuencias intrónicas internas alejadas de la secuencia codificante puede ser muy abundante. Mutaciones localizadas en estas secuencias pueden generar nuevos sitios consenso de *splicing*, activar regiones potenciadoras o inhibir regiones silenciadoras presentes en estas secuencias, encargadas de impedir normalmente su reconocimiento por la maquinaria de *splicing*. Frecuentemente, las mutaciones intrónicas producen la inclusión errónea de **pseudoexones,** secuencias del pre-mRNA que se asemejan a un exón tanto en tamaño como por presentar secuencias flanqueantes implicadas en el *splicing,* pero que en condiciones normales no son nunca reconocidas como un exón por la maquinaria de *splicing* (Buratti et al., 2006; Pagani and Baralle, 2004). Muchas veces, los pseudoexones derivan de secuencias repetidas tipo *Alu* (Vorechovsky, 2010).

Mediante el análisis *in silico* podemos orientarnos sobre el mecanismo molecular por el cual la mutación ejerce su efecto, bien por afectar a la complementariedad de bases entre distintos snRNAs del "spliceosoma", como U1snRNA que se une específicamente al sitio 5´ de *splicing*; o bien por modificar secuencias reconocidas como *enhancers* de *splicing* exónicos e intrónicos (ESEs e ISEs), donde se unen las proteínas SR auxiliares de *splicing*. Para ello, están disponibles distintos programas como son el servidor *Berkeley Drosophila Genome Project* (BDGP): http://www.fruitfly.org/sq_tools/splice.html, *Analyzer Splice Tool* (AST): http://ibis.tau.ac.il/ssat/SpliceSiteFrame.html o *Human Splicing Finder* (http://www.umd.be/HSF/) y *ESE finder* (http://exon.cshl.edu/ESE). Este último facilita la identificación de posibles ESEs basándose en su reconocimiento por cuatro proteínas SR: SF2/ASF, SC35, SRp40 y SRp55.

Para analizar funcionalmente el efecto de una mutación sobre el procesamiento del mRNA o *splicing* es necesario analizar el perfil transcripcional del alelo mutante, bien directamente en células del paciente, o bien mediante la utilización de sistemas celulares modelo de *splicing* que utilizan vectores específicos llamados **minigenes** (Cooper, 2005). Los minigenes son vectores con porciones exónicas de un gen, definidas como sitios funcionales 5´ y 3´ de *splicing,* separadas por secuencias intrónicas donde está localizado el sitio de policlonaje y se clona la secuencia genómica de interés. La expresión transitoria de minigenes es un ensayo *ex vivo*, utilizado comúnmente para identificar el efecto funcional de una mutación comparando el perfil transcripcional de construcciones normal y mutante, así como para explorar más en profundidad los mecanismos subyacentes al procesamiento erróneo del mRNA, como puede ser la identificación del grado de reconocimiento de los sitios de *splicing*, de elementos exónicos o intrónicos potenciadores o represores, así como la identificación de factores que se unan a estos elementos modulando el *splicing* (Baralle and Baralle, 2005).

Como consecuencia de defectos en el *splicing,* usualmente se producen transcritos que introducen un cambio en la fase de lectura y un codón de parada prematura de la traducción (PTC) y que son por tanto, susceptibles a ser degradados

por el mecanismo de NMD, que actúa como sistema de vigilancia del mRNA que contiene PTCs para evitar que puedan traducirse a proteínas truncadas carentes de función (Maquat, 2004). El NMD en mamíferos, generalmente, degrada mRNAs que producen PTCs 50-55 nucleótidos corriente arriba de una unión exón-exón generada tras el procesamiento del mRNA. A 20-24 nucleótidos corriente arriba de esta unión se une un complejo proteico denominado EJC (*Exon Junction Complex*), formado por 12 proteínas que incluyen algunos de los factores del sistema NMD. Cuando el ribosoma comienza la traducción y encuentra un PTC se detiene. Esto permite la formación del complejo SURF que al unirse al EJC provoca la activación del sistema NMD y con ello la degradación del mRNA (Figura 7).

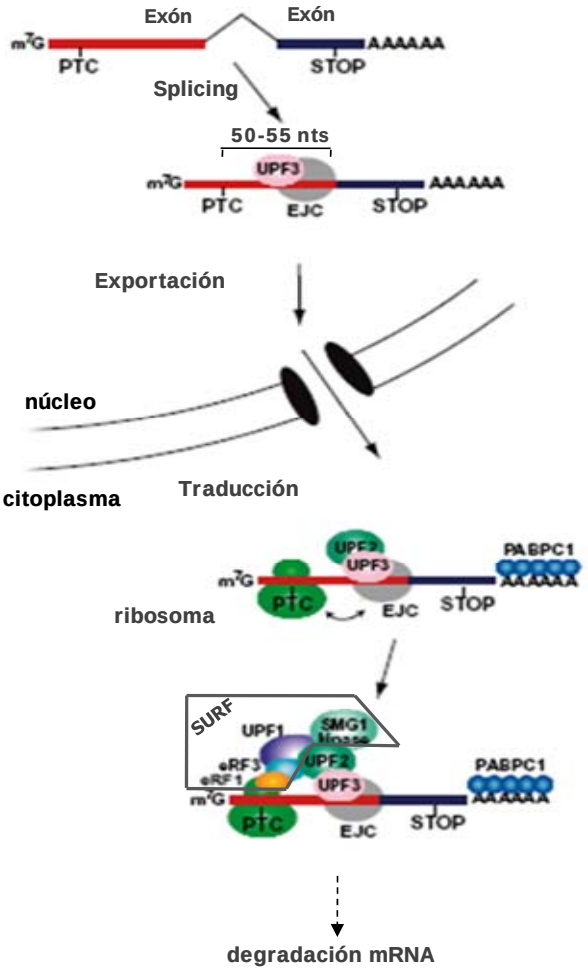

Figura 7. Esquema del mecanismo NMD. Se muestran los distintos pasos de degradación de un mRNA que contiene un PTC (siguiendo la regla del NMD) a 50-55 nucleótidos corriente arriba de una unión exón-exón. El complejo SURF está formado por SMG kinasa, UPF1 y los factores eRF1 y eRF3. Figura modificada de Behm-Ansmant et al., 2007.

1.6.2. Terapias específicas de mutaciones de *splicing*

Una vez identificados los genes involucrados y las mutaciones responsables de la enfermedad, la investigación se centra en los mecanismos moleculares subyacentes, lo cual sirve como base científica para el desarrollo de terapias específicas de mutación. Son muchas las aproximaciones terapéuticas propuestas para modificar el patrón de *splicing* de un premRNA aberrante o eliminar un mRNA aberrante causante de

enfermedad. Entre ellas, se encuentran distintas estrategias como son la sobreexpresión de factores de *splicing*, la utilización de RNA interferente para eliminar selectivamente un mRNA aberrante o inhibir la traducción de alguna de las proteínas implicadas en la regulación del *splicing,* y la utilización de oligonucleótidos antisentido.

La **sobreexpresión de factores de *splicing*** de manera específica para cada una de las mutaciones analizadas permite determinar cuáles son los mecanismos moleculares subyacentes al defecto, sirviendo de base científica para el desarrollo de la aproximación terapéutica más acertada para cada uno de los casos. Como ha sido comentado anteriormente, las proteínas SR y hnRNPs tienen un papel muy importante en la modulación del *splicing*, por lo que, una vez ha sido identificado el efecto regulador de cada una de ellas para cada mutación en concreto, la utilización de pequeñas moléculas que produzcan variaciones ya sea en la actividad o en las cantidades relativas de estas proteínas en el núcleo modularía en gran medida el patrón transcripcional producido (Sumanasekera et al., 2008). En este sentido, se han ensayado múltiples terapias farmacológicas, como el uso de kinetina, aclarubicina, butirato sódico o valproico (Andreassi et al., 2001; Hims et al., 2007). La mayoría actúan activando la transcripción de determinados genes factores de *splicing,* ya que inhiben las deacetilasas de histonas. También se ha descrito que la transfección de factores de *splicing* específicos puede modular el *splicing* (Nissim-Rafinia et al., 2004).

Por otra parte, para mutaciones localizadas en el sitio 5´de *splicing* donde se ve afectada la unión por complementariedad de bases de U1snRNA, el uso de vectores que contienen U1snRNAs modificados ha sido ampliamente estudiada (Guedard-Mereuze et al., 2009; Lund and Kjems, 2002; Roca et al., 2005) y utilizada con éxito para recuperar el patrón transcripcional normal en distintas enfermedades como retinitis pigmentosa (Tanner et al., 2009), deficiencia del factor VII de coagulación (Pinotti et al., 2009) u osteopetrosis infantil maligna (Susani et al., 2004).

Otra aproximación terapéutica ensayada con éxito para modular el *splicing* es el uso de **oligonucleótidos antisentido** (AONs). Estos AONs son pequeñas cadenas de análogos nucleotídicos que hibridan con el mRNA complementario por apareamiento de bases, formando los heterodúplex AONs-mRNA, y actúan bloqueando estéricamente la unión de componentes del "spliceosoma" a los sitios de *splicing*. Han sido utilizados para impedir el reconocimiento de sitios crípticos de *splicing*, cambiar los niveles de genes procesados por *splicing* alternativo o producir el *skipping* de un exón en concreto con el objetivo de restablecer la pauta de lectura y la funcionalidad de la proteína como es el caso de la distrofia muscular de Duchenne donde esta terapia está actualmente en fase clínica (Cirak et al., 2011; Goemans et al., 2011). La terapia antisentido ha sido también utilizada para mutaciones intrónicas que activan la inserción de pseudoexones (Dhir and Buratti, 2010), también en modelos celulares de distintas EMH (Perez et al., 2010).

2. OBJETIVOS

El **objetivo principal** de este trabajo ha sido la caracterización de variaciones en el número de copias (CNVs) y mutaciones sin sentido en acidemia propiónica, así como de mutaciones de *splicing* y sus mecanismos moleculares en diferentes enfermedades metabólicas hereditarias, sirviendo como base para la investigación en nuevas aproximaciones terapéuticas específicas de mutación.

Para ello, se han seguido los siguientes objetivos concretos:

1. Caracterización de CNVs, en concreto grandes deleciones genómicas, en el gen *PCCA* en pacientes con acidemia propiónica.

2. Caracterización de mutaciones sin sentido en los genes *PCCA* y *PCCB* causantes de acidemia propiónica.

3. Análisis *in vitro* y funcional del efecto de compuestos supresores de la terminación de la traducción sobre mutaciones sin sentido en los genes *PCCA* y *PCCB*.

4. Caracterización funcional de mutaciones que afectan al procesamiento del mRNA o *splicing* en diferentes enfermedades metabólicas hereditarias.

5. Análisis del efecto de la sobreexpresión de factores de *splicing,* U1snRNAs modificados y oligonucleótidos antisentido, sobre la recuperación transcripcional y funcional de defectos de *splicing*, como primer paso en la investigación de nuevas aproximaciones terapéuticas moduladoras del *splicing.*

3. MATERIALES Y MÉTODOS

3.1. MATERIALES

3.1.1. Reactivos y aparatos

En el cultivo celular se emplearon los siguientes reactivos: medio mínimo esencial de Eagle (MEM), glutamina de la firma comercial GibcoBRL y suero fetal bovino (FBS) de SIGMA. Los antibióticos fueron suministrados por Antibióticos S.A. La tripsina y los medios de comprobación se obtuvieron de Difco Laboratorios. Invitrogen, GibcoBRL, Gene Tools y Lonza suministraron los reactivos para las transfecciones de células primarias y establecidas. Las botellas de 25 o 75 cm^2 y placas estandarizadas de 6 pocillos (P6) eran de NUNC, Thermo Scientific.

La agarosa y la agarosa *NuSieve®GTG®* son de las casas comerciales Pronadisa y Cambrex, la acrilamida y bisacrilamida de Bio-Rad.

Invitrogen proporcionó los productos necesarios para la purificación de RNA total. La purificación de productos de PCR y de DNA plasmídico se llevó a cabo con los productos de las casas comerciales Promega, Qiagen y Mbiotech. Las firmas comerciales Gentra Systems, Promega, Invitrogen y Roche proporcionaron los productos necesarios para la extracción de DNA genómico.

Los reactivos y enzimas empleados en las reacciones de PCR, RT-PCR y mutagénesis dirigida fueron obtenidos de las firmas comerciales Invitrogen, Roche y Stratagene y se realizaron en un termociclador *Veriti* de Applied Biosystems.

Las reacciones de secuenciación cíclica directa se llevaron a cabo con productos de Applied Biosystems en un secuenciador *ABI* Prism® *3730* de Applied Biosystems. Los oligonucleótidos sintéticos proceden de la firma comercial Sigma y los oligonucleótidos antisentido tipo morfolinos fueron suministrados por la casa comercial GeneTools.

Invitrogen y Life Technologies proporcionaron los vectores necesarios para llevar a cabo los clonajes.

Las enzimas de restricción fueron proporcionadas por Roche Diagnostics, Promega y New England Biolabs.

Los reactivos empleados en las reacciones RT-PCR a tiempo real (qRT-PCR) fueron obtenidos de las firmas comerciales Applied Biosystems y Roche, la PCR fue llevada a cabo en el aparato Lightcycler® 480 de Roche.

Los reactivos utilizados para la detección de proteínas de unión a biotina son de las casas comerciales Miltenyi Biotech, Pierce, Millipore y Roche. La membrana de PVDF procedió de la casa comercial Protan. Se utilizó el anticuerpo anti-avidina conjugado a fosfatasa alcalina (Pierce). La electroforesis se llevó a cabo en el Mini-protean de Bio-Rad y la transferencia en el Mini Trans-Blot Transfer Cell (Bio-Rad).

Para la transcripción-traducción *in vitro*, el kit TNT-*T7 Quick Coupled Transcription/Translation System* lo proporcionó Promega y Amersham el reactivo Amplify. Las radiografías se cuantificaron en el densitómetro Bio-Rad GS-800 Calibrated Imaging Densitometer. La mezcla macada radiactivamente L-[S^{35}]-Met+L-[S^{35}]-Cys (Promix TM L-[S^{35}] *in vitro* cell labelling mix; >1000Ci/mmol) y el isótopo radiactivo NaH[^{14}C]O_3 con una actividad de 44,8 mCi/mmol y 1mCi/ml fueron suministrados por Perkin Elmer.

El *SMARTpool siRNA* contra *SRp40* fue proporcionado por Dharmacon.

3.1.2. Material biológico

3.1.2.1. Pacientes y líneas control

El estudio se ha llevado a cabo en distintos pacientes diagnosticados de acidemia propiónica y metilmalónica en base a su sintomatología clínica y análisis bioquímico. Como fuente de DNA y RNA se han utilizado fibroblastos de piel cultivados, muestras de sangre impregnada en papel o sangre total. Las líneas de fibroblastos control fueron obtenidas del banco de células humanas del Instituto Coriell para la investigación biomédica (Camden, NJ).

Todo el material genético (biopsias de piel y sangre) de pacientes y controles fue obtenido con el consentimiento informado autorizado por los padres y por el hospital que remitió las muestras. Toda la investigación llevada a cabo con este material está autorizado por el Comité de Ética de la Investigación de la Universidad Autónoma de Madrid, respeta los principios fundamentales de la declaración de Helsinki, del Convenio del Consejo de Europa relativo a los derechos humanos y la biomedicina y de la declaración Universal de la UNESCO sobre el genoma humano y los derechos humanos.

3.1.2.2. Líneas celulares establecidas

La línea celular de hepatoma utilizada para este estudio fue Hep3B, cedida por el Dr. S.R. de Córdoba. Alternativamente los estudios sobre *splicing* con minigenes se realizaron en la línea celular establecida HEK293T.

En los estudios de expresión de PCCA y PCCB en células eucariotas se emplearon las líneas celulares establecidas de fibroblastos: **5626-T** (pccA, genotipo: c.1899+3del4/ c.1899+3del4) y **14046-T** (pccBC, genotipo: c.1218_1231del14ins12/ c.1218_1231del14ins12), transformadas con el plásmido T22 (cedido por el Dr. P. H. Gallimore, Universidad de Birmingham, UK), que contiene secuencias del virus SV40.

3.1.2.3. Cepas bacterianas

Las estirpes de *E.coli* utilizada en este estudio han sido TOP10 de Invitrogen y XL1-Blue de Stratagene.

3.1.2.4. Vectores plasmídicos

- *TOPO TA Cloning PCR 2.1-Topo Vector* de Invitrogen.
- pSPL3 de Life Technologies, cedido por el Dr. B. Andresen.
- Los plásmidos portadores de la secuencia codificante para los distintos factores de *splicing* y proteínas SR fueron cedidos por Dr. B. Andresen, Dr. A. Krainer, Dr. J. Valcarcel y el Dr. F. Pagani.
- pCMVA45-12 y pRcCMVB52 (cedidos por el Dr. D. Leclerc y el Prof. R. A. Gravel), portadores de los cDNAs *PCCA* y *PCCB,* respectivamente.

3.2. MÉTODOS

3.2.1. Aislamiento de ácidos nucleicos

La **extracción de DNA genómico** a partir de fibroblastos de piel cultivados o sangre total se realizó mediante fenolizaciones (John et al., 1991) o con el aparato *MagNA Pure Compact* de Roche mediante el *MagNA Pure Compact Nucleic Acid Isolation kit*. A partir de sangre impregnada en papel se llevó a cabo con el kit *Generation DNA Purification Systems* de Gentra Systems.

Para obtener un **DNA plasmídico** de alto grado de pureza, a baja escala, se ha empleado el kit *Wizard® Plus SV Minipreps DNA Purification System* de Promega. Para extracciones a gran escala se ha empleado el sistema de extracción *QIAGEN® Plasmid Maxi kit* de Qiagen.

La **extracción de RNA total** a partir de fibroblastos de piel o células establecidas de hepatoma (línea Hep3B) o HEK293 T se llevó a cabo mediante el reactivo *Tripure Isolation Reagent* de Invitrogen o bien con el aparato *MagNA Pure Compact* de Roche mediante el kit *MagNA Pure Compact RNA isolation* de Roche.

3.2.2. Amplificación de DNA genómico

La amplificación de los distintos exones, junto con su secuencia intrónica adyacente, se llevó a cabo utilizando los reactivos y las instrucciones descritas por las firmas comerciales Invitrogen (*Platinum® Taq DNA polimerasa* y *Platimun® PCR*

Supermix) y Roche (*Fast Start Taq Polimerasa*) en un termociclador *Veriti* de Applied Biosystems.

Para la amplificación de grandes fragmentos se realizó **PCR larga** mediante la polimerasa *AccuTaq DNA* (Sigma), siguiendo las recomendaciones del fabricante. Se amplificaron 500 ng de DNA genómico en un volumen final de reacción de 50 µl que contiene el buffer de la polimerasa 1X, 500 µM de dNTPs, 400 nM de cada uno de los oligos, 2% DMSO y 2,5 U de polimerasa. Los oligos se diseñaron teniendo en cuenta que no hibridaran con secuencias intrónicas repetidas, para lo que se utilizó el programa *RepeatMasker* (www.repeatmasker.org), y que tuvieran una Tm≥70°C para permitir una reacción de amplificación en 2 pasos de la siguiente manera: una desnaturalización inicial de 98°C durante 30 segundos, 30 ciclos a 94°C 15 segundos, 68°C 8-10 minutos y una extensión final de 10 minutos a 68°C. Los productos de la amplificación fueron purificados mediante *Qiaex II Gel Extraction Kit* (Qiagen) para ser secuenciados, bien directamente, o bien previo clonaje en el vector *TOPO TA version 2.1* (Invitrogen) en cuyo caso se utilizaron los oligos propios del vector: *M13 Reverse* 5´-CAGGAAACAGCTATGAC-3´ y *M13 Forward* 5´-GTAAAACGACGGCCAG-3´.

Para poder clonar los productos de PCR larga generados con la polimerasa *AccuTaq DNA* en el vector TOPO, específico para productos de PCR que generen colas de A, éstas se añadieron a los productos amplificados utilizando 1 µl de dATP y 0,5 U de la *Platinum® Taq DNA polimerase* de Invitrogen durante 3 ciclos a 55°C y 15´a 72°C.

3.2.3. Amplificación de cDNA

- El proceso de **RT-PCR** se ha llevado a cabo partiendo de 1µg de RNA total extraído a partir de fibroblastos de piel o células de hepatoma. Los reactivos empleados fueron suministrados por Invitrogen (*Superscript™ III First-Strand Síntesis System for RT PCR* y *Platinum® Taq DNA polimerase),* utilizando oligodT y según las instrucciones de la casa comercial.

- Los niveles de expresión de los genes *PCCA*, *PCCB* y *SRP40* se analizaron mediante cuantificación del cDNA por **RT-PCR a tiempo real (qRT-PCR).** La retrotranscripción se llevó a cabo con el *High Capacity cDNA Reverse Transcription kit* de Applied Biosystems utilizando 1µg de RNA total y siguiendo las recomendaciones del proveedor:

Para la qRT-PCR del mRNA de los **genes *PCCA y PCCB,*** se utilizaron los oligonucleótidos **APA13** localizado en el exón 22 (5´-TGCCAGTTTTCCCAGCTGTC-3´) y **23AS** localizado en el exon 23 (5´- ACCAGACTTGCCGCAGAATT-3´) para el gen *PCCA;* y **cDNA5s** localizado en el exón 5 (5´-ATTGGCTGAATGACTCTGG-3´) y **cDNA8as** localizado en el exón 8 (5´-CAGGGGCAGGTAGTTGAAGA-3´) para el gen *PCCB*. La PCR se llevó a cabo en un volumen total de 20 µl, con 0,25-1 µl de cDNA, 5 µl *LightCycler® 480 SYBR Green I Master* (Roche) y una concentración final de oligos de 125 nM cada uno.

Para el **gen *SRp40*** se utilizó la sonda *Universal Probe Library* #88 y los oligonucleótidos específicos diseñados por el *probe Finder Software (Universal Probe Library)* de Roche Applied Science: **SRp40 S** (5´-CTTCATGGCCGCTCAGAT-3´) y **SRp40 AS** (5´-TGATGTCCGGCTAGTACTTCCT-3´). La reacción se llevó a cabo en la unidad de genómica del Parque Científico de Madrid (Campus de Cantoblanco, Madrid).

La amplificación y análisis se realizó en un aparato LightCycler® 480 de Roche. La eficiencia de la amplificación fue estandarizada mediante la retrotranscripción y posterior amplificación en paralelo del mRNA del gen constitutivo *GAPDH.*

Para llevar a cabo la cuantificación, una vez obtenidos los datos de *crossing point* (Cp) o *cycle threshold* (Ct) de la PCR a tiempo real, tanto para el gen de interés como para los constitutivos, se llevó a cabo el tratamiento matemático para obtener finalmente el parámetro *Relative Quantity* (RQ), que nos permite calcular y comparar la cantidad de mRNA en los distintos extractos celulares, siendo calculado según la siguiente fórmula:

$RQ = 2^{-\Delta\Delta Ct}$; $\Delta\Delta Ct$ = (ΔCt de una muestra - ΔCt la muestra de referencia)

ΔCt = (Ct del gen de estudio - Ct del gen constitutivo [*GAPDH*])

- Para la **<u>semicuantificación del mRNA</u>** en los fibroblastos transfectados con las distintas construcciones de U1, la RT-PCR se llevó a cabo mediante la utilización de un oligo *sense* fluorescente marcado con 6FAM que hibridaba en el exón 11 y uno *antisense* que hibridaba en el exón 14 del gen *PCCA*. La reacción se incubó a 95°C durante 5 minutos, seguida de 30 ciclos a 95°C durante 25 segundos, 55°C durante 25 segundos y 72°C durante 40 segundos. Los productos de amplificación fueron separados en el *ABI Prism 3730 Genetic Analyzer* (Applied Biosystems) y analizados mediante el *software Peakscanne*r (Applied Biosystems)

3.2.4. Purificación de fragmentos de DNA

La purificación de fragmentos de DNA inferiores a 1 Kb, obtenidos tras amplificación por PCR o resultantes de digestión enzimática, se realizó con los productos *SpinClean PCR Purification Kit* de MBiotech, siguiendo las instrucciones de los proveedores. En el caso de que la purificación se realizara a partir de los fragmentos en geles de agarosa se utilizó el *kit QIAEX® II Gel Extraction* (Qiagen).

3.2.5. Secuenciación de DNA

La secuenciación cíclica directa se realizó empleando el método enzimático de terminación de cadena de DNA por incorporación de dideoxinucleótidos trifosfato (ddNTPs) descrito por Sanger et al., 1977. Las reacciones se llevaron a cabo en la unidad de genómica del Parque Científico de Madrid (Campus de Cantoblanco, Madrid) junto con oligonucleótidos sintéticos no fluorescentes y utilizando el kit

BigDye™ Terminator v3.1 Cycle Sequencing de Applied Biosystems, siguiendo el protocolo suministrado por el proveedor, los productos obtenidos fueron resueltos en un secuenciador automático *ABI* Prism® *3730* de Applied Biosystems.

En las reacciones de secuenciación de productos amplificados por PCR se emplearon 300 ng de DNA y para la secuenciación de construcciones plasmídicas se empleó una cantidad de 300-500 ng de DNA. El oligo utilizado para secuenciar estaba a 5 µM. La secuenciación de productos amplificados por PCR se llevó a cabo con oligonucleótidos de igual secuencia a los empleados en las reacciones de amplificación.

3.2.6. Mutagénesis dirigida

La mutagénesis dirigida mediante el proceso de PCR se realizó con el kit *Quickchange™ Site Directed Mutagenesis* de Stratagene.

3.2.7. Clonajes

3.2.7.1. Clonaje en el vector pSPL3. Minigenes

La amplificación por PCR de las secuencias genómicas a estudiar en los genes *PCCA, PCCB* y *MMAB* se llevó a cabo a partir de DNA genómico de controles y de los pacientes portadores de los cambios nucleotídicos. Los productos de estas amplificaciones se clonaron en el vector *TOPO TA version 2.1* (Invitrogen). Se transformaron bacterias *E.coli XL1-Blue* (Stratagene) y se seleccionaron los clones positivos, mediante escisión con el enzima de restricción *EcoRI*. Una vez liberado el fragmento introducido en cada caso se clonó en el vector de *splicing* pSPL3 (Life Technologies) (Figura 8), digerido previamente con el mismo enzima, utilizando el kit *Rapid DNA ligation* de Roche. En algunos casos, el vector pSPL3 digerido se desfosforiló previamente con TSAP *(Thermostable Alkaline Phosphatase)* de Promega. Las construcciones normales y mutantes con orientación correcta, se seleccionaron por secuenciación cíclica directa.

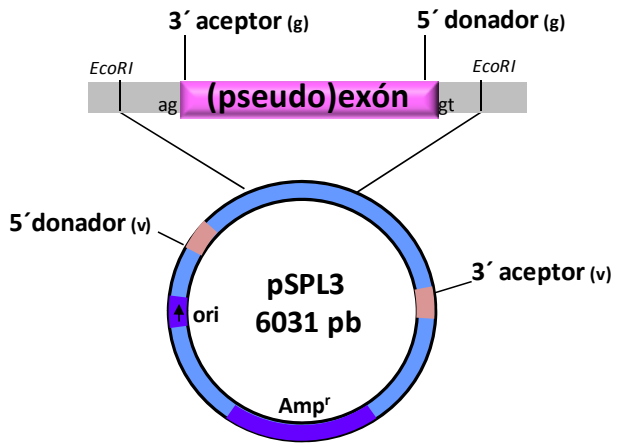

Figura 8. Esquema del vector pSPL3. Se muestran los sitios 3´ aceptor y 5´ donador de *splicing* de la secuencia genómica (g) de estudio, así como del vector (v). Amp^r: gen de resistencia a ampicilina.

3.2.7.2. Clonaje de los cDNA *PCCA* y *PCCB* para ensayos de síntesis *in vitro* de las proteínas PCCA y PCCB

Para expresar *in vitro* la proteína **PCCA**, se utilizó el vector de transcripción *in vitro* pGEM-11Zf(+) (Richard et al., 1999), que contiene el cDNA de *PCCA* (2184 pb). Sobre éste se introdujeron las **mutaciones p.R313*, p.Q371*, p.Y380*, p.S562* y p.Q611*,** por mutagénesis dirigida.

Para la proteína **PCCB** se utilizaron diferentes construcciones. El cDNA de *PCCB* (1617pb) se amplificó utilizando como molde el vector pRcCMVB52, del que disponíamos en el laboratorio, mediante la utilización de un oligo *sense* que introduce las secuencia correspondientes al promotor T7 y al sitio de iniciación de la traducción en eucariotas *(Kozak),* inmediatamente anteriores al codón de inicio ATG, de secuencia: 5'-TAATACGACTCACTATAGGAACAGCCACCATGGCGGCGGCATTACGGGTG-3´. Este producto amplificado se clonó en el vector *TOPO TA version 2.1* (Invitrogen). Las mutaciones **p.Q139*, p.Y314*, p.R514* y p.W531*** se introdujeron después en esta construcción, por mutagénesis dirigida.

Para analizar los mutantes PCCB: **p.G94*, p.R111* y p.R113***, se realizó una construcción híbrida PCCA-PCCB por su dificultad para ser detectadas eficientemente, debido al pequeño tamaño de las proteínas truncadas resultantes y su bajo contenido en metioninas y cisteínas que pudieran ser marcadas con el isótopo radiactivo. El cDNA de *PCCB* se amplificó del codón 1 al 116 mediante oligos que introdujeron un sitio de restricción para la enzima *StuI* y se clonó en el vector pGEM-PCCA, digerido con la misma enzima, que corta después del codón 196 en el cDNA de *PCCA*. De manera que, la construcción final codifica para una proteína que contiene los 196 primeros aminoácidos de la proteína PCCA, seguidos en fase con los primeros 116 aminoácidos de PCCB y después con los aminoácidos del 197 hasta el codón de parada de PCCA, con un peso molecular total de aproximadamente 92KDa (Figura 9).

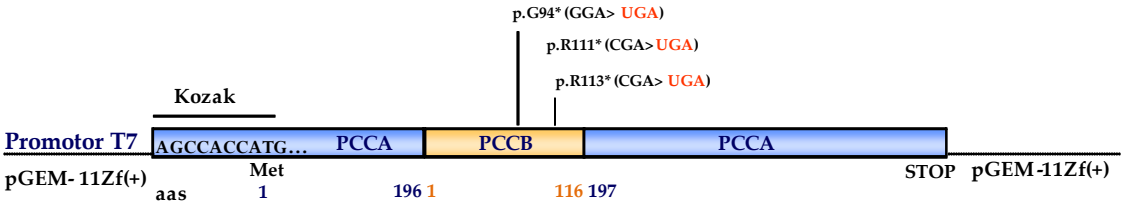

Figura 9. Esquema de la construcción híbrida PCCA-PCCB diseñada, donde queda clonado el cDNA de *PCCB* con las mutaciones p.G94*, p.R111* y p.R113*, en el vector pGEM-PCCA, para su análisis por transcripción-traducción acopladas (TNT).

3.2.8. *Multiplex Ligation Probe Amplification* (MLPA)

Para el análisis por MLPA, se utilizaron 250 ng de DNA extraídos de fibroblastos de cada uno de los pacientes PCCA deficientes con genotipo incompleto, junto con dos controles. El análisis se llevó a cabo tras hibridación de las sondas con cada uno de los exones, posterior ligación de cada una de las partes de las sondas y amplificación de los fragmentos generados, de acuerdo a las instrucciones proporcionadas por el fabricante y utilizando el kit *MLPA SALSA P278 PCCA* de MRC Holland (www.mrc-holland.com). Por último, 2 µl de los productos de PCR fueron mezclados con 0,2 µl del estándar de pesos moleculares marcados con ROX (LIZ-500), separados mediante el secuenciador capilar *ABI PRISM 3730 Genetic Analyzer* (Applied Biosystems) y analizadas posteriormente mediante el *software Peakscanner* (Applied Biosystems) por visualización de los distintos picos que corresponden a cada uno de los exones del gen *PCCA* reconocidos por tener cada uno un tamaño específico. Para la normalización, la señal de cada sonda se calcula dividiendo la medida del área de cada pico entre la suma del área de todos los picos de la muestra. El *ratio* de cada sonda se normaliza a la media obtenida entre 2 controles. Se considera que hay deleciones en un exón cuando el *ratio* es menor de 0,65; entre 0,35 y 0,65 si hay deleciones en heterocigosis y aproximadamente 0 si hay deleciones en homocigosis. Todas las deleciones sospechosas son confirmadas por un segundo análisis por MLPA o análisis por PCR larga.

3.2.9. Síntesis *in vitro* de las proteínas PCCA y PCCB

La expresión *in vitro* de las proteínas PCCA y PCCB se realizó empleando el sistema comercial *TNT-T7 Quick coupled transcription/rabbit reticulocyte translation system* de Promega. Cada reacción se desarrolló a 30°C durante 90 minutos conteniendo 500-750 ng del plásmido o 1,25 µg del producto de amplificación, 10 µl de *TNT T7 Quick Master Mix* y 1µl de L-[S^{35}]-metionina-cisteina.

Para ensayar el efecto de los compuestos supresores de la terminación de la traducción, se añadieron distintas concentraciones de G418 (0,1-2,5 µg/mL), gentamicina sulfato (1,25-20 µg/mL) y PTC124 (0,03-10 µM) a la reacción de síntesis. La muestra (2-4 µl) fue desnaturalizada y analizada posteriormente por SDS-PAGE. Las proteínas marcadas radiactivamente fueron visualizadas por fluorografía utilizando el reactivo *Amplify* y mediante exposición toda la noche a -70°C. Para analizar la densidad óptica de las bandas resultantes correspondientes a los niveles de proteína obtenidos, se utilizó el programa *Quantity One 4.3.1* (Bio-Rad). Los niveles de proteína completa sintetizada fueron calculados como la cantidad de proteína completa producida, en relación a la suma de las proteínas truncada y completa, y expresada en porcentaje.

3.2.10. Cultivo celular, transfecciones y tratamientos

Los cultivos primarios de fibroblastos procedentes de biopsia de piel, tanto de individuos control como de pacientes, así como células establecidas de hepatoma (línea Hep3B de hepatoma humano) y HEK293T se han cultivado en botellas de 25 ó 75 cm^2 ó placas estandarizadas de 6 pocillos (P6). Han sido cultivadas a 37°C en una atmósfera de humedad relativa del 95% y CO_2 5%, utilizando como medio de cultivo medio mínimo esencial de Eagle (MEM) suplementado con glutamina 2mM, suero fetal bovino (FBS) al 10% (v/v), penicilina 100U/mL y estreptomicina 100µg/mL. Las células fueron recogidas con una solución de tripsina 0,25% y EDTA 0,02% y sedimentadas mediante centrifugación.

- Los experimentos de **<u>expresión de minigenes</u>** se llevaron a cabo cultivando 3 x 10^5 células de Hep3B o HEK293T en placas P6. Las transfecciones se llevaron a cabo en medio MEM completo, utilizando 6 µl de Jetpei (*Lipofectin® Reagent*, Invitrogen) y 1,5 µg de la construcción plasmídica pSPL3 normal o mutante. Las células fueron recogidas a las 24 o 48 horas. Para el estudio posterior del perfil transcripcional se utilizaron los oligonucleótidos, SD6 y SA2, específicos del vector pSPL3:

  - **SD6 (*sense*):** 5´-TCTGAGTCACCTGGACAACC-3´
  - **SA2 (*antisense*):** 5´-ATCTCAGTGGTATTTGTGAGC-3´

- Para el **<u>análisis *in vitro* de mutaciones de cambio de aminoácido</u>** se utilizaron las líneas establecidas de los fibroblastos procedentes de las líneas **5626-T** o **14046-T** deficientes en PCCA o PCCB, respectivamente (Clavero et al., 2002; Perez-Cerda et al., 2003) y los vectores pCMVA45-12 y pRcCMVB52 que codifican para las proteínas PCCA y PCCB, respectivamente, en los que se introdujeron, por mutagénesis dirigida, las mutaciones a analizar. La transfección se llevó a cabo empleando *Lipofectamine™ LTX* (Invitrogen) y medio libre de suero *OptiMEM®-1* (GibcoBRL), siguiendo las instrucciones del proveedor, cotransfectando 2 µg de las construcciones PCCA o PCCB mutantes junto con 2 µg de los vectores PCCB y PCCA *wildtype,* respectivamente para obtener la máxima expresión como ha sido descrito con anterioridad (Clavero et al., 2002; Perez-Cerda et al., 2003). Las células fueron recogidas, 72 horas después por tripsinización, para medir la actividad PCC.

- Para ensayar el efecto de la **<u>sobreexpresión de factores de *splicing*</u>** se cotransfectaron 3 x 10^5 células de Hep3B con 1,5 µg del minigen de estudio y hasta 4 µg de los vectores portadores de los distintos factores de *splicing* y proteínas SR: U2AF35, U2AF65, SRp40, SRp55, SC35 y SF2/ASF, y el vector que codifica para la parte RNA de la ribonucleoproteína U1 (U1snRNA), utilizando 8 µl de *Jetpei Lipofectin® Reagent* (Invitrogen). Las células fueron recogidas a las 48 o 72 horas.

En otros experimentos, los fibroblastos de los pacientes portadores de la mutación c.1209+3A>G (*PCCA*), 3-4x10^5 cultivados en P6 o 1,6-1,8x10^6 en botellas de 75 cm^2, se transfectaron con 0,5- 4 µg o 7,5 y 30 µg, respectivamente, de los distintos vectores modificados de U1, empleando *Lipofectamine™ LTX* (Invitrogen) y medio libre de suero *OptiMEM®-1* (GibcoBRL) y siguiendo las instrucciones del proveedor. En otros

casos, 4-5x10^5 fibroblastos se transfectaron con 2 y 4 µg de los vectores utilizando el kit *Amaxa® Human Dermal Nucleofector* según las instrucciones recomendadas por el proveedor. Paralelamente, se transfectó un plásmido control que codificaba para GFP para comprobar la eficiencia de la nucleofección que se analizó mediante citometría de flujo y microscopía de fluorescencia. Las células fueron recogidas a las 24, 48, 72 ó 96 horas según cada caso.

- Para el **silenciamiento del gen *SRP40***, se cultivaron 1,5 x 10^5 células de hepatoma (Hep3B) en placas estandarizadas P6 y se añadió a las 24 horas ON-*TARGETplus SMARTpool siRNA* contra *SRP40* (Dharmacon) 100nM junto con 6 ó 10 µl de *Lipofectamine™ 2000* (Invitrogen) y medio libre de suero *OptiMEM®-1* (GibcoBRL), siguiendo las instrucciones del proveedor.

- Para ensayar el efecto producido por los **oligonucleótidos antisentido tipo morfolinos (AONs)**, 4 x 10^5 fibroblastos de piel del paciente fueron cultivados en placas P6 o 6 x 10^5 en botellas de 25cm^2. Se añadieron los AONs 24 horas después de la siembra a una concentración final de 10, 20 y 30 µM. Para la transfección se utilizó *Endo-Porter* (Gene Tools) a una concentración final de 6 µM. El tiempo de cultivo tras la adición del *Endo-Porter* y los AONs fue de 48-72 horas.

En algunos casos, para rescatar transcritos aberrantes susceptibles a la degradación por el mecanismo NMD, los fibroblastos de los pacientes fueron tratados con cicloheximida (Sigma) a 0,5-0,75 mg/mL, 6 horas antes de ser recogidos.

- Para ensayar el **tratamiento con compuestos supresores de la terminación de la traducción**, 2x10^5 fibroblastos de los pacientes portadores de las diferentes mutaciones sin sentido fueron cultivados en placas P6. Distintas concentraciones de los diferentes compuestos supresores, se añadieron 24 horas después, en medio sin antibiótico: gentamicna sulfato (Sigma Aldrich) (500-750 µg/mL), G418 (Gibco) (50-75µg/mL) y PTC124 (Selleckchem Co) (5-15µM). Para los tratamientos con gentamicina y G418 los compuestos, junto con medio fresco, fueron reemplazados a las 72h y las células se recogieron a los 5 días del tratamiento. Para el tratamiento con PTC124 las células se recogieron a las 72h.

Para los experimentos en los que se utilizaron inhibidores del NMD, las células se cultivaron en las mismas condiciones descritas y se añadió wortmanina (Sigma Aldrich) (5-20µM) o cafeína (Sigma Aldrich) (7,5mM), 8h antes de ser recogidas.

3.2.11. Actividad propionil-CoA carboxilasa

La medida de la actividad propionil-CoA carboxilasa se realizó en extracto de fibroblastos cultivados que fueron recogidos por tripsinización y resuspendidos en un *buffer* Tris-HCl 20mM pH 8, glutation 0,025 % (p/v). Posteriormente se sometieron a tres ciclos sucesivos de congelación/descongelación en N_2 líquido.

La determinación de las actividades enzimáticas PCC y MCC (utilizado como control intraensayo) se realizó siguiendo el protocolo descrito por Suormala et al., 1985. Cada ensayo se llevó a cabo en un volumen final de 200 µl, en la siguiente mezcla de reacción: 20 µmoles Tris-HCl pH 8.0, 0,15 µmoles DTT, 0,628 µmoles Na_2-ATP.$3H_2O$, 1,2 µmoles $MgCl_2.6H_2O$, 20 µmoles KCl, 5% (v/v) Triton X-100, 0,2 µmoles propionil-CoA o 0,2 µmoles 3-metilcrotonil-CoA y 8 µmoles $NaHCO_3$. Se utilizó el isótopo radiactivo $NaH[^{14}C]O_3$ (Perkin Elmer) con una actividad de 44,8 mCi/mmol.

La reacción enzimática comenzó al añadir 30 µl del extracto proteico celular y se llevó a cabo a 30°C durante 20 minutos. La parada de la reacción enzimática tuvo lugar por la adición de 140 µl de TCA 30% (p/v) y las proteínas precipitadas se separaron por centrifugación a 14000 rpm durante 15 min. El sobrenadante fue transferido a un vial de centelleo y sometido a evaporación a temperatura ambiente, siendo posteriormente resuspendido en 500 µl de agua miliQ. Posteriormente, se añadieron a cada vial 5 ml de líquido de centelleo *Optiphase Hisafe 2* (Perkin Elmer) y se procedió a la determinación de cpm en el contador 1209 Rackbeta Liquid Scintillation Counter (Wallac).

La actividad específica residual PCC se expresó en unidades de pmoles $[^{14}C]O_2$ incorporado/min/mg proteína total. La cuantificación de proteínas totales en los extractos proteicos se llevó a cabo según el método descrito por Lowry et al., 1951.

3.2.12. Aislamiento de mitocondrias, electroforesis y detección de la proteína PCCA

Para la detección de la proteína PCCA, la extracción de mitocondrias de fibroblastos de los pacientes se realizó por homogenización y centrifugación diferencial a 4°C en una solución 25mM sacarosa, 10mM Tris-HCl, 2mM EDTA pH 7,4 e inhibidor de proteasas *Complete Mini EDTA-free Protease Inhibitor Cocktail Tablets* (Roche Applied Science), siguiendo el protocolo descrito por Bergman et al., 1989 y posteriormente, resuspendidas en 20-50 µl de una solución 25mM sacarosa, 10mM Tris-HCl, 2mM EDTA pH 7,4. Alternativamente, la extracción de mitocondrias se llevó a cabo a partir de los fibroblastos de los pacientes utilizando el *MACS® Mitochondria Isolation kit human* de Miltenyi Biotec. La determinación de la concentración de proteínas se llevó cabo por el método de Bradford (Bradford, 1976) empleando el reactivo *Bio-Rad Protein Assay* (Bio-Rad). La misma cantidad (~25-30 µg) de las fracciones mitocondriales fue sometida a electroforesis en gel de poliacrilamida al 10%, empleando una solución Tris 25mM, 250 mM glicina, 0,1% (p/v) SDS.

Tras la electroforesis, las proteínas procedentes de las fracciones mitocondriales fueron transferidas a membranas de PVDF (*Immobilon™-P*, Millipore) según el protocolo descrito por Baumgartner et al., 2001. La transferencia se realizó empleando una solución 24 mM Tris base, 192 mM glicina, 20% metanol según el protocolo descrito por Towbin et al., 1979, en el aparato *Mini Trans-Blot Transfer Cell* (Bio-Rad). Una vez finalizada, la membrana fue sometida a tres lavados de 5-10 minutos en PBS y bloqueada durante al menos una hora en una solución PBS-BSA 2% (p/v). Una vez

bloqueada la membrana, se incubó durante 1 hora con una solución de PBS/BSA 0,3 % (p/v) a la que se había añadido avidina conjugada con fosfatasa alcalina (Pierce) en una proporción 1:1000. Tras tres lavados sucesivos de 5 min en PBS, se procedió al revelado de la membrana por adición del sustrato *1-Step™ NBT/BCIP* de la firma comercial Pierce y posterior desarrollo colorimétrico.

3.2.13. Soporte informático y análisis *in sílico*.

Las secuencias tanto de los cDNAs como de los DNAs genómicos de los genes *PCCA, PCCB, MMAB* y *SPR* fueron obtenidas mediante búsqueda informática en las bases de datos públicas *Ensembl* (http://www.ensembl.org/index.html) y *GenBank* de NCBI (http://www.ncbi.nih.gov/). Las mutaciones reportadas en cada gen se consultaron en la base de datos HGMD (*Human Gene Mutation Database® Professional release* 2011.4, www.hgmd.cf.ac.uk) y para su nomenclatura se han seguido las recomendaciones del HGVS (*Human Genome Variation Society*, http://www.hgvs.org/).

Las secuencias de las proteínas se obtuvieron en la base de datos PDB (*Protein Data Bank*) de SWISS-PROT (http://www.expasy.org/sprot/).

Para la búsqueda de secuencias homólogas en las bases de datos públicas se utilizaron programas de BLAST (http://www.ncbi.nlm.nih.gov/BLAST/).

El procesamiento y análisis de secuencias de DNA se llevó a cabo con el programa *Chromas 1.45* (Griffith University, Australia).

Para el diseño de oligos se utilizó el programa *Primer3* (v. 0.4.0) (http://frodo.wi.mit.edu/).

La búsqueda de dianas de restricción en los fragmentos amplificados de los genes *PCCA* y *PCCB* controles y portadores del cambio nucleotídico se realizó mediante el programa *Prophet 5.0* y *NEBcutter V2.0* (New England Biolabs-http://tools.neb.com/NEBcutter2/).

La localización de posibles ESEs (*exonic splicing enhancers*) se llevó a cabo con el programa informático de predicción de secuencias de reconocimiento de factores de *splicing* ESE Finder version 3.0 (http://rulai.cshl.edu/tools/ESE) (Cartegni et al., 2003) y HSFinder v2.4 (http://www.umd.be/HSF/) (Desmet et al., 2009). También, se ha comprobado cómo varían los valores de las secuencias de *splicing* con los cambios nucleotídicos encontrados, mediante programas de predicción de sitios conservados de *splicing,* como el servidor BGDP (*Berkeley Drosophila Genome Project*-http://www.fruitfly.org/seq_tools/splice) (Baralle and Baralle, 2005) y el programa AST (*Analyzer Splice Tool*-http://ibis.tau.ac.il/ssat/SpliceSiteFrame.htm).

Para la predicción de la posible patogenicidad y el efecto funcional de las variaciones nucleotídicas de cambio de aminoácido se utilizaron los *softwares* de

predicción informática PolyPhen-2 (*Polymorphism Phenotyping v2*- http://genetics.bwh.harvard.edu/pph2/) y SIFT (http://sift.bii.a-star.edu.sg/).

Los p-valores se han estimado mediante el análisis estadístico realizado con el *software* SPSS®, efectuando un análisis de varianza (ANOVA) de un factor con la corrección *post-hoc* de *Bonferroni.*

4. RESULTADOS

4.1. CARACTERIZACIÓN DE CNVs EN EL GEN *PCCA* RESPONSABLES DE ACIDEMIA PROPIÓNICA

En el laboratorio se reciben muestras de pacientes con acidemia propiónica de todo el mundo para su diagnóstico molecular. Hasta el momento, 80 pacientes diagnosticados corresponden a defectos en el gen *PCCA* y 110 a defectos en el gen *PCCB*.

El porcentaje de mutaciones identificadas a nivel genómico, al comienzo de este estudio, eran del 99,9% para el gen *PCCB,* pero sólo del 78% para el gen *PCCA*, siendo en ambos casos, en su mayoría, mutaciones de cambio de aminoácido.

Dentro de los casos sin caracterizar en el gen *PCCA* se detectó, en cDNA, la exclusión de determinados exones, como los exones 3 y 4, el exón 23, los exones 13 y 14 y los exones del 13 al 20. Tras realizar el análisis en DNA genómico, se observó en los pacientes homocigotos la ausencia de amplificación del fragmento correspondiente a dichos exones, mientras que en heterocigotos, la amplificación y secuenciación fueron normales. Esto llevó a la sospecha de deleciones a nivel genómico. Tras esta sospecha, se analizó el número de copias de cada fragmento exónico mediante *Multiplex Ligation Probe Amplification* (MLPA) con un ensayo desarrollado a medida en colaboración con *R. Vijzelaar (MRC Holland,)* en el que se incluyeron un total de 20 pacientes entre los que se incluyen aquellos en los que, por el análisis en cDNA, se había visto la exclusión de alguno de los exones, así como pacientes en los que sólo se había identificado una mutación en uno de los alelos.

Los resultados revelaron la existencia de CNVs (en concreto, deleciones) en 18 pacientes, 10 de ellos en homocigosis y 8 en heterocigosis, tal y como se observó en los electroforegramas (Figura 10) y en la cuantificación del *ratio* relativo a la señal de cada una de las sondas correspondientes a cada exón, en comparación con muestras control. Los resultados se muestran en la Tabla 1. Según estos datos, hay dos deleciones recurrentes, la de los exones 3 y 4 que se detectó en 13 alelos (5 pacientes homocigotos y 3 heterocigotos) y la deleción del exón 23 que se detectó en 9 alelos (4 pacientes homocigotos y uno heterocigoto). El resto de las deleciones identificadas sólo se encontraron en un alelo cada una.

Para aquellos casos en los que se disponía de muestras de los padres, se confirmó, por MLPA, la herencia mendeliana de las deleciones.

En total se detectaron 28 alelos independientes con grandes deleciones, correspondientes a una frecuencia del 21,3% del total de alelos mutados en el gen *PCCA*, en una muestra de pacientes genotipados en el laboratorio.

Tabla 1. Deleciones identificadas tras el análisis del cDNA, gDNA y MLPA.

Deleción exónica	Cambio en cDNA	Efecto predecible	Mutación en gDNA	Nº alelos	Origen	Frecuencia relativa (%)*
Δexones 3-4	r.184_300del	p.T62_S100del39	c.184-558del4779	11	Italia, Turquia, Grecia, EE.UU.	8,3
Δexón 23	r.2041_2118del	p.V681_A706del26	c.2041-2924del3889	9	Países árabes	6,8
Δexones 3-4	r.184_300del	p.T62_S100del39	c.184-727del8860	2	Malasia	1,5
Δexones 13-14	r.1066_1284del	p.V356_G428del73	c.1066-?_1284+?del	2	Líbano	1,5
Δexón 1	-	-	c.1-?_105+?del	1	Italia	0,8
Δexones 17-18	r.1430_1643del	p.G477fs	c.1430-?_1643+?del	1	Español	0,8
Δexones 15-19	r.1285_1746del	p.V429_S582del154	c.1285-?_1746+?del	1	Alemania	0,8
Δexones 13-20	r.1066_1845del	p.V356_Q615del260	c.1066-?_1845+?del	1	EE.UU.	0,8

* calculada en relación a 132 alelos *PCCA* analizados en el laboratorio.

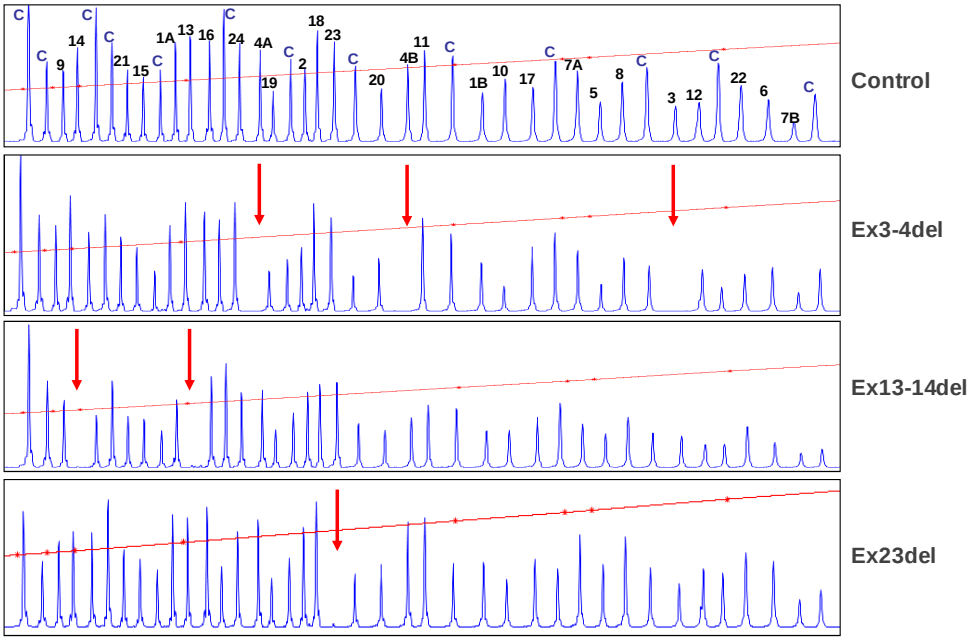

Figura 10. Electroforegramas obtenidos en el análisis por MLPA para un control y distintos pacientes con deleciones en homocigosis. Cada pico representa un exón del gen *PCCA* (indicado con su número) o una sonda control (C). Eje x: tamaño del fragmento, eje y: intensidad de fluorescencia. Las flechas rojas indican los exones delecionados, tal y como revela la ausencia del pico correspondiente. Los exones 1, 4 y 7 son identificados por dos sondas diferentes.

Los puntos de ruptura cromosómicos de las dos deleciones más frecuentes, citadas anteriormente, se analizaron mediante PCR larga y paseo cromosómico (*chromosomal walking*). Para ello, se ha utilizado como molde el DNA genómico de pacientes homocigotos para estas deleciones. La secuenciación a lo largo de los intrones se realizó mediante la utilización de distintos oligos, que fueron diseñados, específicamente, teniendo en cuenta que no hibridasen con secuencias repetidas, utilizando el programa *Repeatmasker*, hasta encontrar la secuencia de ruptura.

En concreto, para caracterizar la **deleción de los exones 3 y 4** se diseñaron oligos que hibridaran en los intrones 2 y 4 de manera que amplificarían un fragmento de ~10 Kb. Como resultado, se obtuvo una banda de ~1Kb en uno de los pacientes y una banda de ~ 5Kb en el resto de los pacientes, lo que indicó que se originaban 2 tipos de deleciones diferentes de aproximadamente 9 y 5 Kb. En el momento de la incorporación a este estudio, ya se había caracterizado la primera deleción correspondiente a 8,7 Kb (c. 184-727del8860), de manera que se caracterizó la de 5 Kb, identificándose una deleción de 4779 nucleótidos con el dinucleótido CA a ambos lados de la deleción, nombrada como c.184-558del4779 o g.13853152_13857931del (de acuerdo al contig NT_ 009952.14) (Figura 11A).

La misma técnica se utilizó para caracterizar la **deleción del exón 23,** de manera que se utilizaron oligos que hibridaran con los intrones 22 y 23, que amplificarían un fragmento de ~14 Kb. El producto amplificado para pacientes homocigotos fue de ~10 Kb, por lo que se esperaría encontrar una deleción de ~4 Kb. Este producto fue secuenciado hasta encontrar el punto de ruptura, identificándose la deleción de 3889 pb, la cual presenta a ambos lados la secuencia GGC. Esta mutación fue nombrada como c.2041-2924del3889 o g.14266781_14270670del (contig NT_00952.14) (Figura 11B).

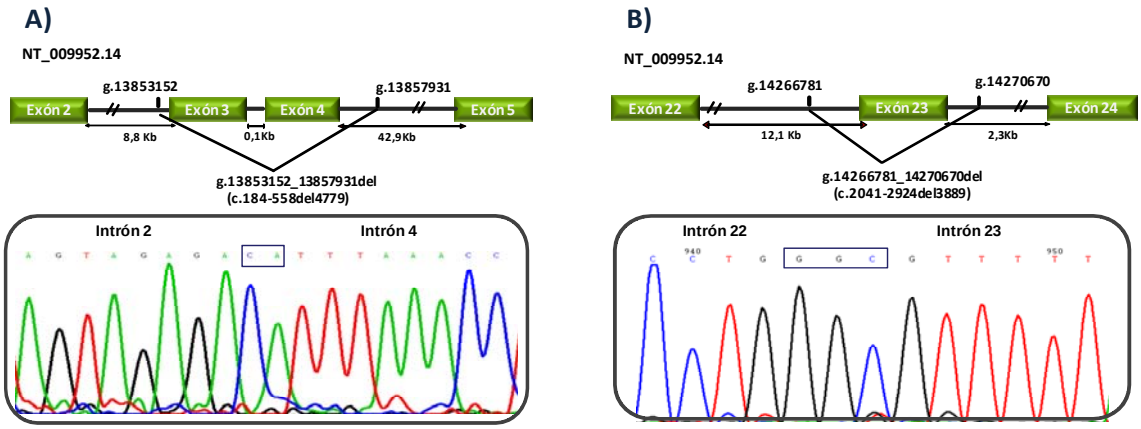

Figura 11. Esquema de la mutación c.184-618del4779 (A) y la mutación c.2041-2924del3889 (B) y análisis de los puntos de ruptura. Se muestra un esquema de las regiones exónicas implicadas (arriba) y el análisis por secuenciación del punto de ruptura (abajo), así como la secuencia repetida hallada a ambos lados (recuadro).

4.2. CARACTERIZACIÓN DE MUTACIONES SIN SENTIDO EN ACIDEMIA PROPIÓNICA Y EFECTO DE COMPUESTOS SUPRESORES DE LA TERMINACIÓN

En una cohorte de 190 pacientes con acidemia propiónica genotipados en el laboratorio (80 son *PCCA* y 110 *PCCB*), se han identificado 12 mutaciones sin sentido diferentes (Figura 12 y Tabla 2), 5 en el gen *PCCA* y 7 en el gen *PCCB*. Siete de ellas fueron descritas por primera vez: las mutaciones p.Q371* (c.111c>T), p.Y380* (c.1140C>A) y p.Q611* (c.1831C>T) en el gen *PCCA* y p.R111* (c.331C>T), p.Q139* (c.415C>T), p.Y314* (c.942C>A) y p.R514* (c.1540 C>T) en el gen *PCCB*, siendo cada una de ellas identificadas únicamente en un paciente.

Según datos del laboratorio junto con datos recogidos en el *Human Gene Mutation Database* (HGMD® *Professional release* 2011.4), las mutaciones sin sentido representan un porcentaje del 8 y 11% en los genes *PCCA* y *PCCB,* respectivamente. En ambos genes la mayoría de las mutaciones corresponden a la introducción del codón de parada UGA (Figura 12 y Tabla 2).

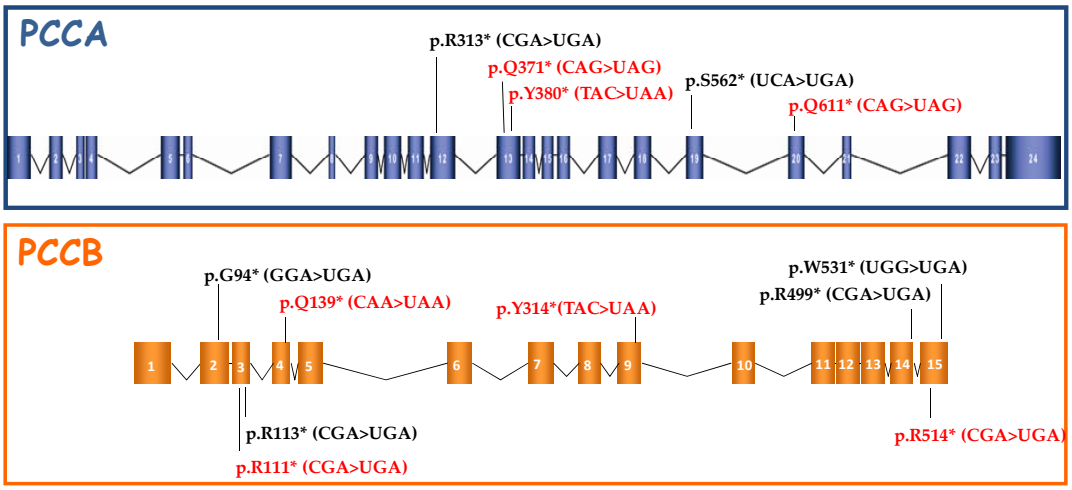

Figura 12. Esquema de la localización de las mutaciones sin sentido estudiadas, en los genes *PCCA* y *PCCB*. Se muestran todos los exones de los genes *PCCA* y *PCCB* en cajas y la localización exacta de cada mutación sin sentido, así como el cambio de codón originado en cada caso. Las mutaciones nuevas aparecen en rojo.

Tabla 2. Mutaciones sin sentido identificadas en una cohorte de 190 pacientes con acidemia propiónica.

Gen	Mutación	Cambio nucleótido	Localización	Codón de parada (4º nt)	Referencia
PCCA	p.R313*	c.937C>T	exón 12	UGA (A)	(Richard et al., 1999)
PCCA	p.Q371*	c.111C>T	exón 13	UAG (G)	este trabajo
PCCA	p.Y380*	c.1140C>A	exón 13	UAA (C)	este trabajo
PCCA	p.S562*	c.1685C>G	exón 19	UGA (G)	(Richard et al., 1999)
PCCA	p.Q611*	c.1831C>T	exón 20	UAG (A)	este trabajo
PCCB	p.G94*	c.280G>T	exón 2	UGA (A)	(Perez et al., 2003)
PCCB	p.R111*	c.331C>T	exón 3	UGA (G)	este trabajo
PCCB	p.R113*	c.415C>T	exón 3	UGA (G)	(Brosch et al., 2008)
PCCB	p.Q139*	c.415C>T	exón 4	UAA (A)	este trabajo
PCCB	p.Y314*	c.942C>T	exón 9	UAA (A)	este trabajo
PCCB	p.R514*	c.1540C>T	exón 15	UGA (A)	este trabajo
PCCB	p.W531*	c.1593G>A	exón 15	UGA (A)	(Rodriguez-Pombo et al., 1998)

4.2.1. Análisis *in vitro* de la supresión de la terminación de las mutaciones sin sentido en los genes *PCCA* y *PCCB*

Se ha analizado el efecto en la supresión de la terminación de los aminoglucósidos gentamicina y geneticina (G418) en los genes *PCCA* y *PCCB,* con las mutaciones sin sentido citadas anteriormente, mediante un ensayo de transcripción-traducción *in vitro* (TNT) en presencia de ^{35}S-Met-Cys. Para ello, se han utilizando distintas construcciones codificantes para las proteínas PCCA o PCCB en las que se han introducido, por mutagénesis dirigida, las mutaciones sin sentido a estudiar.

En ausencia de tratamiento, se observó la correcta síntesis de las distintas proteínas truncadas resultantes de la terminación de la traducción como consecuencia de la mutación, todas ellas del tamaño esperado, no observándose niveles detectables de proteína completa en ninguno de los casos. En alguna ocasión, se observaron bandas adicionales en los productos de traducción, presumiblemente debido bien a otros marcos abiertos de lectura presentes en el vector utilizado, o bien a productos de degradación de las proteínas sintetizadas.

Posteriormente, se ensayó, en todos los mutantes sin sentido descritos, la adición de dosis crecientes de gentamicina (2,5-15 µg/mL) y G418 (0,1-2,5 µg/mL) a la reacción de síntesis para monitorizar y cuantificar la recuperación de proteína completa. La mutación p.W531* en el gen *PCCB* produce una proteína truncada con una deleción de tan sólo 9 aminoácidos en el extremo carboxiterminal, por lo que no se pudo distinguir en tamaño de la proteína completa a la hora de querer observar recuperación o no tras el tratamiento. La figura 13 muestra las autorradiografías

resultantes para alguna de las mutaciones sin sentido tras la adición de los aminoglucósidos.

Tras analizar todas las demás mutaciones, tal y cómo se resume en la figura 14, al menos 8 de ellas fueron susceptibles a la supresión de la terminación mediada por los aminoglucósidos en diferente medida. Las mutaciones p.R313* y p.S562* en el gen *PCCA* fueron las que presentaron mayores niveles de recuperación, siendo ambas portadoras del codón de parada UGA que está descrito como el más susceptible a la supresión mediada por los aminoglucósidos (Manuvakhova et al., 2000). En general se pudo percibir un efecto dosis-dependiente, observándose un mayor nivel de recuperación en la mayoría de los mutantes con 15 µg/mL de gentamicina y 1 µg/mL de G418. A concentraciones mayores la síntesis de proteína total generalmente se inhibió, hecho que también ha sido observado previamente por otros autores (Lai et al., 2004)

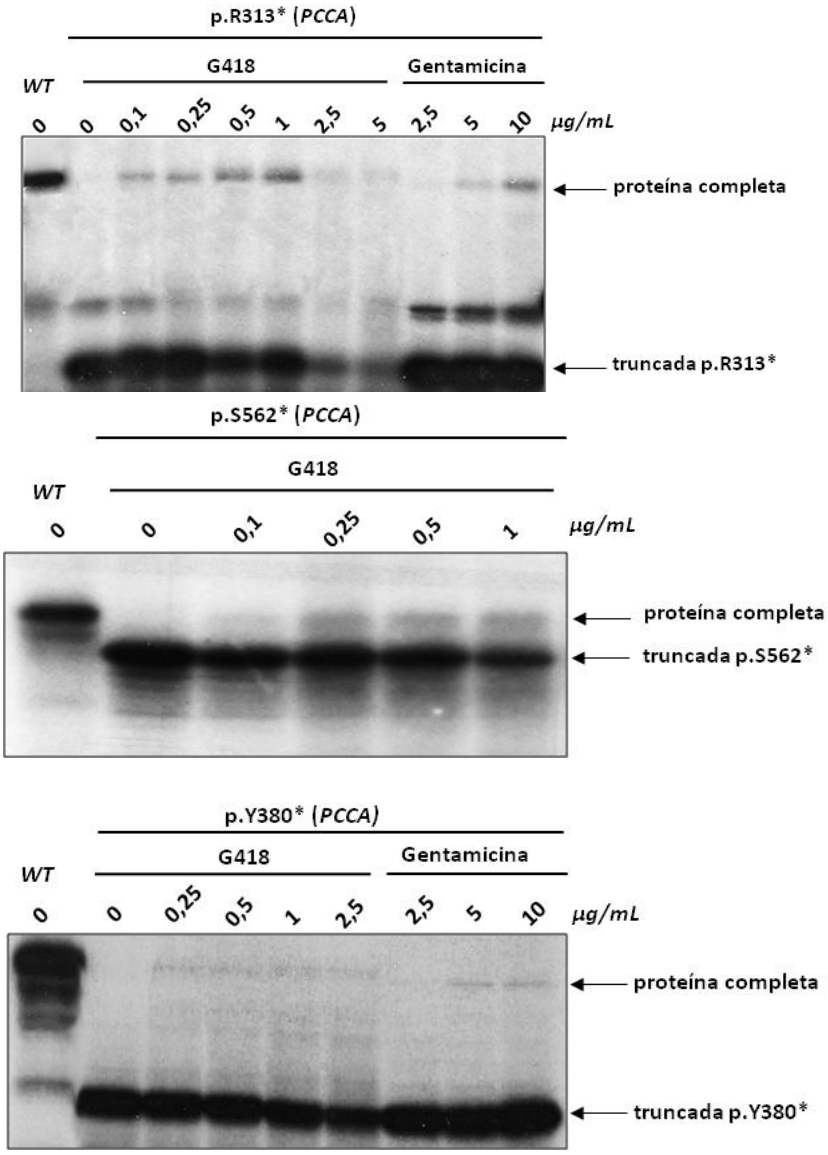

Figura 13. Efecto supresor de los aminoglucósidos en ensayos *in vitro* en el sistema TNT para las mutaciones p.R313*, p.S562* y p.Y380* en el gen *PCCA*.

También se probó la adición de ambos antibióticos juntos para comprobar si se producía un efecto sinérgico, tal y como ha sido descrito con anterioridad (Buck et al., 2009), pero no se obtuvieron mayores niveles de recuperación que los obtenidos con un solo antibiótico.

En los mutantes p.R113*, p.Q139* y p.R514* en el gen *PCCB* no se detectó recuperación de proteína completa en ninguna de las condiciones descritas.

También, se ensayó en el TNT la eficiencia en la supresión del compuesto PTC124 (*Ataluren®*). Se probó a concentraciones entre 0,03-10 µM (Welch et al., 2007) sobre las mutaciones p.R313* y p.S562* en el gen *PCCA* que fueron las más susceptibles a la supresión mediada por los antibióticos aminoglucósidos, pero no se observaron niveles detectables de recuperación de proteína completa.

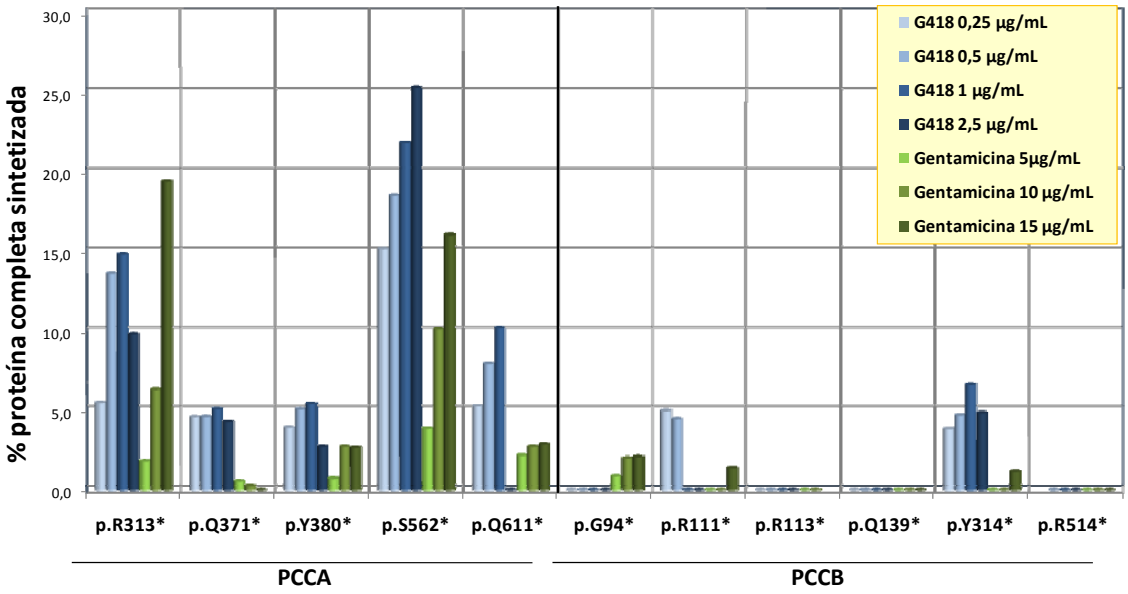

Figura 14. Representación de la estimación de proteína completa obtenida en el sistema de TNT tras el tratamiento de supresión con los aminoglucósidos gentamicina y geneticina para cada una de las mutaciones sin sentido presentes en los genes *PCCA* y *PCCB*. Los resultados mostrados son la media de al menos tres experimentos independientes.

4.2.2. Análisis *in silico* e *in vitro* de las mutaciones de cambio de aminoácido previsiblemente inducidas con la supresión de la terminación

Se ha descrito en la literatura, que los aminoácidos glutamina (Gln) y triptófano (Trp) son las inserciones más comunes en la supresión de la terminación de codones prematuros de parada. De manera que, en la mayoría de los casos la Gln se inserta si el codón de parada es UAG o UAA y el Trp si el codón es UGA (Brooks et al., 2006; Harrell et al., 2002; Nilsson and Ryden-Aulin, 2003).

Para analizar la potencialidad de la recuperación funcional de la supresión de las mutaciones sin sentido descritas en los pacientes con AP, el efecto funcional del

cambio de aminoácido predecible para cada una de ellas fue analizado *in silico* evaluando la patogenicidad de las distintas mutaciones de cambio de aminoácido, e *in vitro* midiendo la actividad PCC residual en un sistema de expresión eucariota, tal y como se describe en materiales y métodos (apartado 3.2.10).

Como se puede observar en la Tabla 3, donde se resumen estos resultados, la mayoría de las mutaciones sin sentido, previsiblemente, bien revierten al aminoácido original, o bien cambian a una mutación de cambio de aminoácido capaz de conservar parcialmente la función enzimática. La predicción *in silico* utilizando el programa *PolyPhen-2* predijo un efecto patogénico para la mayoría de las mutaciones que no se correspondía con los resultados obtenidos mediante el análisis de expresión. Sin embargo, mediante el programa SIFT obtuvimos mejor correlación de manera que la mayoría de las mutaciones con una actividad residual *in vitro* de >30% se predice que son benignas, no afectando significativamente a la función de la proteína. La única excepción fue la mutación p.S562W, que se predice como patogénica por ambos programas bioinformáticos, pero mostró alta actividad residual en el análisis de expresión *in vitro*.

Tabla 3. Análisis *in silico* e *in vitro* del efecto funcional de los cambios previsiblemente inducidos tras la supresión de la terminación para cada una de las mutaciones sin sentido descritas.

Gen	Mutación sin sentido	Cambio previsible	Efecto funcional		
			PolyPhen-2 (score)[a]	*SIFT (score)*[b]	Actividad residual *in vitro*[c]
PCCA	p.R313*	p.R313W	patogénica (1.000)	patogénica (0.00)	2,6±2,3
	p.Q371*	p.Q371Q	aminoácido original	aminoácido original	*wildtype*
	p.Y380*	p.Y380Q	benigna (0.025)	benigna (0.32)	34,5±2,9
	p.S562*	p.S562W	patogénica (0.494)	patogénica (0.03)	67,8±9,5
	p.Q611*	p.Q611Q	aminoácido original	aminoácido original	*wildtype*
PCCB	p.G94*	p.G94W	patogénica (0.999)	benigna (0.08)	38,4±2,5
	p.R111*	p.R111W	patogénica (0.976)	benigna (0.19)	49,7±3,6
	p.R113*	p.R113W	patogénica (0.989)	patogénica (0.02)	11,7±2,7
	p.Q139*	p.Q139Q	aminoácido original	aminoácido original	*wildtype*
	p.Y314*	p.Y314Q	patogénica (1.000)	patogénica (0.00)	10,0±0,6
	p.R514*	p.R514W	patogénica (0.992)	benigna (0.05)	67,1±5,9
	p.W531*	p.W531W	aminoácido original	aminoácido original	*wildtype*

[a] *PolyPhen-2*: http://genetics.bwh.harvard.edu/pph2/. Rango de *score* de 0 (neutral) a 1 (patogénico)
[b] *SIFT*: http://blocks.fhcrc.org/sift/SIFT.html. Rango de *score* de 0 (patogénico) a 1 (neutral)
[c] Relativo a niveles control

4.2.3. Análisis del efecto funcional de la supresión de la terminación de las mutaciones sin sentido en fibroblastos de los pacientes

De entre los pacientes portadores de las mutaciones sin sentido analizadas, en el laboratorio disponíamos de fibroblastos primarios de cinco de ellos, dos de ellos con mutaciones en el gen *PCCA*: P1 (p.R313*/p.R313*), P2 (p.S562*/p.S562*) y tres en el gen *PCCB*: P3 (p.W531*/p.G470fs), P4 (p.Y314*/p.E331*, la segunda mutación corresponde al cambio c.990dupT, no susceptible al tratamiento de supresión) y P5 (p.G94*/p.G470fs), en los que se analizó el efecto de los distintos compuestos supresores mediante cuantificación de la actividad enzimática PCC y medida de los niveles de mRNA.

Para ello, los fibroblastos de los pacientes se cultivaron en presencia de concentraciones crecientes de G418 (30-100 µg/mL) o gentamicina (300-1000 µg/mL) durante 5 días o del compuesto PTC124 (5-100 µM) durante 3 días.

Los resultados referentes a la actividad PCC se muestran en la figura 15. En los pacientes P1, P2, P3 y P5 se detectó un aumento de la actividad PCC (de hasta 50 veces) con varias concentraciones de los distintos compuestos supresores. En general, los mejores resultados se obtuvieron con G418 a 50-75 µg/mL y gentamicina a 300 µg/mL. Con el compuesto PTC124 se observó un efecto algo más moderado.

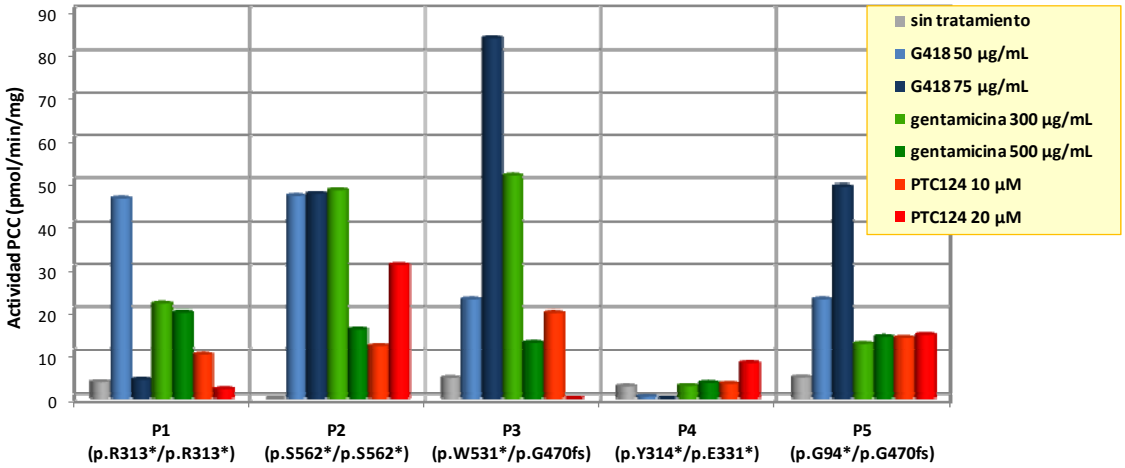

Figura 15. Efecto de los compuestos supresores sobre la actividad PCC en los fibroblastos de los pacientes portadores de mutaciones sin sentido. Los resultados son la media de al menos dos experimentos independientes por duplicado.

Se observó una gran variabilidad en los datos de actividad PCC recuperada en las líneas de los pacientes después del tratamiento con los distintos compuestos supresores (discusión: página 80), siendo amplio el rango de actividad recuperado para cada uno de los tratamientos (Tabla 4). El hecho de que para más de un experimento podamos medir un aumento detectable de actividad PCC en células tratadas indica un efecto positivo del tratamiento, aunque no se pueda alcanzar significancia estadística.

La actividad PCC recuperada se encontraba en un rango de entre 3-15%, respecto a los niveles de actividad de fibroblastos control tratados en paralelo en las mismas condiciones. En estos fibroblastos control, la gentamicina y PTC124 no tuvieron un efecto significativo en los niveles de actividad, mientras que con G418 se observó una reducción del 40-50% (Tabla 5). También se ensayó el tratamiento de los distintos compuestos a tiempos más prolongados no resultando en un aumento de los niveles en la actividad PCC.

Tabla 4. Media y rango de actividad PCC en fibroblastos de los pacientes tras el tratamiento con los compuestos supresores

Paciente/tratamiento	Media actividad PCC (pmol/min/mg)	Rango (pmol/min/mg)
P1 (p.R313*/p.R313*)		
sin tratamiento	3,7	0-11
G418 50 µg/mL	46,5	0-46
G418 75 µg/mL	4,2	0-71
gentamicina 300 µg/mL	22	26-62
gentamicina 500 µg/mL	19,7	0-11
PTC124 10 µM	10	7-14
PTC124 20 µM	2	0-6
P2 (p.S562*/pS562*)		
sin tratamiento	0	0
G418 50 µg/mL	47,1	0-226
G418 75 µg/mL	47,6	0-113
gentamicina 300 µg/mL	48,5	0-97
gentamicina 500 µg/mL	16	0-39
PTC124 10 µM	12	0-48
PTC124 20 µM	31	0-58
P3 (p.W531*/p.G70fs)		
sin tratamiento	4,7	0-11
G418 50 µg/mL	23	0-69
G418 75 µg/mL	83,7	20-197
gentamicina 300 µg/mL	51,75	0-131
gentamicina 500 µg/mL	12,8	0-45
PTC124 10 µM	19,7	0-41
PTC124 20 µM	0	0
P4 (p.Y314*/p.E331*)		
sin tratamiento	2,67	0-8
G418 50 µg/mL	0,5	0-2
G418 75 µg/mL	0	0
gentamicina 300 µg/mL	2,75	0-7
gentamicina 500 µg/mL	3,5	0-14
PTC124 10 µM	3,25	0-13
PTC124 20 µM	8,25	0-30
P5 (p.G94*/p.G470fs)		
sin tratamiento	4,8	0-11
G418 50 µg/mL	23	16-30
G418 75 µg/mL	49,3	43-54
gentamicina 300 µg/mL	12,5	0-25
gentamicina 500 µg/mL	14,25	0-23
PTC124 10 µM	14	0-33
PTC124 20 µM	14,7	12-18

Tabla 5. Media y rango de actividad PCC en fibroblastos controles tras el tratamiento con los compuestos supresores.

Paciente/tratamiento	Media actividad PCC (pmol/min/mg)	Rango (pmol/min/mg)
Fibroblastos control (experimento 1)		
sin tratamiento	1052	1011-1094
G418 50 µg/mL	645	628-662
G418 75 µg/mL	526	509-543
gentamicina 500 µg/mL	1041	1025-1057
PTC124 10 µM	n.d.	
PTC124 20 µM	n.d.	
Fibroblastos control (experimento 2)		
sin tratamiento	2204	1981-2427
G418 50 µg/mL	1252	1146-1359
G418 75 µg/mL	833	830-836
gentamicina 500 µg/mL	2703	1455-2951
PTC124 10 µM	2017	1956-2078
PTC124 20 µM	1231	1118-1344

n.d.= no determinado

Considerando que los mRNAs portadores de mutaciones sin sentido producen PTCs susceptibles a la degradación por el mecanismo NMD (Kuzmiak and Maquat, 2006), analizamos los niveles de transcritos *PCCA* o *PCCB* para cada uno de los pacientes portadores de mutaciones sin sentido, por qRT-PCR. Asimismo, medimos los niveles de mRNA tras los distintos tratamientos, ya que en la literatura se han descrito casos en los que se ha observado un aumento en los niveles de mRNA (Bellais et al., 2010), aunque en otros estudios no se han observado diferencias tras el tratamiento con aminoglucósidos (Buck et al., 2009; Hein et al., 2004; Popescu et al.). En ausencia de tratamiento todos los pacientes presentaban una disminución en los niveles de transcritos portadores de mutaciones sin sentido de entre el 1 y el 35% respecto a niveles controles. Tras el tratamiento de supresión no se observaron grandes variaciones en ninguno de los pacientes analizados, excepto en P2 (p.S562*/p.S562*) donde se observó un incremento en los niveles de transcritos tras el tratamiento con G418 a 50 y 75 µg/mL que coincide con una subida importante en los niveles de actividad (Figura 16).

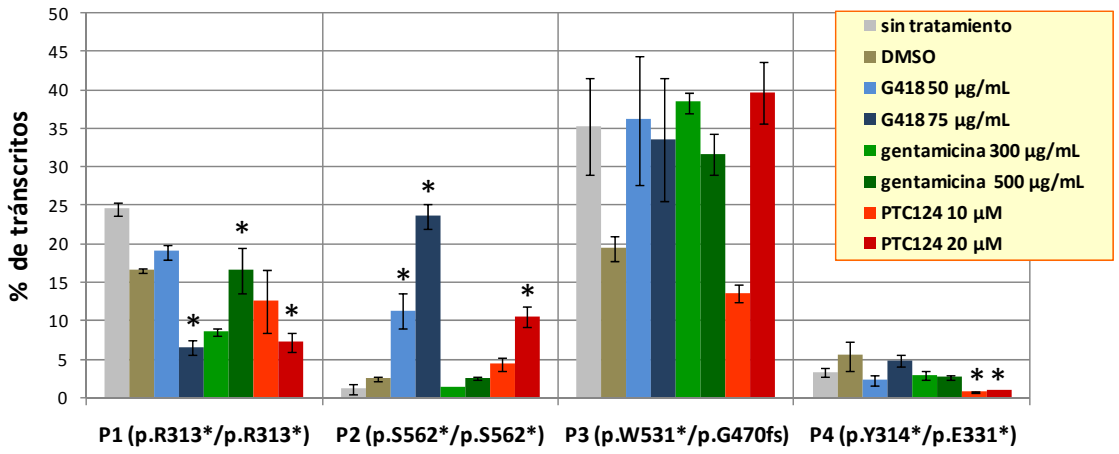

Figura 16. Cuantificación de los niveles de mRNA en fibroblastos de pacientes PCCA y PCCB portadores de mutaciones sin sentido tras el tratamiento con las distintas drogas supresoras. Se representa el porcentaje de transcritos portadores de mutaciones sin sentido obtenidos por qRT-PCR para cada una de los pacientes. Estos datos son los obtenidos de al menos 2 experimentos independientes por duplicado. *p-valor<0,05.

Ya que todos los pacientes presentaban niveles disminuidos de transcritos mutantes, presumiblemente debido al NMD, adicionalmente se ensayó el efecto de inhibidores del NMD para intentar rescatar transcritos mutantes, y estudiar si con ello, se incrementaban los niveles de actividad PCC recuperada tras el tratamiento con los compuestos supresores. Se utilizaron los inhibidores wortmanina y cafeína que producen la fosforilación de un factor esencial en el mecanismo NMD a la vez que mantienen la síntesis proteica (Rio Frio et al., 2008; Usuki et al., 2004). Para este ensayo se seleccionó el P2 homocigoto para la mutación p.S562* que predeciblemente revierte a una mutación de cambio de aminoácido con alta actividad residual (Tabla 3) y muestra cierta recuperación funcional tras el tratamiento con aminoglucósidos (Figura 15). Los fibroblastos de este paciente se incubaron con wortmanina 5-20 µM o cafeína 7,5 mM durante 8 horas. Con wortmanina a 20 µM se observó un aumento de entre 1,5-2 veces del nivel de transcritos mutantes, tal y como ha sido descrito en la literatura con anterioridad (Linde et al., 2007; Rio Frio et al., 2008). Sin embargo, cuando se ensayó la adición de aminoglucósidos después de las 8 horas de tratamiento con los inhibidores no se encontraron diferencias en los niveles de actividad PCC recuperados anteriormente con las células tratadas sólo con aminoglucósidos.

Los niveles de proteína PCCA o PCCB tras el tratamiento no pudieron ser ensayados en los fibroblastos de los pacientes por no disponer de anticuerpos comercialmente disponibles que fueran lo suficientemente sensibles.

4.3. CARACTERIZACIÓN DE MUTACIONES DE *SPLICING* EN DIFERENTES EMH Y ANÁLISIS DE TERAPIAS ESPECÍFICAS

Aproximadamente un 15% de las mutaciones puntuales asociadas a enfermedades genéticas humanas en general, y a EMH en particular, afectan al procesamiento del mRNA o *splicing.* En este trabajo se han analizado mutaciones que afectan al sitio 3´ o 5´ de *splicing* así como mutaciones intrónicas que activan la inserción de pseudoexones. El análisis de dichas mutaciones incluye la secuenciación y cuantificación de los transcritos en fibroblastos de pacientes; el análisis *in silico* para averiguar el efecto de la mutación sobre potenciadores, silenciadores de *splicing* y sitios de reconocimiento de factores de *splicing;* y el análisis funcional mediante minigenes, donde se clonan los exones afectados junto con las regiones intrónicas adyacentes, lo que permite estudiar las mutaciones de forma individual, especialmente relevante para pacientes heterocigotos.

4.3.1. Caracterización de mutaciones de *splicing*

4.3.1.1. Mutaciones que afectan al sitio 3´ aceptor o al sitio 5´ donador de *splicing*

Se realizó al análisis funcional de las siguientes mutaciones que afectan al sitio **3´ aceptor de *splicing*** (Tabla 6 y figura 17):

- La mutación **c.1091-11del6 (IVS10-11del6)**, identificada en el **gen *PCCB*** en un paciente con acidemia propiónica, que produce la deleción de 6 nucleótidos entre las posiciones -11 y -6 del intrón 10, acortando el tracto polipirimidínico (Rodriguez-Pombo et al., 1998).

- La mutación **c.394-1G>C (IVS4-1G>C)** que fue identificada en heterocigosis en el **gen *MMAB*** en un paciente diagnosticado con aciduria metilmalónica. En este paciente también se identificó la mutación c.290G>A que afecta al sitio 5´de *splicing,* la cual ha sido también analizada en este trabajo.

También se analizaron las mutaciones que afectan al sitio **5´ donador de *splicing*** (Tabla 7 y figura 18):

- La mutación **c.1209+3A>G (IVS13+3A>G)**, identificada en el **gen *PCCA***, en varios pacientes con acidemia propiónica (Desviat et al., 2006a).

- La mutación **c.290G>A**, localizada en el último nucleótido del exón 3 del **gen *MMAB*,** identificada en heterocigosis en un paciente diagnosticado con aciduria metilmalónica.

- La mutación **c.304G>T** localizada en el último nucleótido del exón 1 del **gen *SPR*.** Esta mutación fue identificada por primera vez en heterocigosis en tres hermanas con un cuadro clínico atípico, sin retraso cognitivo y con distinto grado de afectación, a

pesar de presentar el mismo genotipo, dos de ellas son prácticamente asintomáticas y la otra presenta fenotipo moderado. La segunda mutación, c.448A>G (p.R150G), ha sido expresada previamente y no presenta actividad, es funcionalmente nula (Bonafe et al., 2001b). Para el análisis por minigenes de la mutación c.304G>T se requirió la construcción de un exón híbrido formado por el exón 2 del gen *SPR*, que aportó su extremo 3' aceptor de *splicing,* fusionado al exón 1, que aportó el sitio 5' donador de *splicing* donde se localiza la mutación de estudio.

Para todas estas mutaciones, en la mayoría de los casos, los minigenes reproducen el efecto en la alteración del *splicing* asociado a la mutación que se observa en las células del paciente, lo que nos ha permitido utilizar, en algunos casos, dichos minigenes como modelos celulares de *splicing* para el ensayo de diferentes aproximaciones terapéuticas con el objetivo de rescatar transcritos correctamente procesados. En otros casos, en los que no se disponía de células del paciente, como es el caso de la mutación c.304G>T del gen *SPR*, el uso de minigenes ha permitido confirmar el defecto de *splicing* asociado a la mutación (Tablas 6 y 7) (Figuras 17 y 18).

Tabla 6. Mutaciones que afectan al sitio 3´de *splicing*

MUTACIÓN (gen)	Perfil transcripcional en fibroblastos	Estudio *in silico*	Minigenes
c.1091-11del6 *(PCCB)*	*Skipping* exón 11	Disminuye el *score* de 0,97 a 0,56	*Skipping* exón 11
c.394-1G>C *(MMAB)*	Activación sitio críptico y deleción de 6 pb del exón 5	Eliminación sitio 3' *splicing* Creación sitio de unión SRp55	*Skipping* exón 5

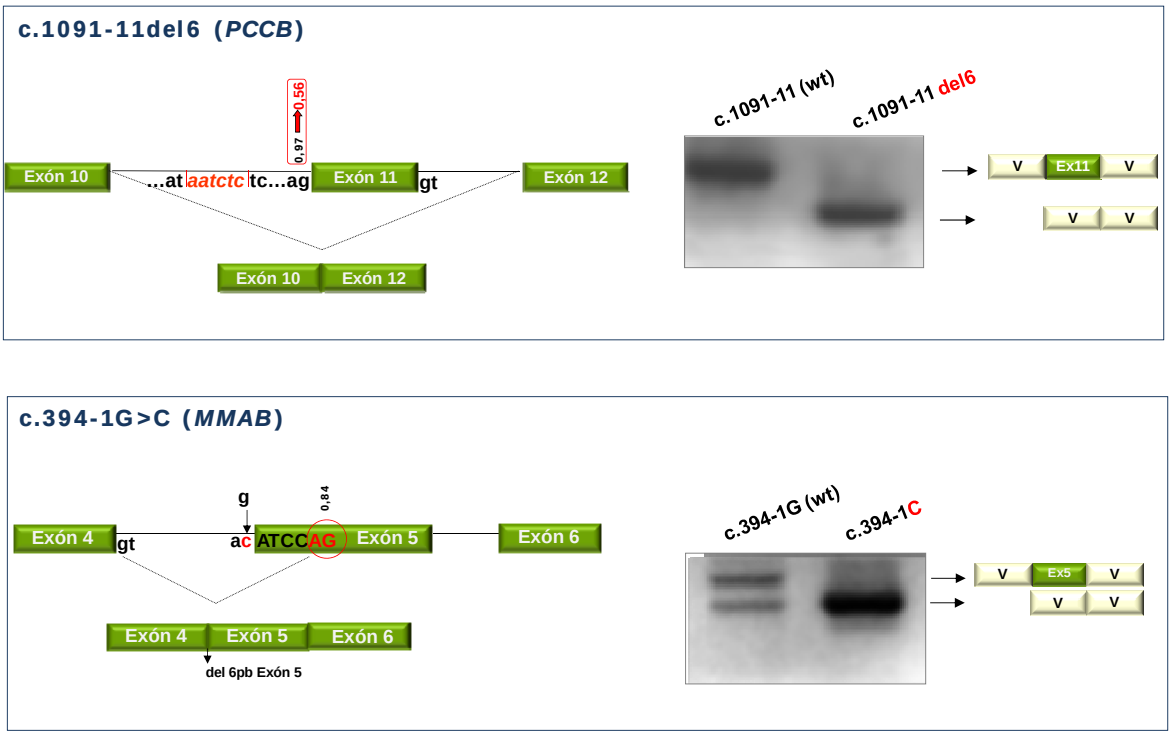

Figura 17. Análisis funcional de las mutaciones que afectan al sitio 3´de *splicing*. Se muestra, a la izquierda, una representación esquemática de la localización de la mutación, los valores *(scores)* de los sitios de *splicing* y el perfil transcripcional observado en los fibroblastos de los pacientes. A la derecha, se muestra el resultado del análisis de la mutación mediante minigenes y la representación esquemática de los transcritos obtenidos tras su caracterización por secuenciación. V: secuencias exónicas del vector.

Tabla 7. Mutaciones que afectan al sitio 5´de *splicing*

MUTACIÓN (gen)	Perfil transcripcional en fibroblastos	Estudio *in silico*	Minigenes
c.1209+3A>G (PCCA)	*Skipping* exón 13. 2-3% de transcritos normales	Disminuye el *score* de 79,4 a 76 y la complementariedad a U1snRNP	*Skipping* exón 13
c.290G>A (MMAB)	*Skipping* exón 3	Disminuye el *score* de 0,99 a 0,50 y la complementariedad a U1snRNP	*Skipping* exón 3
c.304G>T (SPR)	n.d.	Disminuye el *score* de 0,99 a 0,73	*Skipping* exón híbrido y transcritos normales

n.d.= no determinado

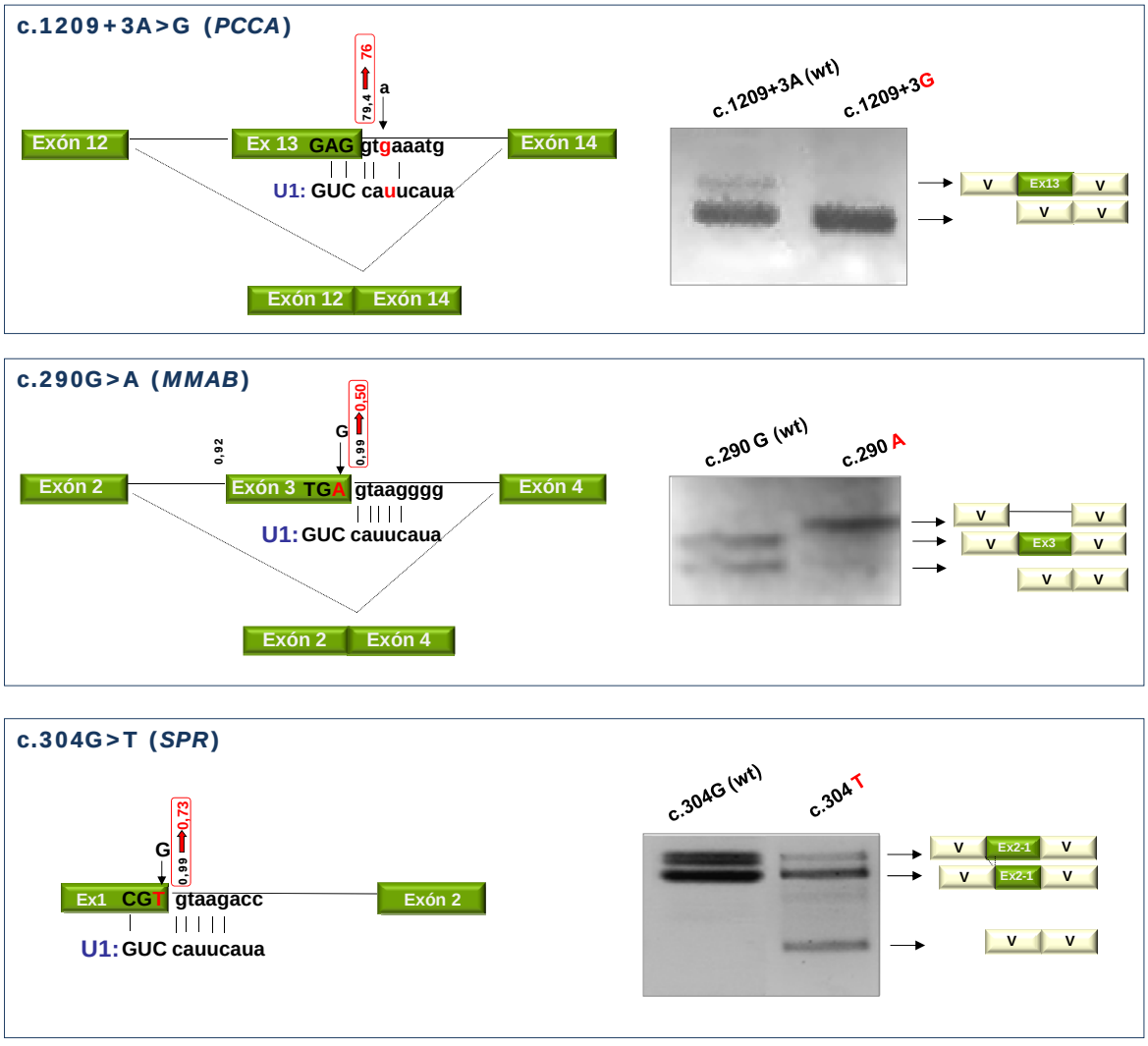

Figura 18. Análisis funcional de las mutaciones que afectan al sitio 5´ de *splicing*. Se muestra, a la izquierda, una representación esquemática de la localización de la mutación y cómo afecta a la complementariedad con U1snRNP, los *scores* de los sitios de *splicing* y el perfil transcripcional observado en los fibroblastos de los pacientes. A la derecha, se muestra el resultado del análisis de la mutación mediante minigenes y la representación esquemática de los transcritos obtenidos tras su caracterización por secuenciación. V: secuencia exónica vector

4.3.1.2. Mutaciones localizadas en secuencias intrónicas que activan la inserción de un pseudoexón

Tras el análisis en cDNA de un paciente diagnosticado bioquímicamente con acidemia propiónica, se observó una inserción de **84 pb** entre los exones 14 y 15 del **gen *PCCA*** que correspondía a una secuencia interna del intrón 14, anteriormente descrita como transcrito minoritario en individuos normales (Campeau et al., 1999 y datos del laboratorio). En el análisis en DNA genómico se identificó en homocigosis la variante **c.1285-1416A>G** localizada en el medio de la región de 84 pb.

Paralelamente, en otro paciente también diagnosticado con acidemia propiónica, se identificó a nivel de cDNA una inserción de **72 pb** entre los exones 6 y 7 del **gen *PCCB*** que también correspondía a una secuencia intrónica. El cambio que se identificó en DNA genómico, también en homocigosis, fue la variante **c.654+462A>G**, localizada 5 nucleótidos aguas abajo de la región de 72 pb. Esta mutación también fue identificada en heterocigosis en un paciente argentino que en el otro alelo portaba una mutación de cambio de aminoácido (c.494G>C, R165P).

Una vez identificadas estas variantes alélicas, se realizó un rastreo en 300 alelos control mediante análisis por enzimas de restricción. En ninguno de los 2 casos se detectó la mutación identificada en los genes *PCCA* o *PCCB* en los alelos control, apoyando el hecho de que éstas fueran patogénicas. (Figura 19).

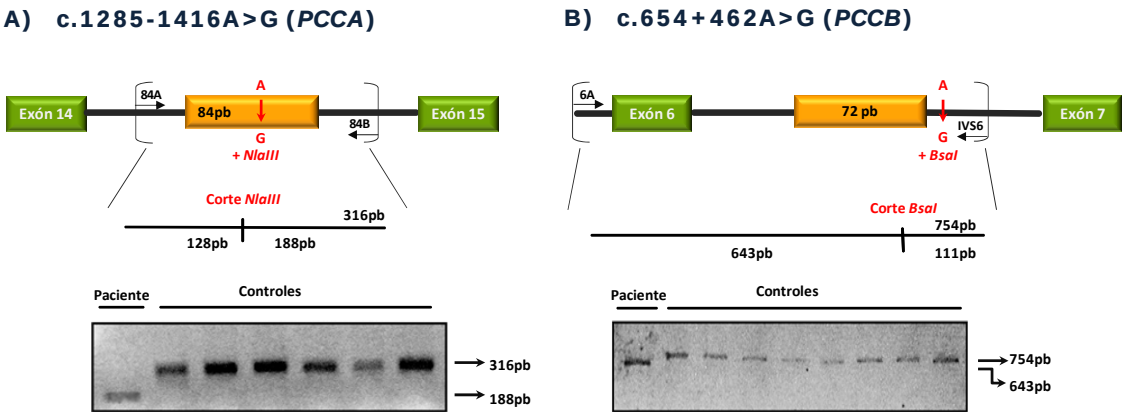

Figura 19. Análisis por enzimas de restricción de las mutaciones intrónicas detectadas. Se muestra el esquema de los fragmentos amplificados para cada una de las mutaciones, así como las dianas de restricción que generan, únicas en todo el fragmento amplificado, y los resultados obtenidos en un conjunto de muestras.

Se observó que la secuencia de las 84 pb en el intrón 14 del gen *PCCA* estaba flanqueada por secuencias potenciales 5´ y 3´ de *splicing,* al igual que la de las 72 pb en el intrón 6 del gen *PCCB,* con valores (*scores*) de *splicing* altos, según datos analizados por programas bioinformáticos (BDGP y AST) (Figura 20), por lo que se pensó que las mutaciones identificadas en los pacientes eran responsables de la exonización de estas secuencias intrónicas que se comportan como pseudoexones. De manera que se analizó *in silico* el posible efecto de cada una de estas mutaciones, observándose, mediante el servidor BDGP, que la mutación **c.654+462A>G** en el gen *PCCB*

incrementa el *score* de *splicing* de 0,93 a 1 en el sitio 5´donador de *splicing* del pseudoexón (Tabla 8).

La mutación **c.1285-1416A>G,** en el gen *PCCA,* se sitúa lejos de las regiones de *splicing* del pseudoexón, y se estudió su efecto sobre secuencias de unión a proteínas SR, que modulan el *splicing,* mediante el programa *ESE Finder*. Dicho análisis reveló que la mutación c.1285-1416A>G crea un sitio de unión de la proteína SRp40 y elimina un sitio de unión de la proteína SRp55 (Tabla 8).

Este estudio *a priori* nos lleva a pensar que estas mutaciones son las causantes de la inserción de estas secuencias intrónicas (pseudoexones) en el mRNA, bien porque activan sitios crípticos de *splicing* (c.654+462A>G), o bien porque afectan al reconocimiento de factores de *splicing* como SRp40 (c.1285-1416A>G).

Para confirmar la implicación de estas mutaciones en la inserción de las los pseudoexones, se realizó un análisis funcional mediante un sistema de minigenes con el vector pSPL3. En este caso, se introdujo la región intrónica que contiene el pseudoexón con las secuencias normal y mutante para estudiar su perfil transcripcional. En el caso del minigen PCCB se clonó además el exón 6. Cada una de las construcciones, normal y mutante, fue transfectada en células de hepatoma. Tras 48h se extrajo el RNA y se realizó la RT-PCR con los oligos SD6 y SA2, específicos del vector pSPL3. Para ambos casos, en las construcciones normales no se observó inclusión de los pseudoexones, pero sí en las construcciones mutantes. El análisis por secuenciación confirmó la identidad de los transcritos en todos los casos. En el caso del minigen portador de la mutación c.654+462A>G (*PCCB*) el transcrito obtenido incluye el pseudoexón, además de una secuencia del vector pSPL3, ya que debido a un artefacto del clonaje se utilizan sitios crípticos de *splicing* presentes en el vector (Tabla 8 y Figura 20).

Esto demuestra la implicación de las mutaciones c.1285-1416A>G y c.654+462A>G en la inclusión intrónica de las secuencias de 84 y 72 pb, respectivamente, que se activan y pasan a ser reconocidas como exones.

La implicación de SRp40 en la inclusión del pseudoexón de 84 pb fue estudiada utilizando RNA de interferencia, cotransfectando el minigen mutante portador de la mutación c.1285-1416A>G y siRNA contra SRp40. Sin embargo, dicha implicación no pudo ser demostrada, ya que, a pesar de que la eficiencia de interferencia fue de ~ 65-75%, no hubo variación en el perfil transcripcional del minigen mutante.

Tabla 8. Mutaciones que activan la inserción de un pseudoexón

Gen	Origen de inserción	Cambio en gDNA	Estudio *in silico*
PCCA	Intrón 14	c.1285-1416A>G	Creación de un sitio de unión a SRp40 y eliminación de un sitio de unión SRp55
PCCB	Intrón 6	c. 654+462A>G	Incrementa el *score* de *splicing* de 0,93 a 1 en el sitio 5´donador del pseudoexón

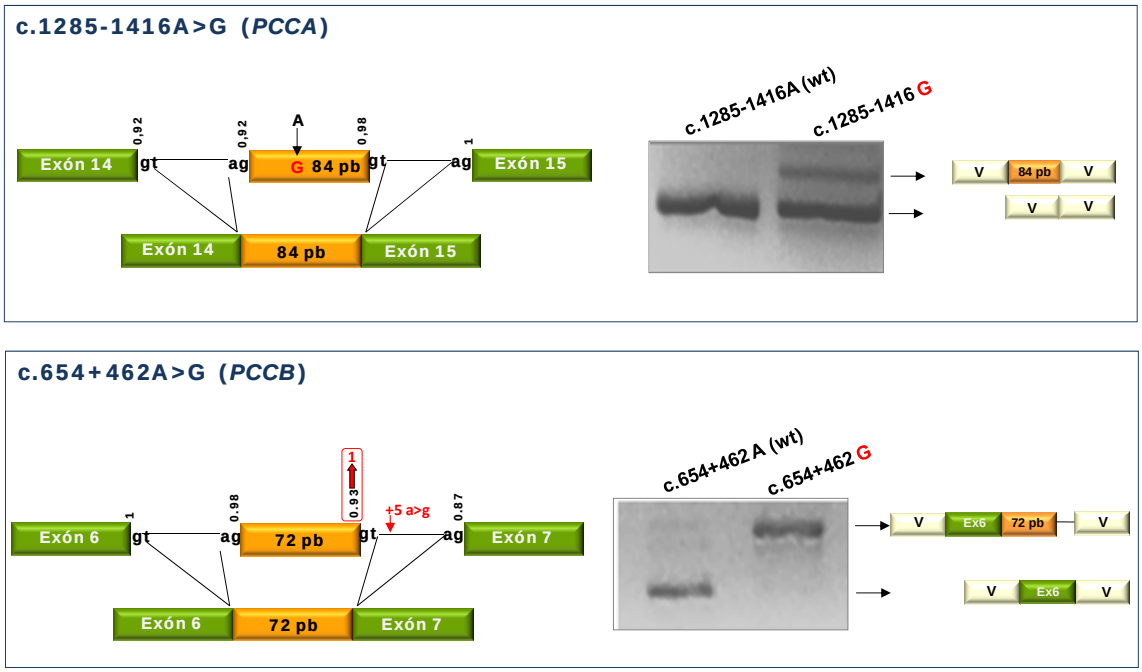

Figura 20. Análisis funcional de las mutaciones que activan la inserción de un pseudoexón. Se muestra, a la izquierda, una representación esquemática de la localización de la mutación, los *scores* de los sitios de *splicing* y el perfil transcripcional observado en los fibroblastos de los pacientes. A la derecha, se muestra el resultado del análisis de la mutación mediante minigenes y la representación esquemática de los transcritos obtenidos tras su caracterización por secuenciación. V: secuencia exónica del vector.

4.3.2. Análisis de terapias moduladoras de mutaciones de *splicing*

Como hemos visto, las mutaciones de *splicing* pueden estar afectando a secuencias más o menos conservadas que son reconocidas por factores de *splicing* específicos. Experimentalmente, se ha descrito cómo cambios en la expresión de alguna de las ribonucleoproteínas que forman parte del "spliceosoma" y, por lo tanto, cambios en la estequiometría entre ellas, pueden tener efectos significativos en el patrón de *splicing* (David and Manley, 2008; Martinez-Contreras et al., 2007). Por ello, hemos ensayado esta estrategia mediante la sobreexpresión de factores de *splicing*, sobre alguna de las mutaciones caracterizadas. Asimismo, hemos ensayado la sobreexpresión de U1snRNAs complementarios a secuencias 5´ de *splicing* mutantes para revertir el defecto en el *splicing*.

Por otra parte, se ha ensayado la utilización de oligonucleótidos antisentido dirigidos a impedir el reconocimiento de las secuencias aceptora o donadora de *splicing* de pseudoexones intrónicos activados por mutaciones.

4.3.2.1. Sobreexpresión de factores de *splicing* sobre mutaciones localizadas en el sitio 3´ de *splicing*

Hay multitud de trabajos que demuestran que las proteínas SR se unen a secuencias exónicas activando el *splicing* (Lavigueur et al., 1993; Sun et al., 1993; Tian & Maniatis, 1993). Concretamente, facilitan la unión de U2AF65 a la secuencia de ramificación a través de la interacción mediada por U2AF35 y las proteínas SR, SC35 y SF2/ASF, que interaccionan entre ellas y con U2AF35 (Tian & Maniatis, 1993, Wu & Maniatis, 1993). Es previsible que la función de los ESEs fuera especialmente importante en mutaciones con sitio 3´ débil, donde se necesitarían secuencias adicionales para la unión de proteínas SR, que ayuden a U2AF a unirse a la secuencia de ramificación (Figura 6). Por este motivo, se procedió a ensayar la sobreexpresión de los factores de *splicing* U2AF35 y U2AF65 y las proteínas SR: SC35, SRP40, SF2/ASF y SRP55 sobre las mutaciones que afectan al sitio **3´de *splicing*: c.1091-11del6, c.394-1G>C**, anteriormente descritas, además de la mutación **c.2041-2A>G**, mediante ensayos de cotransfección de los minigenes mutantes con los vectores portadores de cada uno de los factores a sobreexpresar.

La mutación c.2041-2A>G (IVS22-2A>G) fue identificada en homocigosis en el gen *PCCA* en un paciente diagnosticado con AP. Se observó que producía la exclusión del exón 23 y fue previamente analizada por minigenes (Clavero et al., 2004). En el análisis *in silico* se predijo que esta mutación crea un sitio de unión para la proteína SC35 y elimina un sitio de unión para SRp40. Tras analizar el patrón de *splicing* que había tenido lugar en el minigen mutante tras la sobreexpresión, se observó que, en concreto con la sobreexpresión de la proteína SC35 y U2AF35, desaparecía la banda correspondiente a la exclusión del exón, detectándose mayoritariamente una banda de igual tamaño al obtenido con el minigen normal, tanto cuando se sobreexpresaban por separado como a la vez, así como al tratar las células transfectadas con el minigen mutante con cafeína 10 y 25mM que aumenta la expresión de la proteína SC35 (Shi et

al., 2008). Sin embargo, el análisis por secuenciación reveló que la banda obtenida correspondía a la utilización de un sitio críptico de *splicing* localizado en el exón 23 a 6 nucleótidos aguas abajo de la mutación (Figura 21). Este sitio se sustituyó por mutagénesis dirigida de *ag* a *gg* de manera que el *score* de *splicing* de éste disminuía según el programa informático *Human Splicing Finder* (http://www.umd.be/HSF) de 77,31 a 72,46. Utilizando esta nueva construcción mutante se obtuvo otro transcrito en el que se escogía otro sitio alternativo de *splicing* 9 nucleótidos aguas abajo, en ningún caso escogiéndose el sitio de *splicing* original.

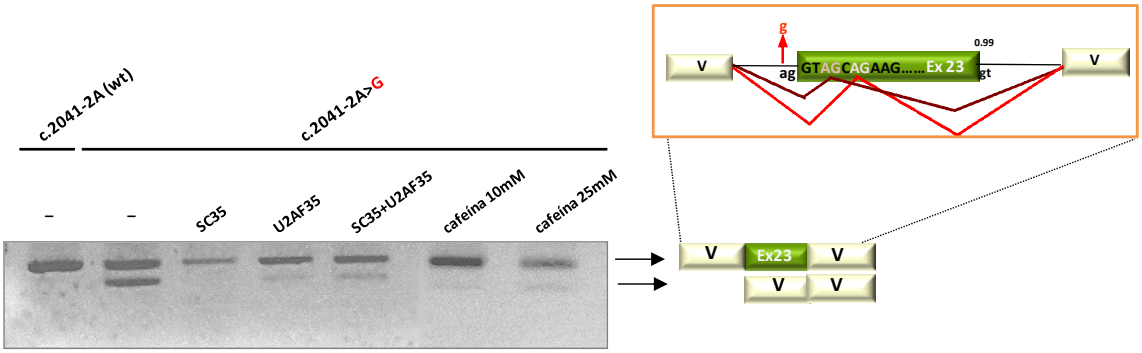

Figura 21. Efecto de la sobreexpresión de factores de *splicing* sobre el perfil transcripcional asociado a la mutación c.2041-2A>G. En el esquema se señalan los diferentes sitios crípticos de *splicing* del exón 23, así como el perfil transcripcional obtenido por RT-PCR tras la cotransfección del minigen mutante junto con los vectores codificantes para la proteína SC35 y U2AF35, y con cafeína 10 y 25mM. V: secuencias exónicas del vector.

Tras los ensayos de sobreexpresión realizados sobre las otras dos mutaciones no se observó, en ningún caso, recuperación de transcritos normales. Por lo que se concluye que las mutaciones **c.1091-11del6 (gen *PCCB*), c.394-1G>C (gen *MMAB*)** y **c.2041-2A>G (gen *PCCA*)** son mutaciones severas no modulables.

4.3.2.2. Sobreexpresión de U1snRNA sobre mutaciones localizadas en el sitio 5´ de *splicing*

El primer paso en la formación del "spliceosoma" es el reconocimiento por complementariedad de bases entre el sitio 5´ de *splicing* del pre-mRNA y el extremo 5´ del RNA de la ribonucleoproteína U1 (Zhuang and Weiner, 1986). Está descrito que al aumentar la complementariedad entre ambos sitios puede aumentar el reconocimiento del sitio 5´ de *splicing* y con ello la inclusión exónica (Pinotti et al., 2008; Tanner et al., 2009); por lo que, para algunas de las mutaciones descritas que afectan al **sitio 5´de *splicing***, se procedió a analizar la sobreexpresión del vector que codifica para el RNA de U1snRNP como posible aproximación terapéutica.

Para la mutación c.290G>A, localizada en el último nucleótido del exón 3 del gen *MMAB,* disminuyendo la complementariedad entre U1snRNA y el sitio 5´de *splicing* (Figura 18), se procedió a ensayar la cotransfección del minigen mutante portador de

esta mutación y el vector que codifica para el RNA de U1snRNP (U1 *wt*). Como resultado, no se observaron diferencias en el perfil transcripcional. Posteriormente, se ensayó la utilización de una construcción de U1, modificado específicamente en el nucleótido de unión a la secuencia mutante (U1-1T), para aumentar así la unión específica entre ambas secuencias e intentar conseguir la recuperación de transcritos normales, pero tampoco fue posible recuperar el perfil transcripcional normal.

La mutación c.1209+3A>G (IVS13+3A>G), que fue identificada en 4 pacientes con acidemia propiónica (3 en homocigosis y 1 en heterocigosis), se localiza en el nucleótido +3 del intrón 13 del gen *PCCA* disminuyendo también la complementariedad de U1snRNA y el sitio 5´de *splicing* (Figura 18). Por ello, se procedió a ensayar, de igual manera, la cotransfección del minigen mutante portador de la mutación y U1snRNA modificado específicamente en el nucleótido de unión a esta secuencia mutante (U1+3C). Sin embargo, tampoco se observó recuperación de transcritos normales.

Está descrito que la región de complementariedad entre U1snRNA y el sitio 5´de *splicing* incluye los 3 últimos nucleótidos del exón y los 8 primeros del intrón (Freund et al., 2005). Con el fin de profundizar en el papel de los distintos nucleótidos en el reconocimiento exónico, y, apoyándonos en concreto en esta última mutación, ya que es una mutación frecuente de la que se disponía de fibroblastos de varios pacientes homocigotos, se modificó, por mutagénesis dirigida, el vector que contiene U1snRNA, de manera que, además del vector U1+3C, se realizaron otras tres construcciones más con modificaciones en los nucleótidos de las posiciones +5 y +6 (U1+3C+5T y U1+3C+5T+6T), importantes en el reconocimiento por parte de ambas secuencias, tal y como se ha descrito en la literatura (Guedard-Mereuze et al., 2009; Zychlinski et al., 2009). Además, se realizó una última construcción modificada además en los nucleótidos de las posiciones -3, +7 y +8 (U1IVS13), de manera que hibridaran perfectamente los 11 últimos nucleótidos del extremo 5´ de U1snRNA con la secuencia mutante en el gen *PCCA* (Figura 22).

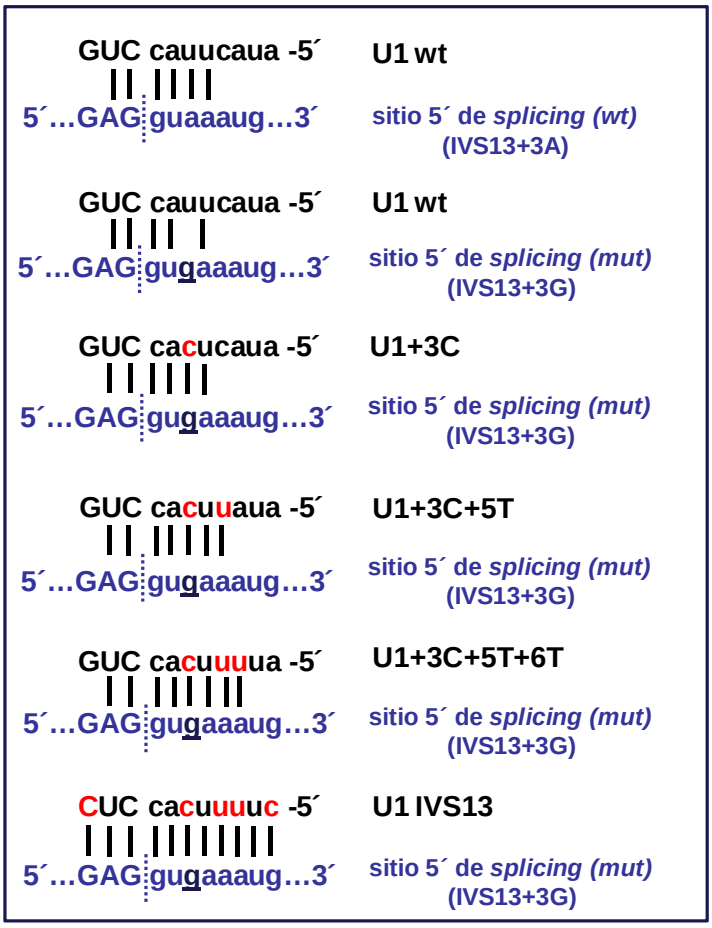

Figura 22. Representación esquemática de la complementariedad de bases entre el sitio 5´ de *splicing* del exón 13 del gen *PCCA* y las diferentes construcciones de U1snRNA.

Dado que el minigen normal correspondiente al exón 13 no reproduce fielmente el patrón de *splicing* que tiene lugar *in vivo,* ya que el porcentaje de transcritos normales es muy minoritario (Figura 18), se decidió ensayar la transfección de los distintos U1snRNAs modificados, directamente sobre los fibroblastos correspondientes a las líneas celulares de dos pacientes que presentan la mutación en homocigosis. En ninguno de los dos casos se observó ningún efecto con las construcciones U1 *wt* y U1+3C; sin embargo, con las otras 3 construcciones se pudo observar recuperación de transcritos normales, siendo prácticamente del 100% con la construcción U1IVS13 (Figura 23A). En las mismas condiciones, se transfectó una línea celular control, no observándose ninguna alteración del perfil transcripcional normal (Figura 23B). Cada una de las bandas identificadas fue caracterizada, en todos los casos, mediante secuenciación.

Como agentes de transfección para estos ensayos se utilizaron tanto *Lipofectamina LTX* como *Nucleofector,* observándose en ambos casos, resultados similares, aunque la eficiencia de transfección medida paralelamente con un plásmido control que codificaba para GFP, fue bastante más alta con la nucleofección. Asimismo, como control adicional, la expresión de las distintas construcciones de U1snRNA transfectadas fue analizada por RT-PCR con oligos específicos del vector: pGEM Q – 5´ATCGAAATTAATACGACTCA-3´ y U1_QR – 5´CTGGGAAAACCACCTTCGT3´- (Raponi et al., 2009), confirmando una eficiente transfeccción en todos los casos. Por otro lado,

no se observó ninguna diferencia importante en ninguna de las dos líneas de fibroblastos utilizadas, homocigotas para la mutación.

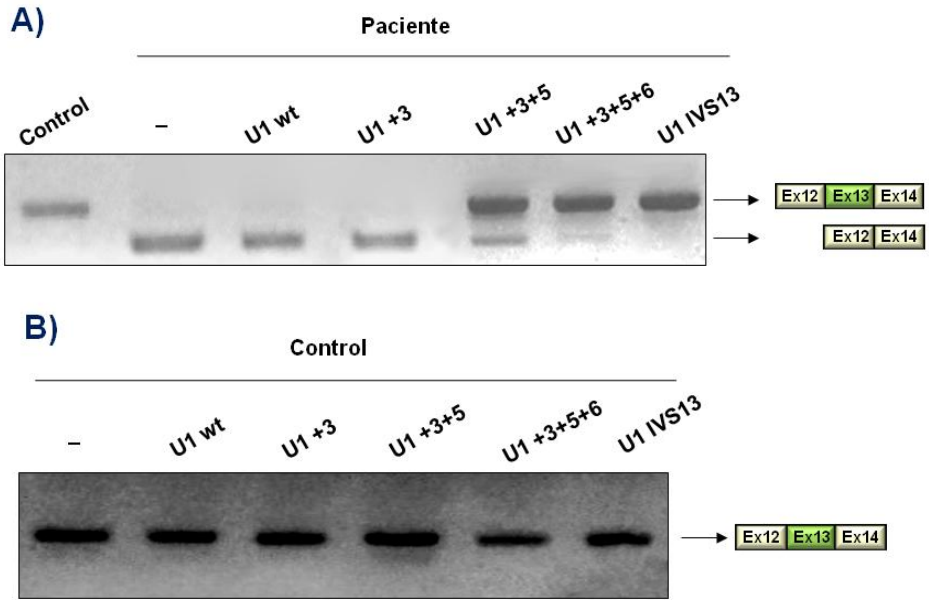

Figura 23. Corrección del *splicing* aberrante mediante la sobreexpresión de U1 snRNAs modificados. Análisis por RT-PCR en fibroblastos de pacientes con la mutación c.1209+3A>G (IVS13+3A>G) (A) y en una línea celular control en las mismas condiciones (B).

En las células de los pacientes, mediante RT-PCR estándar, no observamos ningún transcrito aberrante adicional (por ejemplo, por activación de un sitio críptico de *splicing* o por exclusión de exones adyacentes), sin embargo, éstos podrían estar produciéndose y no ser detectados por estar fuera de fase y ser degradados por el mecanismo NMD. En este caso, estos transcritos aberrantes no serían rescatados por la sobreexpresión de los distintos U1snRNAs modificados, limitando su acción terapéutica. Para descartar esta posibilidad, se ensayó en los mismos experimentos de sobreexpresión de los U1snRNAs modificados, con los que se rescataban transcritos normales (U1+3+5, U1+3+5+6 y U1 IVS13), el efecto de la adición de diferentes concentraciones (10 y 100 µM) de wortmanina, inhibidor del NMD, 6 horas antes de la recogida de células (Rio Frio et al., 2008; Usuki et al., 2004). Mediante RT-PCR no se observaron diferencias en el perfil transcripcional tras comprobar la identidad de las bandas por secuenciación.

También, se llevó a cabo el análisis por RT-PCR semicuantitativa utilizando oligos fluorescentes y analizando, posteriormente, los fragmentos obtenidos por electroforesis capilar, obteniéndose el mismo perfil transcripcional. La cantidad de producto amplificado fue prácticamente la misma en todos los casos indicando que la mayoría del RNA presente en las células de los pacientes es correctamente procesado después de la transfección con las distintas construcciones (Figura 24).

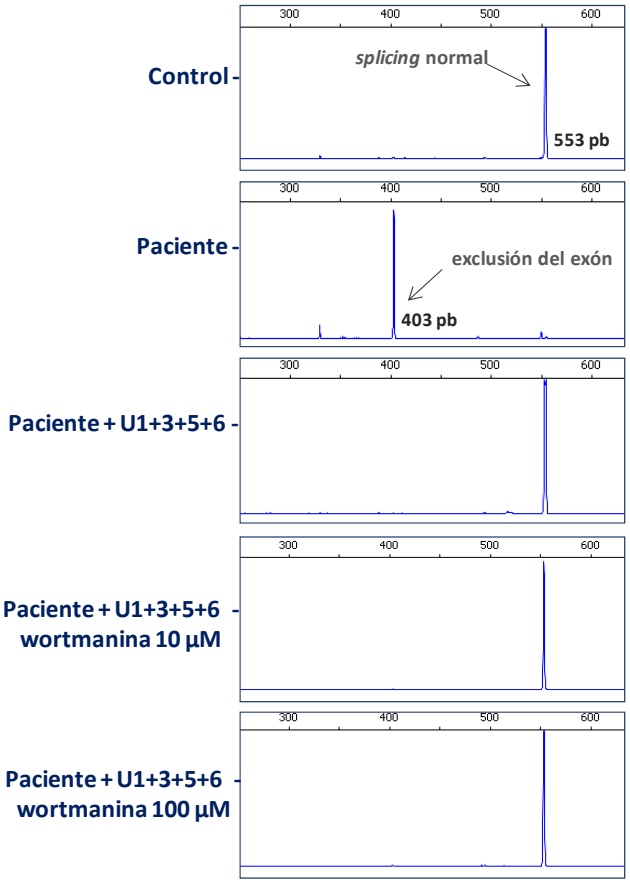

Figura 24. Análisis por electroforesis capilar de los productos de RT-PCR semicuantitativa de la región del exón 13 del gen *PCCA*. Se utilizó un oligonucleótido fluorescente y el *software Peakscanner* (*Applied Biosystems*).
Eje x: tamaño del fragmento (en pb); eje y: intensidad de fluorescencia.

La recuperación funcional de la mutación c.1209+3A>G (IVS13+3A>G), tras la sobreexpresión de U1snRNAs modificados, fue ensayada a través de la medida de la actividad enzimática PCC en los fibroblastos transfectados en las mismas condiciones en las que se observa la recuperación de transcritos normales, pero no se observó un incremento de actividad en ninguno de los casos.

Los cDNAs completos de *PCCA* y *PCCB* fueron también amplificados por PCR en 2 o 3 fragmentos superpuestos, observándose niveles normales y de secuencia completamente normal. Se descartó también la posibilidad de que estuviera teniendo lugar una inhibición inespecífica de la actividad enzimática PCC tras la sobreexpresión de U1, transfectando una línea celular control con las construcciones U1+3+5+6 y U1 IVS13 en la que no se observó ninguna variación en los niveles de actividad PCC.

Mediante detección de la proteína PCCA, empleando un ensayo con avidina para detectar proteínas mitocondriales unidas a biotina, no se detectó proteína PCCA biotinilada después de la sobreexpresión de U1 IVS13 snRNA (Figura 25), que había sido la más efectiva en la recuperación de transcritos normales.

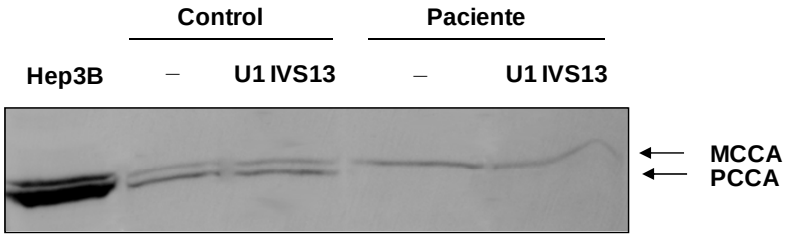

Figura 25. Detección de proteínas mitocondriales biotiniladas en fibroblastos control y de uno de los pacientes portadores de la mutación c.1209+3A>G (IVS13+3A>G) en homocigosis sin transfectar y tras la transfección con la construcción U1 IVS13. Se utilizó la línea de hepatoma Hep3B como control. MCCA, subunidad α de la metilcrotonil CoA carboxilasa.

4.3.2.3. Transfección de oligonucleótidos antisentido para bloquear la inclusión aberrante de pseudoexones

En estudios previos en el laboratorio, se ha estudiado que la inserción de pseudoexones provocada por mutaciones localizadas en secuencias intrónicas puede impedirse con la utilización de oligonucleótidos antisentido tipo morfolino (AONs), que por impedimento estérico bloquean la unión de la maquinaria de *splicing* a los sitios aceptor o donador del pseudoexón, de manera que se utilizan los sitios normales de *splicing,* restableciendo el perfil transcripcional normal.

En este trabajo, esta terapia fue ensayada en un paciente portador en heterocigosis de la mutación intrónica c.654+462A>G en el gen *PCCB,* anteriormente descrita, y responsable de la inclusión aberrante de un pseudoexón de 72 pb. Al encontrarse la mutación en heterocigosis y debido al NMD, el transcrito aberrante sólo fue detectado, aunque en niveles muy bajos, después de tratar los fibroblastos del paciente con cicloheximida (0,5-0,75 mg/mL) durante 6 horas (Figura 26).

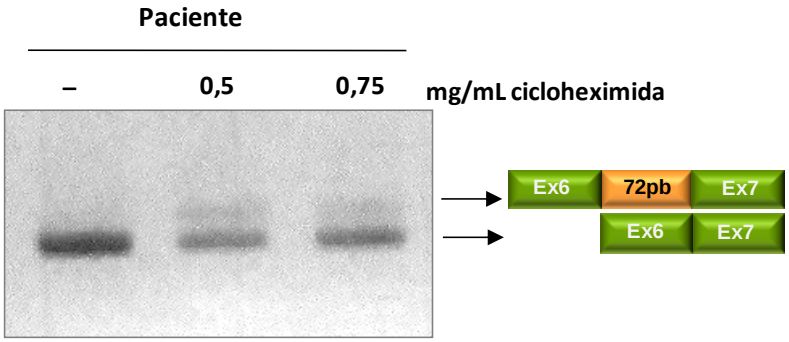

Figura 26. Efecto del tratamiento con cicloheximida sobre los fibroblastos de un paciente portador en heterocigosis de la mutación c.654+462A>G en el gen *PCCB*. La figura muestra el perfil transcripcional obtenido por RT-PCR y la representación esquemática de los productos obtenidos, tras su caracterización por secuenciación.

Para la terapia antisentido se utilizó el morfolino AONB (5´-TCATGTAATAAAGATATATGTACCTCT-3´), dirigido contra el sitio 5´ del pseudoexón de 72 pb, el cual fue ensayado a distintas concentraciones (10, 20 y 30 µM) directamente sobre los fibroblastos del paciente, para, posteriormente, medir la actividad enzimática PCC. Se pudo observar que había una recuperación parcial de actividad, debido a que la mutación se encuentra en heterocigosis, aunque prácticamente se alcanzan valores normales (Figura 27).

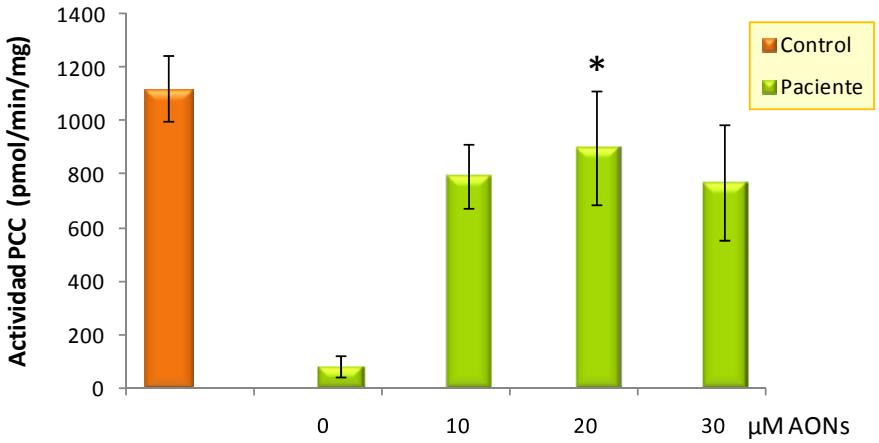

Figura 27. Medida de la actividad propionil CoA carboxilasa en fibroblastos control y del paciente con la mutación c.654+462A>G tras la transfección con distintas concentraciones de AONs. Todos los datos son la media de 3 experimentos independientes por duplicado. *p-valor<0,05.

5. DISCUSIÓN

En este trabajo, se han caracterizado reordenamientos genómicos en el gen *PCCA* y mutaciones sin sentido en los genes *PCCA* y *PCCB* implicados en acidemia propiónica, así como estudiado funcionalmente distintas variantes alélicas que afectan al *splicing,* implicadas en diferentes enfermedades metabólicas hereditarias. Asimismo, hemos ensayado terapias específicas para las mutaciones sin sentido y mutaciones de *splicing* caracterizadas. Con ello, hemos pretendido ampliar el conocimiento de estos defectos profundizando en la aplicación de nuevas estrategias diagnósticas y/o terapéuticas específicas de mutación.

5.1. IDENTIFICACIÓN DE CNVs EN EL GEN *PCCA* RESPONSABLES DE ACIDEMIA PROPIÓNICA

La mayoría de las mutaciones detectadas en los genes *PCCA* y *PCCB* son de cambio de aminoácido. En los últimos años, se han descrito reordenamientos genómicos en muchas enfermedades genéticas, coincidiendo con la aparición de distintas técnicas que permiten medir dosis génica. Las deleciones exónicas en muchas ocasiones se han escapado a los métodos diagnósticos de rutina de PCR y secuenciación. Éstas sólo pueden sospecharse claramente en pacientes homocigotos, en los que en el análisis en gDNA no se observa amplificación de alguno de los exones. En algunos pacientes heterocigotos, los transcritos portadores de deleciones pueden no ser detectados, bien debido a que corresponden a transcritos fuera de fase con PTCs susceptibles a la degradación por NMD (Maquat, 2004), o bien porque los oligos utilizados para la amplificación del cDNA hibriden en los exones delecionados.

En este trabajo, se ha empleado la técnica de MLPA para analizar deleciones en el gen *PCCA* en pacientes con acidemia propiónica, en los que no se habían encontrado mutaciones en uno o ambos alelos por los métodos convencionales de PCR y secuenciación. Mediante esta técnica y PCR larga se identificaron grandes deleciones genómicas, nunca antes descritas en el gen *PCCA*, con una alta frecuencia de alelos delecionados (21,3%). Esta frecuencia puede ser considerada como representativa de la población caucásica, ya que las muestras de los pacientes recibidos en el laboratorio provienen de Australia, Europa y EE.UU. En total, se identificaron 8 deleciones diferentes por MLPA, de la cuales dos fueron las más recurrentes: la deleción de los exones 3-4 y la deleción del exón 23, que tiene una frecuencia de 6,8%. En los alelos que presentaban la deleción de los exones 3 y 4, se detectaron 2 deleciones diferentes en el análisis en gDNA: una de 8,8 y otra de 4,7 kb. La deleción de 4,7 Kb (c.184-618del4479) estaba presente en 11 alelos, lo que corresponde a una frecuencia de 8,3% del total de alelos *PCCA* (Figura 28). Muchos de los pacientes portadores de esta última deleción son de origen Mediterráneo (griegos, turcos o italianos), mientras que la deleción del exón 23 está presente en pacientes de origen árabe. Estos resultados proporcionan información relevante acerca de la epidemiología de la enfermedad y sirven como base para la estrategia de diagnóstico de futuros pacientes dependiendo de su etnia y situación geográfica.

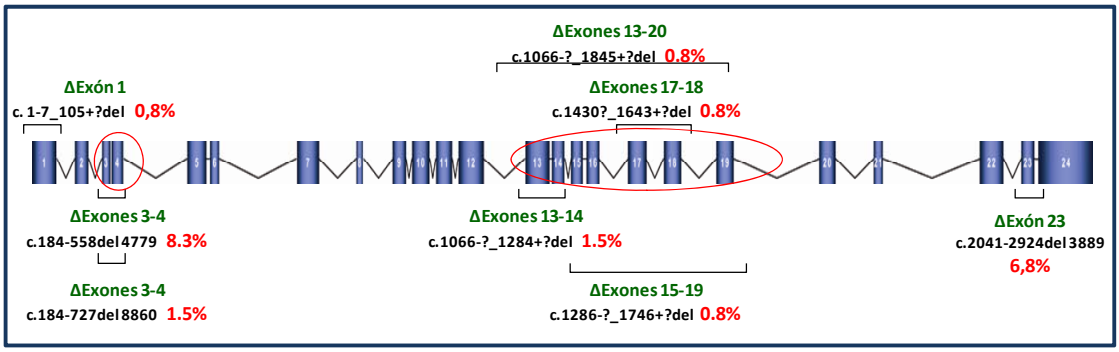

Figura 28. Representación esquemática del gen *PCCA* y localización de las grandes deleciones caracterizadas, así como la frecuencia de cada una de ellas. Se indican, rodeadas en rojo, las regiones *hotspots* para las deleciones.

Con este estudio, el porcentaje de detección de mutaciones en el gen *PCCA* asciende a ~98,5%, con lo que quedan ~1,5% de alelos aún sin caracterizar que corresponden a pacientes con sólo una mutación identificada. El segundo alelo podría portar una mutación en regiones implicadas en la regulación o, más probablemente en regiones intrónicas que normalmente no se secuencian por completo, pudiendo afectar al *splicing* y generar la inserción de un pseudoexón en el mRNA, con lo que estos transcritos aberrantes no serían detectados al ser degradados por el sistema NMD (Du et al., 2007).

En las tres deleciones en las que se han caracterizado los puntos de ruptura, se han identificado secuencias repetitivas, ya sean secuencias *Alu* o repeticiones simples a ambos lados de la deleción, probablemente implicadas en la generación de las deleciones, como ya ha sido descrito con anterioridad por mecanismos de recombinación o errores en la replicación (Chuzhanova et al., 2003; Abeysinghe et al., 2003).

Recientemente, se ha descrito otra deleción de ~73Kb que incluye los exones 17 al 19 en una familia saudí con acidemia propiónica (Kaya et al., 2008). Esto lleva a pensar que hay alguna característica en el gen PCCA que le hace ser más susceptible a este tipo de mutaciones. En concreto parece haber un *hotspot* para deleciones en las regiones entre los intrones 12 y 19 y otro más pequeño alrededor de los intrones 2 y 4 (Figura 28). Como se ha visto en la distrofia muscular de Duchenne, estos eventos se localizan generalmente en intrones muy grandes (Den Dunnen et al., 1989). Este es el caso del gen *PCCA*, que tiene ~440 Kb con intrones también muy grandes, 10 de ellos mayores de 20 Kb, y en la mayoría, las secuencias repetidas representan el 45-55% de la secuencia intrónica según *RepeatMasker*. Según la base de datos de variantes genómicas (http://projects.tcag.ca/variation), hay descrita una inversión y varias CNVs en el gen *PCCA*, lo que indica que los reordenamientos en esta región ocurren con cierta frecuencia.

Todas las deleciones identificadas en los pacientes resultan previsiblemente en una deleción interna en fase en la secuencia de la proteína, a excepción de la deleción de los exones 17-18, que está fuera de fase y de la deleción del exón 1, que tiene un efecto impredecible. Las delecciones descritas pueden incluir, desde 26 aminoácidos (deleción del exón 23), que previsiblemente resulta en una proteína funcionalmente nula ya que incluye el sitio de unión a biotina (Leon-del-Rio and Gravel, 1994), hasta 260 aminoácidos (deleción de los exones 13 al 20). La deleción de los exones 3-4 (39 aminoácidos), que es la más frecuente, fue ensayada en el laboratorio en un sistema de expresión eucariota resultando en una ausencia total de actividad residual confirmando su patogenicidad.

5.2. EFECTO DE COMPUESTOS SUPRESORES DE LA TERMINACIÓN DE LA TRADUCCIÓN EN MUTACIONES SIN SENTIDO EN ACIDEMIA PROPIÓNICA.

En este trabajo, hemos estudiado también mutaciones sin sentido en los genes *PCCA* y *PCCB*, responsables de acidemia propiónica, que corresponden aproximadamente al 10% de los alelos mutantes, con el objetivo de ensayar estrategias terapéuticas basadas en la supresión de la terminación de la traducción mediada por diferentes compuestos.

La acidemia propiónica es un buen modelo para ensayar el efecto de estos compuestos. Actualmente, no hay tratamiento para esta enfermedad y, en muchos casos, el deterioro neurológico es inevitable. Esta terapia puede ser relevante terapéuticamente ya que en AP, pacientes con mutaciones que retienen cierta actividad residual presentan fenotipos intermedios (Perez-Cerda et al., 2000), lo que concuerda con estudios realizados en un modelo *knock out PCCA* de ratón que revelaron que la presencia de al menos un 10-20% de actividad PCC en el hígado, resultante de una baja expresión de un transgen, podía mejorar las consecuencias de la enfermedad y prevenir la letalidad neonatal (Miyazaki et al., 2001).

Aproximadamente un tercio de los alelos causantes de enfermedades genéticas son portadores de PTCs, generando la producción de proteínas truncadas. En los últimos años, la acción de compuestos supresores de la terminación de PTCs en fase inducidos por mutaciones sin sentido, ha sido descrita por como una terapia potencial para este grupo de pacientes. Existe una gran variablidad en los datos reportados para distintos genes causantes de enfermedad y en la respuesta a estos compuestos. Los resultados de esta terapia pueden verse influidos por la naturaleza y fisiopatología de la enfermedad; así como por el tipo de mutaciones sin sentido, la vida media de la proteína, el tiempo en que comienza el tratamiento en relación con la patogénesis de la enfermedad, la eficiencia de la liberación del compuesto y la dosis utilizada. Es necesario, en cada caso, evaluar la especificidad del tratamiento en modelos celulares y animales, previamente, antes de comenzar los estudios clínicos.

En este trabajo, se han identificado siete nuevas mutaciones sin sentido de un total de 12 mutaciones, en una cohorte de 190 pacientes con AP en la población caucásica. El análisis *in vitro* nos ha permitido estudiar el efecto de los compuestos

supresores para cada una de las mutaciones sin sentido, identificadas en los pacientes AP y su secuencia contexto. Ninguna de las mutaciones sin sentido identificadas portaban el tetranucleótido UGAC, descrito por ser el más susceptible a la supresión (Keeling and Bedwell, 2002). Dentro de las mutaciones analizadas en el gen *PCCA* observamos una mayor supresión para las mutaciones p.R313* y p.S562*, ambas portadoras del codón de parada UGA, lo que concuerda con estudios previos (Keeling et al., 2001; Manuvakhova et al., 2000). Sin embargo, en las mutaciones analizadas en el gen *PCCB* no se pudo establecer una conclusión clara, además de que aparentemente la recuperación de proteína completa después del tratamiento supresor fue bastante menor que en las mutaciones en el gen *PCCA*, lo que probablemente pueda ser debido, en parte, a diferencias en el vector de clonaje y el procedimiento experimental.

Con el objetivo de investigar la actividad de la proteína completa sintetizada tras el tratamiento de supresión, se analizó el efecto *in silico* e *in vitro* de las mutaciones de cambio de aminoácido previsiblemente inducidas tras la supresión para cada una de las mutaciones. Tras el análisis se concluyó que la mayor parte de las proteínas PCCA y PCCB completas, predeciblemente generadas, retienen cierta actividad enzimática (Tabla 3). Los resultados *in silico* han de ser interpretados con precaución, siendo aconsejable la utilización de más de un programa y verificarlos experimentalmente siempre que sea posible. En nuestro caso, el efecto de las mutaciones de cambio de aminoácido analizadas experimentalmente mediante un sistema de expresión eucariota, se correlacionó mejor con las predicciones bioinformáticas del programa SIFT (Tabla 3).

De los estudios realizados en fibroblastos de pacientes portadores de las mutaciones sin sentido analizadas, se puede concluir que, al igual que ocurre *in vitro*, aquellas que introducen el codón de parada UGA son las más susceptibles al tratamiento supresor. En concreto, los niveles de actividad PCC más altos se observaron para el P3 (Figura 15), heterocigoto para la mutación p.W531* que previsiblemente revierte al aminoácido original, junto con el P2, homocigoto para la mutación p.S562* que coincide con los niveles más altos de recuperación de proteína completa *in vitro* y que previsiblemente resulta en una proteína con alta actividad residual *in vitro* (Figura 14 y Tabla 3). Los niveles de recuperación más altos se observaron con G418 a 50 y 75 µg/mL y con gentamicina a 300 µg/mL, mientras que a 500 µg/mL en general el efecto es menor, sugiriendo un efecto tóxico a esta dosis. Con PTC124 se observaron unos niveles más moderados de recuperación en los fibroblastos de los pacientes (Figura 15), siendo nulo en los ensayos *in vitro* tal y como ha sido observado previamente por otros autores (Dranchak et al., 2011). Los resultados obtenidos con PTC124 han de ser interpretados con precaución ya que no pudimos confirmar su funcionalidad al no estar disponible el compuesto directamente del proveedor original.

La variación en los niveles de actividad recuperados con los distintos tratamientos para cada uno de los pacientes, puede ser debido, además de a diferencias técnicas, como puede ser el número de pases de cada una de las líneas, lo que produciría variaciones en la respuesta a la supresión, tal y como ha sido observado

con anterioridad (Keeling et al., 2001), y de la variabilidad en los niveles de los distintos aminoácidos incorporados en lugar del PTC en cada caso; también a factores epigenéticos y/o modificadores genéticos. Un ejemplo de ello es la respuesta diferente que se obtuvo durante la fase 2 del tratamiento con PTC124 en pacientes con fibrosis cística, donde sólo en el 50% de ellos se observó una recuperación de proteína funcional, aun siendo portadores, algunos de ellos, de la misma mutación (Kerem et al., 2008).

En algunos casos, en los efectos relativos de cada compuesto, analizados *in vitro* y *ex vivo,* se han observado algunas diferencias, tal y como ha sido observado previamente en aciduria metilmalónica (Buck et al., 2009). Las limitaciones más importantes para la extensión de esta terapia a situaciones *ex vivo* son, por un lado, la especificidad de los agentes supresores por los codones de parada prematuros (en contraposición a los codones de parada originales presentes al final de la fase de lectura), y por otro, los bajos niveles de transcritos disponibles debido al NMD (Rowe and Clancy, 2009). En fibroblastos controles hemos observado que, en concreto con el tratamiento con G418, los niveles de actividad PCC disminuían en torno a un 40-50% (Tabla 5), que podría deberse a una supresión de la terminación sobre el codón de parada original tal y como ha sido observado previamente en otros trabajos (Hein et al, 2004), aunque serían necesarios más estudios al respecto de esta supresión no específica que aclaren este hecho. En los fibroblastos de los pacientes analizados, se observó una bajada significativa de los niveles de transcritos, de los cuales tan sólo entre el 1 y el 35% de ellos evadieron el mecanismo NMD, siendo por tanto susceptibles a la supresión de la terminación mediada por los distintos compuestos y resultando en una proteína PCC completa; esto explica que los niveles de actividad recuperados en los fibroblastos de los pacientes no sean especialmente elevados.

No se observó un efecto sobre la estabilidad del mRNA tras los diferentes tratamientos, tal y como se ha descrito con anterioridad (Buck et al., 2009; Hein et al., 2004; Popescu et al.), aunque hay autores que sí han descrito un aumento en los niveles de mRNA tras el tratamiento con aminoglucósidos (Bellais et al., 2010). Aunque los resultados obtenidos con la utilización del inhibidor del NMD wortmanina no fueron muy concluyentes (ya que aunque sí que se observó un aumento de transcritos mutantes, no así un aumento de los niveles de actividad enzimática tras la adición de los aminoglucósidos), en este sentido se ha ensayado el silenciamiento génico de diferentes factores implicados en el NMD en fibrosis cística, observándose un incremento significativo en los niveles de proteína funcional observados tras la terapia de supresión (Linde et al., 2007). Esta estrategia dirigida a reducir la eficiencia del NMD podría mejorar los beneficios proporcionados por la terapia supresora.

En resumen, nuestros resultados, en concreto en acidemia propiónica, proporcionan una prueba de concepto de que las mutaciones sin sentido identificadas en los genes *PCCA* y *PCCB* pueden ser susceptibles a la supresión de la terminación mediada por diferentes compuestos, con diferentes eficiencias dependiendo de la mutación sin sentido analizada, y que una recuperación funcional terapéuticamente relevante en pacientes es posible, dados los resultados obtenidos en modelos celulares de la enfermedad. El tratamiento con compuestos supresores no tóxicos ya sean

derivados de aminoglucósidos (Hainrichson et al., 2008) u otros compuestos no aminoglucósidos como RT13 y RT14 (Du et al., 2009) o PTC124 (Welch et al., 2007), en fase 3 en ensayos clínicos en fibrosis cística (http://www.ptcbio.com/), sugieren la terapia supresora como prometedora para el tratamiento futuro de esta enfermedad, así como de diversas enfermedades genéticas en pacientes seleccionados portadores de mutaciones sin sentido.

5.3. MUTACIONES DE *SPLICING* EN ENFERMEDADES METABÓLICAS HEREDITARIAS Y TERAPIAS ESPECÍFICAS

En los últimos años, se ha prestado especial atención a las mutaciones genéticas que afectan al *splicing* siendo múltiples las nuevas terapias moleculares y farmacológicas que se han ido desarrollando para este tipo de mutaciones. En particular, en este trabajo se han analizado mutaciones de *splicing* en los genes *PCCA* y *PCCB* responsables de acidemia propiónica, donde el porcentaje de este tipo de mutaciones corresponde a ~15-17% según el HGMD (*HGMD® Professional release 2011.4*), en el gen *MMAB* responsable de aciduria metilmalónica tipo *cblB* (~24%) y en el gen SPR responsable de la deficiencia de sepiapterina reductasa (~16%). En varias de ellas, se han ensayado distintas aproximaciones que sirvieran como herramienta para investigar los mecanismos moleculares del *splicing,* a la vez que como estrategia terapéutica para corregir defectos en el *splicing* responsables de enfermedad.

Las mutaciones descritas en este trabajo han sido analizadas tanto *in silico,* mediante programas bioinformáticos disponibles que predicen el valor de los sitios de *splicing* y la presencia de secuencias reguladoras de unión a factores de *splicing* y proteínas SR (Hartmann et al., 2008), así como funcionalmente en un sistema celular mediante minigenes.

5.3.1. Mutaciones de *splicing* localizadas en secuencias conservadas

En este trabajo se han analizado cinco mutaciones que afectan a **secuencias conservadas de *splicing***: las mutaciones **c.1091-11del6 (*PCCB*), c.394-1G>C (*MMAB*), c.1209+3A>G (*PCCA*), c.290G>A (*MMAB*) y c.304G>T (*SPR*)**. Tres de ellas, se localizan en secuencias intrónicas, de la cuales, una afecta al *ag* invariable del sitio 3´de *splicing,* y las otras dos se localizan en secuencias exónicas, en concreto en el ultimo codón exónico, formando parte de la secuencia conservada implicada en la unión a U1snRNP (Figuras 17 y 18).

Las predicciones *in silico* son una herramienta importante como primer rastreo de cómo una mutación puede afectar al procesamiento del pre-mRNA, pero no siempre son totalmente precisas, por lo que es importante además, realizar el análisis *ex vivo* mediante minigenes para analizar funcionalmente el efecto individual de las distintas mutaciones en el procesamiento del mRNA, especialmente relevante cuando las muestras de los pacientes no están disponibles, como es el caso del análisis de la mutación c.304G>T en el gen *SPR* de la que no fue posible disponer de muestras de

RNA del paciente. Los resultados obtenidos en los minigenes confirmaron que la mutación es responsable de un defecto en el *splicing*, aunque ciertos transcritos procesados correctamente podrían estar presentes resultando en la mutación de cambio de aminoácido p.G102C que retiene cierta actividad residual. Con estos datos podría explicarse el fenotipo intermedio y la variabilidad en las diferentes formas de presentación clínica, que podrían deberse a diferencias interindividuales en la presencia relativa de transcritos correctamente procesados y aberrantes.

El efecto más común de las mutaciones localizadas en secuencias conservadas de *splicing* sobre el perfil transcripcional es el *skipping* del correspondiente exón, produciendo una deleción ya sea en fase o fuera de fase. En algunos casos al interrumpirse los sitios originales 3´ o 5´ de *splicing* se ven activados nuevos sitios crípticos, ya sea en el intrón o en el exón, dando lugar a la generación de transcritos aberrantes. Un ejemplo, es el caso de la mutación c.394-1G>C, en el gen *MMAB*, que activa un sitio críptico 3´ de *splicing* en el exón 5 produciendo la deleción en fase de 2 aminoácidos (p.I117_Q118del), que aun tratándose de una deleción pequeña y en fase no presenta actividad residual siendo por tanto patogénica (datos del laboratorio).

De todas las mutaciones analizadas, en la mayoría de ellas el análisis por minigenes ha reproducido el defecto en el *splicing* observado en las células del paciente, sin embargo no siempre es así (Tablas 6 y 7). En concreto, en la mutación c.394-1G>C descrita anteriormente, en las células del paciente se activa un sitio críptico de *splicing* en el exón, y en el minigen portador de la mutación se produce el *skipping* del exón 5 (Figura 17). En el caso del minigen normal correspondiente al exón 13 del gen *PCCA,* el porcentaje de transcritos normales obtenido es muy minoritario (Figura 18). Estas diferencias puede ser debido al hecho de que en este sistema celular se carezca de la secuencia genómica adyacente completa, cuyo contexto es importante para el correcto reconocimiento exónico, tal y como sucede en la paraplegia espástica hereditaria (Svenson et al. 2001), o bien porque en realidad se produzcan otros transcritos, degradados por el sistema NMD. En cualquier caso, siempre que sea posible, el perfil transcripcional ha de ser confirmado en las células de los pacientes.

En los últimos años, se ha investigado sobre numerosas **aproximaciones terapéuticas** que modifican el patrón de *splicing* de un pre-mRNA mutante o eliminan un mRNA patológico asociado a una determinada mutación. En este trabajo, se han ensayado distintas estrategias terapéuticas como son la sobreexpresión de diversos factores de *splicing* y de U1snRNAs modificados.

Para determinar la importancia de los distintos factores reguladores en el reconocimiento exónico y evaluar la posibilidad de nuevas aproximaciones terapéuticas, se ensayó el efecto de la sobreexpresión de diversos factores de *splicing* y proteínas SR. Las proteínas SR intervienen en el ensamblaje temprano del "spliceosoma", favoreciendo el reclutamiento y la estabilización de U1snRNP y el factor auxiliar de U2snRNP (U2AF) en los sitios 5´ y 3´de *splicing,* respectivamente (Kohtz et al., 1994; Staknis and Reed, 1994; Zuo and Maniatis, 1996), siendo estas interacciones esenciales para definir los límites exón-intrón. En el modelo de reconocimento exónico (*exon definition*), las proteínas SR se unen a múltiples

secuencias en el RNA e interaccionan simultáneamente con factores asociados en el sitio 5´ de *splicing* (U1-70K) y en el sitio 3´ del intrón (U2AF), a través de una red de interacciones proteína-proteína donde están implicados los dominios RS de estas proteínas. La función mejor caracterizada de las proteínas SR en el *splicing* alternativo es la regulación de sitios 3´ débiles, generalmente caracterizados por un sitio 3´ de *splicing* imperfecto pobremente reconocido por U2AF. A través de la unión a ESEs, las proteínas SR favorecen el reclutamiento de U2AF al sitio 3´ y seguidamente de U2snRNP (Zuo and Maniatis, 1996; Graveley et al., 2001; Guth et al., 2001).

Se ensayó el efecto de la **sobreexpresión de los factores U2AF35, U2AF65** y las **proteínas SR:** SC35, SRp40, SF2/ASF y SRp55 sobre las mutaciones descritas que afectan al sitio 3´ de *splicing*: c.1091-11del6, c.394-1G>C, y la mutación c.2041-2A>G que había sido previamente analizada en el laboratorio (Clavero et al., 2004). Se consiguió modular en cierta manera el patrón de *splicing* para la mutación c.2041-2A>G al sobreexpresar la proteína SC35 y el factor U2AF35, o bien con la cafeína que aumenta la expresión de SC35 tal y como se ha visto en genes asociados a cáncer (Shi et al., 2008). A pesar de que se modificó el perfil transcripcional, no se recuperó en ningún caso el perfil transcripcional normal ya que se producía la activación de un sitio críptico presente en el exón 23. Podemos concluir que, las mutaciones que afectan a las bases 100% conservadas como el *ag,* en el sitio 3´ de *splicing* y el *gt,* en el sitio 5´ de *splicing,* son mutaciones severas no modulables. La mutación c.1091-11del6 también se considera severa no modulable, ya que tampoco pudo recuperarse en ningún caso el perfil transcripcional normal, probablemente debido a que la secuencia polipirimidínica que se ve acortada, sea de alta importancia para el ensamblaje de los distintos factores y proteínas del "spliceosoma".

Por otra parte, la **sobreexpresión de la parte RNA de U1snRNP (U1snRNA)** ha sido ensayada para distintas mutaciones que afectan al sitio 5´de *splicing*, por considerarse la interacción por complementariedad de bases entre el sitio 5´de *splicing* y los 11 últimos nucleótidos del extremo 5´ de U1 snRNA, uno de los pasos fundamentales en la definición de este sitio de *splicing*. También se ha demostrado que un mayor apareamiento de bases entre ambas secuencias aumenta la inclusión exónica, la eficiencia del *splicing* y la estabilidad del pre-mRNA (Freund et al., 2005). Análisis funcionales e *in sílico* han determinado que una base desapareada entre U1snRNA y el sitio 5´ de *splicing* puede ser compensada por otros apareamientos de bases que mantengan la complementariedad dentro de un número mínimo de bases apareadas (Carmel et al., 2004; Clark and Thanaraj, 2002; Lund and Kjems, 2002; Roca et al., 2008).

Dentro de las mutaciones descritas que afectan al sitio 5´ donador de *splicing,* agrupadas en las inmediaciones de la unión exón-intrón, el 64% de ellas descritas en el HGMD afectan al dinucleótido conservado *gt* (Krawczak et al., 2007). Las mutaciones fuera del *gt* son más frecuentes en las posiciones -2,-1 del exón y del +3 al +6 del intrón adyacente (Krawczak et al., 2007).

En este trabajo, la sobreexpresión de U1snRNA se ha estudiado en detalle en los fibroblastos de 2 pacientes portadores de la mutación c.1209+3A>G (IVS13+3A>G), en

el gen *PCCA,* en homocigosis, identificada en un total de 7 alelos AP resultando en el *skipping* del exón 13. En humanos, en el sitio +3 ambas bases, A y G, están prácticamente igual de conservadas (Figura 29), habiéndose descrito variaciones similares (+3A>G) que provocan un *splicing* aberrante (Guedard-Mereuze et al., 2009). Respecto a la compensación por parte de otras bases, se ha descrito que, en concreto cuando en la posición +3 se localiza una guanina, el apareamiento correcto en las posiciones +4 a la +6 con el U1snRNA reduce las posibilidades de un defecto en el *splicing* (Guedard-Mereuze et al., 2009; Ohno et al., 1999).

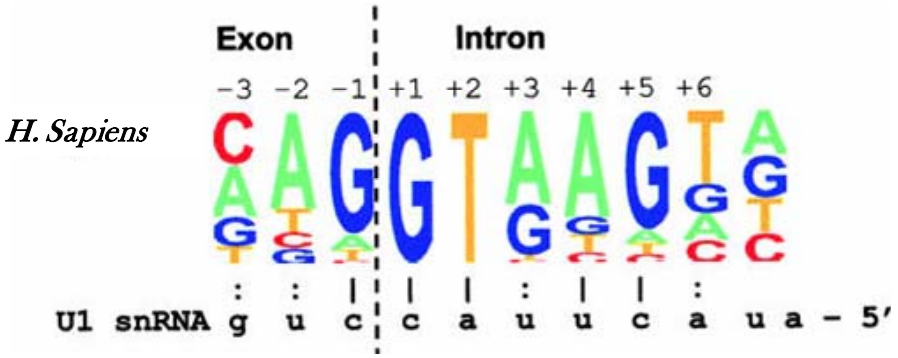

Figura 29: Complementariedad de bases entre el sitio 5´de *splicing* en humanos y U1snRNA. La altura de cada letra indica la frecuencia de los distintos nucleótido en cada una de las posiciones del sitio 5´ de *splicing* obtenidas a partir de la comparación de 49.778 secuencias 5´ de *splicing* (Carmel et al., 2004). La complementariedad de bases con el nucleótido correspondiente en U1snRNA está marcado por una barra vertical para apareamientos altamente frecuentes (>0,7%) o por dos puntos para los menos frecuentes (<0,7%). Imagen modificada de Carmel et al., 2004.

La sobreexpresión de distintos U1snRNAs *wildtype* y modificados compensatoriamente en la posición +3, así como en otros nucleótidos de unión a la secuencia mutante (Figura 22), fue ensayada en los fibroblastos de los pacientes portadores de la mutación c.1209+3A>G en homocigosis. Los resultados indican que, la falta de unión de U1snRNA al sitio 5´ de *splicing* es parcialmente responsable del *skipping* del exón 13 y confirma que, en este caso, el procesamiento correcto del mRNA no sólo depende de los niveles de U1snRNA, ya que la sobreexpresión de U1snRNA *wildtype* no es capaz de rescatar transcritos normales. De hecho, este patrón normal sólo se recupera cuando se introducen cambios además de en la posición +3, en las posiciones +5 o incluso +5 y +6. La recuperación completa, en la que el 100% de los transcritos son normales, sólo se observa con la construcción U1 IVS13 que tiene una complementariedad más extensa con la secuencia 5´ de *splicing* desde las posiciones -3 a la +8 (Figuras 22 y 23). El hecho de que la construcción U1+3C, aun recuperando el número de bases apareadas con el sitio 5´de *splicing* normal, no sea capaz de restablecer el perfil transcripcional, sugiere que la interacción entre ambas secuencias no es el único evento involucrado en el reconocimiento e inserción del exón. Es probable que la mutación afecte a la afinidad del sitio 5´ de *splicing* con otros factores. Se sabe que, en el paso siguiente de la unión de U1snRNP al sitio 5´de *splicing*, éste es desplazado por U6snRNP y U5snRNP que se unen en este mismo sitio (Lund and Kjems, 2002).

De manera que, según estos resultados, en nuestro modelo experimental, la sobreexpresión de un U1snRNA eficiente en revertir el defecto en el *splicing*, requiere la presencia de 7 pares de bases contiguas complementarias al sitio 5´ de *splicing*, una más que en la secuencia normal con U1 wildtype, así mismo, se observa la necesidad de la complementariedad de las bases en las posiciones +5 y +6 para observar una corrección del defecto en el *splicing*. Estos resultados concuerdan con los observados en trabajos similares en otros genes, en los que un U1snRNA de complementariedad más extensa ha sido necesario para la inclusión del exón, en ensayos realizados mediante minigenes (Guedard-Mereuze et al., 2009; Tanner et al., 2009).

Según nuestros datos, tras la utilización de las distintas construcciones de U1snRNAs modificados sobre las células de los pacientes, a pesar de haber observado, en algunos casos, una recuperación de prácticamente el 100% de transcritos normales, no se detectó recuperación de la proteína PCC, ni de la actividad enzimática, en ninguno de los casos. Se descartó la posibilidad de una contribución de transcritos mutantes alternativos, mediante un ensayo de RT-PCR semicuantitativa, en la que se utilizaron oligos fluorescentes y se analizaron los productos obtenidos por electroforesis capilar, en presencia y ausencia del inhibidor del NMD, wortmanina. Se observó que la mutación producía exclusivamente transcritos aberrantes con el *skipping* del exón 13 y que, tras el tratamiento con U1snRNA, se acumulaban niveles normales de transcritos correctamente procesados (Figura 24). Lo que no pudimos descartar fue un efecto inespecífico de U1snRNA en elementos claves necesarios para la traducción o el ensamblaje del heteropolímero PCC que impidiera la formación de una proteína activa, cómo nos pueden llevar a pensar los resultados obtenidos en la detección de la proteína PCCA tras la sobreexpresión de U1snRNAs modificados que resultó en la ausencia de proteína PCCA biotinilada (Figura 25). Se han descrito efectos sobre el *splicing* y la poliadenilación de algunos premRNAs con la utilización de U1snRNAs con extremos 5´ modificados (Gunderson et al., 1998), igualmente no se descartan posibles efectos en el complejo paso entre *splicing* y traducción, aún sin elucidar por completo (Cooper et al., 2009).

En otro tipo de aproximaciones, se ha recuperado en varias ocasiones proteína funcional y actividad enzimática PCC en fibroblastos de los pacientes después de la modulación del *splicing* con oligonucleótidos antisentido, dirigidos para impedir el reconocimiento de pseudoexones, que se introducen de manera aberrante en el mRNA. Es importante comentar que, en la sobreexpresión de U1 se utiliza una molécula de RNA que es un factor de *splicing* natural, modificado de manera que se una de una manera más estable al sitio 5´ de *splicing,* lo que podría inhibir la entrada de otros componentes del "spliceosoma", como el complejo trimérico U4/U6.U5, debido a un retraso en la liberación de U1snRNA del sitio 5´ de *splicing* en diferentes transcritos celulares.

La presencia de transcritos correctamente procesados en el mRNA completo de *PCCA* y *PCCB,* tras la sobreexpresión con U1snRNA, fue comprobada mediante secuenciación, pero otros mRNAs celulares pueden haberse visto afectados, por lo que para analizar a fondo esta cuestión, la aplicación de tecnologías basadas en *exon-array*

pueden ser útiles para la detección de transcritos alternativos. A este respecto, un trabajo muy reciente propone la utilización de U1snRNAs específicos para cada exón de estudio, localizados en secuencias intrónicas, aguas abajo del exón, que al no estar igual de conservadas reducirían la posibilidad de efectos indeseables en otros mRNAs celulares (Fernandez Alanis et al., 2012). Estos U1snRNAs son, además, capaces de recuperar el perfil transcripcional de mutaciones localizadas no sólo en secuencias 5´ de *splicing* sino también en el tracto polipirimidínico o en secuencias exónicas reguladoras, además de recuperar proteína funcional para varias mutaciones de *splicing* mediante la utilización de un vector de expresión como modelo celular de la deficiencia de uno de los factores de coagulación (Fernandez Alanis et al., 2012). Por todo esto, estos U1snRNAs se sugieren como una aproximación terapéutica prometedora para las mutaciones de *splicing*. Asimismo, la sobreexpresión de U1snRNA se ha ensayado en otros estudios en líneas celulares donde sí fue posible revertir parcialmente el fenotipo (Hartmann et al., 2010).

En resumen, tras este estudio, se concluye que la sobreexpresión de U1snRNAs modificados ha de ser analizada además de en minigenes, como ha sido descrito para diferentes genes (Crehalet et al., 2009; Pinotti et al., 2009; Pinotti et al., 2008; Susani et al., 2004; Tanner et al., 2009), en líneas celulares de los pacientes o modelos animales de la enfermedad, como primer paso de la investigación de la aplicabilidad *in vivo* de la terapia. En conjunto, resultados similares como los propuestos recientemente en Fernandez Alanis et al., 2012, aclararían cuestiones acerca de si la recuperación funcional que no ha sido posible rescatar en este estudio es específica del gen o de la mutación analizada. En cualquier caso, los resultados obtenidos sobre la modulación del *splicing* mediante la utilización de factores de *splicing* han de ser interpretados con precaución, ya que éstos ejercen diferentes funciones dentro de la célula (Buratti and Baralle, 2010), que podrían resultar en efectos indeseados que tendrían que ser analizados en detalle.

5.3.2. Mutaciones de *splicing* localizadas en regiones intrónicas profundas

En este trabajo, también hemos analizado dos mutaciones: c.1285-1416A>G (gen *PCCA*) y c.654+462A>G (gen *PCCB*), que se localizan en regiones intrónicas profundas generando la inclusión anormal de secuencias intrónicas (pseudoexones) en el mRNA. Según las predicciones *in silico*, el mecanismo molecular activado por estas dos mutaciones, bien está basado en un aumento en la complementariedad del sitio 5´ de *splicing* del pseudoexón con la secuencia de U1snRNP, lo que se refleja en el score de *splicing* que aumenta de 0,93 a 1 (mutación c.654+462A>G), o bien en el reclutamiento de factores de *splicing* auxiliares como SRp40 (mutación c.1285-1416A>G) (Tabla 8, Figura 20). Este último hecho no pudo ser demostrado experimentalmente mediante RNA interferente contra SRp40, bien porque éste no fuera el único factor implicado, o bien porque el nivel de bajada en la expresión de la proteína no fuera lo suficientemente importante para observar un cambio en el perfil transcripcional.

En aquellas enfermedades en las que se ha podido calcular, la frecuencia de las mutaciones que activan la inserción de un pseudoexón varía en torno al 2-5% de los alelos mutantes (Perez et al., 2010), aunque presumiblemente la frecuencia puede ser mayor debido a que en el análisis rutinario de genotipado de los pacientes, la secuenciación completa de los intrones no se lleva a cabo, además de que, en muchas ocasiones, estos transcritos resultan en un cambio en la pauta de lectura y la inclusión de un PTC y son degradados por el mecanismo NMD. El tratamiento de las células de los pacientes con cicloheximida, emetina, puromicina u otros compuestos que eviten el NMD puede ayudar a la identificación de estas mutaciones difíciles de localizar en el análisis en cDNA.

Para estas mutaciones que activan la inserción de pseudoexones, en este trabajo, se han utilizado **oligonucleótidos antisentido (AONs)** modificados que actúan bloqueando, por impedimento estérico, el reconocimiento y la unión de componentes del "spliceosoma" al pseudoexón, forzando así a la maquinaria de *splicing* a utilizar los sitios naturales. En un estudio anterior, se ensayó, concretamente la utilización de AONs tipo mofolino en los fibroblastos de dos pacientes AP, portadores en homocigosis de las mutaciones c.1285-1416A>G (gen *PCCA*) y c.654+462A>G (gen *PCCB*) recuperándose en ambos casos valores de actividad normal. El efecto de la transfección con los AONs persiste hasta 15 días después de la transfección (Perez et al., 2009). La recuperación de la actividad, al impedir la incorporación del pseudoexón en el mRNA, demuestra que esta inserción es la causa de enfermedad en estos pacientes y que esta aproximación terapéutica puede ser aplicada a pacientes con este tipo de defectos en cualquier gen.

En este trabajo, se empleó esta misma aproximación sobre fibroblastos de un paciente portador de la mutación c.654+462A>G (gen *PCCB*) en heterocigosis, demostrando que existe recuperación parcial de la actividad PCC alcanzándose valores muy próximos a la normalidad. Estos valores pueden considerarse terapéuticamente significativos teniendo en cuenta que para enfermedades recesivas, una actividad residual está asociada con fenotipos intermedios, y que en modelos animales las consecuencias de la enfermedad pueden mejorar incluso con una baja expresión de los niveles de un transgen (Miyazaki et al., 2001).

Además de en acidemia propiónica, esta terapia ha sido utilizada con éxito en otras EMH, como la aciduria metilmalónica, donde se identificaron dos mutaciones intrónicas diferentes que producen la inserción del mismo pseudoexón, que fue eficientemente excluido, recuperando la actividad enzimática (Perez et al., 2009). También ha sido ensayada en un paciente con deficiencia en fosfomanomutasa 2 (PMM2), portador de una mutación en heterocigosis responsable de la inserción de un pseudoexón, donde se obtuvieron resultados similares, con un 23% de proteína inmunorreactiva y un 50 % de actividad recuperadas (Vega et al., 2009). Además de en la deficiencia de 6-pyruvoiltetrahidrobiopterina sintasa (PTPS) (Brasil et al., 2011) y en la enfermedad de Niemann-Pick tipo C (Rodriguez-Pascau et al., 2009). En todos estos casos, los AONs modificados utilizado han sido también tipo morfolino, observándose que la corrección sobre el perfil transcripcional ha sido dosis y secuencia específica, sin observarse signos evidentes de citotoxicidad.

Las mayores dificultades para la utilización *in vivo* de estos AONs, es su vehiculización para que puedan llegar a tejidos de interés, así como la determinación de la dosis óptima que permita obtener simultáneamente la recuperación de los transcritos de interés, sin provocar una toxicidad elevada. Si el AON es administrado sistémicamente debe ser estable en el torrente sanguíneo, resistente a nucleasas, capaz de llegar a las células diana, cruzar la membrana celular, escapar de los endosomas celulares y llegar al núcleo. Con este propósito, se han desarrollado un amplio grupo de derivados de nucleótidos, de nueva generación, modificados químicamente, bien sea en la propia ribosa, mediante la utilización de bases no naturales o mediante alteraciones en el esqueleto fosfato (Kurreck, 2003), entre los que se encuentran, además de los morfolinos utilizados en este trabajo, los *locked nucleic acid* (LNA), que presentan mayor afinidad y más específica a la secuencia diana, resultando en una alta eficiencia a bajas concentraciones (Guterstam et al., 2008). Como agentes de vehiculización de los AONs, se están evaluando los péptidos catiónicos (Du et al., 2011) o la utilización de nanopartículas poliméricas tipo dendrímeros (Dufes et al., 2005). Las nanopartículas de varios tipos ofrecen muchas ventajas como agentes de vehiculización ya que pueden llevar cientos de copias de AONs y pueden ser conjugados con ligandos que le confieran gran afinidad por las células diana. La eficacia de un dendrímero octa-guanidino covalentemente unido a un oligomero antisentido tipo morfolino (vivo-morfolino) ha resultado ser efectivo en modelos celulares, entre ellos de aciduria metilmalónica y en la deficiencia de PTPS (Brasil et al., 2011; Perez et al., 2009), así como en modelos animales de DMD (Wu et al., 2009) y otras enfermedades (Osorio et al., 2011; Owen et al., 2012; Zammarchi et al., 2011).

Para enfermedades neurogenéticas, la incapacidad de los AONs de cruzar la barrera hematoencefálica y llegar de manera eficiente a células diana en el cerebro, limita en gran medida la aplicación clínica de esta estrategia terapéutica. En este sentido, tanto los péptidos catiónicos ricos en arginina (Du et al., 2011), como los dendrímeros carbosilanos (Jimenez et al., 2010), han sido utilizados dirigidos a células del cerebro con resultados prometedores.

La terapia antisentido ensayada en este trabajo tiene la ventaja de que el mRNA correctamente procesado es transcrito en su contexto y mediante su maquinaria natural, siendo más fácil de implementar que la terapia génica. Por otro lado, es específica para cada gen y mutación en concreto, por lo que la aplicación terapéutica de cada AON se limita a uno o pocos pacientes, siendo englobada dentro de la tendencia actual de una medicina personalizada, dirigida a mutaciones concretas, identificadas en cada paciente. Hasta la fecha, los estudios tanto en modelos animales (Alter et al., 2006), como en ensayos clínicos en humanos en DMD son prometedores con resultados que muestran una buena eficacia bioquímica y un buen perfil de seguridad (Cirak et al., 2011 ; Goemans et al., 2011).

En resumen, los resultados presentados en este trabajo tienen un claro valor diagnóstico, habiéndose identificado por primera vez CNVs en el gen *PCCA* mediante la técnica de MLPA, con lo que el porcentaje de detección de mutaciones en este gen ha

ascendido a ~98,5%, implementándose esta técnica en el laboratorio como complementaria para el diagnóstico de pacientes con defectos en el gen *PCCA*. Asimismo, se ha caracterizado el efecto de variantes nucleotídicas exónicas o intrónicas, presentes en varios genes responsables de distintas EMH, sobre el *splicing*. Por otra parte, los resultados que se presentan tienen un valor terapéutico añadido, ya que se demuestra que las mutaciones sin sentido identificadas en los genes *PCCA* y *PCCB* son susceptibles al tratamiento con compuestos supresores de la terminación de la traducción, y que algunas de las mutaciones de *splicing*, identificadas en varios genes responsables de distintas EMH, pueden ser moduladas bien mediante la sobreexpresión de factores de *splicing* o U1snRNAs modificados, o bien mediante la terapia antisentido utilizada para mutaciones intrónicas responsables de la inserción de un pseudoexón, lo que resulta en una recuperación funcional terapéuticamente relevante.

6. CONCLUSIONES

1. Se ha implementado la utilidad de la técnica MLPA para el genotipado de los pacientes de AP con defectos en el gen *PCCA,* ya que se han identificado y caracterizado CNVs patogénicas en un 21% de los alelos mutantes.

2. Se ha establecido la prueba de concepto de que las mutaciones sin sentido en AP pueden ser susceptibles a la supresión de la terminación mediada por distintos compuestos, con diferentes eficiencias dependiendo de la mutación y la secuencia contexto, demostrando una recuperación funcional terapéuticamente relevante en las células de los pacientes. Estos resultados indican que la utilización de compuestos supresores de la terminación puede ser una terapia alternativa o complementaria para un grupo de pacientes AP.

3. El análisis *in silico* y funcional mediante minigenes de variantes nucleotídicas exónicas e intrónicas, identificadas en distintos genes responsables de EMH, ha permitido confirmar su implicación en defectos de *splicing* y explicar el mecanismo molecular subyacente a la expresión fenotípica de la enfermedad.

4. El patrón aberrante de *splicing* asociado a determinadas mutaciones ha podido ser modulado mediante la sobreexpresión de factores de *splicing* y de U1snRNAs complementarios a la secuencia mutante del sitio 5´de *splicing*, lo cual podría ser la base de futuras estrategias terapéuticas.

5. Se ha confirmado la eficiencia de la terapia antisentido para revertir el efecto de una mutación que genera la exonización de una secuencia intrónica, con una recuperación funcional cercana a la normalidad, aun encontrándose la mutación en heterocigosis.

6. Los resultados presentados en este trabajo han permitido profundizar en el conocimiento de los mecanismos patogénicos de las diferentes variantes alélicas, aportando una base científica para la aplicación e investigación de nuevas aproximaciones terapéuticas específicas de mutación.

7. BIBLIOGRAFÍA

Abeysinghe, S.S., Chuzhanova, N., Krawczak, M., Ball, E.V. and Cooper, D.N. (2003) Translocation and gross deletion breakpoints in human inherited disease and cancer I: Nucleotide composition and recombination-associated motifs. *Hum Mutat*, **22**, 229-244.

Al Essa, M., Rahbeeni, Z., Jumaah, S., Joshi, S., Al Jishi, E., Rashed, M.S., Al Amoudi, M. and Ozand, P.T. (1998) Infectious complications of propionic acidemia in Saudia Arabia. *Clin Genet*, **54**, 90-94.

Alter, J., Lou, F., Rabinowitz, A., Yin, H., Rosenfeld, J., Wilton, S.D., Partridge, T.A. and Lu, Q.L. (2006) Systemic delivery of morpholino oligonucleotide restores dystrophin expression bodywide and improves dystrophic pathology. *Nat Med*, **12**, 175-177.

Andreassi, C., Jarecki, J., Zhou, J., Coovert, D.D., Monani, U.R., Chen, X., Whitney, M., Pollok, B., Zhang, M., Androphy, E. and Burghes, A.H. (2001) Aclarubicin treatment restores SMN levels to cells derived from type I spinal muscular atrophy patients. *Hum Mol Genet*, **10**, 2841-2849.

Bain, M.D., Jones, M., Borriello, S.P., Reed, P.J., Tracey, B.M., Chalmers, R.A. and Stacey, T.E. (1988) Contribution of gut bacterial metabolism to human metabolic disease. *Lancet*, **1**, 1078-1079.

Baralle, D. and Baralle, M. (2005) Splicing in action: assessing disease causing sequence changes. *J Med Genet*, **42**, 737-748.

Baumgartner, M.R., Almashanu, S., Suormala, T., Obie, C., Baumgartner, E.R. and Valle, D. (2001) 3-methylcrotonyl-CoA carboxylase deficiency: extension of molecular analysis to patients detected by tandem MS based newborn screening. *J Inher Metab Dis*, **24**, 57.

Beckmann, J.S., Estivill, X. and Antonarakis, S.E. (2007) Copy number variants and genetic traits: closer to the resolution of phenotypic to genotypic variability. *Nat Rev Genet*, **8**, 639-646.

Bedwell, D.M., Kaenjak, A., Benos, D.J., Bebok, Z., Bubien, J.K., Hong, J., Tousson, A., Clancy, J.P. and Sorscher, E.J. (1997) Suppression of a CFTR premature stop mutation in a bronchial epithelial cell line. *Nat Med*, **3**, 1280-1284.

Behm-Ansmant, I., Kashima, I., Rehwinkel, J., Sauliere, J., Wittkopp, N. and Izaurralde, E. (2007) mRNA quality control: an ancient machinery recognizes and degrades mRNAs with nonsense codons. *FEBS Lett*, **581**, 2845-2853.

Bellais, S., Le Goff, C., Dagoneau, N., Munnich, A. and Cormier-Daire, V. (2010) In vitro readthrough of termination codons by gentamycin in the Stuve-Wiedemann Syndrome. *Eur J Hum Genet*, **18**, 130-132.

Bergman, I., Finegold, D., Gartner, J.C., Jr., Zitelli, B.J., Claassen, D., Scarano, J., Roe, C.R., Stanley, C. and Goodman, S.I. (1989) Acute profound dystonia in infants with glutaric acidemia. *Pediatrics*, **83**, 228-234.

Blau, N., Thony, B., Cotton, G.H. and Hyland, K. (2001) Disorders of tetrahydrobioterin and related biogenic amines. In Scriver, C.R., Beaudet, A.L., Sly, W.S., Valle, D., Childs, B. and Vogelstein, B. (eds.), *The Metabolic and Molecular Basis of Inherited Disease*. McGraw-Hill, New York, pp. 1725-1776.

Bonafe, L., Thony, B., Leimbacher, W., Kierat, L. and Blau, N. (2001a) Diagnosis of dopa-responsive dystonia and other tetrahydrobiopterin disorders by the study of biopterin metabolism in fibroblasts. *Clin Chem*, **47**, 477-485.

Bonafe, L., Thony, B., Penzien, J.M., Czarnecki, B. and Blau, N. (2001b) Mutations in the sepiapterin reductase gene cause a novel tetrahydrobiopterin-dependent monoamine-neurotransmitter deficiency without hyperphenylalaninemia. *Am J Hum Genet*, **69**, 269-277.

Bradford, M.M. (1976) A rapid and sensitive method for the quantitation of microgram quantities of protein utilizing the principle of protein-dye binding. *Anal. Biochem.*, **72**, 248-254.

Brasil, S., Viecelli, H.M., Meili, D., Rassi, A., Desviat, L.R., Perez, B., Ugarte, M. and Thony, B. (2011) Pseudoexon exclusion by antisense therapy in 6-pyruvoyl-tetrahydropterin synthase deficiency. *Hum Mutat*.

Brooks, D.A., Muller, V.J. and Hopwood, J.J. (2006) Stop-codon read-through for patients affected by a lysosomal storage disorder. *Trends Mol Med*, **12**, 367-373.

Brosch, S., Rauffeisen, A., Baur, M., Michels, L., Trefz, F.K. and Pfister, M. (2008) [Propionic acidemia and sensorineural hearing loss: is there a connection at the molecular genetics level?]. *HNO*, **56**, 37-42.

Buck, N.E., Wood, L., Hu, R. and Peters, H.L. (2009) Stop codon read-through of a Methylmalonic aciduria mutation. *Mol Genet Metab*, **97**, 244-249.

Buratti, E. and Baralle, D. (2010) Novel roles of U1 snRNP in alternative splicing regulation. *RNA Biol*, **7**.

Buratti, E., Baralle, M. and Baralle, F.E. (2006) Defective splicing, disease and therapy: searching for master checkpoints in exon definition. *Nucleic Acids Res*, **34**, 3494-3510.

Caceres, J.F., Screaton, G.R. and Krainer, A.R. (1998) A specific subset of SR proteins shuttles continuously between the nucleus and the cytoplasm. *Genes Dev*, **12**, 55-66.

Campeau, E., Desviat, L.R., Leclerc, D., Wu, X., Perez, B., Ugarte, M. and Gravel, R.A. (2001) Structure of the PCCA gene and distribution of mutations causing propionic acidemia. *Mol Genet Metab*, **74**, 238-247.

Campeau, E., Dupuis, L., Leclerc, D. and Gravel, R.A. (1999) Detection of a normally rare transcript in propionic acidemia patients with mRNA destabilizing mutations in the PCCA gene. *Hum Mol Genet*, **8**, 107-113.

Carmel, I., Tal, S., Vig, I. and Ast, G. (2004) Comparative analysis detects dependencies among the 5' splice-site positions. *Rna*, **10**, 828-840.

Cartegni, L., Chew, S.L. and Krainer, A.R. (2002) Listening to silence and understanding nonsense: exonic mutations that affect splicing. *Nat Rev Genet*, **3**, 285-298.

Cartegni, L., Wang, J., Zhu, Z., Zhang, M.Q. and Krainer, A.R. (2003) ESEfinder: A web resource to identify exonic splicing enhancers. *Nucleic Acids Res*, **31**, 3568-3571.

Cirak, S., Arechavala-Gomeza, V., Guglieri, M., Feng, L., Torelli, S., Anthony, K., Abbs, S., Garralda, M.E., Bourke, J., Wells, D.J., Dickson, G., Wood, M.J., Wilton, S.D., Straub, V., Kole, R., Shrewsbury, S.B., Sewry, C., Morgan, J.E., Bushby, K. and Muntoni, F. (2011) Exon skipping and dystrophin restoration in patients with Duchenne muscular dystrophy after systemic phosphorodiamidate morpholino oligomer treatment: an open-label, phase 2, dose-escalation study. *Lancet*, **378**, 595-605.

Clancy, J.P., Bebok, Z., Ruiz, F., King, C., Jones, J., Walker, L., Greer, H., Hong, J., Wing, L., Macaluso, M., Lyrene, R., Sorscher, E.J. and Bedwell, D.M. (2001) Evidence that systemic gentamicin suppresses premature stop mutations in patients with cystic fibrosis. *Am J Respir Crit Care Med*, **163**, 1683-1692.

Clark, F. and Thanaraj, T.A. (2002) Categorization and characterization of transcript-confirmed constitutively and alternatively spliced introns and exons from human. *Hum Mol Genet*, **11**, 451-464.

Clavero, S., Martinez, M.A., Perez, B., Perez-Cerda, C., Ugarte, M. and Desviat, L.R. (2002) Functional characterization of

PCCA mutations causing propionic acidemia. *Biochim Biophys Acta*, **1588**, 119-125.

Clavero, S., Perez, B., Rincon, A., Ugarte, M. and Desviat, L.R. (2004) Qualitative and quantitative analysis of the effect of splicing mutations in propionic acidemia underlying non-severe phenotypes. *Hum Genet*, **115**, 239-247.

Coelho, D., Suormala, T., Stucki, M., Lerner-Ellis, J.P., Rosenblatt, D.S., Newbold, R.F., Baumgartner, M.R. and Fowler, B. (2008) Gene identification for the cblD defect of vitamin B12 metabolism. *N Engl J Med*, **358**, 1454-1464.

Cooper, D.N., Stenson, P.D. and Chuzhanova, N.A. (2006) The Human Gene Mutation Database (HGMD) and its exploitation in the study of mutational mechanisms. *Curr Protoc Bioinformatics*, **Chapter 1**, Unit 1 13.

Cooper, T.A. (2005) Use of minigene systems to dissect alternative splicing elements. *Methods*, **37**, 331-340.

Cooper, T.A., Wan, L. and Dreyfuss, G. (2009) RNA and disease. *Cell*, **136**, 777-793.

Coude, F.X., Sweetman, L. and Nyhan, W.L. (1979) Inhibition by propionyl-coenzyme A of N-acetylglutamate synthetase in rat liver mitochondria. A possible explanation for hyperammonemia in propionic and methylmalonic acidemia. *J Clin Invest*, **64**, 1544-1551.

Crehalet, H., Latour, P., Bonnet, V., Attarian, S., Labauge, P., Bonello, N., Bernard, R., Millat, G., Rousson, R. and Bozon, D. (2009) U1 snRNA mis-binding: a new cause of CMT1B. *Neurogenetics*, **11**, 13-19.

Chuzhanova, N., Abeysinghe, S.S., Krawczak, M. and Cooper, D.N. (2003) Translocation and gross deletion breakpoints in human inherited disease and cancer II: Potential involvement of repetitive sequence elements in secondary structure formation between DNA ends. *Hum Mutat*, **22**, 245-251.

Dalphin, M.E., Stockwell, P.A., Tate, W.P. and Brown, C.M. (1999) TransTerm, the translational signal database, extended to include full coding sequences and untranslated regions. *Nucleic Acids Res*, **27**, 293-294.

David, C.J. and Manley, J.L. (2008) The search for alternative splicing regulators: new approaches offer a path to a splicing code. *Genes Dev*, **22**, 279-285.

Den Dunnen, J.T., Grootscholten, P.M., Bakker, E., Blonden, L.A., Ginjaar, H.B., Wapenaar, M.C., van Paassen, H.M., van Broeckhoven, C., Pearson, P.L. and van Ommen, G.J. (1989) Topography of the Duchenne muscular dystrophy (DMD) gene: FIGE and cDNA analysis of 194 cases reveals 115 deletions and 13 duplications. *Am J Hum Genet*, **45**, 835-847.

Desmet, F.O., Hamroun, D., Lalande, M., Collod-Beroud, G., Claustres, M. and Beroud, C. (2009) Human Splicing Finder: an online bioinformatics tool to predict splicing signals. *Nucleic Acids Res*, **37**, e67.

Desviat, L.R., Clavero, S., Perez-Cerda, C., Navarrete, R., Ugarte, M. and Perez, B. (2006a) New splicing mutations in propionic acidemia. *J Hum Genet*, **51**, 992-997.

Desviat, L.R., Perez, B., Perez-Cerda, C., Rodriguez-Pombo, P., Clavero, S. and Ugarte, M. (2004) Propionic acidemia: mutation update and functional and structural effects of the variant alleles. *Mol Genet Metab*, **83**, 28-37.

Desviat, L.R., Perez, B. and Ugarte, M. (2006b) Identification of exonic deletions in the PAH gene causing phenylketonuria by MLPA analysis. *Clin Chim Acta*, **373**, 164-167.

Desviat, L.R., Pérez, B. and Ugarte, M. (2001) Bases moleculares de las enfermedades metabólicas hereditarias. In Sanjurjo, P., Baldellou, A. and Ergon, S. (eds.), *Diagnóstico y tratamiento de las enfermedades metabólicas hereditarias*, Madrid, pp. 1-13.

Dhir, A. and Buratti, E. (2010) Alternative splicing: role of pseudoexons in human disease and potential therapeutic strategies. *Febs J*, **277**, 841-855.

Dietz, H.C. (2011) New therapeutic approaches to mendelian disorders. *N Engl J Med*, **363**, 852-863.

Dranchak, P.K., Di Pietro, E., Snowden, A., Oesch, N., Braverman, N.E., Steinberg, S.J. and Hacia, J.G. (2011) Nonsense suppressor therapies rescue peroxisome lipid metabolism and assembly in cells from patients with specific PEX gene mutations. *J Cell Biochem*, **112**, 1250-1258.

Du, L., Damoiseaux, R., Nahas, S., Gao, K., Hu, H., Pollard, J.M., Goldstine, J., Jung, M.E., Henning, S.M., Bertoni, C. and Gatti, R.A. (2009) Nonaminoglycoside compounds induce readthrough of nonsense mutations. *J Exp Med*, **206**, 2285-2297.

Du, L., Kayali, R., Bertoni, C., Fike, F., Hu, H., Iversen, P.L. and Gatti, R.A. (2011) Arginine-rich cell-penetrating peptide dramatically enhances AMO-mediated ATM aberrant splicing correction and enables delivery to brain and cerebellum. *Hum Mol Genet*, **20**, 3151-3160.

Du, L., Pollard, J.M. and Gatti, R.A. (2007) Correction of prototypic ATM splicing mutations and aberrant ATM function with antisense morpholino oligonucleotides. *Proc Natl Acad Sci U S A*, **104**, 6007-6012.

Du, M., Liu, X., Welch, E.M., Hirawat, S., Peltz, S.W. and Bedwell, D.M. (2008) PTC124 is an orally bioavailable compound that promotes suppression of the human CFTR-G542X nonsense allele in a CF mouse model. *Proc Natl Acad Sci U S A*, **105**, 2064-2069.

Dufes, C., Uchegbu, I.F. and Schatzlein, A.G. (2005) Dendrimers in gene delivery. *Adv Drug Deliv Rev*, **57**, 2177-2202.

Dunant, P., Walter, M.C., Karpati, G. and Lochmuller, H. (2003) Gentamicin fails to increase dystrophin expression in dystrophin-deficient muscle. *Muscle Nerve*, **27**, 624-627.

Echenne, B., Roubertie, A., Assmann, B., Lutz, T., Penzien, J.M., Thony, B., Blau, N. and Hoffmann, G.F. (2006) Sepiapterin reductase deficiency: clinical presentation and evaluation of long-term therapy. *Pediatr Neurol*, **35**, 308-313.

Fearon, K., McClendon, V., Bonetti, B. and Bedwell, D.M. (1994) Premature translation termination mutations are efficiently suppressed in a highly conserved region of yeast Ste6p, a member of the ATP-binding cassette (ABC) transporter family. *J Biol Chem*, **269**, 17802-17808.

Fenton, W.A., Gravel, R.A. and Rosenberg, L.E. (2001) Disorders of propionate and methylmalonate metabolism. In Scriver, C.R., Beaudet, A.L., Sly, W. and Valle, D. (eds.), *The Metabolic and Molecular Bases of Inherited Disease*. McGraw-Hill, New York, pp. 2165-2190.

Fernandez Alanis, E., Pinotti, M., Dal Mas, A., Balestra, D., Cavallari, N., Rogalska, M.E., Bernardi, F. and Pagani, F. (2012) An exon-specific U1 small nuclear RNA (snRNA) strategy to correct splicing defects. *Hum Mol Genet*.

Font-Llitjos, M., Rodriguez-Santiago, B., Espino, M., Sillue, R., Manas, S., Gomez, L., Perez-Jurado, L.A., Palacin, M. and Nunes, V. (2009) Novel SLC7A7 large rearrangements in lysinuric protein intolerance patients involving the same AluY repeat. *Eur J Hum Genet*, **17**, 71-79.

Freund, M., Hicks, M.J., Konermann, C., Otte, M., Hertel, K.J. and Schaal, H. (2005) Extended base pair complementarity between U1 snRNA and the 5' splice site does not inhibit splicing in higher eukaryotes, but rather increases 5' splice site recognition. *Nucleic Acids Res*, **33**, 5112-5119.

Frischmeyer, P.A. and Dietz, H.C. (1999) Nonsense-mediated mRNA decay in health and disease. *Hum Mol Genet*, **8**, 1893-1900.

Gabut, M., Chaudhry, S. and Blencowe, B.J. (2008) SnapShot: The splicing regulatory machinery. *Cell*, **133**, 192 e191.

Garrod, A.E. (1975) The Lancet. The incidence of alkaptonuria: a study in chemical individuality. *Nutr Rev*, **33**, 81-83.

Goemans, N.M., Tulinius, M., van den Akker, J.T., Burm, B.E., Ekhart, P.F., Heuvelmans, N., Holling, T., Janson, A.A., Platenburg, G.J., Sipkens, J.A., Sitsen, J.M., Aartsma-Rus, A., van Ommen, G.J., Buyse, G., Darin, N., Verschuuren, J.J., Campion, G.V., de Kimpe, S.J. and van Deutekom, J.C. (2011) Systemic administration of PRO051 in Duchenne's muscular dystrophy. *N Engl J Med*, **364**, 1513-1522.

Graveley, B.R., Hertel, K.J. and Maniatis, T. (2001) The role of U2AF35 and U2AF65 in enhancer-dependent splicing. *Rna*, **7**, 806-818.

Guedard-Mereuze, S.L., Vache, C., Molinari, N., Vaudaine, J., Claustres, M., Roux, A.F. and Tuffery-Giraud, S. (2009) Sequence contexts that determine the pathogenicity of base substitutions at position +3 of donor splice-sites. *Hum Mutat*, **30**, 1329-1339.

Gunderson, S.I., Polycarpou-Schwarz, M. and Mattaj, I.W. (1998) U1 snRNP inhibits pre-mRNA polyadenylation through a direct interaction between U1 70K and poly(A) polymerase. *Mol Cell*, **1**, 255-264.

Guterstam, P., Lindgren, M., Johansson, H., Tedebark, U., Wengel, J., El Andaloussi, S. and Langel, U. (2008) Splice-switching efficiency and specificity for oligonucleotides with locked nucleic acid monomers. *Biochem J*, **412**, 307-313.

Guth, S., Tange, T.O., Kellenberger, E. and Valcarcel, J. (2001) Dual function for U2AF(35) in AG-dependent pre-mRNA splicing. *Mol Cell Biol*, **21**, 7673-7681.

Hainrichson, M., Nudelman, I. and Baasov, T. (2008) Designer aminoglycosides: the race to develop improved antibiotics and compounds for the treatment of human genetic diseases. *Org Biomol Chem*, **6**, 227-239.

Harrell, L., Melcher, U. and Atkins, J.F. (2002) Predominance of six different hexanucleotide recoding signals 3' of read-through stop codons. *Nucleic Acids Res*, **30**, 2011-2017.

Hartmann, L., Neveling, K., Borkens, S., Schneider, H., Freund, M., Grassman, E., Theiss, S., Wawer, A., Burdach, S., Auerbach, A.D., Schindler, D., Hanenberg, H. and Schaal, H. (2010) Correct mRNA processing at a mutant TT splice donor in FANCC ameliorates the clinical phenotype in patients and is enhanced by delivery of suppressor U1 snRNAs. *Am J Hum Genet*, **87**, 480-493.

Hartmann, L., Theiss, S., Niederacher, D. and Schaal, H. (2008) Diagnostics of pathogenic splicing mutations: does bioinformatics cover all bases? *Frontiers in Biosciences*, **13**, 3252-3272.

Hayasaka, K., Narisawa, K., Satoh, T., Tateda, H., Metoki, K., Tada, K., Hiraga, K., Aoki, T., Kawakami, T., Akamatsu, H. and Matsuo, N. (1982) Glycine cleavage system in ketotic hyperglycinemia: a reduction of H-protein activity. *Pediatr Res*, **16**, 5-7.

Hein, L.K., Bawden, M., Muller, V.J., Sillence, D., Hopwood, J.J. and Brooks, D.A. (2004) alpha-L-iduronidase premature stop codons and potential read-through in mucopolysaccharidosis type I patients. *J Mol Biol*, **338**, 453-462.

Hims, M.M., Ibrahim, E.C., Leyne, M., Mull, J., Liu, L., Lazaro, C., Shetty, R.S., Gill, S., Gusella, J.F., Reed, R. and Slaugenhaupt, S.A. (2007) Therapeutic potential and mechanism of kinetin as a treatment for the human splicing disease familial dysautonomia. *J Mol Med*, **85**, 149-161.

Hofherr, S.E., Senac, J.S., Chen, C.Y., Palmer, D.J., Ng, P. and Barry, M.A. (2009) Short-term rescue of neonatal lethality in a mouse model of propionic acidemia by gene therapy. *Hum Gene Ther*, **20**, 169-180.

Howard, M., Frizzell, R.A. and Bedwell, D.M. (1996) Aminoglycoside antibiotics restore CFTR function by overcoming premature stop mutations. *Nat Med*, **2**, 467-469.

Huang, C.S., Sadre-Bazzaz, K., Shen, Y., Deng, B., Zhou, Z.H. and Tong, L. (2010) Crystal structure of the alpha(6)beta(6) holoenzyme of propionyl-coenzyme A carboxylase. *Nature*, **466**, 1001-1005.

James, P.D., Raut, S., Rivard, G.E., Poon, M.C., Warner, M., McKenna, S., Leggo, J. and Lillicrap, D. (2005) Aminoglycoside suppression of nonsense mutations in severe hemophilia. *Blood*, **106**, 3043-3048.

Jimenez, J.L., Clemente, M.I., Weber, N.D., Sanchez, J., Ortega, P., de la Mata, F.J., Gomez, R., Garcia, D., Lopez-Fernandez, L.A. and Munoz-Fernandez, M.A. (2010) Carbosilane dendrimers to transfect human astrocytes with small interfering RNA targeting human immunodeficiency virus. *BioDrugs*, **24**, 331-343.

John, S.W.M., Weitzner, G., Rozen, R. and Scriver, C.R. (1991) A Rapid Procedure for Extracting Genomic DNA from Leukocytes. *Nucl. Acids Res.*, **19**, 408.

Kanno, J., Hutchin, T., Kamada, F., Narisawa, A., Aoki, Y., Matsubara, Y. and Kure, S. (2007) Genomic deletion within GLDC is a major cause of non-ketotic hyperglycinaemia. *J Med Genet*, **44**, e69.

Kaya, N., Al-Owain, M., Albakheet, A., Colak, D., Al-Odaib, A., Imtiaz, F., Coskun, S., Al-Sayed, M., Al-Hassnan, Z., Al-Zaidan, H., Meyer, B. and Ozand, P. (2008) Array comparative genomic hybridization (aCGH) reveals the largest novel deletion in PCCA found in a Saudi family with propionic acidemia. *Eur J Med Genet*.

Kayler, L.K., Merion, R.M., Lee, S., Sung, R.S., Punch, J.D., Rudich, S.M., Turcotte, J.G., Campbell, D.A., Jr., Holmes, R. and Magee, J.C. (2002) Long-term survival after liver transplantation in children with metabolic disorders. *Pediatr Transplant*, **6**, 295-300.

Keeling, K.M. and Bedwell, D.M. (2010) *Recoding therapies for genetic diseases*. In: Atkins JF, Gesteland RF, eds. Recoding Expansion of Decoding Rules Enriches Gene Expression. Springer Publishing, New York.

Keeling, K.M. and Bedwell, D.M.(2011) Suppression of nonsense mutations as a therapeutic approach to treat genetic diseases. *Wiley Interdiscip Rev RNA*, **2**, 837-852.

Keeling, K.M. and Bedwell, D.M. (2002) Clinically relevant aminoglycosides can suppress disease-associated premature stop mutations in the IDUA and P53 cDNAs in a mammalian translation system. *J Mol Med*, **80**, 367-376.

Keeling, K.M., Brooks, D.A., Hopwood, J.J., Li, P., Thompson, J.N. and Bedwell, D.M. (2001) Gentamicin-mediated suppression of Hurler syndrome stop mutations restores a low level of alpha-L-iduronidase activity and reduces lysosomal glycosaminoglycan accumulation. *Hum Mol Genet*, **10**, 291-299.

Kellermayer, R., Szigeti, R., Keeling, K.M., Bedekovics, T. and Bedwell, D.M. (2006) Aminoglycosides as potential pharmacogenetic agents in the treatment of Hailey-Hailey disease. *J Invest Dermatol*, **126**, 229-231.

Kennerknecht, I., Klett, C. and Hameister, H. (1992) Assignment of the human gene propionyl coenzyme A carboxylase, alpha-chain, (PCCA) to chromosome 13q32 by in situ hybridization. *Genomics*, **14**, 550-551.

Kerem, E., Hirawat, S., Armoni, S., Yaakov, Y., Shoseyov, D., Cohen, M., Nissim-Rafinia, M., Blau, H., Rivlin, J., Aviram, M., Elfring, G.L., Northcutt, V.J., Miller, L.L., Kerem, B. and Wilschanski, M. (2008) Effectiveness of PTC124 treatment of cystic fibrosis caused by nonsense mutations: a prospective phase II trial. *Lancet*, **372**, 719-727.

Kohtz, J.D., Jamison, S.F., Will, C.L., Zuo, P., Luhrmann, R., Garcia-Blanco, M.A. and Manley, J.L. (1994) Protein-protein interactions and 5'-splice-site recognition in mammalian mRNA precursors. *Nature*, **368**, 119-124.

Kolvraa, S. (1979) Inhibition of the glycine cleavage system by branched-chain amino acid metabolites. *Pediatr Res*, **13**, 889-893.

Kong, J. and Liebhaber, S.A. (2007) A cell type-restricted mRNA surveillance pathway triggered by ribosome extension into the 3' untranslated region. *Nat Struct Mol Biol*, **14**, 670-676.

Kraus, J.P., Williamson, C., Firgaira, F., Yang-Feng, T., Münke, M., Francke, U. and Rosenberg, L.E. (1986) Cloning and screening with nanogram amounts of immunopurified mRNAs: cDNA clonning and chromosomal mapping of cystathionine b-synthase and the b subunit of propionyl-CoA carboxylase. *Proc Natl Acad Sci U S A*, **83**, 2047-2051.

Krawczak, M., Reiss, J. and Cooper, D.N. (1992) The mutational spectrum of single base-pair substitutions in mRNA splice junctions of human genes: causes and consequences. *Hum Genet*, **90**, 41-54.

Krawczak, M., Thomas, N.S., Hundrieser, B., Mort, M., Wittig, M., Hampe, J. and Cooper, D.N. (2007) Single base-pair substitutions in exon-intron junctions of human genes: nature, distribution, and consequences for mRNA splicing. *Hum Mutat*, **28**, 150-158.

Kurreck, J. (2003) Antisense technologies. Improvement through novel chemical modifications. *Eur J Biochem*, **270**, 1628-1644.

Kuzmiak, H.A. and Maquat, L.E. (2006) Applying nonsense-mediated mRNA decay research to the clinic: progress and challenges. *Trends Mol Med*, **12**, 306-316.

Lai, C.H., Chun, H.H., Nahas, S.A., Mitui, M., Gamo, K.M., Du, L. and Gatti, R.A. (2004) Correction of ATM gene function by aminoglycoside-induced read-through of premature termination codons. *Proc Natl Acad Sci U S A*, **101**, 15676-15681.

Lamhonwah, A., Barankiewicz, T., Willard, H., Mahuran, D., Quan, F. and Gravel, R.A. (1986) Isolation of cDNA clones coding for the a - b chains of human propionyl-CoA carboxylase: chromosomal assignments and DNA polymorphism associated with PCCA and PCCB genes. *Proc Natl Acad Sci U S A*, **83**, 4864-4868.

Lavigueur, A., La Branche, H., Kornblihtt, A.R. and Chabot, B. (1993) A splicing enhancer in the human fibronectin alternate ED1 exon interacts with SR proteins and stimulates U2 snRNP binding. *Genes Dev*, **7**, 2405-2417.

Lee, Y.W., Lee, D.H., Kim, N.D., Lee, S.T., Ahn, J.Y., Choi, T.Y., Lee, Y.K., Kim, S.H., Kim, J.W. and Ki, C.S. (2008) Mutation analysis of PAH gene and characterization of a recurrent deletion mutation in Korean patients with phenylketonuria. *Exp Mol Med*, **40**, 533-540.

Lehnert, W., Sperl, W., Suormala, T. and Baumgartner, E.R. (1994) Propionic acidaemia: clinical, biochemical and therapeutic aspects. Experience in 30 patients. *Eur J Pediatr*, **153**, S68-80.

Leon-del-Rio, A. and Gravel, R.A. (1994) Sequence requirements for the biotinylation of carboxyl-terminal fragments of human propionyl-CoA carboxylase a subunit expressed in Escherichia coli. *J Biol Chem*, **269**, 22964-22968.

Linde, L., Boelz, S., Nissim-Rafinia, M., Oren, Y.S., Wilschanski, M., Yaacov, Y., Virgilis, D., Neu-Yilik, G., Kulozik, A.E., Kerem, E. and Kerem, B. (2007) Nonsense-mediated mRNA decay affects nonsense transcript levels and governs response of cystic fibrosis patients to gentamicin. *J Clin Invest*, **117**, 683-692.

Linde, L. and Kerem, B. (2008) Introducing sense into nonsense in treatments of human genetic diseases. *Trends Genet*, **24**, 552-563.

Lowry, O.H., Rosebrough, N.J., Farr, A.L. and Randall, R.J. (1951) Protein measurement with the Folin phenol reagent. *J Biol Chem*, **193**, 265-275.

Lukong, K.E., Chang, K.W., Khandjian, E.W. and Richard, S. (2008) RNA-binding proteins in human genetic disease. *Trends Genet*, **24**, 416-425.

Lund, M. and Kjems, J. (2002) Defining a 5' splice site by functional selection in the presence and absence of U1 snRNA 5' end. *Rna*, **8**, 166-179.

Manuvakhova, M., Keeling, K. and Bedwell, D.M. (2000) Aminoglycoside antibiotics mediate context-dependent suppression of termination codons in a mammalian translation system. *Rna*, **6**, 1044-1055.

Maquat, L.E. (2004) Nonsense-mediated mRNA decay: splicing, translation and mRNP dynamics. *Nat Rev Mol Cell Biol*, **5**, 89-99.

Martinez-Contreras, R., Cloutier, P., Shkreta, L., Fisette, J.F., Revil, T. and Chabot, B. (2007) hnRNP proteins and splicing control. *Adv Exp Med Biol*, **623**, 123-147.

McCaughan, K.K., Brown, C.M., Dalphin, M.E., Berry, M.J. and Tate, W.P. (1995) Translational termination efficiency in mammals is influenced by the base following the stop codon. *Proc Natl Acad Sci U S A*, **92**, 5431-5435.

Mellon, A.F., Deshpande, S.A., Mathers, J.C. and Bartlett, K. (2000) Effect of oral antibiotics on intestinal production of propionic acid. *Arch Dis Child*, **82**, 169-172.

Merinero, B., Perez, B., Perez-Cerda, C., Rincon, A., Desviat, L.R., Martinez, M.A., Sala, P.R., Garcia, M.J., Aldamiz-Echevarria, L., Campos, J., Cornejo, V., Del Toro, M., Mahfoud, A., Martinez-Pardo, M., Parini, R., Pedron, C., Pena-Quintana, L., Perez, M., Pourfarzam, M. and Ugarte, M. (2008) Methylmalonic acidaemia: examination of genotype and biochemical data in 32 patients belonging to mut, cblA or cblB complementation group. *J Inherit Metab Dis*, **31**, 55-66.

Miousse, I.R., Watkins, D., Coelho, D., Rupar, T., Crombez, E.A., Vilain, E., Bernstein, J.A., Cowan, T., Lee-Messer, C., Enns, G.M., Fowler, B. and Rosenblatt, D.S. (2009) Clinical and molecular heterogeneity in patients with the cblD inborn error of cobalamin metabolism. *J Pediatr*, **154**, 551-556.

Miyazaki, T., Ohura, T., Kobayashi, M., Shigematsu, Y., Yamaguchi, S., Suzuki, Y., Hata, I., Aoki, Y., Yang, X., Minjares, C., Haruta, I., Uto, H., Ito, Y. and Muller, U. (2001) Fatal propionic acidemia in mice lacking propionyl-CoA carboxylase and its rescue by postnatal, liver-specific supplementation via a transgene. *J Biol Chem*, **276**, 35995-35999.

Neville, B.G., Parascandalo, R., Farrugia, R. and Felice, A. (2005) Sepiapterin reductase deficiency: a congenital dopa-responsive motor and cognitive disorder. *Brain*, **128**, 2291-2296.

Nilsson, M. and Ryden-Aulin, M. (2003) Glutamine is incorporated at the nonsense codons UAG and UAA in a suppressor-free Escherichia coli strain. *Biochim Biophys Acta*, **1627**, 1-6.

Nissim-Rafinia, M., Aviram, M., Randell, S.H., Shushi, L., Ozeri, E., Chiba-Falek, O., Eidelman, O., Pollard, H.B., Yankaskas, J.R. and Kerem, B. (2004) Restoration of the cystic fibrosis

transmembrane conductance regulator function by splicing modulation. *EMBO Rep*, **5**, 1071-1077.

Ohno, K., Brengman, J.M., Felice, K.J., Cornblath, D.R. and Engel, A.G. (1999) Congenital end-plate acetylcholinesterase deficiency caused by a nonsense mutation and an A-->G splice-donor-site mutation at position +3 of the collagenlike-tail-subunit gene (COLQ): how does G at position +3 result in aberrant splicing? *Am J Hum Genet*, **65**, 635-644.

Ohura, T., Ogasawara, M., Ikeda, H., Narisawa, K. and Tada, K. (1993) The molecular defect in propionic acidemia: exon skipping caused by an 8-bp delection from an intron in the PCCB allele. *Hum Genet*, **92**, 397-402.

Osorio, F.G., Navarro, C.L., Cadinanos, J., Lopez-Mejia, I.C., Quiros, P.M., Bartoli, C., Rivera, J., Tazi, J., Guzman, G., Varela, I., Depetris, D., de Carlos, F., Cobo, J., Andres, V., De Sandre-Giovannoli, A., Freije, J.M., Levy, N. and Lopez-Otin, C. (2011) Splicing-directed therapy in a new mouse model of human accelerated aging. *Sci Transl Med*, **3**, 106ra107.

Owen, L.A., Uehara, H., Cahoon, J., Huang, W., Simonis, J. and Ambati, B.K. (2012) Morpholino-mediated increase in soluble flt-1 expression results in decreased ocular and tumor neovascularization. *PLoS One*, **7**, e33576.

Padovani, D. and Banerjee, R. (2006) Assembly and protection of the radical enzyme, methylmalonyl-CoA mutase, by its chaperone. *Biochemistry*, **45**, 9300-9306.

Pagani, F. and Baralle, F.E. (2004) Genomic variants in exons and introns: identifying the splicing spoilers. *Nat Rev Genet*, **5**, 389-396.

Pampols, T. (2010) Inherited metabolic rare disease. *Adv Exp Med Biol*, **686**, 397-431.

Perez-Cerda, C., Clavero, S., Perez, B., Rodriguez-Pombo, P., Desviat, L.R. and Ugarte, M. (2003) Functional analysis of PCCB mutations causing propionic acidemia based on expression studies in deficient human skin fibroblasts. *Biochim Biophys Acta*, **1638**, 43-49.

Perez-Cerda, C., Merinero, B., Rodriguez-Pombo, P., Perez, B., Desviat, L.R., Muro, S., Richard, E., Garcia, M.J., Gangoiti, J., Ruiz Sala, P., Sanz, P., Briones, P., Ribes, A., Martinez-Pardo, M., Campistol, J., Perez, M., Lama, R., Murga, M.L., Lema-Garrett, T., Verdu, A. and Ugarte, M. (2000) Potential relationship between genotype and clinical outcome in propionic acidaemia patients. *Eur J Hum Genet*, **8**, 187-194.

Perez-Cerda, C., Perez, B., Merinero, B., Desviat, L.R., Rodriguez-Pombo, P. and Ugarte, M. (2004) Prenatal diagnosis of propionic acidemia. *Prenat Diagn*, **24**, 962-964.

Perez, B., Desviat, L.R., Rodriguez-Pombo, P., Clavero, S., Navarrete, R., Perez-Cerda, C. and Ugarte, M. (2003) Propionic acidemia: identification of twenty-four novel mutations in Europe and North America. *Mol Genet Metab*, **78**, 59-67.

Perez, B., Rincon, A., Jorge-Finnigan, A., Richard, E., Merinero, B., Ugarte, M. and Desviat, L.R. (2009) Pseudoexon exclusion by antisense therapy in methylmalonic aciduria (MMAuria). *Hum Mutat*, **30**, 1676-1682.

Perez, B., Rodriguez-Pascau, L., Vilageliu, L., Grinberg, D., Ugarte, M. and Desviat, L.R. (2010) Present and future of antisense therapy for splicing modulation in inherited metabolic disease. *J Inherit Metab Dis*, **33**, 397-403.

Pinol-Roma, S. and Dreyfuss, G. (1992) Shuttling of pre-mRNA binding proteins between nucleus and cytoplasm. *Nature*, **355**, 730-732.

Pinotti, M., Balestra, D., Rizzotto, L., Maestri, I., Pagani, F. and Bernardi, F. (2009) Rescue of coagulation factor VII function by the U1+5A snRNA. *Blood*, **113**, 6461-6464.

Pinotti, M., Rizzotto, L., Balestra, D., Lewandowska, M.A., Cavallari, N., Marchetti, G., Bernardi, F. and Pagani, F. (2008) U1-snRNA-mediated rescue of mRNA processing in severe factor VII deficiency. *Blood*, **111**, 2681-2684.

Politano, L., Nigro, G., Nigro, V., Piluso, G., Papparella, S., Paciello, O. and Comi, L.I. (2003) Gentamicin administration in Duchenne patients with premature stop codon. Preliminary results. *Acta Myol*, **22**, 15-21.

Popescu, A.C., Sidorova, E., Zhang, G. and Eubanks, J.H. Aminoglycoside-mediated partial suppression of MECP2 nonsense mutations responsible for Rett syndrome in vitro. *J Neurosci Res*, **88**, 2316-2324.

Raponi, M., Buratti, E., Dassie, E., Upadhyaya, M. and Baralle, D. (2009) Low U1 snRNP dependence at the NF1 exon 29 donor splice site. *Febs J*, **276**, 2060-2073.

Richard, E., Desviat, L.R., Perez, B., Perez-Cerda, C. and Ugarte, M. (1999) Genetic heterogeneity in propionic acidemia patients with alpha-subunit defects. Identification of five novel mutations, one of them causing instability of the protein. *Biochim Biophys Acta*, **1453**, 351-358.

Rincon, A., Aguado, C., Desviat, L.R., Sanchez-Alcudia, R., Ugarte, M. and Perez, B. (2007) Propionic and Methylmalonic Acidemia: Antisense Therapeutics for Intronic Variations Causing Aberrantly Spliced Messenger RNA. *Am J Hum Genet*, **81**, 1262-1270.

Rio Frio, T., Wade, N.M., Ransijn, A., Berson, E.L., Beckmann, J.S. and Rivolta, C. (2008) Premature termination codons in PRPF31 cause retinitis pigmentosa via haploinsufficiency due to nonsense-mediated mRNA decay. *J Clin Invest*, **118**, 1519-1531.

Roca, X., Olson, A.J., Rao, A.R., Enerly, E., Kristensen, V.N., Borresen-Dale, A.L., Andresen, B.S., Krainer, A.R. and Sachidanandam, R. (2008) Features of 5'-splice-site efficiency derived from disease-causing mutations and comparative genomics. *Genome Res*, **18**, 77-87.

Roca, X., Sachidanandam, R. and Krainer, A.R. (2005) Determinants of the inherent strength of human 5' splice sites. *Rna*, **11**, 683-698.

Rodriguez-Pascau, L., Coll, M.J., Vilageliu, L. and Grinberg, D. (2009) Antisense oligonucleotide treatment for a pseudoexon-generating mutation in the NPC1 gene causing Niemann-Pick type C diseaseb. *Hum Mutat*, **30**, E993-E1001.

Rodriguez-Pombo, P., Hoenicka, J., Muro, S., Perez, B., Perez-Cerda, C., Richard, E., Desviat, L.R. and Ugarte, M. (1998) Human propionyl-CoA carboxylase beta subunit gene: exon-intron definition and mutation spectrum in Spanish and Latin American propionic acidemia patients. *Am J Hum Genet*, **63**, 360-369.

Roe, C.R., Millington, D.S., Maltby, D.A., Bohan, T.P. and Hoppel, C.L. (1984) L-carnitine enhances excretion of propionyl coenzyme A as propionylcarnitine in propionic acidemia. *J Clin Invest*, **73**, 1785-1788.

Rowe, S.M. and Clancy, J.P. (2009) Pharmaceuticals targeting nonsense mutations in genetic diseases: progress in development. *BioDrugs*, **23**, 165-174.

Ruiz Pons, M., Sánchez-Valverde Visus, F., Dalmau Serra, J. and SHS España, S.L. (2004) *Tratamiento nutricional de los errores innatos del metabolismo*. ERGON.

Saillour, Y., Cossee, M., Leturcq, F., Vasson, A., Beugnet, C., Poirier, K., Commere, V., Sublemontier, S., Viel, M., Letourneur, F., Barbot, J.C., Deburgrave, N., Chelly, J. and Bienvenu, T. (2008) Detection of exonic copy-number changes using a highly efficient oligonucleotide-based comparative genomic hybridization-array method. *Hum Mutat*, **29**, 1083-1090.

BIBLIOGRAFÍA

Sanger, F., Nicklen, S. and Coulson, A.R. (1977) DNA Sequencing with Chain Terminating Inhibitors. *Proc. Natl. Acad. Sci. USA*, **74**, 5463-5467.

Sanjurjo, P., Aquino, L. and Aldamiz-Echevarría, L. (2001) *Enfermedades congénitas del metabolismo: generalidades, grupos clínicos y algoritmos diagnósticos*, Madrid.

Schouten, J.P., McElgunn, C.J., Waaijer, R., Zwijnenburg, D., Diepvens, F. and Pals, G. (2002) Relative quantification of 40 nucleic acid sequences by multiplex ligation-dependent probe amplification. *Nucleic Acids Res*, **30**, e57.

Shchelochkov, O.A., Li, F.Y., Geraghty, M.T., Gallagher, R.C., Van Hove, J.L., Lichter-Konecki, U., Fernhoff, P.M., Copeland, S., Reimschisel, T., Cederbaum, S., Lee, B., Chinault, A.C. and Wong, L.J. (2009) High-frequency detection of deletions and variable rearrangements at the ornithine transcarbamylase (OTC) locus by oligonucleotide array CGH. *Mol Genet Metab*.

Shi, J., Hu, Z., Pabon, K. and Scotto, K.W. (2008) Caffeine regulates alternative splicing in a subset of cancer-associated genes: a role for SC35. *Mol Cell Biol*, **28**, 883-895.

Sperl, W., Murr, C., Skladal, D., Sass, J.O., Suormala, T., Baumgartner, R. and Wendel, U. (2000) Odd-numbered long-chain fatty acids in propionic acidaemia. *Eur J Pediatr*, **159**, 54-58.

Staknis, D. and Reed, R. (1994) SR proteins promote the first specific recognition of Pre-mRNA and are present together with the U1 small nuclear ribonucleoprotein particle in a general splicing enhancer complex. *Mol Cell Biol*, **14**, 7670-7682.

Stanczak, C.M., Chen, Z., Zhang, Y.H., Nelson, S.F. and McCabe, E.R. (2007) Deletion mapping in Xp21 for patients with complex glycerol kinase deficiency using SNP mapping arrays. *Hum Mutat*, **28**, 235-242.

Stewart, P.M. and Walser, M. (1980) Failure of the normal ureagenic response to amino acids in organic acid-loaded rats. Proposed mechanism for the hyperammonemia of propionic and methylmalonic acidemia. *J Clin Invest*, **66**, 484-492.

Sumanasekera, C., Watt, D.S. and Stamm, S. (2008) Substances that can change alternative splice-site selection. *Biochem Soc Trans*, **36**, 483-490.

Suormala, T., Baumgartner, M.R., Coelho, D., Zavadakova, P., Koich, V., Koch, H.G., Berghauser, M., Wraith, J.E., Burlina, A., Sewell, A., Herwig, J. and Fowler, B. (2004) The cblD defect causes either isolated or combined deficiency of methylcobalamin and adenosylcobalamin synthesis. *J Biol Chem*, **279**, 42742-42749.

Suormala, T., Wick, H., Bonjour, J.P. and Baumgartner, E.R. (1985) Rapid differential diagnosis of carboxylase deficiencies and evaluation for biotin-responsiveness in a single blood sample. *Clin Chim Acta*, **145**, 151-162.

Susani, L., Pangrazio, A., Sobacchi, C., Taranta, A., Mortier, G., Savarirayan, R., Villa, A., Orchard, P., Vezzoni, P., Albertini, A., Frattini, A. and Pagani, F. (2004) TCIRG1-dependent recessive osteopetrosis: mutation analysis, functional identification of the splicing defects, and in vitro rescue by U1 snRNA. *Hum Mutat*, **24**, 225-235.

Tanner, G., Glaus, E., Barthelmes, D., Ader, M., Fleischhauer, J., Pagani, F., Berger, W. and Neidhardt, J. (2009) Therapeutic strategy to rescue mutation-induced exon skipping in rhodopsin by adaptation of U1 snRNA. *Hum Mutat*, **30**, 255-263.

Tate, W.P., Poole, E.S., Horsfield, J.A., Mannering, S.A., Brown, C.M., Moffat, J.G., Dalphin, M.E., McCaughan, K.K., Major, L.L. and Wilson, D.N. (1995) Translational termination efficiency in both bacteria and mammals is regulated by the base following the stop codon. *Biochem Cell Biol*, **73**, 1095-1103.

Tazi, J., Durand, S. and Jeanteur, P. (2005) The spliceosome: a novel multi-faceted target for therapy. *Trends Biochem Sci*, **30**, 469-478.

Thompson, G.N. and Chalmers, R.A. (1990) Increased urinary metabolite excretion during fasting in disorders of propionate metabolism. *Pediatr Res*, **27**, 413-416.

Thompson, G.N., Walter, J.H., Bresson, J.L., Ford, G.C., Lyonnet, S.L., Chalmers, R.A., Saudubray, J.M., Leonard, J.V. and Halliday, D. (1990) Sources of propionate in inborn errors of propionate metabolism. *Metabolism*, **39**, 1133-1137.

Thony, B., Auerbach, G. and Blau, N. (2000) Tetrahydrobiopterin biosynthesis, regeneration and functions. *Biochem J*, **347 Pt 1**, 1-16.

Thony, B. and Blau, N. (2006) Mutations in the BH4-metabolizing genes GTP cyclohydrolase I, 6-pyruvoyl-tetrahydropterin synthase, sepiapterin reductase, carbinolamine-4a-dehydratase, and dihydropteridine reductase. *Hum Mutat*, **27**, 870-878.

Towbin, H., Staehelin, T. and Gordon, J. (1979) Electrophoretic transfer of proteins from polyacrylamide gels to nitrocellulose shetts: procedures and some applications. *Proc. Nat. Acad. Sci. USA*, **76**, 4350-4354.

Ugarte, M., Perez-Cerda, C., Rodriguez-Pombo, P., Desviat, L.R., Perez, B., Richard, E., Muro, S., Campeau, E., Ohura, T. and Gravel, R.A. (1999) Overview of mutations in the PCCA and PCCB genes causing propionic acidemia. *Hum Mutat*, **14**, 275-282.

Ule, J. (2008) Ribonucleoprotein complexes in neurologic diseases. *Curr Opin Neurobiol*, **18**, 516-523.

Usuki, F., Yamashita, A., Higuchi, I., Ohnishi, T., Shiraishi, T., Osame, M. and Ohno, S. (2004) Inhibition of nonsense-mediated mRNA decay rescues the phenotype in Ullrich's disease. *Ann Neurol*, **55**, 740-744.

Vega, A.I., Perez-Cerda, C., Desviat, L.R., Matthijs, G., Ugarte, M. and Perez, B. (2009) Functional analysis of three splicing mutations identified in the PMM2 gene: toward a new therapy for congenital disorder of glycosylation type Ia. *Hum Mutat*, **30**, 795-803.

Vorechovsky, I. (2010) Transposable elements in disease-associated cryptic exons. *Hum Genet*, **127**, 135-154.

Wang, G.S. and Cooper, T.A. (2007) Splicing in disease: disruption of the splicing code and the decoding machinery. *Nat Rev Genet*, **8**, 749-761.

Wang, J., Smith, P.J., Krainer, A.R. and Zhang, M.Q. (2005) Distribution of SR protein exonic splicing enhancer motifs in human protein-coding genes. *Nucleic Acids Res*, **33**, 5053-5062.

Welch, E.M., Barton, E.R., Zhuo, J., Tomizawa, Y., Friesen, W.J., Trifillis, P., Paushkin, S., Patel, M., Trotta, C.R., Hwang, S., Wilde, R.G., Karp, G., Takasugi, J., Chen, G., Jones, S., Ren, H., Moon, Y.C., Corson, D., Turpoff, A.A., Campbell, J.A., Conn, M.M., Khan, A., Almstead, N.G., Hedrick, J., Mollin, A., Risher, N., Weetall, M., Yeh, S., Branstrom, A.A., Colacino, J.M., Babiak, J., Ju, W.D., Hirawat, S., Northcutt, V.J., Miller, L.L., Spatrick, P., He, F., Kawana, M., Feng, H., Jacobson, A., Peltz, S.W. and Sweeney, H.L. (2007) PTC124 targets genetic disorders caused by nonsense mutations. *Nature*, **447**, 87-91.

Wilschanski, M., Yahav, Y., Yaacov, Y., Blau, H., Bentur, L., Rivlin, J., Aviram, M., Bdolah-Abram, T., Bebok, Z., Shushi, L., Kerem, B. and Kerem, E. (2003) Gentamicin-induced correction of CFTR function in patients with cystic fibrosis and CFTR stop mutations. *N Engl J Med*, **349**, 1433-1441.

Wolf, B., Hsia, Y.E., Sweetman, L., Gravel, R., Harris, D.J. and Nyhan, W.L. (1981) Propionic acidemia: a clinical update. *J Pediatr*, **99**, 835-846.

Wong, L.J., Dimmock, D., Geraghty, M.T., Quan, R., Lichter-Konecki, U., Wang, J., Brundage, E.K., Scaglia, F. and Chinault, A.C. (2008) Utility of oligonucleotide array-based comparative genomic hybridization for detection of target gene deletions. *Clin Chem*, **54**, 1141-1148.

Wu, B., Li, Y., Morcos, P.A., Doran, T.J., Lu, P. and Lu, Q.L. (2009) Octa-guanidine morpholino restores dystrophin expression in cardiac and skeletal muscles and ameliorates pathology in dystrophic mdx mice. *Mol Ther*, **17**, 864-871.

Yorifuji, T., Muroi, J., Uematsu, A., Nakahata, T., Egawa, H. and Tanaka, K. (2000) Living-related liver transplantation for neonatal-onset propionic acidemia. *J Pediatr*, **137**, 572-574.

Zammarchi, F., de Stanchina, E., Bournazou, E., Supakorndej, T., Martires, K., Riedel, E., Corben, A.D., Bromberg, J.F. and Cartegni, L. (2011) Antitumorigenic potential of STAT3 alternative splicing modulation. *Proc Natl Acad Sci U S A*, **108**, 17779-17784.

Zhang, F., Gu, W., Hurles, M.E. and Lupski, J.R. (2009) Copy number variation in human health, disease, and evolution. *Annu Rev Genomics Hum Genet*, **10**, 451-481.

Zhuang, Y. and Weiner, A.M. (1986) A compensatory base change in U1 snRNA suppresses a 5' splice site mutation. *Cell*, **46**, 827-835.

Zuo, P. and Maniatis, T. (1996) The splicing factor U2AF35 mediates critical protein-protein interactions in constitutive and enhancer-dependent splicing. *Genes Dev*, **10**, 1356-1368.

Zwickler, T., Lindner, M., Aydin, H.I., Baumgartner, M.R., Bodamer, O.A., Burlina, A.B., Das, A.M., DeKlerk, J.B., Gokcay, G., Grunewald, S., Guffon, N., Maier, E.M., Morava, E., Geb, S., Schwahn, B., Walter, J.H., Wendel, U., Wijburg, F.A., Muller, E., Kolker, S. and Horster, F. (2008) Diagnostic work-up and management of patients with isolated methylmalonic acidurias in European metabolic centres. *J Inherit Metab Dis*, **31**, 361-367.

Zychlinski, D., Erkelenz, S., Melhorn, V., Baum, C., Schaal, H. and Bohne, J. (2009) Limited complementarity between U1 snRNA and a retroviral 5' splice site permits its attenuation via RNA secondary structure. *Nucleic Acids Res*, **37**, 7429-7440.

8. PUBLICACIONES

Parte de este trabajo se encuentra recogido en las siguientes publicaciones:

- **Sanchez-Alcudia, R.**, Perez, B., Ugarte, M. and Desviat, L.R. (2012) Feasibility of nonsense mutations readthrough as a novel therapeutical approach in propionic acidemia. *Hum Mutat*. (en prensa).

- Arrabal, L., Teresa, L., **Sanchez-Alcudia, R.**, Castro, M., Medrano, C., Gutierrez-Solana, L., Roldan, S., Ormazabal, A., Perez-Cerda, C., Merinero, B., Perez, B., Artuch, R., Ugarte, M. and Desviat, L.R. (2011) Genotype-phenotype correlations in sepiapterin reductase deficiency. A splicing defect accounts for a new phenotypic variant. *Neurogenetics*, **12**, 183-191.

- **Sanchez-Alcudia, R.**, Perez, B., Perez-Cerda, C., Ugarte, M. and Desviat, L.R. (2011) Overexpression of adapted U1snRNA in patients' cells to correct a 5' splice site mutation in propionic acidemia. *Mol Genet Metab*, **102**, 134-138.

- Jorge-Finnigan, A., Aguado, C., **Sanchez-Alcudia, R.**, Abia, D., Richard, E., Merinero, B., Gamez, A., Banerjee, R., Desviat, L.R., Ugarte, M. and Perez, B. (2010) Functional and structural analysis of five mutations identified in methylmalonic aciduria cblB type. *Hum Mutat*, **31**, 1033-1042.

- Perez, B., Angaroni, C., **Sanchez-Alcudia, R.**, Merinero, B., Perez-Cerda, C., Specola, N., Rodriguez-Pombo, P., Wajner, M., de Kremer, R.D., Cornejo, V., Desviat, L.R. and Ugarte, M. (2010) The molecular landscape of propionic acidemia and methylmalonic aciduria in Latin America. *J Inherit Metab Dis*, **33**, S307-314.

- Desviat, L.R., **Sanchez-Alcudia, R.**, Perez, B., Perez-Cerda, C., Navarrete, R., Vijzelaar, R. and Ugarte, M. (2009) High frequency of large genomic deletions in the PCCA gene causing propionic acidemia. *Mol Genet Metab*, **96**, 171-176.

- Rincon, A., Aguado, C., Desviat, L.R., **Sanchez-Alcudia, R.**, Ugarte, M. and Perez, B. (2007) Propionic and methylmalonic acidemia: antisense therapeutics for intronic variations causing aberrantly spliced messenger RNA. *Am J Hum Genet*, **81**, 1262-1270.

RESEARCH ARTICLE

Human Mutation

OFFICIAL JOURNAL HGVS HUMAN GENOME VARIATION SOCIETY www.hgvs.org

Feasibility of Nonsense Mutations Readthrough as a Novel Therapeutical Approach in Propionic Acidemia

Rocío Sánchez-Alcudia, Belén Pérez, Magdalena Ugarte, and Lourdes R. Desviat*

Centro de Diagnóstico de Enfermedades Moleculares, Centro de Biología Molecular Severo Ochoa, UAM-CSIC, Centro de Investigación Biomédica en Red de Enfermedades Raras (CIBERER), Madrid, Spain

Communicated by Dr. Jan Kraus

Received 11 August 2011; accepted revised manuscript 26 January 2012.
Published online DD MM YYYY in Wiley Online Library (www.wiley.com/humanmutation).DOI: 10.1002/humu.22047

ABSTRACT: Aminoglycosides and other compounds can promote premature termination codon (PTC) readthrough constituting a potential therapy for patients with nonsense mutations. In a cohort of 190 propionic ~~academia~~ (PA) patients, we have identified 12 different nonsense mutations, six of them novel, accounting for 10% of the mutant alleles. Using an in vitro system, we establish the proof-of-principle that nonsense mutations in the *PCCA* and *PCCB* genes encoding both subunits of the propionyl-CoA carboxylase (PCC) enzyme can be partially suppressed by aminoglycosides, with different efficiencies depending on the sequence context. To correct the metabolic defect, the amino acid incorporated at the PTC should support protein function, and this has been evaluated in silico and by in vitro expression analysis of the predicted missense changes, most of which retain partial activity, confirming the feasibility of the approach. In patients' fibroblasts cultured with readthrough drugs, we observe a fourfold to 50-fold increase in the PCC activity, reaching up to 10–15% level of treated control cells. The ability to partially correct nonsense *PCCA* and *PCCB* alleles represents a potential therapy or supplementary treatment for a number of propionic acidemia (PA) patients, encouraging further clinical trials with readthrough drugs without toxic effects such as PTC124 or other newly developed compounds.
Hum Mutat 00:1–8, 2012. © 2012 Wiley Periodicals, Inc.

KEY WORDS: nonsense mutations; aminoglycosides; ataluren; PCCA; PCCB

Introduction

There is now compelling evidence that aminoglycosides can suppress premature termination codon (PTC) mutations in mammalian transcripts both in vitro and in vivo at levels that restore physiologically relevant amounts of protein [Kuzmiak and Maquat, 2006; Linde and Kerem, 2008]. Historically, the first demonstration that aminoglycosides could suppress PTC in a defective human gene was carried out in cystic fibrosis [Bedwell et al., 1997; Howard et al., 1996]. Since then, PTC readthrough has been documented in vitro and in cellular and animal models of different disorders, including cystic fibrosis, Duchenne muscular dystrophy, Hurler's syndrome, diabetes, cystinosis, X-linked retinitis pigmentosa, and ataxia–telangiectasia among others [Barton-Davis et al., 1999; Grayson et al., 2002; Keeling et al., 2001; Lai et al., 2004].

Aminoglycosides promote readthrough by mimicking the conformational change in 16S RNA that would be induced by a correct codon–anticodon pair, thereby compromising the integrity of codon–anticodon proofreading during translation. Thus, a near-cognate amino acid is inserted at the stop codon, resulting in the synthesis of a full-length protein. As a general rule, glutamine is inserted at nonsense UAG or UAA codons, whereas UGA miscode to tryptophan [Harrell et al., 2002; Nilsson and Ryden-Aulin, 2003]. Several studies have shown that the sequence context, that is, the identity of the stop codon as well as the surrounding sequence, strongly influence readthrough efficiency. In particular, stop codon UGA followed by a C is most susceptible to aminoglycoside-mediated readthrough [Keeling and Bedwell, 2002; Manuvakhova et al., 2000].

Several human trials were carried out to test the efficacy of the aminoglycoside gentamicin on functional restoration of full-length protein in cystic fibrosis and Duchenne and Becker muscular dystrophy patients. However, results were hampered by the toxic side effects (nephrotoxicity and ototoxicity) of long-term treatment and the need for regular intravenous administration [Finkel, 2010]. With the aim of identifying alternative compounds for optimal suppression of nonsense mutations without eliciting toxic side effects, several studies using high throughput screens or designer aminoglycosides have been carried out [Du et al., 2009; Hainrichson et al., 2008; Welch et al., 2007]. One promising compound identified in high throughput screens is PTC124 or ataluren, which shows potent PTC suppression while preserving the natural termination codon and offering the advantages of having no obvious toxic effects and being orally bioavailable [Welch et al., 2007]. Several clinical trials are ongoing to evaluate the safety and activity of ataluren in cystic fibrosis ~~and hemophilia type A and B~~ (http://www.ptcbio.com/).

It is clear that the nature and pathophysiology of the disorder as well as the spectrum of nonsense mutations may influence the therapeutical outcome with readthrough drugs; thus, the feasibility of this treatment strategy must be evaluated in each case. In the past years, our group has studied the molecular basis of propionic acidemia (PA; MIM# 606054), one of the most frequent organic acidemias worldwide, caused by mutations in the *PCCA* (MIM# 23200) and *PCCB* genes (MIM# 232050), encoding both subunits of the biotin-dependent propionyl-CoA carboxylase enzyme (PCC,

Additional Supporting Information may be found in the online version of this article.

*Correspondence to: Lourdes R. Desviat, Centro de Biología Molecular Severo Ochoa, UAM-CSIC, Universidad Autónoma de Madrid, 28049 Madrid, Spain. E-mail: lruiz@cbm.uam.es

Contract grant sponsors: Ministerio de Ciencia e Innovación (SAF2010-17272); Centro de Investigación Biomédica en Red de Enfermedades Raras (CIBERER INTRA/10/720.1); Fundación Ramón Areces (to the Centro de Biología Molecular Severo Ochoa).

E.C. 6.4.1.3). PCC catalyzes the conversion of propionyl-CoA to methylmalonyl-CoA and is one of the key enzymes in the catabolic pathway of the amino acids valine, isoleucine, methionine, and threonine, as wells as of odd-chain fatty acids and the side chain of cholesterol. The PCC holoenzyme is an $\alpha_6\beta_6$ dodecamer, with the α subunit containing the biotin carboxyl carrier protein and the biotin carboxylase domains, whereas the β subunit supplies carboxyltransferase activity. Recent crystallographic evidence has shown that α subunits are arranged as monomers decorating a central β_6 hexamer [Huang et al., 2010].

PA shows a wide range of clinical manifestations ranging from a severe neonatal form with ketoacidosis, poor feeding, lethargy, failure to thrive, seizures, and encephalopathy to a milder, later-onset chronic form with less impaired neurological outcome. Progression of symptoms, if not promptly treated, leads to death within few days or to severe brain damage [Fenton et al., 2001]. Current treatment of PA relies on several, often combined, strategies such as administration of biotin and metronidazole, restriction of precursor amino acids, supplementation of L-carnitine, and prevention of the catabolic state. Liver or combined liver–kidney transplantation has been performed in some cases, improving the outcome and quality of life of patients [de Baulny et al., 2005]. However, in most of the cases, treatment does not effectively prevent neurological deterioration and the long-term outcome is unsatisfactory [Fenton et al., 2001].

Mutation analysis has identified more than 70 pathogenic mutations in each of the *PCCA* and *PCCB* genes, including missense, frameshift, insertion, deletion, and nonsense changes [Desviat et al., 2004] (Human Gene Mutation Database [HGMD®] professional release, 2011). In this study, we have focused on the nonsense mutations identified in a large cohort of PA patients and investigated the potential drug-mediated readthrough to restore PCC function as a therapeutical approach.

Materials and Methods

Patients' Fibroblasts and Mutation Analysis

Primary fibroblasts from PA patients carriers of nonsense mutations and primary fibroblast cell line GM 08680 from the Human Genetic Mutant Cell Repository, National Institute of General Medical Sciences (Camden, NJ) used as control were grown in minimum essential medium supplemented with 1% glutamine, 10% fetal bovine serum, and antibiotics. Ethical approval for the use of human samples in this study was granted by the Institutional Ethics Committee (Universidad Autónoma de Madrid Madrid, Spain). Mutation analysis was carried out with complementary DNA (cDNA) and/or genomic DNA samples from fibroblasts or whole blood, as previously described [Rincon et al., 2007]. Mutation nomenclature follows the recommended guidelines of the Human Genome Variation Society (www.HGVS.org). Nucleotide numbering is based on cDNA reference sequence GenBank accession numbers NM_000282.3 (*PCCA*) and NM_000532.4 (*PCCB*). Mutation nomenclature was validated using Mutalyzer 2.0 β-8 (http://www.mutalyzer.nl/2.0).

Cloning of Reporter Vectors for Transcription–Translation Assays

To assay the in vitro translation of PCCA proteins, *PCCA* cDNA (2106 bp) cloned in the pGEM-11Zf(+) vector [Richard et al., 1999] was used. The *PCCA* mutations p.R313*, p.Q371*, p.Y380*, p.S562*, and p.Q611* were introduced by PCR mutagenesis using the QuickChange mutagenesis kit (Agilent Technologies, Santa Clara, CA). For *PCCB*, different constructs were used. *PCCB* cDNA (1620 bp) was amplified using a sense primer that introduces the T7 promoter and the consensus Kozak sequences adjacent to the ATG initiation codon (5′-TAATACGACTCACTATAGGAACAGCCACC-ATGGCGGCGGCATTACGGGTG-3′) and cloned in pCR2.1-TOPO vector (Invitrogen, Carlsbad, CA). *PCCB* mutations p.Q139*, p.Y314*, p.R514*, and p.W531* were then introduced by PCR mutagenesis in this construct. For the remaining *PCCB* mutations p.G94*, p.R111*, and p.R113*, predictably resulting in small truncated proteins with low methionine and cysteine content (labeled amino acids used in the transcription–translation [TNT] assay), precluding efficient labeling and detection, a hybrid construct encoding a PCCA–PCCB fusion protein was cloned. *PCCB* cDNA was amplified from codon 1 to codon 116 with primers introducing an *Stu*I restriction site and cloned in pGEM–PCCA digested with the same enzyme that cuts after codon 196 in *PCCA* cDNA. The final construct encodes for a protein containing the first 196 amino acids from PCCA, followed in frame with the first 116 amino acids from PCCB and then with amino acids 197 to 704 from the PCCA protein, with an overall molecular weight of approximately 92 kDa. The construct was fully sequenced and validated in TNT assays, where a band of the expected molecular weight was detected. *PCCB* mutations p.G94*, p.R111*, and p.R113* were then introduced by PCR mutagenesis. In these cases, PCR products obtained using primers to amplify the complete hybrid cDNA and the T7 promoter sequence were used as templates for the TNT assay. Bands of the expected molecular weight of the truncated proteins were observed after the TNT reaction.

Coupled TNT Assay

T7 transcription/rabbit reticulocyte translation system from Promega (Madison, WI) was used for protein synthesis. Each reaction was done at 30°C for 90 min and contained 500–750 ng of plasmid or 1.25 μg of amplified product, 10 μl of TNT T7 Quick Master Mix (Promega), and 1 μl of L-[^{35}S]-methionine-cysteine (EasyTag EXPRESS ^{35}S Protein Labeling Mix, [^{35}S], 7mCi; PerkinElmer, Waltham, MA). To assay the effect of the readthrough drugs, a range of different concentrations of G418 (0.1–2.5 μg/ml; Gibco BRL, Grant Island, NY), gentamicin sulfate (1.25–20 μg/ml; Sigma–Aldrich, St. Louis, MO), and PTC 124 (0.03–10 μM; Selleckchem, Shanghai, China) were added to the TNT reaction, according to previously published procedures [Keeling and Bedwell, 2002]. The [^{35}S]-labeled polypeptides resulting from these reactions were separated by sodium dodecyl sulfate-polyacrylamide gel electrophoresis and then revealed after overnight exposure at–70°C in autoradiography films. Protein quantification was performed using a calibrated densitometer GS-800 (Bio-Rad Laboratories, Hercules, CA). The readthrough levels were calculated as the amount of full-length protein produced relative to the sum of the truncated and full-length protein and expressed as percentages.

Messenger RNA Quantification

The levels of *PCCA* and *PCCB* transcripts in patients' fibroblasts were analyzed by quantitative reverse-transcription polymerase chain reaction (qRT-PCR) in a LightCycler® 480 instrument (Roche Applied Sciences, Indianapolis, IN). For messenger RNA (mRNA) isolation, cultured patients' fibroblasts were harvested and mRNA was obtained with TriPure Isolation Reagent (Roche Applied Sciences) or with the MagNA Pure Compact RNA isolation kit and system (Roche Applied Sciences), following the manufacturer's recommendations.

Table 1. Nonsense Mutations Identified in a Cohort of 190 PA Patients

Gene	Mutation	nt change	Location	Stop codon (fourth nt)	Reference
PCCA	p.R313*	c.937C>T	Exon 12	UGA (A)	[Richard, et al., 1999]
PCCA	p.Q371*	c.1111C>T	Exon 13	UAG (G)	This work
PCCA	p.Y380*	c.1140C>A	Exon 13	UAA (C)	This work
PCCA	p.S562*	c.1685C>G	Exon 19	UGA (G)	[Richard, et al., 1999]
PCCA	p.Q611*	c.1831C>T	Exon 20	UAG (A)	This work
PCCB	p.G94*	c.280G>T	Exon 2	UGA (A)	[Perez, et al., 2003]
PCCB	p.R111*	c.331C>T	Exon 3	UGA (G)	This work
PCCB	p.R113*	c.415C>T	Exon 3	UGA (G)	[Brosch, et al., 2008]
PCCB	p.Q139*	c.415C>T	Exon 4	UAA (A)	This work
PCCB	p.Y314*	c.942C>A	Exon 9	UAA (A)	This work
PCCB	p.R514*	c.1540C>T	Exon 15	UGA (A)	This work[a]
PCCB	p.W531*	c.1593G>A	Exon 15	UGA (A)	[Rodriguez-Pombo, et al., 1998]

[a]Previously reported in a meeting abstract and recorded in the HGMD.

Total RNA obtained as described above was retrotranscribed using the High-Capacity cDNA Archive Kit (Applied Biosystems) and amplified using the LightCycler® 480 SYBR Green I Master (Roche Applied Sciences) with primers located in exon 22 (5′-TGCCAGTTTTCCCAGCTGTC-3′) and exon 23 (5′-ACCAGACTTGCCGCAGAATT-3′) of the *PCCA* gene, and in exon 5 (5′-ATTGGCTGAATGACTCTGG-3′) and exon 8 (5′-CAGGGGCAGGTAGTTGAAGA-3′) of the *PCCB* gene. Glyceraldehyde 3-phosphate dehydrogenase (GAPDH) mRNA expression level was used as an endogenous control. PCR was performed in a total volume of 20 µl, containing 0.5–2 µl of cDNA product, 5 µl of LightCycler® 480 SYBR Green I Master (Roche Applied Sciences), and PCR primers at a final concentration of 125 nM each. The data were analyzed using the LightCycler® software (Roche Applied Sciences) to correlate relative initial template concentration to the cycle threshold (Ct), obtaining the relative quantity (RQ), which is defined as follows: $RQ = 2^{-\Delta\Delta Ct}$, where $\Delta\Delta Ct = (\Delta Ct$ patient cell line$-\Delta Ct$ control cell line) and $\Delta Ct =$ (Ct target gene [*PCCA*, *PCCB*]–(Ct housekeeping gene [*GAPDH*]).

Determination of PCC Activity

PCC activity was determined in fibroblast protein extracts by measuring the enzyme-dependent incorporation of [^{14}C]-bicarbonate into acid-nonvolatile products, as described in Suormala et al. [1985]. Protein was measured by the Lowry method.

In Silico and In Vitro Expression Analysis of Missense Changes

The in silico analysis of the predicted missense change introduced by aminoglycoside treatment was performed with the bioinformatics applications: PolyPhen-2 (http://genetics.bwh.harvard.edu/pph2/) and SIFT (http://sift.bii.a-star.edu.sg/).

For in vitro analysis, stably transformed fibroblasts derived from a *PCCA*- and *PCCB*-deficient cell line [Clavero et al., 2002; Perez-Cerda et al., 2003] were used. *PCCA* and *PCCB* missense mutations were introduced by PCR mutagenesis (QuickChange Mutagenesis kit; Agilent Technologies) in the pCMVA45-12 and pRcCMVB52 vectors coding for wild-type *PCCA* and *PCCB* cDNAs, respectively. Transfection was achieved by lipofection using Lipofectamine LTX (Invitrogen) cotransfecting 2 µg of the mutant PCCA or PCCB vectors and 2 µg of the wild-type partner PCCB or PCCA constructs to achieve maximal expression, as previously described [Clavero et al., 2002; Perez-Cerda et al., 2003]. PCC activity was assayed in cells harvested 72 hr after transfection. Experiments were performed in duplicate.

Readthrough Drug Treatment in Patients' Fibroblasts

All cells used had less than 10 passages. Cells (2×10^5) were plated in P6-wells and 24 hr after readthrough drugs were added in medium without antibiotics. Different concentrations of gentamicin sulfate (500–750 µg/ml; Sigma–Aldrich), G418 (50–75 µg/ml; Gibco BRL), and PTC124 (5, 10, and 15 µM; Selleckchem) were used, according to previous studies [Bellais et al., 2010; Lai et al., 2004]. For treatment with gentamicin and G418, fresh media and drugs were replaced at 72 hr and cells were harvested after 5 days of treatment. For PTC124 treatment, cells were harvested 72 hr after its addition. For experiments using nonsense-mediated decay (NMD) inhibitors, cells were plated and treated as described above, and 8 hr before harvesting, 5–20 µM wortmannin (Sigma–Aldrich) or 7.5 mM caffeine (Sigma–Aldrich) was added. After cell harvest, mRNA was quantified and PCC activity was analyzed in parallel.

Results

Spectrum of Nonsense Mutations in PA Patients

As reference laboratory, our center receives samples from PA patients worldwide to perform genetic analysis of the *PCCA* and *PCCB* genes. In the past years, 80 *PCCA* and 110 *PCCB* patients have been genotyped, with a mutation detection rate of 99.9%. In this cohort of patients, we have identified 12 different nonsense mutations (Table 1), five in the *PCCA* gene and seven in the *PCCB* gene; six of them are novel—namely, p.Q371* (c.1111C>T), p.Y380* (c.1140C>A), and p.Q611* (c.1831C>T) in the *PCCA* gene, and p.R111* (c.331C>T), p.Q139* (c.415C>T), and p.Y314* (c.942C>A) in the *PCCB* gene—each of them identified in only one patient. The other nonsense mutations identified have been previously reported and are described in the HGMD (HGMD professional release, 2011). According to our results and those in the HGMD, nonsense mutations represent 8 and 11% of the mutations in the *PCCA* and *PCCB* genes, respectively. Most of them correspond to UGA stop codons (Table 1).

In Vitro Readthrough of PA Nonsense Mutations

To test the effect of aminoglycosides as representative compounds with readthrough potential, we assayed the expression of nonsense-bearing PCCA and PCCB proteins in the presence of gentamicin and G418 in a mammalian-coupled TNT assay. In the absence of treatment, truncated proteins of the expected size for each of the 12 nonsense mutations described above were synthesized in levels

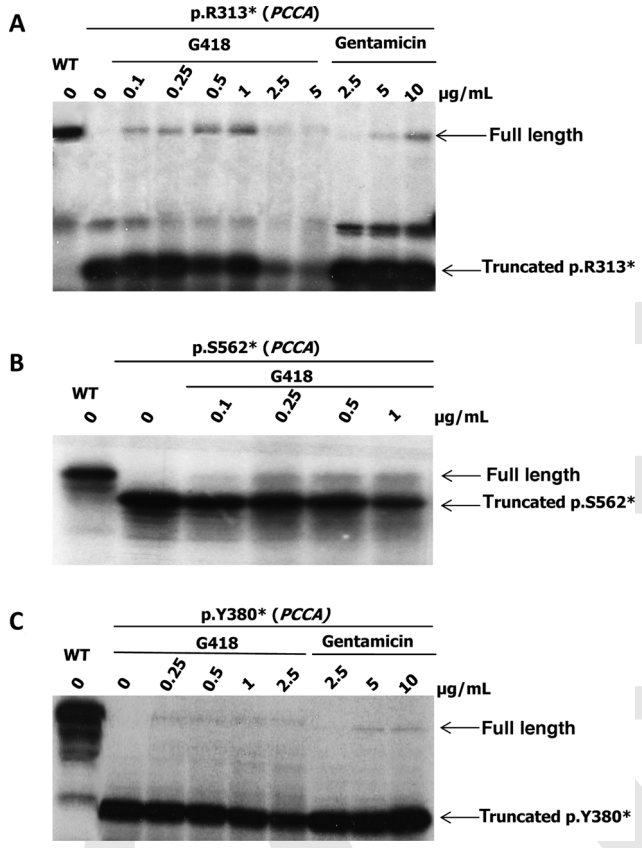

Figure 1. Effect of aminoglycosides on in vitro readthrough of nonsense mutations in the *PCCA* and *PCCB* genes in the TNT system. The figure shows representative experiments for the p.R313*, p.S562*, and p.Y380* mutations in the *PCCA* gene.

comparable to wild-type protein. No full-length protein was detectable for the mutants tested. Occasional extra bands were observed in the translation products, presumably corresponding to other open reading frames in the template vector or degradation products of the synthesized proteins. Increasing doses of gentamicin (2.5–15 µg/ml) and G418 (0.1–2.5 µg/ml) were added to the synthesis reaction, and the appearance of full-length protein was monitored and quantified. Figure 1 shows the results of representative experiments, and a summary of the results obtained for all mutations at selected aminoglycoside concentrations is depicted in Figure 2. In the case of *PCCB* mutant protein p.W531* resulting in a carboxy-terminal deletion of nine amino acids, the small difference in size precluded precise separation of wild-type and truncated protein; so, no quantification of the effect of aminoglycosides could be carried out. Depending on the mutation tested, the estimated amount of full-length protein varied from less than 1 to 25%. The results demonstrate that at least eight naturally occurring mutations are amenable to suppression by aminoglycosides to a detectable extent. Mutations with highest levels of aminoglycoside-mediated readthrough were p.R313*, p.S562*, and p.Q611* in the *PCCA* gene. A dose-dependent effect was generally observed, with the highest readthrough occurring for most mutants at 15 µg/ml of gentamicin and at 1 µg/ml of G418. In general, at higher concentrations, overall protein synthesis was inhibited, as previously observed by other authors [Lai et al., 2004]. When both drugs were added together to the synthesis reaction, we observed no synergistic effects (data not shown). For mutants p.R113*, p.Q139*, and p.R514* in the *PCCB* gene, no full-length protein was detectable in the conditions tested.

PTC124 (ataluren) was also tested in the TNT assay at concentrations 0.03–10 µM for mutations p.R313* and p.S562* in the *PCCA* gene, shown to be responsive to aminoglycoside-mediated nonsense suppression. No full-length protein was detectable in these conditions.

In Silico and In Vitro Analysis of the Predicted Missense Changes Induced by Aminoglycoside Treatment

Gln and Trp are the two most common amino acid insertions for stop codon readthrough; glutamine is inserted at nonsense UAG or UAA codons, whereas UGA miscode to tryptophan [Brooks et al., 2006; Harrell et al., 2002; Nilsson and Ryden-Aulin, 2003]. The predicted amino acid changes in our series of PA nonsense mutations were analyzed both by an in silico approach evaluating the pathogenicity of the missense mutation and by expression analysis in a eukaryotic system to quantify the associated PCC residual activity. With this study, we sought to analyze the feasibility and the potential of a functional recovery of the suppressed nonsense mutations in PA. The results are shown in Table 2. Most nonsense mutations will predictably be translated reverting to the original amino acid or change to a missense mutation that is capable of

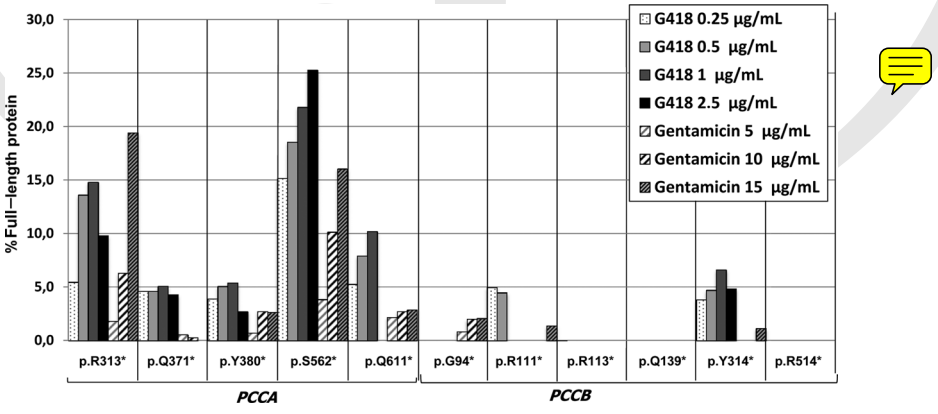

Figure 2. Estimation of full-length protein synthesized from each mutant construct in the TNT system as a result of the different aminoglycoside treatments. The results are the mean of at least three experiments.

Table 2. In Silico and In Vitro Analysis of the Functional Effect of the Predicted Changes Resulting from Nonsense Mutation Readthrough

Gene	Nonsense mutation	Predicted change	Predicted functional effect		In vitro residual activity (%)[c]
			PolyPhen-2 (score)[a]	SIFT (score)[b]	
PCCA	p.R313*	p.R313W	Damaging (1.000)	Damaging (0.00)	2.6 ± 2.3
	p.Q371*	p.Q371Q	Original amino acid	Original amino acid	Wild type
	p.Y380*	p.Y380Q	Benign (0.025)	Tolerated (0.32)	34.5 ± 2.9
	p.S562*	p.S562W	Damaging (0.494)	Damaging (0.03)	67.8 ± 9.5
	p.Q611*	p.Q611Q	Original amino acid	Original amino acid	Wild type
PCCB	p.G94*	p.G94W	Damaging (0.999)	Tolerated (0.08)	38.4 ± 2.5
	p.R111*	p.R111W	Damaging (0.976)	Tolerated (0.19)	49.7 ± 3.6
	p.R113*	p.R113W	Damaging (0.989)	Damaging (0.02)	11.7 ± 2.7
	p.Q139*	p.Q139Q	Original amino acid	Original amino acid	Wild type
	p.Y314*	p.Y314Q	Damaging (1.000)	Damaging (0.00)	10.0 ± 0.6
	p.R514*	p.R514W	Damaging (0.992)	Tolerated (0.05)	67.1 ± 5.9
	p.W531*	p.W531W	Original amino acid	Original amino acid	Wild type

[a]PolyPhen-2 (http://genetics.bwh.harvard.edu/pph2/). Score ranges from 0 (neutral) to 1 (damaging).
[b]SIFT (http://blocks.fhcrc.org/sift/SIF.html). Score ranges from 0 (damaging) to 1 (neutral).
[c]Relative to wild-type levels.

supporting partial enzyme function, as verified by expression analysis. The in silico prediction using PolyPhen-2 predicted a damaging effect for most of the missense changes with different scores that, in general, did not correlate with the results of the expression analysis. Using SIFT, we obtained a better correlation, as mutations predicted to be tolerated, exhibited in vitro relative activity values greater than 30%. The only exception was mutation p.S562W, predicted to be damaging by both programs and found to have the highest residual activity by expression analysis (Table 2).

Ex Vivo Readthrough of PA Nonsense Mutations: Functional Analysis in Patients' Fibroblasts

Available primary fibroblasts from PA patient carriers of nonsense mutations in at least one allele were cultured for 5 days in the presence of increasing amounts of gentamicin (300–1000 μg/ml) or G418 (30–100 μg/ml), or for 3 days with PTC124 (5–100 μM), and PCC activity was subsequently analyzed. The samples included patients P1 and P2, homozygous for the *PCCA* mutations p.R313* and p.S562*, respectively, and the following heterozygous *PCCB*-deficient patients P3 (p.W531*/p.G470fs), P4 (p.Y314*/p.E331*, the second mutation corresponding to variant c.990dupT, not susceptible to readthrough treatment), and P5 (p.G94*/p.G470fs).

In all fibroblast samples, a detectable increase in the PCC activity (up to 50-fold) could be observed at several concentrations of the readthrough compounds (Fig. 3 and Supp. Table S1), with best results generally obtained with 300 μg/ml gentamicin and 50–75 μg/ml G418. Overall, the recovered PCC activity was up to 10–15% of the activity levels in control fibroblasts treated in parallel. In the latter, gentamicin had no significant effect, whereas G418 and PTC124 resulted in a 40–60% reduction in PCC activity (Supp. Table S1). Treatment at longer times in patient fibroblasts did not result in higher PCC activity levels (data not shown). The absence of commercially available antibodies sensitive enough to detect PCCA and PCCB proteins in human fibroblasts precluded protein analysis.

Considering that mRNAs encoding nonsense mutations resulting in premature stop codons may be subject to degradation via NMD, thus reducing the amount of mutant mRNA available for translational readthrough [Kuzmiak and Maquat, 2006], we analyzed *PCCA* and *PCCB* transcript levels by qRT-PCR. All patient cells had decreased amounts, with values ranging from 1–35% of wild-type levels. After readthrough drug treatment, we measured mRNA levels in P1–P4 fibroblasts, and no significant differences were observed, except for sample P2 with G418 and PTC124 (Fig. 4).

We further investigated the effect of NMD inhibitors wortmannin and caffeine, which act by phosphorylation of an essential NMD

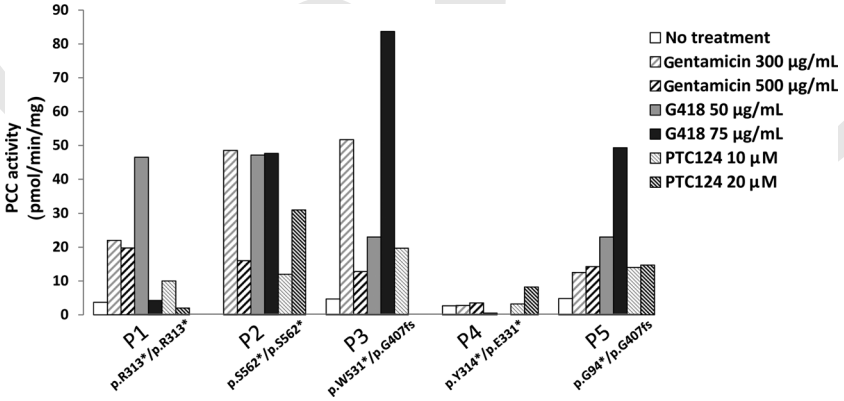

Figure 3. Effect of readthrough drugs on the PCC activity in fibroblasts from patient carriers of nonsense mutations. The results are the mean from at least two experiments performed in duplicate.

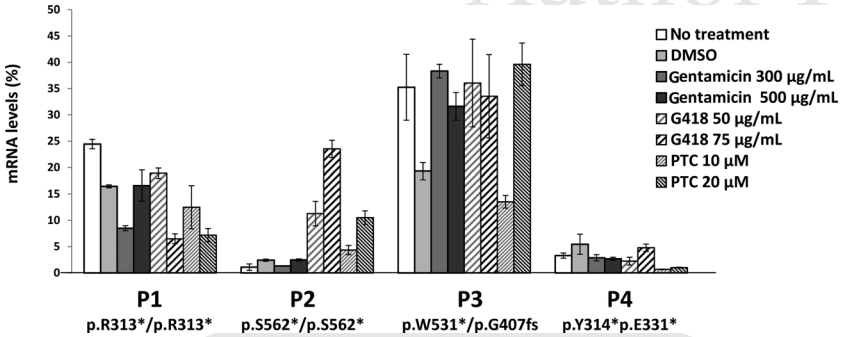

Figure 4. Quantification by qRT-PCR of *PCCA* (for P1 and P2) and *PCCB* (P3 and P4) mRNA levels in fibroblast samples untreated or cultured with different concentrations of readthrough drugs. The *x*-axis represents the results of the relative quantification expressed as percentages. Data represent the mean ± SD of two experiments performed in triplicate. DMSO, dimethyl sulfoxide.

factor while preserving protein synthesis [Usuki et al., 2004; Rio Frio et al., 2008]. Fibroblasts from patient P2 homozygous for mutation p.S562* predictably reverting to a missense change with high residual activity (Table 2) and responsive to aminoglycoside treatment were incubated with 5–20 µM wortmannin or 7.5 mM caffeine for 8 hr. With 20 µM wortmannin, a 1.5-fold to twofold increase in *PCCA* transcript levels was evidenced, in line with previous observations [Linde et al., 2007; Rio Frio et al., 2008]. However, this increase only resulted in less than 25% wild-type transcript levels, and no substantial differences in restored PCC activity were observed between cells treated with aminoglycosides alone or in combination with wortmannin or caffeine (data not shown).

Discussion

PA is a good model for evaluating drug-induced readthrough. There is currently no effective treatment available, and in many cases, neurological deterioration is unavoidable. However, studies in a *PCCA* knockout mouse model have revealed that the presence of as low as 10–20% of PCC activity in liver, resulting from a low expression transgene, can significantly improve the outcome, preventing neonatal lethality [Miyazaki et al., 2001]. Here, we report six novel nonsense mutations, and a total of 12 different nonsense changes in a cohort of 190 Caucasian PA patients. Roughly, 10% of the patients carry at least one nonsense mutation, which is relevant, as certain compounds have been shown to suppress PTCs in genetic disease and allow for generation of full-length protein. Given the data variability in the literature for different disorders, it is at present unknown whether different nonsense mutations in a specific gene will be responsive or not to readthrough drugs. Our results provide a proof-of-concept that naturally occurring nonsense mutations in PA can be effectively suppressed by readthrough drugs, with different efficiencies depending on the nonsense mutation tested, and that a therapeutically relevant functional recovery in patients is feasible, given the results obtained in cellular models of disease.

Our in vitro study with the TNT system is focused on naturally occurring nonsense mutations, therefore precluding a thorough analysis of different sequence contexts on readthrough effect. In the nonsense mutations identified, no optimal UGAC tetranucleotides reported to have the highest response to aminoglycosides [Keeling and Bedwell, 2002], were present. Considering *PCCA* mutants, we do observe a trend toward higher nonsense suppression for mutations p.R313* and p.S562* with an UGA stop codon, correlating with previous studies [Keeling et al., 2001; Manuvakhova et al., 2000]. However, for *PCCB* mutants, no clear conclusions can be drawn. Overall, treatment effects appear to be more significant for *PCCA* mutations, which could be due to differences in the reporter vector or in the experimental procedures in each case.

After confirming in vitro nonsense suppression in PA, our study goes one step further to investigate the biological activity of the synthesized protein, which is lacking in other studies, just focused at the detection of full-length protein. Taking into account the predicted amino acid insertion at the termination codon as a consequence of aminoglycoside treatment and the results of in silico and in vitro analysis, we can conclude that a major fraction of the full-length PCCA and PCCB proteins generated will retain PCC enzymatic activity (Table 2). Our results confirm that in silico predictions, although useful, should be interpreted with caution and may work for some proteins or for some mutations better than for others. More than one program should be used to obtain reliable results, as each uses different algorithms, ~~including or not available structural and phylogenetic analysis~~ [Thusberg and Vihinen, 2009]. In our hands, SIFT resulted in a more accurate prediction of the missense effect, as verified using a well-established expression analysis system [Clavero et al., 2002].

Studies with cultured patient cell carriers of nonsense mutations and devoid of PCC activity showed that in certain conditions, aminoglycoside treatment generated detectable activity, with values reaching up to 10–15% of treated control cells, similar to other studies where functional recovery was quantified [Keeling et al., 2001]. P3 fibroblasts heterozygous for the *PCCB* mutation p.W531* predictably reverting to the original amino acid exhibited the highest functional recovery, along with P2 fibroblasts homozygous for the *PCCA* mutation p.S562*, with highest in vitro readthrough and predictably resulting in a protein with high residual activity. Overall, genotypes with UGA stop codons appear to be most responsive. The increase in PCC activity with gentamicin is generally lower at 500 µg/ml than at 300 µg/ml, suggestive of a toxic effect. It should be noted that in cultured primary fibroblasts, the concentration of aminoglycosides used are much higher than in in vitro assays due to associated permeability problems, which may increase with continued passage of the cells [Keeling et al., 2001]. In this respect, the different functional response may also reflect differences in cell passage number, as well as variability in the amounts of different amino acids incorporated at the stop codon, or the fact that patients' fibroblasts P1 and P2 are homozygous, whereas the other fibroblasts are heterozygous for the nonsense mutation. In some cases, the relative effects of each compound differ in the in vivo and in vitro systems,

which is a common observation [Buck et al., 2009]. In addition, some authors have reported positive results with G418, whereas in the same assay, PTC124 was not effective [Dranchak et al., 2011], in line with our results in the TNT system.

One major limitation in vivo may be the availability of nonsense-bearing transcripts, given the role of NMD in their degradation. Indeed, greatly decreased PCC mRNA levels were detected, although ~~in the PA, fibroblasts analyzed~~ up to 35% of the transcripts escape NMD and are available for full-length protein synthesis in the presence of aminoglycosides, which explains the functional recovery observed. No significant effect on mRNA stability was observed with the different treatments for P1, P3, and P4, whereas some effect was detected for sample P2, although no clear conclusions can be drawn from the results. In the literature, some authors reported no increase in mRNA levels with aminoglycosides [Buck et al., 2009; Hein et al., 2004; Popescu et al., 2010], whereas others have described some restoration of mRNA levels with gentamicin [Bellais et al., 2010]. Although results using wortmannin were not conclusive, the potential role of NMD inhibitors in response to readthrough drugs in PA remains to be clarified.

The results of this study further support the results of previous studies in other gene defects and provide evidence of the feasibility of treatment for PA. As in other autosomal recessive diseases, the presence of small levels of functional protein can be therapeutically relevant, and patients with mutations retaining some activity have been described to exhibit milder phenotypes [Perez-Cerda et al., 2000]. The results encourage further testing with other compounds [Du et al., 2009; Hainrichson et al., 2008; Welch et al., 2007], which may be capable of higher readthrough efficiencies, as well as follow-up animal studies. Future prospects in PA for PTC124 and other drugs will have to await the results of clinical trials, especially those currently running for methylmalonic aciduria (http://www.ptcbio.com/), another organic aciduria due to an enzyme deficiency of the propionate oxidation pathway.

Acknowledgments

The authors thank Dr. C. Pérez-Cerdá for her collaboration and expert advice with patients' samples, E. Martinez for her help in the experiments, and Sven Calduch for technical assistance.

References

Barton-Davis ER, Cordier L, Shoturma DI, Leland SE, Sweeney HL. 1999. Aminoglycoside antibiotics restore dystrophin function to skeletal muscles of mdx mice. J Clin Invest 104:375–381.

Bedwell DM, Kaenjak A, Benos DJ, Bebok Z, Bubien JK, Hong J, Tousson A, Clancy JP, Sorscher EJ. 1997. Suppression of a CFTR premature stop mutation in a bronchial epithelial cell line. Nat Med 3:1280–1284.

Bellais S, Le Goff C, Dagoneau N, Munnich A, Cormier-Daire V. 2010. In vitro readthrough of termination codons by gentamycin in the Stuve–Wiedemann Syndrome. Eur J Hum Genet 18:130–132.

Brooks DA, Muller VJ, Hopwood JJ. 2006. Stop-codon read-through for patients affected by a lysosomal storage disorder. Trends Mol Med 12:367–373.

Buck NE, Wood L, Hu R, Peters HL. 2009. Stop codon read-through of a methylmalonic aciduria mutation. Mol Genet Metab 97:244–249.

Clavero S, Martinez MA, Perez B, Perez-Cerda C, Ugarte M, Desviat LR. 2002. Functional characterization of PCCA mutations causing propionic acidemia. Biochim Biophys Acta 1588:119–125.

de Baulny HO, Benoist JF, Rigal O, Touati G, Rabier D, Saudubray JM. 2005. Methylmalonic and propionic acidaemias: management and outcome. J Inherit Metab Dis 28:415–423.

Desviat LR, Perez B, Perez-Cerda C, Rodriguez-Pombo P, Clavero S, Ugarte M. 2004. Propionic acidemia: mutation update and functional and structural effects of the variant alleles. Mol Genet Metab 83:28–37.

Dranchak PK, Di Pietro E, Snowden A, Oesch N, Braverman NE, Steinberg SJ, Hacia JG. 2011. Nonsense suppressor therapies rescue peroxisome lipid metabolism and assembly in cells from patients with specific PEX gene mutations. J Cell Biochem 112:1250–1258.

Du L, Damoiseaux R, Nahas S, Gao K, Hu H, Pollard JM, Goldstine J, Jung ME, Henning SM, Bertoni C, Gatti RA. 2009. Nonaminoglycoside compounds induce readthrough of nonsense mutations. J Exp Med 206:2285–2297.

Fenton WA, Gravel RA, Rosenberg LE. 2001. Disorders of propionate and methylmalonate metabolism. In: Scriver CR, Beaudet AL, Sly W, Valle D, editors. The metabolic and molecular bases of inherited disease. New York: McGraw-Hill. pp 2165–2190.

Finkel RS. 2010. Read-through strategies for suppression of nonsense mutations in Duchenne/ Becker muscular dystrophy: aminoglycosides and ataluren (PTC124). J Child Neurol 25:1158–1164.

Grayson C, Chapple JP, Willison KR, Webster AR, Hardcastle AJ, Cheetham ME. 2002. In vitro analysis of aminoglycoside therapy for the Arg120stop nonsense mutation in RP2 patients. J Med Genet 39:62–67.

Hainrichson M, Nudelman I, Baasov T. 2008. Designer aminoglycosides: the race to develop improved antibiotics and compounds for the treatment of human genetic diseases. Org Biomol Chem 6:227–239.

Harrell L, Melcher U, Atkins JF. 2002. Predominance of six different hexanucleotide recoding signals 3′ of read-through stop codons. Nucleic Acids Res 30:2011–2017.

Hein LK, Bawden M, Muller VJ, Sillence D, Hopwood JJ, Brooks DA. 2004. Alpha-L-iduronidase premature stop codons and potential read-through in mucopolysaccharidosis type I patients. J Mol Biol 338:453–462.

Howard M, Frizzell RA, Bedwell DM. 1996. Aminoglycoside antibiotics restore CFTR function by overcoming premature stop mutations. Nat Med 2:467–469.

Huang CS, Sadre-Bazzaz K, Shen Y, Deng B, Zhou ZH, Tong L. 2010. Crystal structure of the alpha(6)beta(6) holoenzyme of propionyl-coenzyme A carboxylase. Nature 466:1001–1005.

Keeling KM, Bedwell DM. 2002. Clinically relevant aminoglycosides can suppress disease-associated premature stop mutations in the IDUA and P53 cDNAs in a mammalian translation system. J Mol Med 80:367–376.

Keeling KM, Brooks DA, Hopwood JJ, Li P, Thompson JN, Bedwell DM. 2001. Gentamicin-mediated suppression of Hurler syndrome stop mutations restores a low level of alpha-L-iduronidase activity and reduces lysosomal glycosaminoglycan accumulation. Hum Mol Genet 10:291–299.

Kuzmiak HA, Maquat LE. 2006. Applying nonsense-mediated mRNA decay research to the clinic: progress and challenges. Trends Mol Med 12:306–316.

Lai CH, Chun HH, Nahas SA, Mitui M, Gamo KM, Du L, Gatti RA. 2004. Correction of ATM gene function by aminoglycoside-induced read-through of premature termination codons. Proc Natl Acad Sci USA 101:15676–15681.

Linde L, Boelz S, Nissim-Rafinia M, Oren YS, Wilschanski M, Yaacov Y, Virgilis D, Neu-Yilik G, Kulozik AE, Kerem E, Kerem B. 2007. Nonsense-mediated mRNA decay affects nonsense transcript levels and governs response of cystic fibrosis patients to gentamicin. J Clin Invest 117:683–692.

Linde L, Kerem B. 2008. Introducing sense into nonsense in treatments of human genetic diseases. Trends Genet 24:552–563.

Manuvakhova M, Keeling K, Bedwell DM. 2000. Aminoglycoside antibiotics mediate context-dependent suppression of termination codons in a mammalian translation system. RNA 6:1044–1055.

Miyazaki T, Ohura T, Kobayashi M, Shigematsu Y, Yamaguchi S, Suzuki Y, Hata I, Aoki Y, Yang X, Minjares C, Haruta I, Uto H, Ito Y, Müller U. 2001. Fatal propionic acidemia in mice lacking propionyl-CoA carboxylase and its rescue by postnatal, liver-specific supplementation via a transgene. J Biol Chem 276:35995–35999.

Nilsson M, Ryden-Aulin M. 2003. Glutamine is incorporated at the nonsense codons UAG and UAA in a suppressor-free *Escherichia coli* strain. Biochim Biophys Acta 1627:1–6.

Perez-Cerda C, Clavero S, Perez B, Rodriguez-Pombo P, Desviat LR, Ugarte M. 2003. Functional analysis of PCCB mutations causing propionic acidemia based on expression studies in deficient human skin fibroblasts. Biochim Biophys Acta 1638:43–49.

Perez-Cerda C, Merinero B, Rodriguez-Pombo P, Perez B, Desviat LR, Muro S, Richard E, Garcia MJ, Gangoiti J, Ruiz Sala P, Sanz P, Briones P, Ribes A, Martínez-Pardo M, Campistol J, Pérez M, Lama R, Murga ML, Lema-Garrett T, Verdú A, Ugarte M. 2000. Potential relationship between genotype and clinical outcome in propionic acidaemia patients. Eur J Hum Genet 8:187–194.

Popescu AC, Sidorova E, Zhang G, Eubanks JH. 2010. Aminoglycoside-mediated partial suppression of MECP2 nonsense mutations responsible for Rett syndrome in vitro. J Neurosci Res 88:2316–2324.

Richard E, Desviat LR, Perez B, Perez-Cerda C, Ugarte M. 1999. Genetic heterogeneity in propionic acidemia patients with alpha-subunit defects. Identification of five novel mutations, one of them causing instability of the protein. Biochim Biophys Acta 1453:351–358.

Rincon A, Aguado C, Desviat LR, Sanchez-Alcudia R, Ugarte M, Perez B. 2007. Propionic and methylmalonic acidemia: antisense therapeutics for intronic variations causing aberrantly spliced messenger RNA. Am J Hum Genet 81:1262–1270.

Rio Frio T, Wade NM, Ransijn A, Berson EL, Beckmann JS, Rivolta C. 2008. Premature termination codons in PRPF31 cause retinitis pigmentosa via haploinsufficiency due to nonsense-mediated mRNA decay. J Clin Invest 118:1519–1531.

Suormala T, Wick H, Bonjour JP, Baumgartner ER. 1985. Rapid differential diagnosis of carboxylase deficiencies and evaluation for biotin-responsiveness in a single blood sample. Clin Chim Acta 145:151–162.

Thusberg J, Vihinen M. 2009. Pathogenic or not? And if so, then how? Studying the effects of missense mutations using bioinformatics methods. Hum Mutat 30:703–714.

Usuki F, Yamashita A, Higuchi I, Ohnishi T, Shiraishi T, Osame M, Ohno S. 2004. Inhibition of nonsense-mediated mRNA decay rescues the phenotype in Ullrich's disease. Ann Neurol 55:740–744.

Welch EM, Barton ER, Zhuo J, Tomizawa Y, Friesen WJ, Trifillis P, Paushkin S, Patel M, Trotta CR, Hwang S, Wilde RG, Karp G, Takasugi J, Chen G, Jones S, Ren H, Moon YC, Corson D, Turpoff AA, Campbell JA, Conn MM, Khan A, Almstead NG, Hedrick J, Mollin A, Risher N, Weetall M, Yeh S, Branstrom AA, Colacino JM, Babiak J, Ju WD, Hirawat S, Northcutt VJ, Miller LL, Spatrick P, He F, Kawana M, Feng H, Jacobson A, Peltz SW, Sweeney HL. 2007. PTC124 targets genetic disorders caused by nonsense mutations. Nature 447:87–91.

Queries

Q1: AU: Sodium dodecyl sulfate-polyacrylamide gel electrophoresis: Is this the correct definition for SDS-PAGE? Please change if this is not correct.

Q2: AU: Quantitative reverse-transcription polymerase chain reaction: Is this the correct definition for qRT-PCR? Please change if this is not correct.

Q3: AU: Please provide the following location details for Applied Biosystems: city and state (if USA), or city, state, and country (if other than USA).

Q4: AU: Glyceraldehyde 3-phosphate dehydrogenase: Is this the correct definition for GAPDH? Please change if this is not correct.

Q5: AU: Please define "WT" given in Figure 1 either in the figure or in the caption.

Q6: AU: Please define SIFT.

Q7: AU: Using SIFT, . . . values greater than 30%. The meaning of this sentence is not clear. Please rewrite or confirm that the sentence is correct.

Q8: AU: Dimethyl sulfoxide: Is this the correct definition for DMSO? Please change if this is not correct.

Q9: AU: "including or not available structural and phylogenetic analysis": The meaning of this phrase is not clear. Please rewrite or confirm that the phrase is correct.

Q10: AU: Indeed, greatly . . . the functional recovery observed. This sentence has been edited for clarity. Please check and confirm whether it is correct.

Q11: AU: As per style of the journal, complete list of authors should be provided in the reference list. Hence, the list of authors have been updated for the following references: Du et al., 2009; Linde et al., 2007; Miyazaki et al., 2001; Perez-Cerda et al., 2000; Welch et al., 2007. Please check.

Q12: AU: Reference Popescu et al., 2010 has been updated as per PubMed. Please check.

Neurogenetics (2011) 12:183–191
DOI 10.1007/s10048-011-0279-4

ORIGINAL ARTICLE

Genotype–phenotype correlations in sepiapterin reductase deficiency. A splicing defect accounts for a new phenotypic variant

Luisa Arrabal · Libertad Teresa · Rocío Sánchez-Alcudia · Margarita Castro · Celia Medrano · Luis Gutiérrez-Solana · Susana Roldán · Aida Ormazábal · Celia Pérez-Cerdá · Begoña Merinero · Belén Pérez · Rafael Artuch · Magdalena Ugarte · Lourdes R. Desviat

Received: 14 January 2011 / Accepted: 18 February 2011 / Published online: 24 March 2011

Abstract Sepiapterin reductase (SR) catalyzes the final step in the de novo synthesis of tetrahydrobiopterin, essential cofactor for phenylalanine, tyrosine, and tryptophan hydroxylases. SR deficiency is a very rare disease resulting in monoamine neurotransmitter depletion. Most patients present with clinical symptoms before the first year of age corresponding to a dopa-responsive dystonia phenotype with diurnal fluctuations, although some patients exhibit more complex motor and neurological phenotypes. Herein, we describe four new cases from Spain, their clinical phenotype and the biochemical and genetic analyses. Two mutations in the *SPR* gene were functionally expressed to provide a basis to establish genotype–phenotype correlations. Mutation c.751A>T is functionally null, correlating with the severe phenotype observed. The novel mutation c.304G>T was identified in three siblings with a strikingly mild phenotype without cognitive delay and close to asymptomatic in the eldest sister. Minigene analysis demonstrated that this mutation located in the last nucleotide of exon 1 affects splicing although some normal transcripts can be produced, resulting in the missense mutant p.G102C that retains partial activity. These results may account for the mild phenotype and the variable clinical presentations observed, which could depend on interindividual differences in relative abundance of correctly spliced and aberrant transcripts.

Keywords Dopa-responsive dystonia · Sepiapterin reductase · Neurotransmitter deficiency · Splicing mutation · Genotype–phenotype

L. Arrabal · S. Roldán
Servicio de Neuropediatría, Hospital Virgen de las Nieves, Granada, Spain

L. Teresa · R. Sánchez-Alcudia · M. Castro · C. Medrano · C. Pérez-Cerdá · B. Merinero · B. Pérez · M. Ugarte (✉) · L. R. Desviat (✉)
Centro de Diagnóstico de Enfermedades Moleculares, Centro de Biología Molecular Severo Ochoa, UAM-CSIC, Universidad Autónoma de Madrid, 28049 Madrid, Spain
e-mail: mugarte@cbm.uam.es
e-mail: lruiz@cbm.uam.es

L. Teresa · R. Sánchez-Alcudia · M. Castro · C. Medrano · A. Ormazábal · C. Pérez-Cerdá · B. Merinero · B. Pérez · R. Artuch · M. Ugarte · L. R. Desviat
Centro de Investigación Biomédica en Red de Enfermedades Raras (CIBERER)
URL: http://www.ciberer.es/

L. Gutiérrez-Solana
Sección de Neurología Pediátrica, Hospital Niño Jesús, Madrid, Spain

A. Ormazábal · R. Artuch
Clinical Biochemistry Department, Hospital Sant Joan de Déu, Esplugues, Barcelona, Spain

Introduction

Sepiapterin reductase (SR, EC 1.1.1.153) deficiency (MIM #612716) is a very rare autosomal recessive disorder of tetrahydrobiopterin (BH_4) metabolism. BH_4 is an essential cofactor required by phenylalanine (Phe), tryptophan, and tyrosine (Tyr) hydroxylases, as well as by nitric oxide

synthases and glyceryl–ether monooxygenase [1]. The impairment of tyrosine and tryptophan hydroxylase activities that catalyze the rate-limiting steps in the biosynthesis of neurotransmitters dopamine and serotonin, respectively, explains the neurological deterioration in patients with BH_4 defects [2]. BH_4 is synthesized de novo from guanosine triphosphate (GTP) in three steps, catalyzed by the enzymes GTP cyclohydrolase I, 6-pyruvoyl tetrahydrobiopterin synthase, and the SR enzyme that catalyzes the final reduction of 6-pyruvoyltetrahydropterin to BH_4. Three additional enzymes can replace SR, aldose reductase, carbonyl reductase, and dihydrofolate reductase, in a pathway that is active in peripheral tissues but not in brain, explaining why patients with SR deficiency do not present with hyperphenylalaninemia [3].

The diagnosis of SR deficiency is based on cerebrospinal fluid (CSF) analysis of pterins and biogenic amines, revealing decreased concentrations of homovanillic acid (HVA), 5-hydroxyindolacetic acid (5-HIAA), and elevated levels of 7,8-dihydrobiopterin and of sepiapterin. The presence of pathogenic mutations in the *SPR* gene encoding the SR enzyme and/or the documentation of low SR activity in fibroblasts allows confirmation of the diagnosis [4, 5]. Clinically, most patients present symptoms in the first years of age, although diagnosis is usually delayed probably due to lack of physician's awareness of the disease and to the need of specialized diagnostic procedures. Commonly, patients exhibit progressive psychomotor retardation and different neurological abnormalities including tremor, seizures, oculogyric crises, and, notably, dystonia with diurnal fluctuations and responsive to L-dopa [6, 7]. Thus, autosomal recessive SR deficiency accounts for a small fraction of dopa-responsive dystonia cases which are prevalently caused by a dominant GTP cyclohydrolase I defect [8]. There are some isolated cases of SR deficiency associated with a milder phenotype coming to attention in adulthood, although with delayed milestones and/or abnormal gait already in childhood [8–10]. In most cases treatment response is excellent although cognitive impairment may persist, highlighting the importance of an early diagnosis of SR deficiency.

To date, 31 patients with SR deficiency are included in the database of BH_4 deficiencies BIODEF (http://www.biopku.org) and a total of 12 different mutations are reported in the *SPR* gene, mostly of the missense or nonsense type. One missense mutation, p.R150G (c.448A>G), has been expressed in a prokaryotic system to assay its functional effect revealing a complete loss of SR activity [3]. Only one splicing mutation has been identified, affecting the conserved 3′ acceptor splice site of intron 2 (IVS2-2a>g; c.596-2a>g).

The aim of this work has been to expand the knowledge of the genotypes and phenotypes of SR deficiency reporting four new cases, three of them without cognitive delay belonging to the same family and presenting distinct phenotypes, from a clearly symptomatic patient to an almost asymptomatic one. The mutations identified in the *SPR* gene have been functionally expressed providing the basis to understand the phenotypic presentation of the disease.

Clinical reports

Case 1 was diagnosed at 23 months of age after presenting psychomotor retardation, hypotonia, hypersalivation, hypersomnolence, ataxia, and extrapyramidal signs. Brain MRI, EEG, routine blood tests, and the study of amino acids and organic acids in body fluids were normal. Diagnosis was made after a routine screening in CSF for neurotransmitter deficiencies performed to all cases presenting neurological affectation and after excluding other metabolic diseases. Plasma prolactin levels were increased up to 24.6 ng/ml (normal range, 1.6–18 ng/ml) pointing to a central dopamine deficiency, as prolactin release is normally inhibited by central dopamine concentrations. Enzymatic and genetic analysis in fibroblasts confirmed the SR deficiency (Table 1). He is being treated with L-dopa/carbidopa (1.2 mg/kg/day) and 5-hydroxytryptophan (1 mg/kg/day) with a clear neurological improvement.

Case 2 is an 11-year-old girl born from healthy non-consanguineous parents after an uneventful pregnancy. She showed normal development until 7 years of age when her parents referred gait difficulties. Left foot equinovarus was evidenced at that moment. She also referred weakness and weariness. Symptoms showed a diurnal variation and were notably alleviated after a nap. In the evening she was virtually inactive and appeared exhausted. She had postural tremor when she was excited, abnormal ocular movements (upper deviation), and oral dyskinesias when tired or stressed. She showed paucity of movement and bradykinesia, a mask-like facial expression, and difficulties in initiating speech, with slurry sentences. Further examination revealed rigidity of lower limbs, slightly worse in the left hemi-body, and axial hypotonia. She had asymmetric postural dystonia with equinovarus left foot and bent spine. The left side was predominantly affected. Hyperactive reflexes and ankle clonus were present as well as myoclonic movements of hands and face. Cognitive level, general examination, and cranial nerves were normal. Ptosis, hypersalivation, or dysautonomia were not present. She was performing acceptably in a normal school setting although attention deficit was referred. Brain MRI, routine blood tests, and screening for inborn errors of metabolism were normal. In order to rule out a Segawa

Table 1 Biochemical and genetic analysis of the four cases with SR deficiency

	Case 1, 2 years	Case 2, 11 years	Case 3, 14 years	Case 4, 18 years	Reference values (2 years)	Reference values (>10 years)
CSF metabolites (nmol/l)						
5-HIAA (nM)	9 (50[a])	25	NP	NP	125–303	63–185
HVA (nM)	111 (125[a])	48	NP	NP	274–863	156–410
Neopterin (nM)	18	19	NP	NP	9–30	11–45
Biopterin (nM)	52	39	NP	NP	10–40	10–36
Sepiapterin (nM)	16	7.8	NP	NP	<0.5	<1
Phe loading test						
Phe/Tyr 0 h	NP	1.2	1.1	1.1	NA	0.5–1.2
Phe/Tyr 1 h	NP	5.1	5.5	5.8	NA	2.0–6.3
Phe/Tyr 2 h	NP	5.8	7.2	4.8	NA	1.17–4.15
Phe/Tyr 4 h	NP	4.3	8.9	4.8	NA	0.6–1.88
Fibroblasts						
SR enzyme activity (μU/mg protein)	4	NP	NP	NP	93–193	NA
Genetic analysis						
Mutations in the *SPR* gene	[c.751A>T] +[c.751A>T]	[c.448A>G]+[c.304G>T]	[c.448A>G]+[c.304G>T]	[c.448A>G]+[c.304G>T]	NA	NA

Mutations are named according to HGVS guidelines (http://www.hgvs.org/mutnomen) and the RefSeq NM_003124.4

NP not performed, *NA* not applicable

[a] Data after 3 years of treatment

disease, biogenic amines and pterins were analyzed in CSF. Moreover, a phenylalanine loading test was also performed. Genetic analysis confirmed the SR deficiency. L-Dopa treatment was initiated with 1 mg/kg/day combined with carbidopa. Treatment induced a spectacular improvement in a few days in terms of energy, strength, and mood. The dosage of L-dopa was increased until 5 mg/kg/day, with no adverse effects. 5-Hydroxytryptophan caused vomiting and was not tolerated.

The elder sisters (cases 3 and 4) were then evaluated. The younger sister (14 years old, case 3) did not refer any symptoms but in the clinical examination, she presented mask face, strabismus, mild dystonic gait with mild hypertonia of limbs, and slurry speech without any other symptoms. She did not show diurnal variations. She had a normal performance at school. She refused treatment at the beginning but she is actually receiving 5 mg/kg/day of L-dopa-carbidopa. The 18-year-old sister (case 4) only presented with slight head and hand tremor when stressed. She referred anxiety at times. No other clinical signs were observed and she has had no treatment to date. She completed high school without problems. Phenylalanine loading test and genetic analysis were performed in both cases 3 and 4. However, informed consent for CSF sampling was refused as well as for further SR activity studies using fibroblasts or lymphoblasts from any of the three sisters.

Methods

Biochemical analysis Biogenic amines (5-HIAA and HVA) and pterins in CSF were analyzed by HPLC with electrochemical and fluorescence detection, as previously reported [11–13].

Oral Phe loading test was performed as previously reported [14]. Briefly, 100 mg/kg/day of Phe was orally administered and Phe, Tyr, and Phe/Tyr ratio were calculated in baseline conditions and after 1, 2, and 4 h post Phe load. Phenylalanine and tyrosine concentrations were analyzed after acidic extraction from blood spots by ion pair HPLC with ultraviolet detection, according to a previously reported procedure [15]. Reference values were previously established in age-matched controls [14], after excluding inborn errors of metabolism of pterins and biogenic amines.

Genetic analysis DNA was isolated from blood using the Magnapure System (Roche). The three *SPR* gene exons and their flanking intronic sequences were amplified separately, using PCR primers (available upon request) designed using Primer3 software (http://fokker.wi.mit.edu/primer3/). The PCR products were sequenced using BigDye Terminator v.3.1 mix (Applied Biosystems, Foster City, CA) with the same primers used for amplification, and analysis by capillary electrophoresis on an ABI Prism® 3700 Genetic Analyzer (Applied Biosystems). Variant alleles were identified by comparison with the wild-type sequence (RefSeq NM_003124.4). Mutations were named according to the guidelines provided by HGVS (http://www.hgvs.org/mutnomen).

Sepiapterin reductase enzymatic assay The method is based on the conversion of sepiapterin to 7,8-dihydrobiopterin which is measured as its oxidized product (biopterin) by HPLC [3, 4]. Protein (5–20 μg) from total cellular extract from patient fibroblasts or 5 μg of soluble protein from induced *Escherichia coli* cells were incubated for 30 min in the dark in a reaction mixture containing 0.1 M potassium phosphate, pH 6.4; 125 mM L-sepiapterin; and 0.25 mM NADPH. The samples were subsequently oxidized for 30 min by addition of oxidizing solution containing 0.5% I_2 and 1% KI in 1 M HCl. Excess iodine was removed with ascorbic acid and the samples are then deproteinized using Ultrafree-MC filters (Millipore) and kept at −70°C until HPLC analysis. Biopterin is measured by HPLC with fluorescence detection at λ_{EX}, 360 nm and λ_{EM}, 440 nm.

Expression analysis in E. coli Plasmid pHSR9 encoding *SPR* cDNA (kindly provided by Dr. B. Thony) [3] was used for expression analysis. Mutations were introduced by site-directed mutagenesis using the Quikchange Mutagenesis kit (Stratagene). Sequence analysis confirmed the identity of the mutant clone and that no other mutation was present in the full-length cDNA. Expression of the recombinant wild-type and mutant SR proteins was carried out essentially as described [3]. Briefly, *E. coli* BL21 (DE3)pLysS cells (Promega) transformed with the corresponding plasmids were induced with 1 mM IPTG for 5 h, harvested by centrifugation and resuspended in 100 mM potassium phosphate (pH 6.4) with 0.4 mg/ml lysozyme and protease inhibitor (Complete Mini EDTA-free from Roche). Cell lysis was achieved by freeze thawing and the soluble protein amount was determined using the Bradford assay (Biorad).

Western blot analysis Forty micrograms of protein from the soluble extracts were resolved in a 12.5% SDS-polyacrylamide gel, transferred to a nitrocellulose membrane (Millipore) and detected using an anti-SR antibody (Abnova) applied in a 1:1,000 dilution, a secondary goat anti-rabbit antibody conjugated to peroxidase (Santa Cruz Biotechnologies) diluted 1:10,000 and the enhanced chemiluminiscence detection system ECL (Amersham).

High-resolution melting analysis Exon 1 of the *SPR* gene was amplified from patient 2 and from 100 control DNA samples (Human Random Control DNA panels from ECACC, Sigma) by real-time PCR using primers 5′-CGTGCTGTGTGCTTGCTG-3′ (sense) and 5′-CCCCAGCGGTGGAGGAAGTG-3′ (antisense). The PCR reactions were performed with 30 ng DNA in a 20-μl final volume using LightCycler® 480 High Resolution Melting Master (Roche Applied Sciences, Indianapolis) in a LightCycler® 480 apparatus. The primers and magnesium chloride were used at 0.2 and 3 mM, respectively. Post-amplification fluorescent melting curves were analyzed with LightCycler® 480 Gene Scanning software following the manufacturer's manual (Roche Applied Sciences, Indianapolis). All curves were analyzed after normalization, temperature shifting automated grouping, and inspection of difference plots. The grouping software uses a curve shape-matching algorithm to identify wild-type from mutant samples and cutoffs are based on variability from the wild-type curve. The presence of the c.304G>T mutation in patient sample was identified by a change in the melting curve shape compared to the wild-type profile, achieved by plotting the fluorescence difference between melt curves [16].

In silico and ex vivo (minigenes) splicing analysis In silico analysis of the effect on splicing of the novel change identified was done using different softwares: BDGP (www.fruitfly.org/seq_tools/plice.html), MaxEnt (http://genes.mit.edu/burgelab/maxent/Xmaxentscan_scoreseq.html), Splice Site Analyzer (http://ast.bioinfo.tau.ac.il/SpliceSiteFrame.htm), and Human Splicing Finder (http://www.umd.be/HSF/). For evaluation of ex vivo splicing using minigenes the pSPL3 vector was used (kindly provided by Dr. B. Andresen). Since the c.304G>T mutation is located in the last nucleotide of exon 1 with no upstream 3′ splice site, a hybrid exon was constructed containing part of exon 2 (with its 3′ splice site) fused with exon 1 with its 5′ splice site. A region of exon 1 including the 5′ splice site was amplified from a control DNA using a sense primer that introduces a SalI restriction site and cloned in TOPO vector (resulting in TOPO-Ex1 vector). Part of exon 2 including its 3′ splice site was amplified using primers introducing BamHI (sense primer) and SalI (antisense primer) restriction sites, digested with both enzymes and cloned in TOPO-Ex1 vector previously digested with both enzymes. Primers are available upon request. The correct clone containing the hybrid exon2–exon 1 was verified by sequencing analysis. The insert was subsequently excised with BamHI and EcoRV, purified using the QIAEX II Gel Extraction kit (Qiagen, Hilden), and subsequently cloned into the pSPL3 vector previously digested with the same enzymes, by use of the Rapid Ligation kit (Roche Applied Sciences, Indianapolis). The identity of the resulting pSPL3-Ex2-1 clone was verified by sequencing. The c.304G>T mutation was then introduced by site-directed mutagenesis with the Quikchange mutagenesis kit (Stratagene) and confirmed by sequencing. For the minigene assay, 2 μg of the wild-type or mutant pSPL3-Ex2-1 were transfected into the human hepatoma cell line Hep3B or in HEK293T cells using JetPEI reagent (Polyplus Transfection, New York) following the manufacturer's recommendations. At 24–48 h post-transfection, the cells were harvested and total RNA purified. RT-PCR was then performed using the pSPL3-specific primers SD6 and SA2 (Exon Trapping System, Gibco, BRL Carlsbad, CA). Amplified products were separated by agarose gel electrophoresis and the excised bands further analyzed by direct sequencing after extraction with QIAEX II Gel Extraction kit (Qiagen, Hilden).

Results

Biochemical and clinical findings

The biochemical parameters and the genotypes for the four cases included in this work are shown in Table 1. Cases 1 and 2 presented the typical SR deficiency pattern in CSF consisting of increased concentrations of biopterin and sepiapterin and concomitant reduction of both 5-HIAA (mildly decreased in case 2) and HVA (end metabolites of serotonin and dopamine, respectively). Phenylalanine loading test performed for the three siblings (cases 2–4) showed an increased Phe/Tyr ratio in all cases, especially at 2 and 4 h after Phe load (Table 1). Clinically, case 1 presented the severe classical phenotype with psychomotor retardation, hypotonia, ataxia, and extrapyramidal signs. Case 2 showed some motor signs compatible with the diagnosis of SR deficiency. Her elder sister (case 3) showed a very mild phenotype which was not noticed by the family while the eldest (case 4) was minimally asymptomatic, only referring slight head and hand tremor.

Follow-up under treatment

In case 1, CSF neurotransmitter analyses were used to monitor therapy. After 1 year of treatment, HVA and 5-HIAA levels slightly increased (HVA 114 nmol/l and 5-HIAA 26 nmol/l) without variation in pterin levels. The levels of 5-methyltetrahydrofolate in CSF decreased to the lower reference range, and treatment with folinic acid (0.5 mg/kg/day) was implemented. The chronic use of carbidopa has been described to lead to a systemic depletion of the pool of metabolically active reduced folates [17]. Doses of L-dopa/carbidopa and 5-

hydroxytryptophan have progressively been increased up to 3.2 and 2.2 mg/kg/day, respectively. After 3 years of therapy, HVA and 5-HIAA concentration were still decreased (HVA 125 nmol/l and 5-HIAA 50 nmol/l) although the HVA/5-HIAA ratio was normalized. With treatment, the patient is able to walk better, his speech has improved, diurnal somnolence has disappeared, and abnormal ocular movements only appear when he is weary. In general, a slight psychomotor delay persists with walk and speech difficulties and drooling.

In case 2, the effectiveness of treatment was closely evaluated by the neuropediatrician including video documentation. The patient shows a remarkable psychomotor improvement from the beginning of treatment. The patient is able to walk normally, is less rigid, and shows a more vivid facial expression. She has improved at school, with better results specially in mathematics. Her IQ is 83 (Weschler Intelligence Scale for Children IV). She is happier, more active, and bright tempered than before. Her dystonic posturing and movement disorders have resolved. Case 3 is currently receiving 5 mg/kg/day of L-dopa–carbidopa and shows improvement in energy and strength. Case 4 refused any treatment.

Genetic analysis

Molecular analysis of the *SPR* gene revealed the previously reported nonsense mutation p. K251X (c.751A>T) in homozygous fashion in case 1 and compound heterozygosity for p.R150G (c.448A>G) and the novel variation c.304G>T in the three sibs (cases 2–4). The novel c.304G>T variation affects the last nucleotide of exon 1 of the *SPR* gene and could potentially cause the missense change p.G102C or affect the splicing process. The presence of this novel change in 200 control alleles was ruled out by high-resolution melting analysis.

Functional assays of the mutations

The p.K251X mutation is located in the last exon of the *SPR* gene and predictably results in a protein with a small C-terminal deletion of 11 amino acids. Both mutations p. K251X and the novel p.G102C putatively resulting from the c.304G>T change were functionally evaluated by expression analysis in *E. coli* using plasmid pHSR9. After 5 h induction with IPTG, the SR protein present in the soluble extract was detected by Western blotting confirming similar protein amounts for wild-type and mutant (with p.K251X or p.G102C) protein (Fig. 1a). SR activities measured in the same extracts are shown in Fig. 1b. The p.K251X mutant protein has <1% residual activity while p.G102C retains partial activity (15% of wild-type levels).

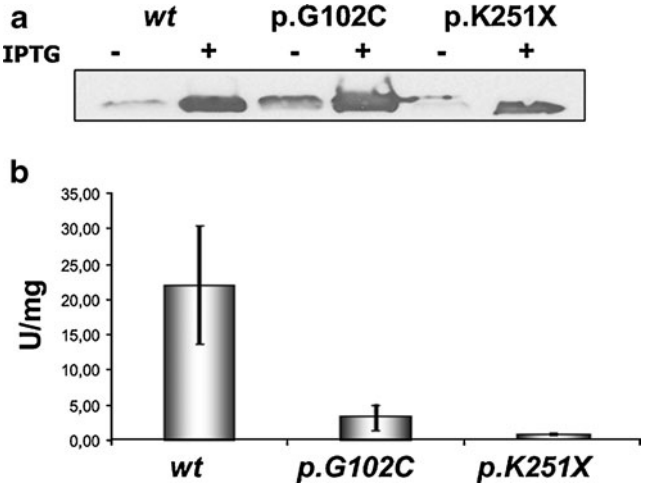

Fig. 1 Results of the expression analysis in *E. coli* of the p.K251X and p.G102C mutant SR proteins. Panel **a** shows the Western blot analysis in cultures transformed with the corresponding wild-type or mutant pHSR9 plasmids uninduced and after induction with IPTG. Panel **b** shows the corresponding enzyme activity measured in induced cells. The results are the mean from at least three experiments

As mentioned above, the presence of the nucleotide change c.304G>T on the last nucleotide of exon 1 included in the 5′ splice site suggested a possible effect of on splicing. To analyze this, different bioinformatic programs were used to determine the splicing scores of wild-type and mutant splice site. All the programs predicted a decrease in splicing score of the 5′ splice site of exon 1 with the c.304G>T change. This decrease was from 92.8 to 81.94 according to human splice finder, from 85.57 to 73 according to human splice analyzer, from 9.84 to 5.04 according to MaxEnt and from 0.99 to 0.73 according to the BDGP software. This prompted us to evaluate functionally its effect on splicing and for this purpose a minigene was constructed containing exon 2 with its 3′ splice site fused with exon 1 where the mutation is present (Fig. 2a). After transfection in HEK293T cell line, the transcripts derived from the minigene were analyzed by RT-PCR and sequencing analysis. The results are shown in Fig. 2b. The wild-type minigene resulted in correct splicing with hybrid exon2-1 inclusion, although sequencing analysis revealed that in some molecules, splicing occurred at a cryptic 3′ splice site within the exonic sequence. The mutant minigene resulted in a different transcriptional profile with an amplification product without exon2-1 resulting from splicing between vector sequences as well as the products corresponding to exon inclusion observed for wild-type minigene transfection (Fig. 2b). The same results were obtained after transfecting a human hepatoma cell line (Hep3B). These results confirm a splicing defect for the c.304G>T mutation, although some amounts of normal splicing could occur, resulting in a mutant protein with the missense change p.G102C.

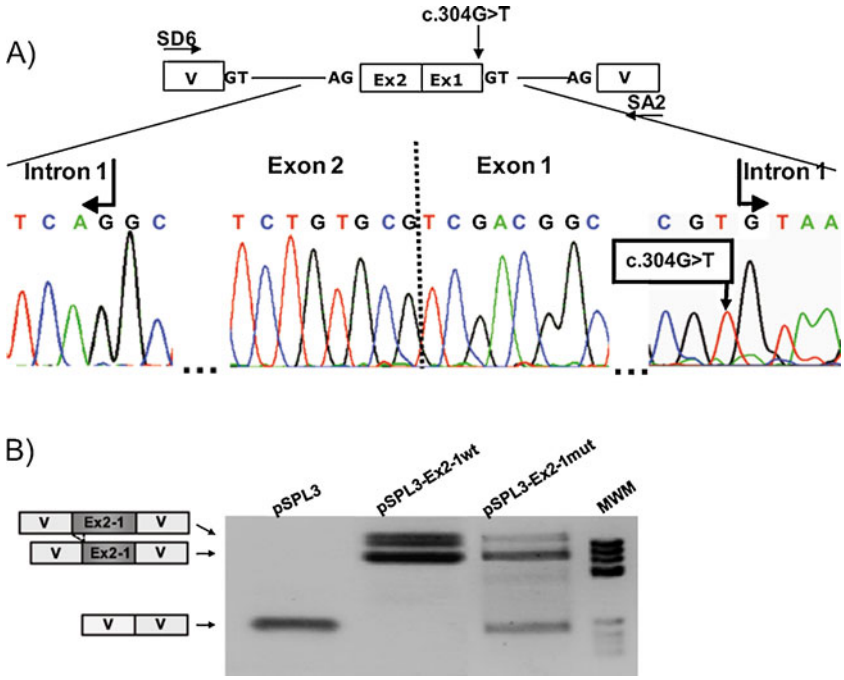

Fig. 2 Minigene analysis of the c.304G>C change. **a** Schematic drawing of the hybrid exon cloned in pSPL3, with the corresponding sequence analysis. **b** The gel shows the RT-PCR analysis in HEK293T cells transfected with the empty vector, the wild-type and mutant EX2-1 minigene. On the left is the schematic drawing showing the composition of the bands which were characterised by sequence analysis. *V*, vector exonic sequences. *MWM*, molecular weight marker

Discussion

Patients reported with SR deficiency typically exhibit clinical features between the second and sixth months of life with progressive global delay. Different clinical symptoms have been reported, most frequently including oculogyric crises and dystonic movements with diurnal variation [7]. Other less frequent symptoms include Parkinsonian tremor, diurnal somnolence, ataxia, or seizures.

Very few cases have been reported with normal cognitive function [8, 10]. Case 1 reported here exhibited a clinical phenotype clearly evoking the diagnosis of SR deficiency. However, cases 2–4 presented here represent a less commonly recognized phenotype as they do not have cognitive impairment and the index case (case 2) had a late-onset presentation while her sisters are very mildly affected or nearly asymptomatic. For case 2 the diurnal fluctuation of her clinical signs and the fact that they were alleviated with sleep was the most suggestive data supporting the diagnosis of dopa-responsive dystonic disorder. Subsequent evaluation of her sisters confirmed the diagnosis of SR deficiency for the three of them. These cases add to the present knowledge of the phenotypical variability in SR deficiency.

Biochemical analysis in CSF of cases 1 and 2 was characteristic of SR deficiency, in agreement with previous reports, highlighting the need for CSF investigations in patients with neurological disorders for correct diagnosis. Verbeek et al. described that in all published patients, 5-HIAA value is always <15% of the lower reference range and often even undetectable [18]. This is indeed the results for case 1, most severely affected. However, in case 2 this value was 39%, which might indicate a milder serotonine deficiency relevant to explain the normal cognitive function in our patient compared to classical cases previously reported in the literature. Recently, a case with normal cognitive function and CSF 5-HIAA around 50% of control values has been reported [19]. Regarding pterins, the most informative parameter is the quantification of sepiapterin in CSF, with an increase that is key for the diagnosis, since biopterin and neopterin could be in the normal range [18]. In the cases reported here, sepiapterin was also clearly elevated which clearly pointed to a diagnosis of SR deficiency. Performing a Phe loading test can also be useful for diagnosis, as hepatic BH_4 concentrations can be limiting for phenylalanine hydroxylation on a Phe challenge, although sufficient in physiological conditions [3]. Interestingly, the oral Phe loading test revealed similar positive results among the three siblings, irrespective of the different clinical presentation. We could not analyze CSF from the elder sisters and no SR enzyme activity could be assessed which could have helped to characterise this very mild form of the disease.

In case 1, analysis of CSF neurotransmitter levels at different times during long-term treatment showed a progressive increase in HVA and 5-HIAA levels although never reaching the control range, despite an excellent neurological improvement, as has been reported for other cases [20].

The genetic analysis of the cases reported here, which are to date the only diagnosed cases in Spain, resulted in the identification of a nonsense mutation p.K251X, previously

identified in other patients [7, 18], one missense mutation (p.R150G) that appears to be a common mutation present in several patients (BIODEF database, http://www.biopku.org), and the novel change c.304G>T. In this work we have confirmed the pathogenicity of both the p.K251X mutation, which predictably results in a protein with a small C-terminal deletion and of the novel change c.304G>T. The p.K251X mutation results in null residual activity, correlating with the severe phenotype exhibited by the patient. Previously reported patients with this mutation exhibited delayed psychomotor development and a complex movement disorder, with symptoms appearing in the first months of life [7, 18]. Data from the crystal structure of mouse SR show that residue D258 (corresponding to D257 in human SR, absent in the truncated protein resulting from p.K251X) is directly involved in the positioning of the pterin substrate in the active site [21]. Thus, D258 is a critical residue determining substrate binding specificity and anchoring and consequently, C-terminal truncation mutants show no residual activity [22], correlating with our results and explaining the genotype–phenotype correlation in the patients with p.K251X.

The novel c.304G>T change was not present in 200 control alleles and we have demonstrated that it results, at least partially, in a splicing defect, although some normally spliced transcript with the missense change p.G102C may occur. This type of "leaky" or partially penetrant splicing mutations has been associated to phenotypic variability [23]. Expression analysis revealed that the protein with the missense mutation p.G102C retains partial activity consistent with the fact that residue G102 is semi-conserved across species and is not directly involved in substrate binding or catalysis [21].

In this scenario, we can envisage different situations for the three siblings heterozygous for the c.304G>T change, as the ratio of correctly spliced (with p.G102C) to aberrant transcript may vary depending on intertissue and interindividual differences in splicing factors. This would allow a molecular explanation for the clinical differences (from mild to nearly asymptomatic) among cases 2–4 with the genotype [p.R150G] + [c.304G>T]. Given that the p.R150G mutation has been previously shown to be functionally null [3], the other allele (c.304G>T) must be the responsible for the mild phenotype. It seems plausible that small differences in the amount of mutant p.G102C protein with partial activity may account for the variable clinical expressivity of the disease.

The results presented in this work underlie the importance of revising the precise effect of exonic nucleotide substitutions, not just assuming that they result in a missense change. Approximately 80% of the natural 5′ splice sites have a G at position −1 (last exonic nucleotide) [24] and its substitution is a frequent pathological mechanism with consequences in mRNA splicing [25–27]. In silico tools are useful to guide the decision for further analysis, as they can offer a prediction of the impact of nucleotide substitutions on splicing [28]. However, RNA analysis is necessary to confirm a splicing defect. When patients' tissue or cells expressing the gene under study are not available, minigenes are a robust and reliable tool to demonstrate a splicing defect, although one must bear in mind that the precise effect in vivo is not always reproduced. For the c.304G>T mutation, the minigene assay resulted in skipping of the hybrid exon cloned in pSPL3. In vivo, activation of exonic or intronic cryptic splice sites or intron retention is the expected consequence as the mutation affects the first exon.

In conclusion, the identification of the cases reported here expand the knowledge of genotype–phenotype correlations in SR deficiency and underlie the importance of CSF sepiapterin and neurotransmitter analysis also in movement and gait disorders with fluctuations of symptoms, in patients with no cognitive delay and mild phenotypes.

Acknowledgments This work was supported by grant SAF2007-61350 from Comisión Interministerial de Ciencia y Tecnología. The authors also acknowledge the support received from Centro de Investigación Biomédica en Red de Enfermedades Raras (CIBERER) and the institutional grant from the Fundación Ramón Areces to the Centro de Biología Molecular Severo Ochoa.

References

1. Thony B, Auerbach G, Blau N (2000) Tetrahydrobiopterin biosynthesis, regeneration and functions. Biochem J 347(Pt 1):1–16
2. Blau N, Thony B, Cotton GH, Hyland K (2001) Disorders of tetrahydrobioterin and related biogenic amines. In: Scriver CR, Beaudet AL, Sly WS, Valle D, Childs B, Vogelstein B (eds) The metabolic and molecular basis of inherited disease, 8th edn. McGraw-Hill, New York, pp 1725–1776
3. Bonafe L, Thony B, Penzien JM, Czarnecki B, Blau N (2001) Mutations in the sepiapterin reductase gene cause a novel tetrahydrobiopterin-dependent monoamine-neurotransmitter deficiency without hyperphenylalaninemia. Am J Hum Genet 69:269–277
4. Bonafe L, Thony B, Leimbacher W, Kierat L, Blau N (2001) Diagnosis of dopa-responsive dystonia and other tetrahydrobiopterin disorders by the study of biopterin metabolism in fibroblasts. Clin Chem 47:477–485
5. Thony B, Blau N (2006) Mutations in the BH4-metabolizing genes GTP cyclohydrolase I, 6-pyruvoyl-tetrahydropterin synthase, sepiapterin reductase, carbinolamine-4a-dehydratase, and dihydropteridine reductase. Hum Mutat 27:870–878
6. Neville BG, Parascandalo R, Farrugia R, Felice A (2005) Sepiapterin reductase deficiency: a congenital dopa-responsive motor and cognitive disorder. Brain 128:2291–2296
7. Echenne B, Roubertie A, Assmann B, Lutz T, Penzien JM, Thony B et al (2006) Sepiapterin reductase deficiency: clinical presen-

tation and evaluation of long-term therapy. Pediatr Neurol 35:308–313
8. Clot F, Grabli D, Cazeneuve C, Roze E, Castelnau P, Chabrol B et al (2009) Exhaustive analysis of BH4 and dopamine biosynthesis genes in patients with Dopa-responsive dystonia. Brain 132:1753–1763
9. Friedman J, Hyland K, Blau N, MacCollin M (2006) Dopa-responsive hypersomnia and mixed movement disorder due to sepiapterin reductase deficiency. Neurology 67:2032–2035
10. Steinberger D, Blau N, Goriuonov D, Bitsch J, Zuker M, Hummel S et al (2004) Heterozygous mutation in 5′-untranslated region of sepiapterin reductase gene (SPR) in a patient with dopa-responsive dystonia. Neurogenetics 5:187–190
11. Ormazabal A, Garcia-Cazorla A, Fernandez Y, Fernandez-Alvarez E, Campistol J, Artuch R (2005) HPLC with electrochemical and fluorescence detection procedures for the diagnosis of inborn errors of biogenic amines and pterins. J Neurosci Methods 142:153–158
12. Zorzi G, Redweik U, Trippe H, Penzien JM, Thony B, Blau N (2002) Detection of sepiapterin in CSF of patients with sepiapterin reductase deficiency. Mol Genet Metab 75:174–177
13. Fukushima T, Nixon JC (1980) Analysis of reduced forms of biopterin in biological tissues and fluids. Anal Biochem 102:176–188
14. Lopez-Laso E, Ormazabal A, Camino R, Gascon FJ, Ochoa JJ, Mateos ME et al (2006) Oral phenylalanine loading test for the diagnosis of dominant guanosine triphosphate cyclohydrolase 1 deficiency. Clin Biochem 39:893–897
15. Madira WM, Xavier F, Stern J, Wilcox AH, Barron JL (1992) Determination and assessment of the stability of phenylalanine and tyrosine in blood spots by HPLC. Clin Chem 38:2162–2163
16. Bastien R, Lewis TB, Hawkes JE, Quackenbush JF, Robbins TC, Palazzo J et al (2008) High-throughput amplicon scanning of the TP53 gene in breast cancer using high-resolution fluorescent melting curve analyses and automatic mutation calling. Hum Mutat 29:757–764
17. Ramaekers VT, Blau N (2004) Cerebral folate deficiency. Dev Med Child Neurol 46:843–851
18. Verbeek MM, Willemsen MA, Wevers RA, Lagerwerf AJ, Abeling NG, Blau N et al (2008) Two greek siblings with sepiapterin reductase deficiency. Mol Genet Metab 94:403–409
19. Leu-Semenescu S, Arnulf I, Decaix C, Moussa F, Clot F, Boniol C et al (2010) Sleep and rhythm consequences of a genetically induced loss of serotonin. Sleep 33:307–14
20. Kusmierska K, Jansen EE, Jakobs C, Szymanska K, Malunowicz E, Meilei D, et al (2009) Sepiapterin reductase deficiency in a 2-year-old girl with incomplete response to treatment during short-term follow-up. J Inherit Metab Dis. Short report # 137 Online
21. Auerbach G, Herrmann A, Gutlich M, Fischer M, Jacob U, Bacher A et al (1997) The 1.25 a crystal structure of sepiapterin reductase reveals its binding mode to pterins and brain neurotransmitters. EMBO J 16:7219–7230
22. Fujimoto K, Ichinose H, Nagatsu T, Nonaka T, Mitsui Y, Katoh S (1999) Functionally important residues tyrosine-171 and serine-158 in sepiapterin reductase. Biochim Biophys Acta 1431:306–314
23. Svenson IK, Ashley-Koch AE, Gaskell PC, Riney TJ, Cumming WJ, Kingston HM et al (2001) Identification and expression analysis of spastin gene mutations in hereditary spastic paraplegia. Am J Hum Genet 68:1077–1085
24. Roca X, Olson AJ, Rao AR, Enerly E, Kristensen VN, Borresen-Dale AL et al (2008) Features of 5′-splice-site efficiency derived from disease-causing mutations and comparative genomics. Genome Res 18:77–87
25. Krawczak M, Thomas NS, Hundrieser B, Mort M, Wittig M, Hampe J et al (2007) Single base-pair substitutions in exon–intron junctions of human genes: nature, distribution, and consequences for mRNA splicing. Hum Mutat 28:150–158
26. von Brederlow B, Bolz H, Janecke A, La OCA, Rudolph G, Lorenz B et al (2002) Identification and in vitro expression of novel *CDH23* mutations of patients with Usher syndrome type 1D. Hum Mutat 19:268–273
27. Yamada K, Fukao T, Zhang G, Sakurai S, Ruiter JP, Wanders RJ et al (2007) Single-base substitution at the last nucleotide of exon 6 (c.671G>A), resulting in the skipping of exon 6, and exons 6 and 7 in human succinyl-CoA:3-ketoacid CoA transferase (SCOT) gene. Mol Genet Metab 90:291–297
28. Houdayer C, Dehainault C, Mattler C, Michaux D, Caux-Moncoutier V, Pages-Berhouet S et al (2008) Evaluation of in silico splice tools for decision-making in molecular diagnosis. Hum Mutat 29:975–982

Molecular Genetics and Metabolism 102 (2011) 134–138

Contents lists available at ScienceDirect

Molecular Genetics and Metabolism

journal homepage: www.elsevier.com/locate/ymgme

Overexpression of adapted U1snRNA in patients' cells to correct a 5′ splice site mutation in propionic acidemia

Rocío Sánchez-Alcudia, Belén Pérez, Celia Pérez-Cerdá, M. Ugarte *, Lourdes R. Desviat *

Centro de Diagnóstico de Enfermedades Moleculares, Centro de Biología Molecular Severo Ochoa, UAM-CSIC, Universidad Autónoma de Madrid, Madrid, Spain
Centro de Investigación Biomédica en Red de Enfermedades Raras (CIBERER), Madrid, Spain

ARTICLE INFO

Article history:
Received 26 October 2010
Accepted 26 October 2010
Available online 5 November 2010

Keywords:
Propionic acidemia
Propionyl-CoA carboxylase
U1snRNA
5′ splice site mutation
Splicing

ABSTRACT

Splicing defects account for 16% of the mutant alleles in the PCCA and PCCB genes, encoding both subunits of the propionyl-CoA carboxylase (PCC) enzyme, defective in propionic acidemia, one of the most frequent organic acidemias causing variable neurological impairment. Most of the splicing mutations identified affect the conserved 3′ splice (3′ ss) or 5′ splice (5′ ss) sites, the latter predictably through lowering the strength of base pairing with U1snRNA. Among the 5′ ss mutations we have focused on the c.1209+3A>G (IVS13+3A>G) mutation in the PCCA gene, identified in four patients (three homozygous and one heterozygous) of common geographical origin and causing exon 13 skipping. To study the potential of splicing modulation to restore PCC function, we analyzed the effect of transient transfections in patients' cells with modified U1snRNA adapted to compensate the mutant change and other mismatches at different positions of the 5′ ss. Using this strategy normal transcript could be efficiently recovered with the concomitant disappearance of the aberrant exon skipping transcript, as observed after standard RT-PCR and sequence analysis or using fluorescent primers and semiquantitative RT-PCR. Different efficiencies with up to 100% exon inclusion were observed depending on the transfection conditions and specifically on the adapted U1snRNA used, confirming previously reported dependencies between nucleotides at the 5′ ss for its correct recognition by the spliceosome. The reversal of the splicing defect did not result in a significant increase in enzyme activity, suggesting other factors must be taken into account for the application of overexpression of splice factors such as U1 as therapeutic strategy for splice defects.

1. Introduction

Splicing defects are among the most frequent pathogenic mechanisms underlying genetic diseases. Splicing is performed by a multi-component machine called the spliceosome, composed by five small ribonucleoproteins (snRNPs) and hundreds of additional proteins [1]. Three sequence elements at the exon–intron junctions of the genes are recognized sequentially by components of the spliceosome and are thus essential for splicing: the 5′ donor splice site (5′ ss), the 3′ acceptor splice site (3′ ss) and the branchpoint sequence [2]. Spliceosome formation is initiated by binding of U1 snRNP to the 5′ ss via the formation of an RNA duplex between the 5′ ss and the 5′ end of U1 snRNA, although recent work has raised the possibility of a recognition mechanism at least partially independent of U1 [3,4]. A 5′ ss provides up to eleven potential positions for U1 binding, although typically, seven are the nucleotides involved in base pairing [5]. It has been suggested that there probably is a minimal number of 5–6 base pairing to U1 for a functional 5′ ss, although the different nucleotide positions are not functionally equivalent [6]. Mutations that lower the complementarity to U1 usually cause splicing defects although the position and the nature of the mutated nucleotide determine the precise effect. It is important to determine the underlying molecular basis of the splicing defects as it expands the opportunities for therapeutic intervention aimed at specific types of mutations and applicable to different genetic diseases.

Propionic acidemia (PA; MIM#606054) affects approximately 1 in 30,000 live births worldwide [7,8] and results from a deficiency of propionyl-CoA carboxylase (PCC, E.C. 6.4.1.3), inherited in autosomal recessive fashion. PCC catalyzes the conversion of propionyl-CoA to methylmalonyl-CoA and is one of the key enzymes in the catabolic pathway of the amino acids valine, isoleucine, methionine and threonine, as wells as of odd-chain fatty acids and the side chain of cholesterol. The enzyme is a heteropolymer of α and β subunits encoded by the PCCA and PCCB genes, respectively.

PA shows a wide range of clinical manifestations ranging from a severe neonatal form with ketoacidosis, poor feeding, lethargy, failure

Abbreviations: 3′ ss, 3′ splice site; 5′ ss, 5′ splice site; U1, U1snRNA; NMD, nonsense mediated decay; PCC, propionyl-CoA carboxylase; PA, propionic acidemia.

* Corresponding authors. Centro de Diagnóstico de Enfermedades Moleculares, Centro de Biología Molecular Severo Ochoa, UAM-CSIC, Universidad Autónoma de Madrid, 28049 Madrid, Spain. Fax: +34 91 1964420.
E-mail addresses: mugarte@cbm.uam.es (M. Ugarte), lruiz@cbm.uam.es (L.R. Desviat).

1096-7192/$ – see front matter © 2010 Elsevier Inc. All rights reserved.
doi:10.1016/j.ymgme.2010.10.013

to thrive, seizures and encephalopathy to a milder, later-onset chronic form with less impaired neurological outcome. Progression of symptoms, if not promptly treated, leads to death within few days or to severe brain damage. Current treatment which is based on dietary restriction does not effectively prevent neurological deterioration [9].

One of the most frequent defects in this genetic disease is splicing mutations. In PA, updated information at the Human Gene Mutation Database (HGMD Professional Release 2010) shows a frequency of ~16% of splicing mutations for both the PCCA and PCCB genes. From these, 65–70% corresponds to 5′ donor site mutations which thus constitute a good target for mutation specific therapeutic approaches. In several diseases, the use of U1snRNA complementary to the mutated site has been described as a potentially therapeutic strategy to correct donor splice site defects dependent on U1 binding. This strategy, initially employed to determine the role of U1 snRNP in 5′ ss recognition [10], has been exploited using minigenes as splice models of disease. Mutant U1snRNA engineered to bind specifically to the mutant donor site are cotransfected along with the minigenes resulting in the correction of the splicing defects [11–15]. In this work we have exploited this strategy for the first time in patients' cells to explore the feasibility of the functional recovery of the defect in a cellular model of disease.

2. Methods

2.1. Minigenes

For evaluation of in vitro splicing, a gene fragment including exon 13 and flanking intronic regions was amplified from patients and control DNA and cloned into the TOPO vector (Invitrogen). The insert was excised with Eco RI and was subsequently cloned into pSPL3 vector (Life Tecnhnologies [Gibco BRL], kindly provided by Dr. B. Andresen). Clones containing the normal and mutant inserts in the correct orientation were identified by restriction-enzyme analysis and automated DNA sequencing. $3–4\times10^5$ Hep3B cells grown in 6-well plates were transfected using Jet Pei with a total of 10.5 μg of wild-type or mutant minigenes. 24–48 h after transfection, RNA was purified from cells and RT-PCR analysis was performed using the pSPL3-specific primers SD6 and SA2. Amplified products were separated by agarose gel electrophoresis and analyzed by direct sequencing.

2.2. RT-PCR analysis in patients' fibroblasts

This study included fibroblast cell lines from two patients homozygous for mutation c.1209+3A>G. Total mRNA was isolated with Tripure Isolation Reagent (Invitrogen) and subsequently RT-PCR was performed using primers located in exon 11 (5′-TGGGAATGCTTTATGGCTTA-3′) and exon 14 (5′-CGGTTCTTGGTACTGAGACAATC-3′).

2.3. U1 snRNA constructs

The U1 vector [13] was kindly provided by Dr. F. Pagani (International Centre for Genetic Engineering and Biotechnology, Trieste, Italy). The mutant U1 vectors were obtained by site directed mutagenesis using the Quickchange mutagenesis kit (Invitrogen). The desired mutations (Fig. 2a) were confirmed by sequence analysis.

2.4. U1 transfection experiments

$3–4\times10^5$ patients' fibroblasts grown in 6-well plates were transfected using Lipofectamine LTX (Invitrogen) with various amounts (00.5–4 μg) of the U1 constructions. 48 h later RNA was isolated and RT-PCR with PCCA specific primers was performed. To assay the functional rescue of the mutation by measuring PCC activity, $1.6–1.8\times10^6$ fibroblast cells were grown in 75 cm^2 flasks and transfected with amounts between 7.5 and 30 μg of the U1 constructs and harvested after 24, 72 or 96 h. In other experiments, $4–5\times10^5$ fibroblast cells were transfected with 2 and 4 μg of the U1 constructs using the Amaxa® Human Dermal Nucleofector kit according to the instructions provided by the manufacturer. In some cases, the NMD inhibitor wortmannin (10 or 100 μM) was added six hours prior to cell harvest. Cells were harvested 72 h posttransfection. In parallel, cells were transfected with a control plasmid encoding GFP and fluorescent cells were monitored by microscopy. The percentage of transfected fibroblasts reached 50–60% with the Nucleofector kit, 10-fold higher than with lipofection.

2.5. Fragment analysis

For mRNA quantification in fibroblasts transfected with the different U1 constructs as described earlier, RT-PCR was performed using a 6FAM fluorescently labeled forward primer hybridizing to exon 11 of the PCCA gene and a reverse primer hybridizing to exon 14. Reactions were incubated at 95 °C for 5 min followed by 30 cycles at 95 °C for 25 s, 55 °C for 25 s and 72 °C for 40 s. Amplification products were separated on an ABI Prism 3730 Genetic Analyzer (Applied Biosystems) and analyzed using the Peakscanner software (Applied Biosystems).

2.6. PCC activity assay

PCC activity was assayed as ^{14}C propionate incorporation into non-volatile products according to the method described in Ref. [16].

2.7. PCCA protein detection

For the detection of biotin-bound proteins, transfected fibroblasts were harvested by trypsinization, resuspended in sucrose buffer (0.25 M sucrose, 10 mM Tris–HCl pH 7.4, EDTA 2 mM, PMSF 0.2 mM) and disrupted with a Teflon Potter homogenizer. Mitochondria were isolated by differential centrifugation at 4 °C [17], suspended in sucrose buffer and protein concentration determined by the Bradford assay. Equal amounts of total protein (30 μg) from each fibroblast sample were loaded on a denaturing 10% polyacrylamide gel. After electrophoresis, proteins were transferred to PVDF membranes (Immobilon™-P, Millipore) and the biotin containing proteins were detected with an avidin alkaline phosphatase conjugate (Pierce), using NBT/BCIP (Pierce) as alkaline phosphatase substrate for color development.

3. Results

3.1. Splicing analysis

The splicing mutation c.1209+3A>G (IVS13+3A>G) in the PCCA gene causes in-frame exon 13 skipping [18] (Fig. 1a), which predictably originates a protein with an internal deletion of 48 amino acids (p.V356_E403del48). *In silico* analysis predicts a decrease in strength of the 5′ ss due to the mutation (from 79.4 to 76.1 according to Shapiro and Senapathy [19]; from 83.74 to 78.72 according to Human Splicing Finder) [20] and a probable exon skipping effect (CRYP-SKYP software [21]).

To date, we have identified this mutation in four patients (three homozygous and one heterozygous) of common geographical/ethnic origin. In homozygous patients no other polymorphic or potentially pathogenic changes were detected in exon 13 and flanking intronic sequences and only the exon skipping transcript is detected in fibroblast samples (Fig. 1a).

To recapitulate the splicing defect in a cellular model which could be used to test U1 overexpression as therapeutic strategy, minigenes

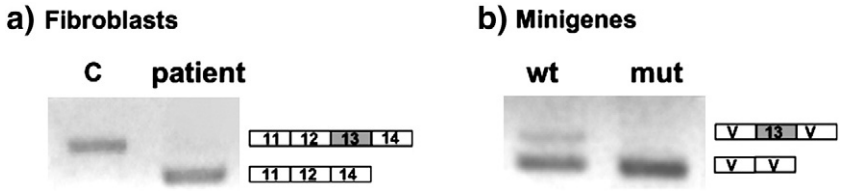

Fig. 1. Results of the RT-PCR analysis in fibroblasts (a) and in Hep3B cells transfected with wild-type (wt) and mutant (mut) minigenes (b). The schematic representation of the amplified bands is shown on the right of each gel. Numbers refer to the PCCA exons and V refers to exonic vector sequences.

with wild-type and mutant sequence were constructed and transfected in a hepatoma cell line. RT-PCR analysis showed the presence of two bands for the wild-type construct, corresponding to vector–vector splicing and to a transcript with exon 13. Mutant minigenes resulted exclusively in a band corresponding to vector–vector splicing (Fig. 1b). As patient cells homozygous for the mutation were available, we decided to test them directly for the U1 overexpression approach.

3.2. U1 constructs transfection in patients' cells

The 5′ ss of exon 13 of the PCCA gene shows complementarity to the 5′ end of U1snRNA in 6 out of the consensus 9 positions (from −3 to +6) [10] (Fig. 2a). Mutation IVS13 + 3A>G introduces a mismatch in position +3, thus lowering the complementarity to U1snRNA. Different mutant U1 plasmids were constructed to compensate for the mutation (U1 + 3) and for other mismatched bases (U1 + 3 + 5; U1 + 3 + 5 + 6 and U1IVS13, the latter with extended complementarity in positions −3 and +7 + 8) (Fig. 2a). Fibroblasts from controls and from patients homozygous for the mutation were transfected with the plasmid coding for wild-type U1 and with the different mutated plasmids and after 48 h cells were trypsinized, RNA was isolated and RT-PCR performed with PCCA cDNA specific primers. The results of a representative experiment are shown in Fig. 2b. While with wt U1 and U1 + 3 no effect was observed, when U1 + 3 + 5, U1 + 3 + 5 + 6 or U1IVS13 were transfected, a reversion of the splicing defect could be detected. In all cases, the identity of the amplified bands was confirmed by sequencing analysis. The levels of normal spliced band with exon 13 reached ~100%, although some variability was detected depending on the patient cell line used, amount and plasmid used and transfection conditions. A control cell line transfected with the same constructs showed no alteration of the normal splice pattern (Fig. 2c). Both lipofectamine LTX and nucleofector technology were used obtaining similar results, although the transfection efficiency was greatly increased with nucleofection, as measured in parallel with a control plasmid coding for GFP. As additional control, the expression of transfected U1 was analyzed by RT-PCR with specific primers [22], confirming efficient transfection in all cases. No substantial difference was observed using two different patient derived cell lines homozygous for the mutant change.

Although by standard RT-PCR we never observed in patient cells any additional aberrant transcripts (e.g. due to activation of cryptic

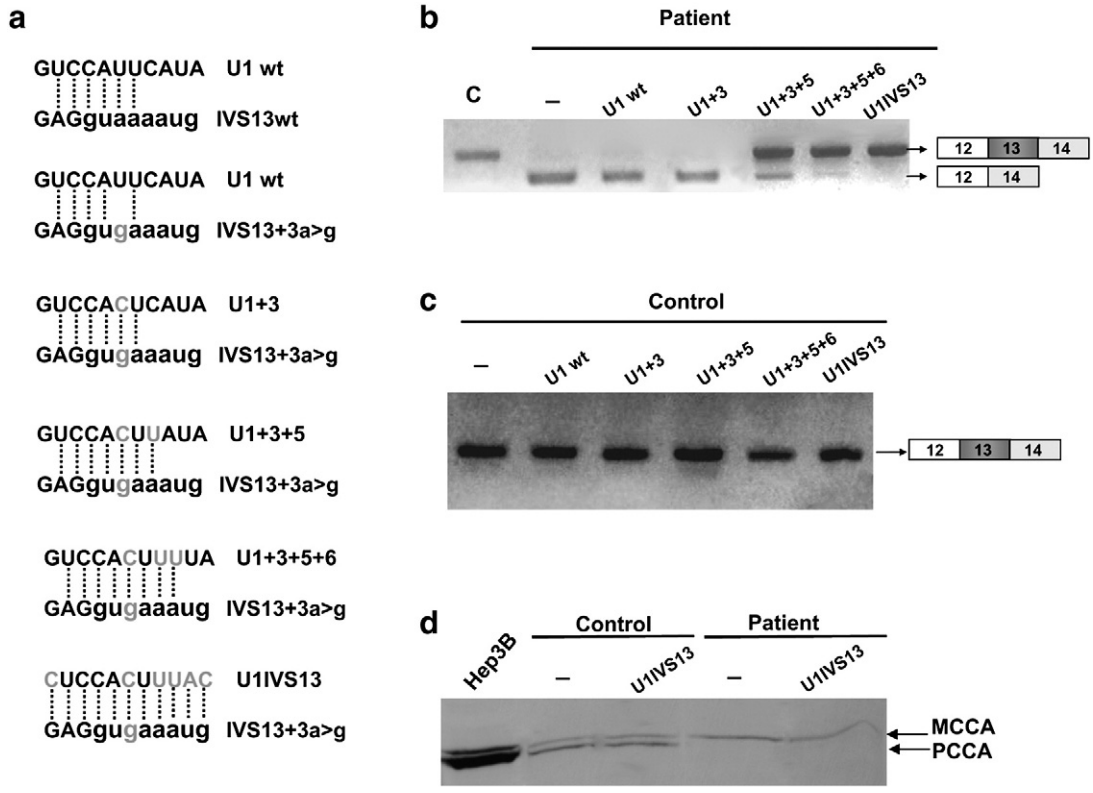

Fig. 2. Correction of aberrant splicing due to the IVS13 + 3A>G mutation by modified U1 snRNA. a) Schematic representation of base pairing between the 5′ ss of exon 13 and the different U1 constructs. b) RT-PCR analysis of a control cell line (C) and patient cells untransfected and after transfection of the different U1 vectors. c) RT-PCR analysis in a control cell line. The schematic composition of the bands as determined by sequence analysis is shown on the right of the gels. wt, wild-type d) detection of mitochondrial biotinylated proteins in control and patient fibroblasts untransfected and transfected with U1IVS13. Hepatoma Hep3B cells were used as control. MCCA, α-subunit of methylcrotonyl CoA carboxylase.

splice sites, or to skipping of nearby exons), it can be envisaged that they could be produced resulting in out of frame transcripts being subjected to degradation by the nonsense mediated decay (NMD) mechanism. These aberrant transcripts would not be rescued by use of adapted U1, limiting its therapeutical potential. Therefore, the effect of using the NMD inhibitor wortmannin was analyzed in the U1 transfection experiments and semiquantitative RT-PCR was performed using fluorescent primers and fragment analysis after capillary electrophoresis in an automated sequencer. No difference in the transcriptional profile and identity of the bands as confirmed by sequence analysis was observed when wortmannin 10 or 100 μM was added for 6 h previous to cell harvest. When a fluorescent primer was used for PCR in conditions determined to be within the linear phase of amplification, the transcriptional profile was the same and the amount of product was comparable in all cases indicating that most of the RNA in the patient cells is efficiently spliced after transfection with either U1 + 3 + 5, U1 + 3 + 5 + 6 or U1IVS13 (Fig. 3).

PCC activity was measured in patients' cells after transfection in the conditions used for 100% rescue of normal splicing, using both U1 + 3 + 5 + 6 and U1IVS13. In some experiments, after transfection, the cell pellet was split in two and one used for enzyme measurements and the other for RNA isolation and RT-PCR analysis confirming transcript rescue in the transfected cells. Different conditions were assayed, either using lipofection or nucleofection and adding in some cases the NMD inhibitor wortmannin, as described in Methods. PCC activity was assayed 24, 72 and 96 h posttransfection. However, in all the conditions tested, no significant increase in activity was detectable in transfected cells, remaining in the range of <2% wild-type levels. No biotinylated PCCA protein could be detected after U1 treatment using an avidin assay to detect mitochondrial biotin-bound proteins (Fig. 2d). Both PCCA and PCCB cDNAs were amplified in 2–3 overlapping fragments observing normal levels and normal sequence. Unspecific inhibition of PCC enzymatic activity by U1 was ruled out in a control cell line transfected with U1 + 3 + 5 + 6 and U1IVS13 constructs.

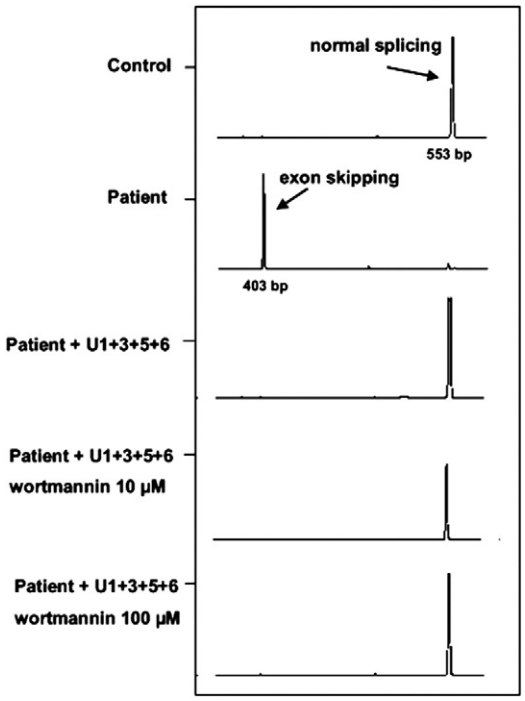

Fig. 3. Capillary electrophoresis of semiquantitative RT-PCR of a fragment spanning exon 13 of the PCCA gene. Detection of the normal and aberrant (without exon 13) PCCA transcripts using a fluorescent dye marked primer and an automated sequencer and fragment analysis with the Peakscanner software (Applied Biosystems). X-axis, length of the fragment in nucleotide; y-axis, fluorescence intensity.

4. Discussion

The c.1209 + 3A>G mutation in intron 13 of the PCCA gene has been identified in a total of seven PA alleles and results in exon 13 skipping. Both A and G are consensus nucleotides in that position and similar variations have been reported to induce aberrant splicing in some cases but not in others [23,24]. Functional and *in silico* studies highlight the role of matching nucleotides to U1 snRNA at positions + 4 to + 6 to render the 5′ ss less prone to a splicing defect in the case of a + 3A>G substitution [23–25]. A survey of natural 5′ ss shows that when the nucleotide at + 3 is a G, the frequencies of accordant nucleotides at positions + 4 to + 6 are higher than those observed in 5′ ss with an A at + 3 [6,25]. Our results indicate that the strength of the wild-type 5′ ss of PCCA intron 13 with six consecutive matches to U1 snRNA may lie just above a critical threshold and in this case, lack of complementarity to U1 snRNA at positions + 5 and + 6 presumably results in its dependence of an A at the + 3 position for correct splicing. This mutation adds to the list of pathogenic + 3A>G mutations [23] providing additional clues for the clinical interpretation of similar changes.

In this work we sought to suppress the splicing defect by overexpression of U1 snRNA adapted to compensate the mismatch at the + 3 position. Initial studies were performed with minigenes but the corresponding wild-type constructs failed to recapitulate accurately the transcriptional profile observed in fibroblasts probably due to lack of necessary genomic sequence context [26]. Therefore, patients' fibroblasts homozygous for the sequence change were used as cellular models for transfection with U1 vector constructs with compensatory mutations. The results indicate that in vivo loss of U1 binding to the mutated 5′ ss is at least partially responsible for the observed exon skipping and confirms that correct splicing is not determined simply by the levels of U1snRNA, as overexpression of wild-type U1 snRNA does not rescue splicing. Indeed, this is only achieved to a detectable extent when additional mutations other than at the mismatched + 3 position are introduced in the U1 snRNA, leading to base pairing also at positions + 5 or + 5 and + 6. Complete restoration of normal splicing with the absence of the exon skipping band was achieved with U1IVS13 with extended complementarity from positions − 3 to + 8 (Fig. 2b). These results are in accordance with similar studies in other genes, where an extended U1 snRNA-5′ ss interaction is necessary for exon inclusion in a minigene based assay [14,23]. To our knowledge, this work represents the first report of U1 mediated suppression of a splicing defect in patients' cells. A semiquantitative RNA assay using fluorescent primers and fragment analysis in the presence or absence of the NMD inhibitor wortmannin indicated that the mutation produces exclusively the exon skipping transcript and that after mutated U1 treatment, the correctly spliced transcript accumulates in similar amounts as in control fibroblasts.

The failure of U1 + 3 to suppress the mutation even though it restores the number of base pairs to the same as in wild-type exon 13 splicing suggests that it is not only the interaction between U1snRNA and the 5′ ss which is involved in the exon skipping event. It is probable that the mutation affects the affinity of the 5′ ss for other splice factors. After U1 binding to the 5′ ss, subsequent spliceosome assembly results in the displacement of U1 by U6 snRNA which is known to base-pair to positions + 2 to + 6 of the 5′ ss [27]. Alternatively, the compensatory mutation at position + 3 introduced in U1snRNA may render it unstable (although we could detect it by RT-PCR with specific primers for exogenous U1) or non-functional [6] thus explaining its inability to revert exon skipping. Similar results have been reported for minigenes with 5′ ss mutations which have been targeted using U1 with compensatory mutations [14]. In our experimental model, efficient U1 suppression of the mutation requires 7 contiguous base pairs with the

mutant splice site, one more than that occurring between the wild-type 5′ ss and wild-type U1.

The feasibility of U1 treatment for functional rescue of an enzymatic defect has to date only been explored using a splicing-competent full-length construct as cellular model of Factor VII deficiency caused by a G>A mutation at position +5 [11]. The results showed U1 mediated rescue of factor VII mRNA splicing resulting in detectable levels of functional activity (9.5% of wild-type levels). However, no studies have been carried out to date in patient derived cell lines. In our hands, although the use of different adapted U1 efficiently rescue ~100% normally spliced transcripts in cells from patients with the IVS13 + 3A>G mutation, no recovery of PCC protein or activity could be detected in any case. No other transcript is detectable after inhibiting NMD and using a sensitive fluorescent assay. Correctly spliced transcripts accumulate in normal amounts after U1 treatment, ruling out the contribution of alternative mutant transcripts to the results observed. In addition, an unspecific effect of U1 transfection on PCCA and PCCB mRNA processing was ruled out. However, we cannot rule out an unspecific effect of U1 on key elements necessary for translation or assembly of the PCC heteropolymer which precludes the formation of an active enzyme. The absence of biotinylated PPCA protein in the patient's fibroblasts treated with U1 supports this notion. U1snRNA with altered 5′ ends have been described to have unintended effects on splicing and polyadenylation of some pre-mRNAs [28]. The complex interplay between splicing and translation has not yet been completely elucidated [2]. Additional evidence from other patients' cell lines with different gene defects targeted with adapted U1 will clarify whether this is a limitation only for this cellular disease model. It is interesting to note that in PA we have recently showed efficient protein and enzymatic recovery in patients' cells after splicing modulation with an antisense oligonucleotide targeting an activated pseudoexon [29]. In that case, reversion of the splicing defect detectable by RT-PCR correlated with functional enzyme production. It must be envisaged that in this work the therapeutic RNA molecule is a natural splice factor modified to bind more stably to certain 5′ ss which in turn can inhibit the entry of other spliceosomal components such as U4/U6.U5 due to a delayed release of the U1 snRNP from the 5′ ss [30]. For PCCA mRNA, detection of correctly spliced transcripts assures that U1 was efficiently displaced but this may not be the case for other cellular mRNAs. Application of exon-array technologies for the detection of alternative transcripts after U1 treatment may be used to investigate this issue.

The results presented in this work indicate that the results of splicing modulation with adapted U1 obtained with minigenes, which have been reported for several genes [11–15], should be complemented using patient derived cell lines or animal models of disease, as a necessary first step in the investigation of the in vivo applicability of U1 therapy. Results from other genes will clarify if the lack of functional rescue is specific for the gene and the mutation described here. In any case we should interpret with caution the results of splicing modulation using splice factors exerting different cellular roles [4] as they may result in unforeseen side effects which should be analyzed in detail.

Acknowledgments

This work was supported by grant SAF2007-61350 from *Comisión Interministerial de Ciencia y Tecnología*. The institutional grant from the *Fundación Ramón Areces* to the Centro de Biología Molecular Severo Ochoa is also acknowledged.

References

[1] J. Tazi, S. Durand, P. Jeanteur, The spliceosome: a novel multi-faceted target for therapy, Trends Biochem. Sci. 30 (8) (2005) 469–478.
[2] T.A. Cooper, L. Wan, G. Dreyfuss, RNA and disease, Cell 136 (4) (2009) 777–793.
[3] M. Raponi, D. Baralle, Can donor splice site recognition occur without the involvement of U1 snRNP? Biochem. Soc. Trans. 36 (Pt 3) (2008) 548–550.
[4] E. Buratti, D. Baralle, Novel roles of U1 snRNP in alternative splicing regulation, RNA Biol. 7 (4) (2010).
[5] X. Roca, A.R. Krainer, Recognition of atypical 5′ splice sites by shifted base-pairing to U1 snRNA, Nat. Struct. Mol. Biol. 16 (2) (2009) 176–182.
[6] I. Carmel, S. Tal, I. Vig, G. Ast, Comparative analysis detects dependencies among the 5′ splice-site positions, Rna 10 (5) (2004) 828–840.
[7] S.E. Hofherr, J.S. Senac, C.Y. Chen, D.J. Palmer, P. NG, M.A. Barry, Short-term rescue of neonatal lethality in a mouse model of propionic acidemia by gene therapy, Hum. Gene Ther. 20 (2) (2009) 169–180.
[8] L.R. Desviat, B. Perez, C. Perez-Cerda, P. Rodriguez-Pombo, S. Clavero, M. Ugarte, Propionic acidemia: mutation update and functional and structural effects of the variant alleles, Mol. Genet. Metab. 83 (1–2) (2004) 28–37.
[9] W.A. Fenton, R.A. Gravel, L.E. Rosenberg, Disorders of propionate and methylmalonate metabolism, in: C.R. Scriver, A.L. Beaudet, W. Sly, D. Valle (Eds.), The Metabolic and Molecular Bases of Inherited Disease, McGraw-Hill, New York, 2001, pp. 2165–2190.
[10] Y. Zhuang, A.M. Weiner, A compensatory base change in U1 snRNA suppresses a 5′ splice site mutation, Cell 46 (6) (1986) 827–835.
[11] M. Pinotti, D. Balestra, L. Rizzotto, I. Maestri, F. Pagani, F. Bernardi, Rescue of coagulation factor VII function by the U1 + 5A snRNA, Blood 113 (25) (2009) 6461–6464.
[12] M. Pinotti, L. Rizzotto, D. Balestra, M.A. Lewandowska, N. Cavallari, G. Marchetti, F. Bernardi, F. Pagani, U1-snRNA-mediated rescue of mRNA processing in severe factor VII deficiency, Blood 111 (5) (2008) 2681–2684.
[13] L. Susani, A. Pangrazio, C. Sobacchi, A. Taranta, G. Mortier, R. Savarirayan, A. Villa, P. Orchard, P. Vezzoni, A. Albertini, A. Frattini, F. Pagani, TCIRG1-dependent recessive osteopetrosis: mutation analysis, functional identification of the splicing defects, and in vitro rescue by U1 snRNA, Hum. Mutat. 24 (3) (2004) 225–235.
[14] G. Tanner, E. Glaus, D. Barthelmes, M. Ader, J. Fleischhauer, F. Pagani, W. Berger, J. Neidhardt, Therapeutic strategy to rescue mutation-induced exon skipping in rhodopsin by adaptation of U1 snRNA, Hum. Mutat. 30 (2) (2009) 255–263.
[15] H. Crehalet, P. Latour, V. Bonnet, S. Attarian, P. Labauge, N. Bonello, R. Bernard, G. Millat, R. Rousson, D. Bozon, U1 snRNA mis-binding: a new cause of CMT1B, Neurogenetics 11 (1) (2009) 13–19.
[16] T. Suormala, H. Wick, J.P. Bonjour, E.R. Baumgartner, Rapid differential diagnosis of carboxylase deficiencies and evaluation for biotin-responsiveness in a single blood sample, Clin. Chim. Acta 145 (2) (1985) 151–162.
[17] S.E. Old, D.C. DeVivo, Pyruvate dehydrogenase complex deficiency: biochemical and immunoblot analysis of cultured skin fibroblasts, Ann. Neurol. 26 (1989) 746–754.
[18] L.R. Desviat, S. Clavero, C. Perez-Cerda, R. Navarrete, M. Ugarte, B. Perez, New splicing mutations in propionic acidemia, J. Hum. Genet. 51 (11) (2006) 992–997.
[19] M.B. Shapiro, P. Senapathy, RNA splice junctions of different classes of eukaryotes: sequence statistics and functional implications in gene expression, Nucleic Acids Res. 15 (17) (1987) 7155–7174.
[20] F.O. Desmet, D. Hamroun, M. Lalande, G. Collod-Beroud, M. Claustres, C. Beroud, Human splicing finder: an online bioinformatics tool to predict splicing signals, Nucleic Acids Res. 37 (9) (2009) e67.
[21] P. Divina, A. Kvitkovicova, E. Buratti, I. Vorechovsky, Ab initio prediction of mutation-induced cryptic splice-site activation and exon skipping, Eur. J. Hum. Genet. 17 (6) (2009) 759–765.
[22] M. Raponi, E. Buratti, E. Dassie, M. Upadhyaya, D. Baralle, Low U1 snRNP dependence at the NF1 exon 29 donor splice site, FEBS J. 276 (7) (2009) 2060–2073.
[23] S.L. Guedard-Mereuze, C. Vache, N. Molinari, J. Vaudaine, M. Claustres, A.F. Roux, S. Tuffery-Giraud, Sequence contexts that determine the pathogenicity of base substitutions at position +3 of donor splice-sites, Hum. Mutat. 30 (9) (2009) 1329–1339.
[24] P.P. Madsen, M. Kibaek, X. Roca, R. Sachidanandam, A.R. Krainer, E. Christensen, R.D. Steiner, K.M. Gibson, T.J. Corydon, I. Knudsen, R.J. Wanders, J.P. Ruiter, N. Gregersen, B.S. Andresen, Short/branched-chain acyl-CoA dehydrogenase deficiency due to an IVS3 + 3A>G mutation that causes exon skipping, Hum. Genet. (2005) 1–11.
[25] K. Ohno, J.M. Brengman, K.J. Felice, D.R. Cornblath, A.G. Engel, Congenital end-plate acetylcholinesterase deficiency caused by a nonsense mutation and an A−>G splice-donor-site mutation at position +3 of the collagenlike-tail-subunit gene (COLQ): how does G at position +3 result in aberrant splicing? Am. J. Hum. Genet. 65 (3) (1999) 635–644.
[26] M. Baralle, N. Skoko, A. Knezevich, L. De Conti, D. Motti, M. Bhuvanagiri, D. Baralle, E. Buratti, F.E. Baralle, NF1 mRNA biogenesis: effect of the genomic milieu in splicing regulation of the NF1 exon 37 region, FEBS Lett. 580 (18) (2006) 4449–4456.
[27] X. Roca, R. Sachidanandam, A.R. Krainer, Determinants of the inherent strength of human 5′ splice sites, Rna 11 (5) (2005) 683–698.
[28] S.I. Gunderson, M. Polycarpou-Schwarz, I.W. Mattaj, U1 snRNP inhibits pre-mRNA polyadenylation through a direct interaction between U1 70 K and poly(A) polymerase, Mol. Cell 1 (2) (1998) 255–264.
[29] A. Rincon, C. Aguado, L.R. Desviat, R. Sanchez-Alcudia, M. Ugarte, B. Perez, Propionic and methylmalonic acidemia: antisense therapeutics for intronic variations causing aberrantly spliced messenger RNA, Am. J. Hum. Genet. 81 (6) (2007) 1262–1270.
[30] M. Lund, J. Kjems, Defining a 5′ splice site by functional selection in the presence and absence of U1 snRNA 5′ end, Rna 8 (2) (2002) 166–179.

RESEARCH ARTICLE

Human Mutation

OFFICIAL JOURNAL HGVS HUMAN GENOME VARIATION SOCIETY www.hgvs.org

Functional and Structural Analysis of Five Mutations Identified in Methylmalonic Aciduria *cblB* Type

Ana Jorge-Finnigan,[1] Cristina Aguado,[1] Rocio Sánchez-Alcudia,[1] David Abia,[2] Eva Richard,[1] Begoña Merinero,[1] Alejandra Gámez,[1] Ruma Banerjee,[3] Lourdes R. Desviat,[1] Magdalena Ugarte,[1]* and Belen Pérez[1]

[1]*Centro de Diagnéstico de Enfermedades Moleculares, Centro de Biología Molecular-SO UAM-CSIC, Universidad Autónoma de Madrid, Campus de Cantoblanco, Madrid, Spain/Centro de Investigación Biomédica en Red de Enfermedades Raras (CIBERER), ISCIII, Madrid, Spain;* [2]*Servicio de Bioinformática, Centro de Biología Molecular-SO UAM-CSIC, Madrid, Spain;* [3]*Department of Biological Chemistry, University of Michigan Medical Center, Ann Arbor, Michigan*

Communicated by David S. Rosenblatt

Received 11 November 2009; accepted revised manuscript 1 June 2010.
Published online 15 June 2010 in Wiley Online Library (wileyonlinelibrary.com). DOI 10.1002/humu.21307

ABSTRACT: ATP:cob(I)alamin adenosyltransferase (ATR, E.C.2.5.1.17) converts reduced cob(I)alamin to the adenosylcobalamin cofactor. Mutations in the *MMAB* gene encoding ATR are responsible for the *cblB* type methylmalonic aciduria. Here we report the functional analysis of five *cblB* mutations to determine the underlying molecular basis of the dysfunction. The transcriptional profile along with minigenes analysis revealed that c.584G>A, c.349-1G>C, and c.290G>A affect the splicing process. Wild-type ATR and the p.I96T (c.287T>C) and p.R191W (c.571C>T) mutant proteins were expressed in a prokaryote and a eukaryotic expression systems. The p.I96T protein was enzymatically active with a K_M for ATP and K_D for cob(I)alamin similar to wild-type enzyme, but exhibited a 40% reduction in specific activity. Both p.I96T and p.R191W mutant proteins are less stable than the wild-type protein, with increased stability when expressed under permissive folding conditions. Analysis of the oligomeric state of both mutants showed a structural defect for p.I96T and also a significant impact on the amount of recovered mutant protein that was more pronounced for p.R191W that, along with the structural analysis, suggest they might be misfolded. These results could serve as a basis for the implementation of pharmacological therapies aimed at increasing the residual activity of this type of mutations.
Hum Mutat 31:1033–1042, 2010. © 2010 Wiley-Liss, Inc.

KEY WORDS: methylmalonic aciduria cblB type; ATR; MMAB; misfolding; splicing; cobalamin

Introduction

ATP:cob(I)alamin adenosyltransferase (ATR, E.C.2.5.1.17) is an enzyme involved in vitamin B_{12} metabolism that converts reduced cob(I)alamin to adenosylcobalamin, the active cofactor of methylmalonyl-CoA mutase (MUT, EC 5.4.99.2), which catalyzes the reversible rearrangement of methylmalonyl-CoA to succinyl-CoA in the catabolism of branched-chain amino acids, odd-chain fatty acids, and cholesterol. Mutations in the human *MMAB* gene encoding the ATR enzyme are responsible for the *cblB* type methylmalonic aciduria (MIM# 607568) [Dobson et al., 2002; Leal et al., 2003]. *CblB* patients present either a severe form with neonatal ketoacidosis, lethargy, failure to thrive, and encephalopathy or a milder, chronic form with less impaired neurological outcome. A cellular in vitro response to hydroxocobalamin (OHCbl) has been reported in certain cases, but this response appears to be unclear in vivo.

The human *MMAB* gene product, the ATR enzyme, is a member of the PduO family of cobalamin adenosyltransferases, which catalyzes the transfer of adenosine from ATP to cobalamin generating AdoCbl. To date, 24 mutations have been identified in the *MMAB* gene in *cblB*-type patients (HGMD® Professional Release 2009.3). Recently, the crystal structures of the homologous ATR proteins from *T. acidophilum* and *L. reuteri*, along with the human enzyme with ATP bound, have been determined [Saridakis et al., 2004; Schubert and Hill, 2006; St. Maurice et al., 2007], allowing for evaluation of the structural impact of pathogenic mutations in ATR. The enzyme is a homotrimer, each subunit composed of a five-helix bundle and an active site located at the subunit interface. Several mutations identified in patients have been mimicked in prokaryotic orthologs and their kinetic parameters determined. They revealed the existence of mutants with reduced affinity for the substrate and cofactor (p.R191W) and with negligible activity and presumed instability in vivo (p.R186W, p.R190H, and p.E193K) [Zhang et al., 2006]. In another study, a *Salmonella* ATR-deficient strain was used to express mutations generated by random mutagenesis in the human ATR coding sequence, allowing the delineation of the active site of the enzyme and the putative residues implicated in cob(II)alamin reduction [Fan and Bobik, 2008].

In this study, we report the genetic analysis of four methylmalonic aciduria *cblB*-type patients and the functional analysis of the identified mutations. In order to determine the molecular basis of in vitro B_{12} responsiveness we have functionally analyzed two missense changes, p.I96T and p.R191W, identified in three B_{12} responsive patient-derived cell lines, in prokaryotic and eukaryotic in vitro expression systems. We have also included the functional analysis of the three mutations affecting splicing (c.290G>A, c.584G>A, and c.349−1G>C) in an ex vivo assay using minigenes.

Cristina Aguado's present address is Universidad Pompeu Fabra.

*Correspondence to: Magdalena Ugarte, Centro de Biología Molecular "Severo Ochoa" CSIC-UAM, C/Nicolás Cabrera No. 1, Universidad Autónoma de Madrid, 28049 Madrid, Spain. E-mail: mugarte@cbm.uam.es

Materials and Methods

Genetic and Biochemical Analysis in Patients' Fibroblasts

Patient 1 (P1), previously described in Merinero et al. [2008], had a neonatal presentation of the disease. Patients 2 (P2) and 3 (P3) are siblings; P2 developed a late onset of the disease (at 4 years) and died shortly afterward. P3 was genetically diagnosed without presenting clinical symptoms, and to date, he is clinically normal. Patient 4 (P4) was referred to our laboratory for genetic analysis (Table 1). Since diagnosis, both the asymptomatic patients P3 and P4 are under therapy with protein restriction, carnitine supplementation, OHCbl administration, oral (5 ml/d) in P3, and intramuscular (5 mg/15 days) in P4 and metronidazol (only P4). During therapy the patients show differences at the biochemical level: P3 shows milder plasma C3 levels (~10 μM) compared to P4 (80 μM); P3 has normal plasma odd-chain fatty acid levels (OLCFA) (<0.4%), whereas P4 has increased ones (~4%). Urine MMA varies in P3 (<200–6000 mmol/mol creat), whereas there are no data available from P4. P3 has a perfect clinical development according to the clinician. P4 has a normal neurological and cardiological evaluation with normal renal function, weight (percentile 25–50) and height (percentile 10) and he is doing well at school. Due to reduction of bone density in lumbar spine, alandronate, calcium, and vitamin D were administered within growth and bone density. During his life he has showed some other metabolic decompensations associated with infections, vomiting, metabolic ketoacidosis, etc., without requiring hospital admission. In these crises the patient required nutritional adaptation. It is worth noting that the patient has excellent dietary compliance. This work has been approved by our institutional ethics committee, and informed consent has been obtained from the patients and their legal caregivers.

Fibroblast cell lines from patients were cultured under standard conditions in MEM supplemented with 10% fetal bovine serum, 200 mM glutamine, and antibiotics. Incorporation of radioactivity from [1-^{14}C] propionate into acid-precipitable material was assayed in intact fibroblasts grown in basal medium ±1 μg/ml OHCbl as previously described [Perez-Cerda et al., 1989]. All data are summarized in Table 1.

To identify mutations in the *MMAB* gene, cDNA sequence analysis was performed. The identified changes were confirmed by sequencing the corresponding genomic DNA region. Genotype analysis was performed using the primers and conditions described previously [Martinez et al., 2005]. Fibroblast cell lines were used as a source of DNA and RNA, which were isolated using the MagnaPure system following the manufacturer's protocol (Roche Applied Sciences, Indianapolis, IN). Mutation nomenclature follows the recommended guidelines of the Human Genome Variation Society (www.HGVS.org). Nucleotide numbering is based on cDNA reference sequences GenBank accession number NM_052845.3.

Functional Analysis of the Splicing Mutations

For evaluation of in vitro splicing, the pSPL3 vector (Life Technologies, Gibco, BRL, Grant Island, NY, kindly provided by Dr. B. Andresen, Aarhus University, Denmark) was used. Gene fragments corresponding to exons and flanking intronic regions were amplified from patients P2 and P4 and from a DNA control and cloned into the TOPO vector (Invitrogen, Carlsbad, CA) as previously described [Rincon et al., 2007]. A total of 2 μg of the wild-type or mutant minigenes was transfected into the following cell lines: Hep3B, HEK293, or COS7 using JetPEI, following the manufacturer's recommendations. Twenty-four to 48 hr postransfection, cells were harvested, RNA was purified, and RT-PCR analysis was performed using the pSPL3-specific primers SD6 and SA2 (Exon Trapping System, Gibco, BRL). The identity of amplified bands was determined by sequence analysis.

Prokaryotic and Eukaryotic Expression Analysis of Missense Changes

Mutation p.I96T (c.287T>C) and p.R191W (c.571C>T) were introduced using the QuikChange Site Directed Mutagenesis kit (Stratagene, Cedar Drive, TX). The oligonucleotides used for mutagenesis were: *MMAB* I96Tsense (5′AGTTCAGCTACTGGGTTTGCTCTG3′), *MMAB* I96T antisense (5′CAGAGCAAACCCAGTAGCTGAACT3′), *MMAB*R191W sense (5′CCGTGTGCCGCTGGGCCGAGAGAC3′) and *MMAB* R191W antisense (5′GTCTCTCGGCCCAGCGGCACACGG3′).

For prokaryotic expression analysis we used the NL173 plasmid, based on pET41a, which contains the human ATR sequence without the mitochondrial targeting sequence. Human ATR protein was expressed in *Escherichia coli* (BL21Star^{TM}DE3 One Shot Cells) and purified following the method described by Leal et al. [2004]. Bacterial cells were transformed with the NL173 plasmid encoding either the normal or mutant (p.I96T and p.R191W) ATRs. Protein expression was induced with 1 mM IPTG; 5 hr after induction, cells were collected by centrifugation and frozen at −70°C until further use. Cell pellets were resuspended at 4°C in 50 mM potassium phosphate buffer, pH 8, 100 mM NaCl, 1 mM DTT, 1 mM protease inhibitor phenylmethylsulphonyl fluoride, 1 mM EDTA, 0.05 mg/ml DNase, 0.3 mg/ml lysozyme. After 1 hr of incubation, the cell suspension

Table 1. Genotype, Clinical and Biochemical Phenotype in Four Methylmalonic Aciduria Patients *cblB* Type

Patient	MUT activity[b] (nmol/min/mg)	[1-^{14}C]-propionate −/+[c]	Allele 1	Allele 2	Onset	Outcome
P1	0.99	0.06/0.25	p.I96T (c.287T>C)	p.R191W (c.571C>T)	Neonatal (4 days)	7 y/severe encephalopathy
P2[a]	0.76	0.26/1.01	p.I96T (c.287T>C)	p.S174fs (c.584G>A)	Late onset (4 years)	Died at 4 y
P3[a]	NS	NS	p.I96T (c.287T>C)	p.S174fs (c.584G>A)	studied due to previous affected sister (3 months)	5 y/asymptomatic
P4	0.55	0.08/0.07	p.I117_Q118del (c.349−1G>C)	p.G66fs (c.290G>A)	Neonatal (4 days)	12 y/asymptomatic

NS, not studied. Mutation nomenclature follows the recommendations of HGVS and cDNA numbering is based on GenBank accession number NM_052845.3.
[a]Patients 2 (P2) and 3 (P3) are siblings.
[b]MUT activity in control fibroblasts with 36 μM AdoCbl was 0.94±0.40 nmol/min/mg protein.
[c][1-^{14}C]-Propionate uptake (nmol/10 hr/mg protein) in control fibroblasts without/with (−/+) hydroxocobalamin in the culture medium was 1.90±1.18/2.34±1.61.

was sonicated and centrifuged to obtain the crude soluble cell extract, which was subjected to ammonium sulphate precipitation and subsequent anion-exchange chromatography using a Sepharose Q column, as previously described [Leal et al., 2004]. In all purification steps, protein concentration was determined by the Bradford assay. Fractions eluted from the Sepharose Q column were subjected to SDS-PAGE to identify those enriched with the ATR protein. In some cases before ATR enzymatic assay, wild-type and mutant ATR proteins were further purified by hydroxyapatite chromatography at 4°C using as mobile phase a gradient of 10–400 mM potassium phosphate buffer pH 8, and 5 mM KCl. Fractions containing ATR of the highest purity were pooled and concentrated using an Amicon concentrator to a final concentration of 10 mg/ml.

Full-length cDNA of wild-type *MMAB* was generated from total RNA fibroblasts by RT-PCR and cloned into pGEM-T vector (Promega, Madison, WI). Subsequently, *MMAB* cDNA was further excised and inserted into *Hind*III/*Eco*RV sites of pFLAG–CMV-5c expression vector (Sigma, St. Louis, MO) to obtain *MMAB* cDNA coupled with FLAG-tag at the C-terminus (pFLAG–*MMAB*).

Eukaryotic expression analysis was performed in the P4 fibroblast cell line stably transformed with pBABE kindly provided by Dr. JA Enriquez (University of Zaragoza, Spain). A total of 4×10^5 transformed cells were transfected using 2.5 μg of normal or mutant pFLAG–*MMAB* constructs using lipofectamine 2000 (Invitrogen); then the cells were grown at 27 or 37°C. Harvested cells were used to determine ATR activity, which was indirectly measured by the analysis of [^{14}C]-propionate incorporation into acid-precipitable material in intact cells grown in basal medium [Perez-Cerda et al., 1989]. Propionate oxidation is catalyzed by two mitochondrial enzymes: the biotin-dependent propionyl-CoA carboxylase and the AdoCbl-dependent methylmalonyl-CoA mutase. AdoCbl is synthesized by ATR, and the patients with defects in the *MMAB* gene exhibit deficient propionate incorporation. Statistical analysis was performed using an *F*-test analysis of variance followed by a one-tailed paired *t*-test. Values of $P < 0.05$ were considered significant.

Enzyme Activity Assays

ATR activity was measured as previously published [Johnson et al., 2001] with minor modifications. Assays contained 200 mM Tris-HCl pH 8.0, 1.6 mM KH_2PO4, 2.8 mM $MgCl_2$, 100 mM KCl, 0.4 mM ATP, and 80 μM OHCbl (Sigma-Aldrich, St. Louis, MO). A total of 800 μl aliquots of the reaction mixture was dispensed into cuvettes kept at 37°C. Titanium (III) citrate (10 μl) was added, the reaction initiated by the addition of 10–100 μg of purified protein, and the decrease in absorbance at 388 nm was monitored. Anaerobic procedures were used to prepare the reaction mix, the protein solution and titanium(III)citrate.

Measurement of Dissociation Constants

The equilibrium dissociation constants (K_d) for cob(II)alamin analogs were determined fluorimetrically as described by Chowdhury and Banerjee [1999] with modifications. To determine the K_d values, 40–150 μg of protein in 50 mM Tris-HCl buffer, pH 8.0, were added to a quartz cuvette and successive aliquots (1–10 μl) of the cobalamin analogue (2–7 mM) were added, then the fluorescence (excitation wavelength: 280 nm, emission wavelength 340 nm) was measured after each addition. The K_d for cob(II)alamin was determined under anaerobic conditions by monitoring the shift in the UV-visible spectrum from 300 to 750 nm using 10 μM cob(II)alamin and varying concentrations of ATR as described previously [Yamanishi et al., 2005]. The kinetic data were analyzed using the IGOR Pro6 software (WaveMetrics Inc, Lake Oswego, OR).

Western Blot Analysis

Protein concentration in fibroblast and bacterial cell extracts was determined using the BIO-RAD protein assay (Bio-Rad, Bio-Rad Laboratories, Munchen, Germany) following the manufacturer's protocol. Equal amounts of total protein for bacterial cell extracts were loaded onto a 10% Laemmli SDS-PAGE System. After SDS-PAGE or native gel electrophoresis, proteins were transferred to a nitrocellulose transfer membrane (GE Healthcare, Buckinghamshire, UK) using a BIO-RAD apparatus in Tris (25 mM)–glycine (192 mM)–methanol (20%) without SDS for 1 hr. Poinceau staining was used to monitor equal loading of protein. Immunodetection was carried out using commercially available anti-ATR antibodies (ProteinTech Group Inc, Chicago, IL) as primary antibodies diluted 1:1,000. The secondary antibodies used were conjugated goat–antimouse IgG-horseradish peroxidase (1:10,000) (Santa Cruz Biotechnology Inc, Santa Cruz, CA) and were detected using the Enhanced Chemiluminescence System (GE Healthcare). Relative protein amounts were determined using a calibrated densitometer GS-800 (BioRad, Hercules, CA).

Oligomeric State of ATR

Size-exclusion chromatography using a Superdex 200 (1.2×92 cm) column was performed to assess the oligomeric state of the wild-type and mutant ATR proteins. A total of 100 μg of protein purified by ammonium sulphate precipitation and anion-exchange chromatography was applied to the column in 50 mM Tris-HCl buffer pH 8.0, 100 mM KCl, and a flow rate of 2.0 ml min^{-1}. Molecular mass value estimations were obtained using a calibration curve generated with molecular weight standards (BioRad).

Blue native electrophoresis was performed using 4–16% Native PAGE gels, Native Marker, and Native running buffer from Invitrogen. Samples were prepared with 4 × Native sample buffer with G-250 sample additive (Invitrogen). The electrophoretic separation was performed at 4°C for 1 hr at 150 V, followed by another hour at 250 V. Lanes containing purified ATR and molecular weight marker were stained using 2% Coomassie Brilliant Blue R-250 (BioRad) solution in acetic acid and destained in acetic acid: methanol: water (0.5:2:2). The remaining lanes were transferred to a PVDF membrane using the iBLOT system from Invitrogen. Immunodetection was carried out as described above.

Protein Stability Studies

The stability of the wild-type and mutant p.I96T and p.R191W proteins expressed in the prokaryotic system was investigated by incubating the transformed cells at 37 or 27°C following IPTG induction. Soluble supernatant was incubated at 37 or 27°C, aliquots were removed at different time points, and the cell extracts were subjected to SDS-PAGE. Western blot analysis was performed as described above. Following densitometric analysis, relative protein levels were expressed as percentage referred to time 0.

Structural Analysis and Molecular Dynamics

Visualization of the crystal structure of ATR and localization of the mutant residue I96 was performed using DSViewerPro5.0 (Accelrys Inc, San Diego, CA) with the PDB coordinates file 2IDX.

Human ATP:cobalamin adenosyltransferase (hATR) monomers were modeled using as a template the B and C chains from the PDB structure 2IDX [Schubert and Hill, 2006], and the program MODELLER9v7 [Eswar et al., 2006]. The ATP binding loop "KIYTK" was kept in the bound conformation from chain B, while the unresolved loop "SSAREAHLKYT" in the B chain was taken from the C chain. Trimer reconstruction was performed by superposition of the modeled monomer over the 2IDX structure with the help of the MAMMOTH program [Ortiz et al., 2002]. All three active sites were modeled as occupied by an ATP molecule.

Models of mutants p.R191W and p.I96T were generated with the program PyMOL [DeLano, 1998–2003] using the modeled trimer as template. Protonation states of ionizable groups at pH 6.5 for the three systems were calculated using the H++ server [Gordon et al., 2005]. The positions of hydrogen atoms, standard atomic charges, and radii for all the atoms were assigned according to the ff03 force field [Duan et al., 2003]. The complexes were immersed in cubic boxes of TIP3P water molecules [William et al., 1983] large enough to guarantee that the shortest distance between the solute and the edge of the box was larger than 13 Å. Counterions were also added to maintain electroneutrality. Three consecutive minimizations were performed involving: (1) only hydrogen atoms, (2) only the water molecules and ions, and (3) the entire system.

Simulation Details

Starting minimized structures, prepared as stated above, were simulated in the NPT ensemble using Periodic Boundary Conditions and Particle Mesh Ewald to treat long-range electrostatic interactions. The systems were then heated and equilibrated in two steps: (1) 200 ps of molecular dynamics (MD) heating the whole system from 100 to 300 K, and (2) equilibration of the entire system during 1.0 ns at 300 K. The equilibrated structures were the starting points for the 15 ns MD simulations at constant temperature (300 K) and pressure (1 atm). SHAKE algorithm was used to keep bonds involving H atoms at their equilibrium length, allowing a 2-fs time step for the integration of Newton's equations of motion. ff03 and TIP3P force fields, as implemented in AMBER 10 package [Case et al., 2008], were used to describe the proteins, the peptides, and the water molecules, respectively. Sample frames at 10-ps intervals from the molecular dynamics trajectory were subsequently used for the analysis.

In Silico Stability Analysis

Absolute free energies of the hATR complex and its mutants (p.R191W and p.I96T) were estimated using the MM-GBSA [Still et al., 2002] approach as implemented in the AMBER10 package. MM-GBSA method approaches the free energy of the complexes as a sum of a molecular mechanic (MM) interaction term, a solvation contribution through a generalized Born (GB) model, and a surface area (SA) contribution to account for the nonpolar part of solvation. Distributions of the observed free energies, measured every 10 ps snapshots along with the molecular dynamics simulations, were plotted using the R package [Gentleman, 1997].

In addition, to better characterize the changes produced by the mutated residues, an energy decomposition analysis in a pairwise fashion (between the residues surrounding the mutations) was performed using a cutoff of 5 Å from the mutated residues. Polar contribution to solvation free energies were calculated with GB, whereas nonpolar contributions were estimated to be proportional to the area lost upon binding using the LCPO method to calculate accessible surface areas [Weiser et al., 1999].

These calculations were performed, for each 10-ps snapshot from the simulations, using the appropriate module within AMBER 10 package. Free-energy decomposition interaction matrix was represented in an energy dependent color gradient using the program matrix2png [Pavlidis and Noble, 2003].

Results

P1, P2, and P4 patients showed normal MUT activity and P1 and P2 exhibited in vitro responsiveness to B_{12} (Table 1). The age of onset and the clinical outcome of these patients are summarized in Table 1. The p.I96T (c.287T>C) sequence change was identified in three of the patients (P1, P2, and P3). This mutation was found in combination with the missense change p.R191W (c.571C>T) and in two siblings in combination with c.584G>A mutation, affecting the last nucleotide of exon 7 in the *MMAB* gene. This last mutation results in exon 7 skipping (r.520_584del) in patient fibroblasts, which would result in a premature stop codon (p.S174fs) (Fig. 1A).

The RT-PCR pattern and subsequent sequence analysis of the amplified products obtained from patient P4 fibroblasts, showed the presence of two bands, one of them corresponding to the skipping of exon 3 (r.197_290del), which is predicted to generate a truncated protein and the other one corresponding to an in-frame deletion of two amino acids (r.349_354del6, p.I117_Q118del) due to activation of a cryptic splice site inside exon 5. The genomic DNA analysis showed two nucleotide changes c.290G>A and c.349−1G>C in the last nucleotide of exon 3 and in the 3′ splice site of intron 4, respectively (Fig. 1B).

Functional Analysis of the Splicing Mutations

In this work, we have investigated the functional effect of the three nucleotide changes affecting splicing (c.290G>A, c.349−1G>C, and c.584G>A) using a cell-based splicing assay. In the patient fibroblasts, only transcripts resulting from the skipping of exon 7 and exon 3 derived from the c.584G>A and c.290G>A alleles are detected. However, if correct splicing occurred occasionally, a mutant protein with the p.R195H and p.G97E changes would result. A minigene functional splicing assay was employed to investigate this possibility. All splicing mutations were cloned in minigenes and transfected in Hep3B, HEK293, or COS cells. All the mutants resulted in aberrant splicing. In addition of the strong 3′ and 5′ splice sites, the pSPL3 vector has after the multiple cloning site, cryptic 3′ and 5′ splice sites. In the case of the c.290G>A and c.584G>A mutant constructs, both splicing sequences were used—the classical and the cryptic one—and therefore the fragment amplified contained a vector sequence generated from use of the weaker cryptic spice sites (Fig. 2) In the case of c.584G>A a small but detectable amount of the correctly spliced transcript (resulting in the p.R195H change) was observed.

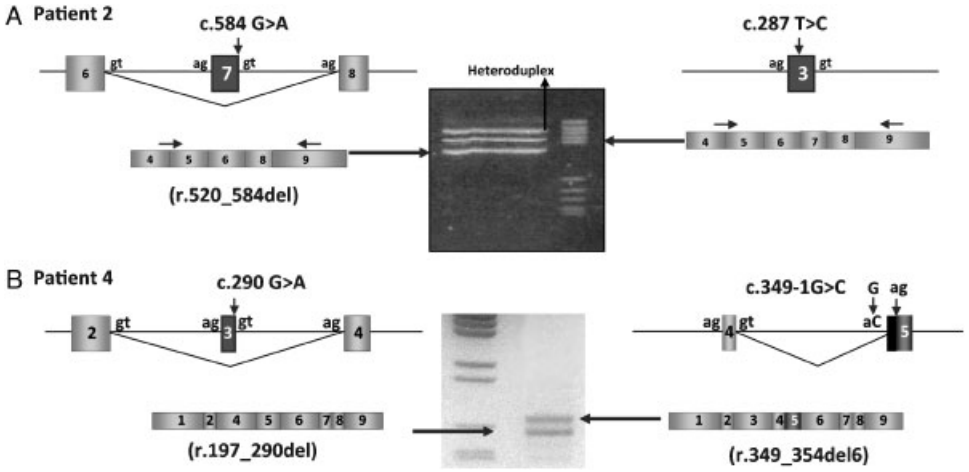

Figure 1. Schematic representation of the mutations mapped in genomic DNA and RT-PCR pattern from fibroblast. **A:** Patient P2 carries one nucleotide change located on exon 7 (c.584G > A) and a missense change on exon 3 (c.287C > T; p.I96T). The transcriptional profile shows three bands corresponding to the skipping of exon 7 transcribed from the allele bearing the c.584G > A change, a normal band from the allele bearing the c.287 T > C and a heteroduplex extra band (upper band). **B:** Patient 4 carries a change located on the last nucleotide of exon 3 (c.290 G > A) and an intronic change (c.349−1G > C) in intron 4. The RT-PCR pattern shows a smaller band without exon 3 resulting from the c.290G > A change and a larger one with an in-frame deletion of the first six nucleotides of exon 5 from the allele bearing c.349−1G > C.

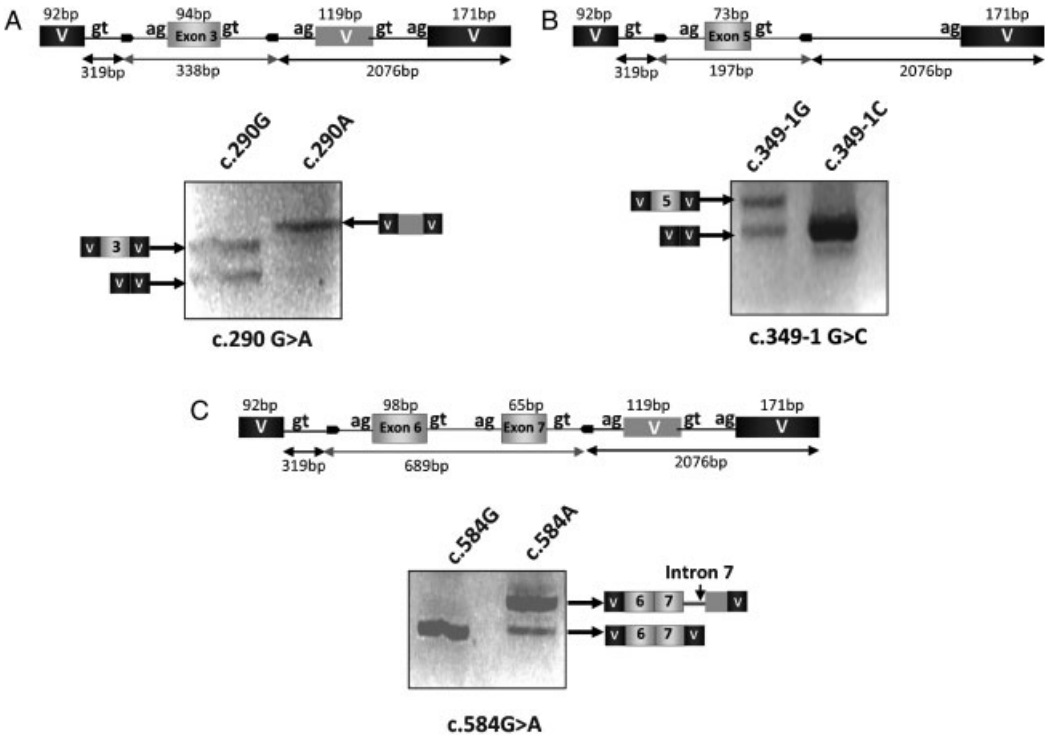

Figure 2. Splicing cellular minigene analysis. RT-PCR pattern obtained after transfection with the corresponding wild-type and mutant minigene constructs and schematic representation of each minigene construct. The PCR from the c.290G > A and c.349−1G > A minigenes was performed using minigene-specific primers while in the c.584G > A, a specific forward primer located at the junction of the vector sequence, and exon 6 was used to prevent different bands obtained when minigene-specific primers are used. All fragments were sequenced and the schematic representation of the resultant transcripts is indicated. Gene fragments corresponding to exon 3 (**A**) or exon 5 (**B**) and flanking 3′ and 5′ intronic regions were amplified from patients and cloned into the pSPL3 vector (gray line and box). For the c.584G > A minigene, the amplified fragment included exon 6, intron 6, and exon 7 and also the intronic sequence adjacent to both exons. The exonic sequences of the pSPL3 vector are highlighted in black boxes (V-boxes: vector sequence) and shaded boxes refers to the sequences involved when the cryptic splice sites are used (**A** and **C**). The sequence of the RT-PCR fragment obtained with the normal minigene (c.290G, c.349−1G, and c.584G) revealed the presence of a normal transcript with the corresponding exon included. In the two former cases we have also detected a slight band corresponding to a complete skipping of exon 3 and 5 that cannot be amplified in the third case. The sequence of the fragment obtained after transfection with the mutant construction containing the c.290A or c.584A changes revealed the presence of a vector sequence of 119 bp inserted in the aberrant transcript due to activation of a 3′ and 5′ cryptic splice site located in the vector sequence following the poly-cloning site.

Functional and Structural Analysis of the Missense Mutations

Because the three patients responsive to B_{12} in vitro share the p.I96T mutation described previously [Merinero et al., 2008], we sought to analyze the kinetic stability properties of the mutant protein. Residue I96 is located in helix α1 (Fig. 3A), distant from the ATP binding site, whereas residue R191 projects into the central cavity of the trimeric protein. Given the location of the I96 residue in α1 helix, the mutation could change the stability of the protein and/or perturb binding of the substrates, ATP, and cobalamin, but is not predicted to be involved in trimer formation.

Absolute free energies for wild-type hATR and the mutants, p.R191W and p.I96T, were estimated by the MM-GBSA method and predicted a decrease in stability for the p.R191W mutant ($-15{,}026.93 \pm 68.35$ kcal/mol) compared to the wild-type ATR (-15436.88 ± 72.76 kcal/mol) or the p.I96T mutant ($-15{,}441.07 \pm 67.06$ kcal/mol). In fact, a significant difference was not found between wild-type ATR and the p.I96T mutant (Supp. Fig. S1).

In addition, pair-wise interaction energies were calculated for the residues surrounding the mutations. In p.R191W, a network of hydrogen bonds at the trimer centre involving R191 and E91 residues was detected, linking the three monomers (Fig. 3B). The equivalent interaction in p.R191W mutant is substantially diminished (Fig. 3C). However, this energy loss is compensated,

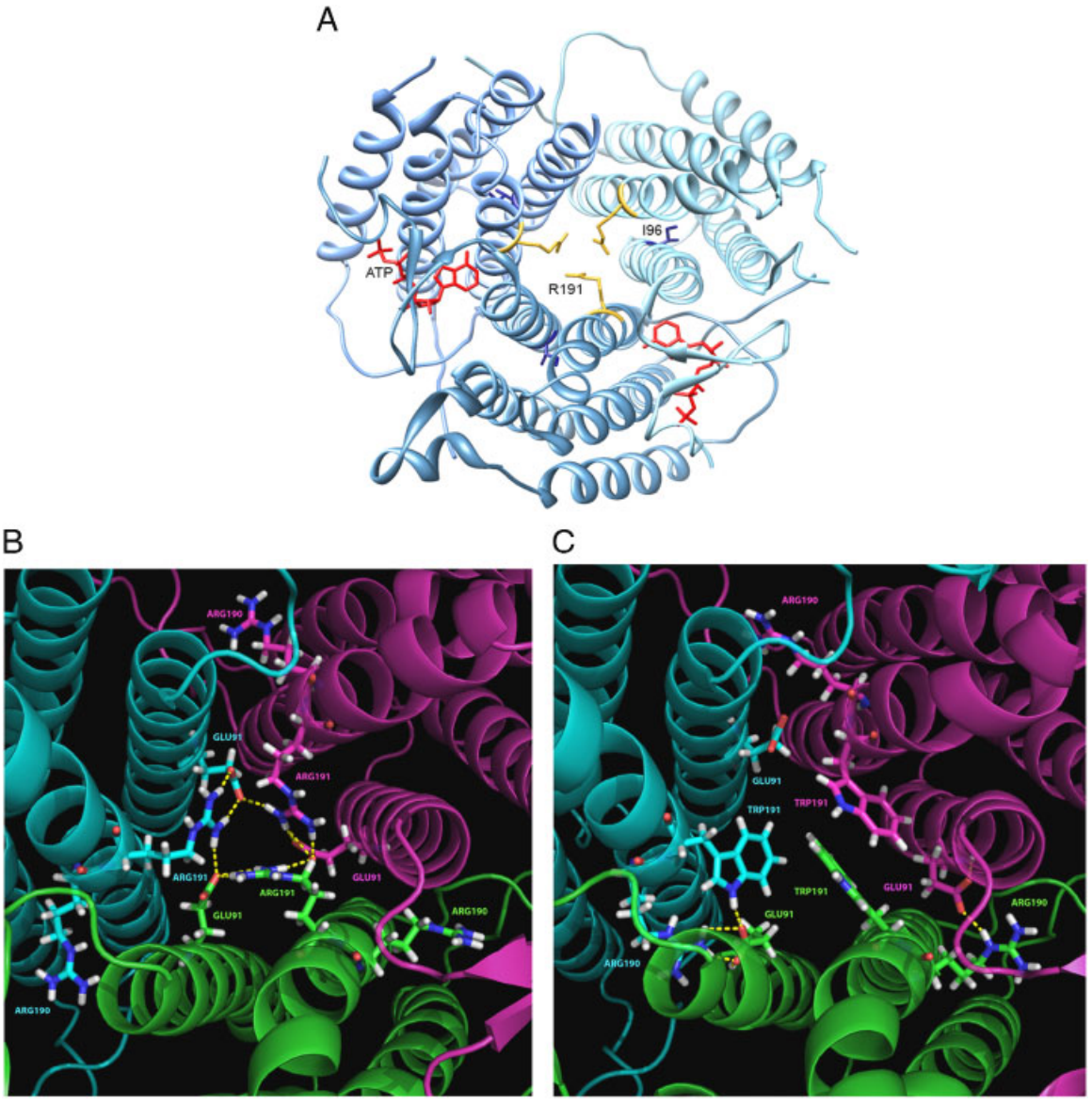

Figure 3. Structural analysis of missense mutation. **A:** Location of the p.I96T and p.R191W mutations in the crystal structure of human ATR. The enzyme is a homotrimer, with each subunit (shown in a different shade of blue) composed of a five-helix bundle and with the active site located at the subunit interfaces. Residue I96 is located in helix α1, distant from the ATP binding site, while residue R191 projects into the central cavity of the trimeric protein. ATP (red) and the residues, I96 (blue) and R191 (gold) are shown in stick representation. This figure was generated from the PDB file 2idx. **B:** Wild-type hATR trimer core (represented as cartoon) showing hydrogen bonds (dashed yellow lines) between residues E91, R190, and R191 (represented as sticks). **C:** R191W mutant hATR trimer core (represented as cartoons) showing hydrogen bonds (dashed yellow lines) between residues E91, R190, and R191 (represented as sticks).

Table 2. Comparison of Kinetic Parameters for Wild-Type and p.I96T ATR

	Wild type	p.I96T
Specific activity (nmol min^{-1} mg^{-1})	200 ± 10	123 ± 19
K_M (μM) ATP	6.2 ± 1.3	7.8 ± 1.9
K_d (μM) AdoCbl	1.7 ± 0.4	2.58 ± 0.62
K_d (μM) OHCbl	8.5 ± 1.1	7.8 ± 1.6
K_d (μM) CNCbl	7.8 ± 0.5	13.3 ± 0.3
K_d (μM) Cob(II)alamin	3.6 ± 1.6	1.37 ± 0.33

Data are the mean of at least two independent experiments each performed in duplicate.

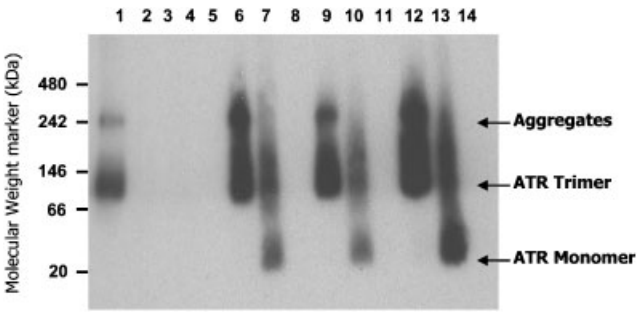

Figure 4. Oligomeric state of ATR. Blue native gel electrophoresis of cell extracts subjected to immunodetection for ATR. Lane 1, 1 μg of purified wild-type hATR; lane 2, total extract from nontransformed BL21 bacteria; lanes 3–5, whole-cell extracts from uninduced bacteria transformed with wild-type ATR plasmid (lane 3), p.I96T ATR (lane 4), and p.R191W ATR (lane 5); lanes 6–14 induced transformed bacteria. Lanes 6, 7, and 8, whole-cell extracts of wild-type (1 μg), p.I96T (2.5 μg), or p.R191W (20 μg); lanes 9, 10, and 11, supernatant of wild-type (1 μg), p.I96T (2.5 μg), and p.R191W (20 μg) after centrifugation of sonicated cell extracts; lanes 12, 13, and 14, pellets from wild-type (1 μg), p.I96T (2.5 μg), and p.R191W (20 μg) obtained after centrifugation.

at least in part, by a new inter subunit hydrogen bond pattern established between the R190 and E91 residues. In addition, the effect of the stacked conformation adopted by the mutant W191 residue creates a distortion in the trimer core that is reflected by other changes involving the interaction profile of E84, especially those related to R194 and R195, and the interaction between R190 and bound ATP (data not shown). On the contrary, a significant difference in the pair-wise interaction energy when comparing the I96T mutant to the wild-type protein was not observed.

Wild-type and mutant (p.I96T) ATR were expressed in *E. coli* and purified. The degree of purification was estimated to be 95% after the first step and ~99% after the final step. The specific activity and kinetic parameters for wild-type and p.I96T ATR were measured in parallel (Table 2), and similar results were obtained with and without the last hydroxyapatite purification step. The p.I96T mutant exhibits a slight reduction in specific activity, retaining 60% of wild-type levels with no significant differences in the K_ds for ATP or cobalamins, with the exception of CNCbl, which showed a 1.7-fold increase in K_d.

The oligomeric profile of the p.I96T mutant protein was analyzed by size-exclusion chromatography following ammonium sulphate precipitation and anion-exchange chromatography. Under these conditions, the protein exists mainly as a trimeric, similar to wild-type ATR (data not shown). Electrophoresis under nondenaturing conditions detected aggregates of ATR in the crude cell lysates (supernatants or pellets) with either wild-type or mutant ATR, although the size distributions were different (Fig. 4). Wild-type ATR showed lower molecular weight aggregates (~250 kDa), while the majority of the protein was present in a trimeric form. The p.I96T mutant showed both trimeric and monomeric forms. Both supernatant and crude extracts of mutant proteins showed a significant reduction in the amount of protein recovered, more pronounced in the case of p.R191W that could not be detected under any conditions (Fig. 4).

Next, we investigated the relative stabilities of the p.I96T and p.R191W mutants expressed in bacteria grown at 37°C or 27°C (Fig. 5). The p.I96T mutant was found to have a significantly decreased half life (Fig. 5A) compared to wild-type protein at 37°C (34 vs. 85 hr). At lower temperature (27°C) the half-lives for both proteins increased (Fig. 5B).

R191 projects into the central cavity of the trimeric ATR structure (Fig. 3A); interactions between this residue from adjacent monomers might play a role in stabilizing the quaternary structure of the protein. In fact, the p.R191W mutant was highly unstable at 37°C (Fig. 5A) with a half-life of 1.3 hr. The expression level of the mutant increased when the cells were grown at 27°C, with a corresponding increase in its half-life to 26.5 hr (Fig. 5B).

Wild-type and mutant ATRs were also expressed as fusion proteins with a FLAG tag in a *cblB* fibroblast cell line (P4). Cells were cultured at 37 and 27°C, and the [^{14}C]-propionate incorporation levels were determined as an indirect measure of ATR activity in the transfected cells. At 37°C, the mutant p.I96T and p.R191W proteins showed a statistically significant reduction in [^{14}C]-propionate incorporation: 65 and 52% of wild-type levels, respectively. When the cells were grown at 27°C, [^{14}C]-propionate incorporation levels of p.I96T and p.R191W mutants increased to levels close to wild-type ones (Fig. 6).

Discussion

The focus of this work was the functional analysis of five *cblB* mutations and the investigation of the underlying molecular mechanism of in vitro B_{12} responsiveness observed in three MMA patients belonging to the *cbl*B class. The results obtained indicate that all five nucleotide changes are disease-causing mutations, opening the possibility for genetic counseling, carrier identification, and prenatal diagnosis in at-risk families, and allowing determination of possible phenotype–genotype correlations and mutation-specific therapies.

Regarding the functional analysis of the exonic and intronic nucleotide changes affecting splicing, our results suggest that there are negligible levels of normal transcript associated with the mutations studied, from fibroblasts from patients and in cell lines (Hep3B, Hek293, and COS cells) transfected with the corresponding minigenes. Based on our data, the in vitro responsiveness in these patients might be associated with the missense changes, p.I96T or p.R191W. In relation to patient P4, who bears two splicing mutations, no stimulation of [^{14}C]-propionate was observed when cells were supplemented with OHCbl. However, given that the patient is clinically asymptomatic, the in-frame deletion of two amino acids resulting from the c.349−1G>C allele might a retain certain degree of activity. Addressing this will be the aim of future investigations.

The three in vitro B_{12} responsive patients (P1, P2, and P3) share the missense mutation p.I96T, which was expressed in a prokaryotic system in order to analyze its structural and kinetic properties. The mutant protein showed a modest reduction in specific activity but normal binding affinity for ATP and cob(II)alamin substrates. Inconsistent results were obtained in

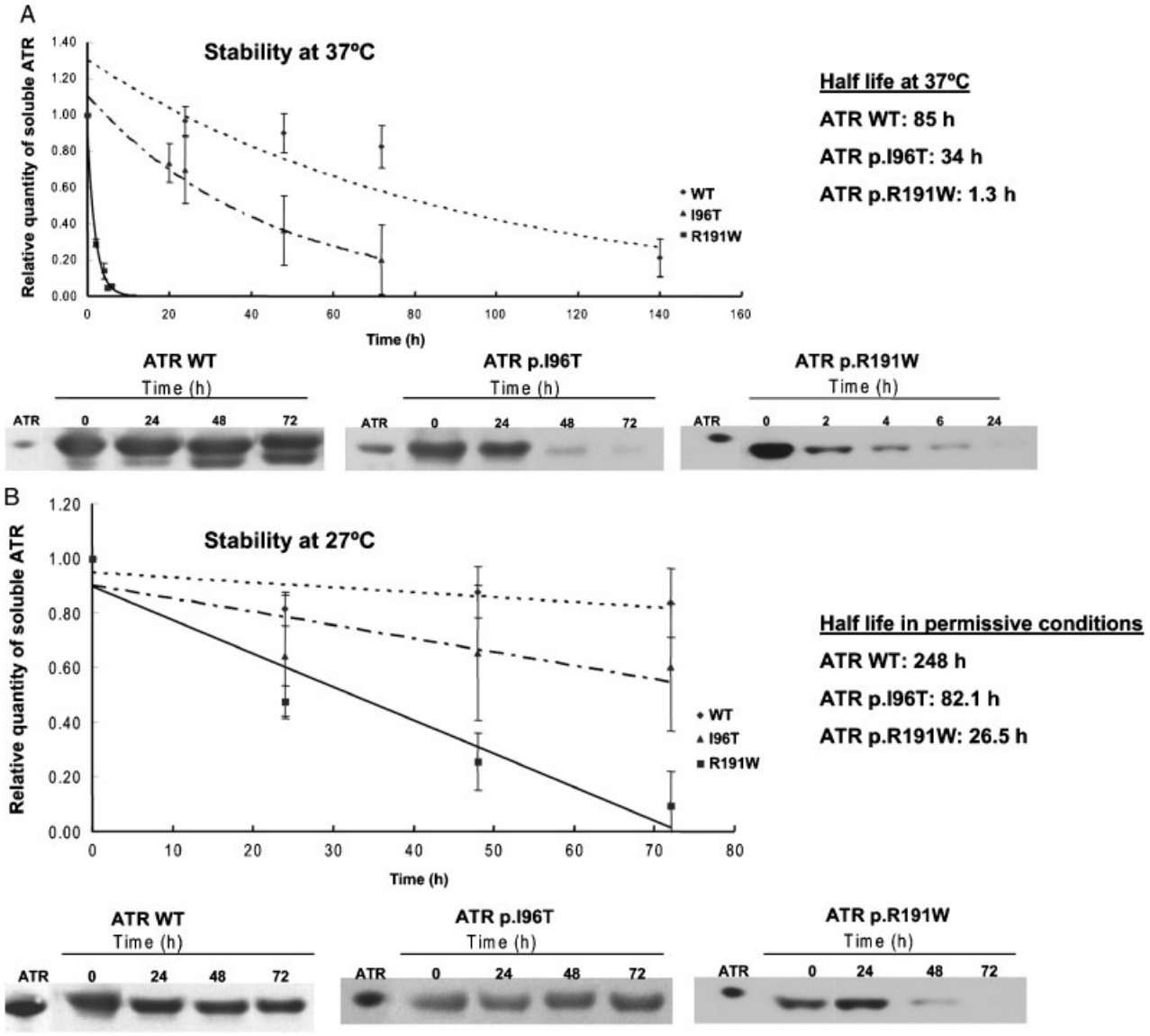

Figure 5. Degradation time course for wild-type p.I96T and p.R191W ATR at 37°C and 27°C. Crude cell extracts from cultures expressing wild-type or p.I96T or p.R191W ATR were incubated at 37°C (**A**) or 27°C (**B**) and aliquots were removed at different time points at 37 and 27°C, respectively, and subjected to SDS-PAGE and Western blot analysis as described in the Methods section. Protein amounts were quantified by laser densitometry. The data are the mean ± SD and represent the percent density of each protein relative to its density at time 0. The half-life of each protein is noted.

evaluating the effect of the mutations on the oligomeric structure of the protein. Thus, size-exclusion chromatography revealed a normal oligomeric profile, while native gel electrophoresis indicated an aberrant profile. In the former case, the purification of ATR prior to Superdex chromatography might have led to the separation of monomers, whereas the soluble or crude extracts loaded on the native gel allowed detection of all the ATR forms and involved only minor manipulation. However, the significantly lower levels of mutant protein observed by native gel electrophoresis, and the lower stability suggests that loss of biological function in the p196T mutant might be due to abnormal folding rather than a change in oligomeric state. Impaired protein folding can enhance degradation (e.g., in Gaucher and lysosomal storage disorders), lead to deposition of misfolded protein (e.g., in Alzheimer's disease) or result in an inactive form [Gamez et al., 2000; Majtan et al., 2010].

When both mutant proteins are expressed in *E. coli* under permissive low-temperature conditions, the steady-state levels of ATR and its half-life are increased. Similar results were obtained using a eukaryotic expression system where the level of ^{14}C-propionate incorporation was similar to control values when the transfected cells were grown at 27°C. Expression studies of the p.R191W mutation in *E. coli* have been previously described using a GST fusion protein in which its stability was not mentioned [Zhang et al., 2006]. In contrast, in *Salmonella enterica,* the p.R191W mutant was expressed at lower levels than the control, indicating that it impairs proper folding and leads to degradation mediated by cellular proteases [Fan and Bobik, 2008]. The residual activity associated with the pR191W mutant was reported to be 30% in the *E. coli* system and undetectable in *S. enterica* [Fan and Bobik, 2008; Zhang et al., 2006]. Mutations affecting residues close to the 191 position, for example, R190H and p.E193K, are also

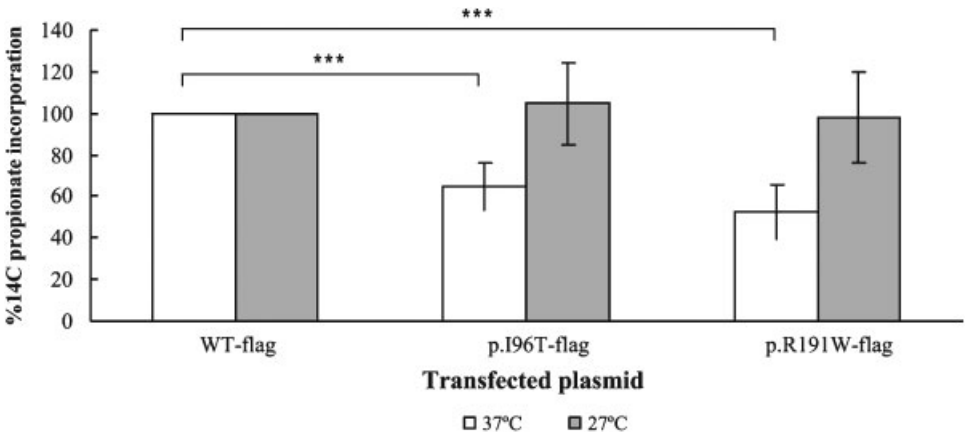

Figure 6. Functional analysis of the p.I96T and p.R191W mutants in a *cblB* null fibroblast cell line. A fibroblast cell line was transfected with a vector encoding wild-type or mutant (p.I96T or p.R191W) *MMAB* cDNA and the culture was incubated at 37 or 27°C. The cells were harvested followed by incorporation of [^{14}C]-propionate into trichloroacetic acid-precipitable material in the absence of OHCbl that was quantified as an indirect measure of ATR activity. The data are the mean ± SD of the percentage of [^{14}C]-propionate incorporation for each transfection versus the wild-type transfection ($n = 4$). The *P*-values were calculated for the pairs indicated in the figure (***P-value < 0.001).

unstable in all expression systems [Fan and Bobik, 2008; Zhang et al., 2006] and might represent a region critical for stability.

Our data suggest that p.R191W and p.196T mutants result in severe folding problems, although when expressed as fusion proteins with the Flag peptide in an eukaryotic expression system, residual activity was observed. However, because transient expression was performed using the P4 cell line, it is possible that in addition to FLAG stabilization, complementation with the endogenous ATR might have contributed to the rather high residual activity of these mutants.

The responsiveness to in vitro OHCbl supplementation could be explained partially by a stabilizing effect of the cofactor, which could act as a natural chaperone, as has been described for other cofactors, for example, tetrahydrobiopterin in phenylalanine hydroxylase deficiency [Erlandsen et al., 2004; Perez et al., 2005; Pey et al., 2004]. Other mechanisms may also be operating in the OHCbl-responsive cell line, P1, because the p.R191W mutant (albeit with a GST tag) exhibits a 16-fold higher K_M for cobalamin [Zhang et al., 2006]. Defects in ATR might also affect its interaction with MMAA or MUT proteins, assuming that the three enzymes operate in a complex and increased levels of B_{12} might have an stabilizing effect [Banerjee, 2006; Banerjee et al., 2009].

In addition to the genetic diagnosis of the disease, knowledge of the mutational spectrum in each population provides insights into genotype–phenotype correlations. Based on the clinical outcome, patients bearing the p.I96T mutation exhibit a highly variable phenotype. Thus, although one of them is clinically asymptomatic, the other two are either dead or severely neurologically impaired. These findings also suggest that the missense changes, p.I96T and p.R191W, might be categorized as a loss-of-function folding mutations that are usually associated with variable genotype–phenotype correlation [Andresen et al., 1997; Pey et al., 2003, 2007]. Interindividual differences in gene expression of the protein quality control and proteasomal proteins have been described as phenotypic modifiers in several misfolding diseases [Dipple and McCabe, 2000a,b].

In conclusion, functional analysis of the mutations described in this study is relevant to our understanding of the pathogenic mechanisms of MMA and also for the design of mutation-specific therapies. In several genetic disorders such as phenylketonuria or Gaucher's disease [Bernier et al., 2004; Mu et al., 2008; Pey et al., 2008], pharmacological rescue of folding mutants or upregulation of gene expression for mutants with residual activity is currently envisaged as a possible option for correcting, at least partially, the phenotype. In the case of the p.I96T and p.R191W mutant proteins, pharmacological chaperones or compounds such as statins [Murphy et al., 2007], which may result in activation of *MMAB* gene expression, should be explored as potential strategies to treat the disease if increased steady-state levels and activity of the protein can be achieved.

Acknowledgments

Ana Jorge-Finnigan is funded by Fondo de Investigaciones Sanitarias. This work was supported by grants from *Comisión Interministerial de Ciencia y Tecnología* (SAF2007-61350), *Fondo de Investigaciones Sanitarias* (PI060512), Fundación Ramón Areces, and the National Institutes of Health (DK45776). An institutional grant from the *Fundación Ramón Areces* to the Centro de Biología Molecular Severo Ochoa is gratefully acknowledged. We acknowledge the generous allocation of computer time at the Barcelona Supercomputing Center.

References

Andresen BS, Bross P, Udvari S, Kirk J, Gray G, Kmoch S, Chamoles N, Knudsen I, Winter V, Wilcken B, Yokota I. 1997. The molecular basis of medium-chain acyl-CoA dehydrogenase (MCAD) deficiency in compound heterozygous patients: is there correlation between genotype and phenotype? Hum Mol Genet 6:695–707.

Banerjee R. 2006. B12 trafficking in mammals: A for coenzyme escort service. ACS Chem Biol 1:149–159.

Banerjee R, Gherasim C, Padovani D. 2009. The tinker, tailor, soldier in intracellular B12 trafficking. Curr Opin Chem Biol 13:477–484.

Bernier V, Lagace M, Bichet DG, Bouvier M. 2004. Pharmacological chaperones: potential treatment for conformational diseases. Trends Endocrinol Metab 15: 222–228.

Chowdhury S, Banerjee R. 1999. Role of the dimethylbenzimidazole tail in the reaction catalyzed by coenzyme B12-dependent methylmalonyl-CoA mutase. Biochemistry 38:15287–15294.

Case TAD, CheathamIII TE, Simmerling CL, Wang J, Duke RE, Luo R, Crowley M, Walker RC, Zhang W, Merz KM, Wang B, Hayik S, Roitberg A, Seabra G, Kolossváry I, Wong KF, Paesani F, Vanicek J, Wu X, Brozell SR, Steinbrecher T, Gohlke H, Yang L, Tan C, Mongan J, Hornak V, Cui G, Mathews DH, Seetin MG, Sagui C, Babin V, Kollman PA. 2008. AMBER 10. San Francisco: University of California.

DeLano WL. 1998–2003. The PyMOL Molecular Graphics System. Version 0.93. San Carlos, CA: DeLano Scientific LLC.

Dipple KM, McCabe ER. 2000a. Modifier genes convert "simple" Mendelian disorders to complex traits. Mol Genet Metab 71:43–50.

Dipple KM, McCabe ER. 2000b. Phenotypes of patients with "simple" Mendelian disorders are complex traits: thresholds, modifiers, and systems dynamics. Am J Hum Genet 66:1729–1735.

Dobson CM, Wai T, Leclerc D, Kadir H, Narang M, Lerner-Ellis JP, Hudson TJ, Rosenblatt DS, Gravel RA. 2002. Identification of the gene responsible for the cblB complementation group of vitamin B12-dependent methylmalonic aciduria. Hum Mol Genet 11:3361–3369.

Duan Y, Wu C, Chowdhury S, Lee MC, Xiong G, Zhang W, Yang R, Cieplak P, Luo R, Lee T, Caldwell J, Wang J, Kollman P. 2003. A point-charge force field for molecular mechanics simulations of proteins based on condensed-phase quantum mechanical calculations. J Comput Chem 24: 1999–2012.

Erlandsen H, Pey AL, Gamez A, Perez B, Desviat LR, Aguado C, Koch R, Surendran S, Tyring S, Matalon R, Scriver CR, Ugarte M, Martínez A, Stevens RC. 2004. Correction of kinetic and stability defects by tetrahydrobiopterin in phenylketonuria patients with certain phenylalanine hydroxylase mutations. Proc Natl Acad Sci USA 101:16903–16908.

Eswar N, Webb B, Marti-Renom MA, Madhusudhan MS, Eramian D, Shen MY, Pieper U, Sali A. 2006. Comparative protein structure modeling using Modeller. Curr Protoc Bioinformatics Chapter 5:Unit 56.

Fan C, Bobik TA. 2008. Functional characterization and mutation analysis of human ATP:Cob(I)alamin adenosyltransferase. Biochemistry 47:2806–2813.

Gamez A, Perez B, Ugarte M, Desviat LR. 2000. Expression analysis of phenylketonuria mutations: effect on folding and stability of the phenylalanine hydroxylase protein. J Biol Chem 275:29737–29742.

Gentleman R. 1997. R. Version 2.9.2. Vienna: R Foundation for Statistical Computing. http://www.R-project.org.

Gordon JC, Myers JB, Folta T, Shoja V, Heath LS, Onufriev A. 2005. H++: a server for estimating pKas and adding missing hydrogens to macromolecules. Nucleic Acids Res 33:W368–W371.

Johnson CL, Pechonick E, Park SD, Havemann GD, Leal NA, Bobik TA. 2001. Functional genomic, biochemical, and genetic characterization of the Salmonella pduO gene, an ATP:cob(I)alamin adenosyltransferase gene. J Bacteriol 183: 1577–1584.

Leal NA, Olteanu H, Banerjee R, Bobik TA. 2004. Human ATP:Cob(I)alamin adenosyltransferase and its interaction with methionine synthase reductase. J Biol Chem 279:47536–47542.

Leal NA, Park SD, Kima PE, Bobik TA. 2003. Identification of the human and bovine ATP:Cob(I)alamin adenosyltransferase cDNAs based on complementation of a bacterial mutant. J Biol Chem 278:9227–9234.

Majtan T, Liu L, Carpenter JF, Kraus JP. 2010. Rescue of cystathionine beta-synthase (CBS) mutants with chemical chaperones: purification and characterization of eight CBS mutant enzymes. J Biol Chem 285:15866–15873.

Martinez MA, Rincon A, Desviat LR, Merinero B, Ugarte M, Perez B. 2005. Genetic analysis of three genes causing isolated methylmalonic acidemia: identification of 21 novel allelic variants. Mol Genet Metab 84:317–325.

Merinero B, Perez B, Perez-Cerda C, Rincon A, Desviat LR, Martinez MA, Sala PR, Garcia MJ, Aldamiz-Echevarria L, Campos J, Cornejo V, Del Toro M, Mahfoud A, Martínez-Pardo M, Parini R, Pedrón C, Peña-Quintana L, Pérez M, Pourfarzam M, Ugarte M. 2008. Methylmalonic acidaemia: examination of genotype and biochemical data in 32 patients belonging to mut, cblA or cblB complementation group. J Inherit Metab Dis 31:55–66.

Mu TW, Ong DS, Wang YJ, Balch WE, Yates 3rd JR, Segatori L, Kelly JW. 2008. Chemical and biological approaches synergize to ameliorate protein-folding diseases. Cell 134:769–781.

Murphy C, Murray AM, Meaney S, Gafvels M. 2007. Regulation by SREBP-2 defines a potential link between isoprenoid and adenosylcobalamin metabolism. Biochem Biophys Res Commun 355:359–364.

Ortiz AR, Strauss CE, Olmea O. 2002. MAMMOTH (matching molecular models obtained from theory): an automated method for model comparison. Protein Sci 11:2606–2621.

Pavlidis P, Noble WS. 2003. Matrix2png: a utility for visualizing matrix data. Bioinformatics 19:295.

Perez B, Desviat LR, Gomez-Puertas P, Martinez A, Stevens RC, Ugarte M. 2005. Kinetic and stability analysis of PKU mutations identified in BH4-responsive patients. Mol Genet Metab 86:S11–S16.

Perez-Cerda C, Merinero B, Sanz P, Jimenez A, Garcia MJ, Urbon A, Diaz Recasens J, Ramos C, Ayuso C, Ugarte M. 1989. Successful first trimester diagnosis in a pregnancy at risk for propionic acidaemia. J Inherit Metab Dis 12:274–276.

Pey AL, Desviat LR, Gamez A, Ugarte M, Perez B. 2003. Phenylketonuria: genotype–phenotype correlations based on expression analysis of structural and functional mutations in PAH. Hum Mutat 21:370–378.

Pey AL, Perez B, Desviat LR, Martinez MA, Aguado C, Erlandsen H, Gamez A, Stevens RC, Thorolfsson M, Ugarte M, Martínez A. 2004. Mechanisms underlying responsiveness to tetrahydrobiopterin in mild phenylketonuria mutations. Hum Mutat 24:388–399.

Pey AL, Stricher F, Serrano L, Martinez A. 2007. Predicted effects of missense mutations on native-state stability account for phenotypic outcome in phenylketonuria, a paradigm of misfolding diseases. Am J Hum Genet 81:1006–1024.

Pey AL, Ying M, Cremades N, Velazquez-Campoy A, Scherer T, Thony B, Sancho J, Martinez A. 2008. Identification of pharmacological chaperones as potential therapeutic agents to treat phenylketonuria. J Clin Invest 118:2858–2867.

Rincon A, Aguado C, Desviat LR, Sanchez-Alcudia R, Ugarte M, Perez B. 2007. Propionic and methylmalonic acidemia: antisense therapeutics for intronic variations causing aberrantly spliced messenger RNA. Am J Hum Genet 81:1262–1270.

Saridakis V, Yakunin A, Xu X, Anandakumar P, Pennycooke M, Gu J, Cheung F, Lew JM, Sanishvili R, Joachimiak A, Arrowsmith CH, Christendat D, Edwards AM. 2004. The structural basis for methylmalonic aciduria. The crystal structure of archaeal ATP:cobalamin adenosyltransferase. J Biol Chem 279:23646–23653.

Schubert HL, Hill CP. 2006. Structure of ATP-bound human ATP:cobalamin adenosyltransferase. Biochemistry 45:15188–15196.

St. Maurice M, Mera PE, Taranto MP, Sesma F, Escalante-Semerena JC, Rayment I. 2007. Structural characterization of the active site of the PduO-type ATP:Co(I)rrinoid adenosyltransferase from *Lactobacillus reuteri*. J Biol Chem 282:2596–2605.

Still WC, Tempczyk A, Hawley RC, Hendrickson T. 2002. Semianalytical treatment of solvation for molecular mechanics and dynamics. J Am Chem Soc 112:6127–6129.

Weiser J, Shenkin PS, Still WC. 1999. Approximate atomic surfaces from linear combinations of pairwise overlaps (LCPO). J Comput Chem 20:217–230.

William LJ, Jayaraman C, Jeffry DM, Roger WI, Michael LK. 1983. Comparison of simple potential functions for simulating liquid water. J Chem Phys 79:926–935.

Yamanishi M, Labunska T, Banerjee R. 2005. Mirror "base-off" conformation of coenzyme B12 in human adenosyltransferase and its downstream target, methylmalonyl-CoA mutase. J Am Chem Soc 127:526–527.

Zhang J, Dobson CM, Wu X, Lerner-Ellis J, Rosenblatt DS, Gravel RA. 2006. Impact of cblB mutations on the function of ATP:cob(I)alamin adenosyltransferase in disorders of vitamin B12 metabolism. Mol Genet Metab 87: 315–322.

J Inherit Metab Dis (2010) 33 (Suppl 2):S307–S314
DOI 10.1007/s10545-010-9116-4

NEWBORN SCREENING

The molecular landscape of propionic acidemia and methylmalonic aciduria in Latin America

Belén Pérez · Celia Angaroni · Rocio Sánchez-Alcudia · Begoña Merinero · Celia Pérez-Cerdá · N. Specola · P. Rodríguez-Pombo · Moacir Wajner · Raquel Dodelson de Kremer · Verónica Cornejo · Lourdes R. Desviat · Magdalena Ugarte

Received: 2 December 2009 / Revised: 9 April 2010 / Accepted: 19 April 2010 / Published online: 15 June 2010

Abstract In this work, we review the clinical and genetic data in 14 Latin American propionic acidemia (PA) and 15 methylmalonic aciduria (MMAuria) patients. In the PA patients, we have identified four different changes in the *PCCA* gene, including one novel one (c.414+5G>A) affecting the splicing process. The *PCCB* mutational spectrum included two prevalent changes accounting for close to 60% of the mutant alleles studied and one novel change (c.494G>C) which by functional analysis is clearly pathogenic. We have also identified the deep intronic change c.654+462A>G, and the results of the antisense treatment in the patient's cell line confirmed the functional recovery of PCC activity. All PA patients bearing out-of-frame mutations presented the disease earlier while patients bearing in hemizygous fashion p.E168K and p.R165W presented the disease later. Regarding the MMAuria patients, we have found three novel mutations in the *MUT* gene (c.1068G>A, c.1587_1594del8 and c.593delA) and one in the *MMAB* gene (c.349-1 G>C). Two patients with MMAuria with homocystinuria *cblC* type are carriers of the frequent c.271dupA mutation. All mut^0, *cblB* and *cblC* patients presented the symptoms early and in general had more neurological complications, while *cblA* and mut^- patients exhibited a late-onset presentation, and in general the long-term outcome was better. The results presented in this work emphasize the importance of the genetic analysis of the patients not only for diagnostic purposes but also to research into novel therapies based on the genotype.

Communicated by: Georg Hoffmann

Competing interest: None declared

B. Pérez · R. Sánchez-Alcudia · B. Merinero · C. Pérez-Cerdá · P. Rodríguez-Pombo · L. R. Desviat · M. Ugarte
Centro de Diagnóstico de Enfermedades Moleculares,
Centro de Biología Molecular-SO UAM-CSIC,
Universidad Autónoma de Madrid,
Campus de Cantoblanco,
28049 Madrid, Spain

B. Pérez · R. Sánchez-Alcudia · B. Merinero · C. Pérez-Cerdá · P. Rodríguez-Pombo · L. R. Desviat · M. Ugarte (✉)
Centro de Investigación Biomédica en Red
de Enfermedades Raras (CIBERER),
Madrid, Spain
e-mail: mugarte@cbm.uam.es

C. Angaroni · R. D. de Kremer
Centro de Estudio de las Metabolopatías Congénitas, CEMECO,
Facultad de Ciencias Médicas, Universidad de Córdoba,
Hospital de Niños,
Córdoba, Argentina

C. Angaroni
Cátedra de Genética Bioquímica, Facultad de Ciencias Químicas,
Universidad Católica de Córdoba,
Córdoba, Argentina

N. Specola
Unidad de Metabolismo, Hospital de Niños de La Plata,
La Plata, Argentina

M. Wajner
Serviço de Genetica Médica, Hospital de Clinicas,
Porto Alegre, RS, Brazil

V. Cornejo
Laboratorio de Genética y Enfermedades Metabólicas, INTA,
Universidad de Chile,
Santiago de Chile, Chile

Introduction

Propionic acidemia (PA, MIM# 606054) and methylmalonic aciduria (MMAuria, MIM# 251000) are the most frequent forms of branched-chain organic acidurias, a class of diseases caused by defects in the catabolism of propionyl-CoA to succinyl-CoA from the branched-chain amino acids, valine and isoleucine, and other propiogenic substrates such as methionine, threonine, odd-chain fatty acids, and cholesterol. These two autosomal recessive disorders are caused by defective conversion of propionyl-CoA to D-methylmalonyl-CoA by the biotin-dependent enzyme propionyl-CoA carboxylase (PCC, EC#6.4.1.3) and of L-methylmalonylCoA to succinyl-CoA by the cobalamin-dependent enzyme methylmalonyl-CoA mutase (MUT, EC#5.4.99.2), respectively.

The biotin-dependent mitochondrial enzyme PCC consists of two non-identical subunits, α- and β-encoded by the *PCCA* (MIM#232000) and *PCCB* (MIM#232050) genes, respectively. To date, more than 140 variant alleles in patients from around the world have been reported in both genes (Desviat et al. 2004) (http://www.hgmd.cf.ac.uk). Missense mutations are predominant (~40%), followed by small insertions/deletions and splicing mutations and, in the case of the *PCCA* gene, by large genomic deletions (Desviat et al. 2009).

Isolated MMAuria is caused by impairment of the apoenzyme MUT (*mut* complementation group) or associated to the defective transport and synthesis of adenosylcobalamin cofactor (Adocbl) in the mitochondria (*cblA, cblB* and *cblDvariant2* complementation groups). Two different defects have been described in the *mut* group, mut^0 and mut^- , based on the presence or absence of in vitro responsiveness to B_{12} (Fowler et al. 2008).

The majority of the changes identified in *cblA* affected patients are nonsense or frame-shift mutations with p.R145X identified as prevalent (Dobson et al. 2002; Lerner-Ellis et al. 2004; Martinez et al. 2005). Mutations in the human *MMAB* gene encoding the ATP:cob(I)alamin adenosyltransferase (ATR) enzyme are responsible for the *cblB* type MMAuria.

MMAuria and homocystinuria *cblC* type *(MMACHC;* MIM 277400, 609831) is the most common genetic defect in cobalamin metabolism (Lerner-Ellis et al. 2006; Rosenblatt and Wayne 2001). To date, 55 different mutations in patients worldwide have been identified, and a duplication of an A at the c.271 position (c.271dupA or p.R91KfsX14) has been identified as the most frequent mutation (Lerner-Ellis et al. 2006; Morel et al. 2006; Nogueira et al. 2008; Richard et al. 2009).

The aim of this work was to bring together the clinical and genetic data of PA and MMAuria Latin American patients in order to provide insight about the genotype–phenotype correlations and as the basis for the investigation and development of "tailor-made" therapies based on the sequence variants identified in each individual.

Materials and methods

The study included 25 fibroblast cell lines and 4 genomic DNAs from 14 PA patients, 13 isolated MMAuria patients and 2 MMAuria with homocystinuria referred to Madrid from Argentina, Brazil, Chile, and Venezuela for genetic analysis. All patients were diagnosed after presenting clinical symptoms and not through neonatal screening. The clinical data were referred by physicians, and a number of patients have been tested with different standard IQ tests at different ages. According to their IQ, we have classified them as: IQ >79 normal, 50–79 mildly retarded, and IQ <50 severely retarded. Conventional treatment (hypoproteic diet, carnitine, B_{12} and biotin administration) were given to most patients.

To identify mutations in all 7 genes, sequence analysis of the cDNAs was performed as previously described in Martinez et al. (2005), Rodriguez-Pombo et al. (1998), and Richard et al. (2009) from fibroblasts grown in standard conditions or supplemented with puromycin (200 μg/mL) for 5 h. The changes identified were confirmed by sequencing the corresponding genomic DNA region. When no mutation, or only one mutation, was found in the cDNA sequence, all exons and intron/exon junctions were sequenced. The primers used for cDNA and genomic DNA amplifications were designed using the ENSEMBL database (http://www.ensembl.org/index.html) and the corresponding GenBank accession number. The amplification of the intronic genomic region of the *PCCA, PCCB* and *MUT* genes was done as previously described (Rincon et al. 2007). The familiar genetic analysis was carried out for heterozygous patients to confirm the presence of the mutations in different alleles and for homozygous patients to rule out the presence of a genomic deletion.

In the patients with MMAuria with homocystinuria, exon 2 of the *MMACHC* gene was directly analyzed by gene scanning using high resolution melting analysis or sequenced due to the high frequency of the c.271dupA mutation in the *MMACHC* Spanish population (Richard et al. 2009).

Total mRNA and genomic DNA were isolated using the MagnaPure system following the manufacturer's protocol (Roche Applied Science, Indianapolis, USA). RT-PCR was performed using the SuperScript III First-Strand enzyme (Invitrogen, Carlsbad, CA, USA). The DNA mutations are numbered based on cDNA sequence and intronic position described in the ENSEMBL database (http://www.ensembl.

org/index.html) as recommended by the Human Genome Variation Society (http://www.hgvs.org/mutnomen). Nucleotide numbering is based on cDNA reference sequences GenBank accession numbers NM_000282, NM_000532, NM_000255, NM_172250 NM_052845, NM_015702.1 and NM_015506 for *PCCA, PCCB, MUT, MMAA, MMAB, MMADHC* and *MMACHC*, respectively, considering nucleotide +1 as the A of the ATG translation initiation codon.

Transfection with antisense morpholino oligonucleotides and determination of PCC enzymatic activity were done as previously described (Rincon et al. 2007). The functional analysis of the new change p.R165P identified in the *PCCB* gene was performed as previously described (Perez-Cerda et al. 2003).

Results

Propionic acidemia

In this cohort of PA patients, we have identified 3 PCCA- and 11 PCCB-affected patients. The genotype and the clinical findings are summarized in Table 1. The mutational spectrum of PCCA patients included five different mutations all previously described (Desviat et al. 2004; Rodriguez-Pombo et al. 1998) except for the novel intronic change (c.414+5g>a) affecting the splicing process as predicted by the drastic decrease in splicing score of the 5' donor site of exon 5 according to splice prediction programs (www.fruitfly.org/seq_tools/splice.html and http://ast.bioinfo.tau.ac.il/SpliceSiteFrame.htm). RT-PCR analysis in the patient's cell line grown in the presence of puromycin showed the insertion of 43 nucleotides resulting from the activation of a nearby intronic cryptic splice site (r.414ins43).

In the *PCCB* gene, nine different mutations were identified. All nucleotide changes but one (c. 494G>C) have been previously described (Desviat et al. 2004). The novel change c.494G>C (p.R165P) was transiently expressed in a eukaryotic expression system showing a residual activity of 2% of wild-type levels.

Most PCCB disease-causing mutations were identified in only one allele with the exception of c.1218_1231del14ins12 and c.502G>A which together accounted for 60% of the mutant alleles studied, similar to the results reported in other cohorts of Caucasian patients (Ugarte et al. 1999; Desviat et al. 2004).

We have performed an antisense morpholino oligonucleotide (AMO) transfection to rescue the normal splicing in the patient's cell line, P8, bearing the deep intronic change c.654+462 A>G. PCC activity in the patient's cells was measured 72 h after AMO transfection (10–30 μM), showing the functional recovery of the defect reaching near-normal levels of PCC activity (data not shown)

Among the 14 PA patients, 1 PCCA and 2 PCCB deficient have died (at ages 9 months to 8 years) and 11 patients are at the moment alive (range 2–29 years old). Two PCCA patients and six PCCB patients exhibited early-onset symptoms, most of them carriers of out-of-frame mutations. The five late-onset PCCB patients are alive and all are homozygous or hemyzygous for the missense mutations p.E168K or p.R165W.

Methylmalonic acidurias

We have identified six *mut* patients, six *cblA*, one *cblB* and two *cblC* (Table 2). The mutational spectrum included nine different sequence variants in the *MUT* gene, three of them novel, two small deletions (c.593delA and c.1587_1594del8), and one nonsense change (c.1068G>A).

The mutational spectrum of MMAuria *cblA* type included four different nucleotide changes, all of them previously described (Martinez et al. 2005). The transcriptional profile of the two cell lines bearing the change c.733G>A (P22 and P25) revealed the skipping of exon 4 (r.563_733del). The rest of the mutations were small duplications causing premature termination codons (PTC).

The *cblB*-affected patient had two splicing mutations, one of which is novel (c.349-1G>A) located in the 3′ splice site of intron 4. RT-PCR analysis in the patient's fibroblasts showed the presence of two bands, one of them corresponding to the skipping of exon 3 (r.197_290del) produced by mutation c.290G>A and the other one corresponding to an in-frame deletion of two amino acids (r.349_354del6, p.I117_Q118del) resulting from the allele bearing the novel change c.349-1G>A, due to the activation of a cryptic splice site inside exon 5.

All *mut* type patients are alive (range 8 months to 17 years old) while both *cblC* cases have died. Concerning the age of presentation, ten exhibited the early onset presentation; all five mut^0, one *cblB*, one *cblA*, and the two *cblC*-affected patients. The mut^- and the remaining three *cblA* patients presented the symptoms later in infancy.

Discussion

The genotype data presented in this work represents a useful diagnostic tool making possible adequate genetic counselling, carrier identification, and prenatal diagnosis in at-risk families, allowing the exploration of phenotype-genotype correlations and, most importantly, allowing the investigation of new treatments specifically tailored to the mutations in each patient.

The mutational spectrum of Latin American PA and MMAuria patients is arguably similar to those described in historically related populations such as the Spanish or other

Table 1 Genotypes and clinical findings in Latin American propionic acidemia patients

Patient no.	Gene	Country	Allele 1	Allele 2	Onset of symptoms (age)[a]	Clinical findings[a]
P1	PCCA	Brasil	c.923dupT (p.L308fs)	c.1268C>T (p.P423L)	Early-onset (first days)	Seizures despite therapy. Anemia, leucopenia. Gastrostomy. Severe cortical atrophy, spongiform leucoencephalopathy. Mental retardation, language problems, normal motor activity. Alive 5 y
P2	PCCA	Brasil	c.1118T>A (p.M373K)	c.1118T>A (p.M373K)	Early-onset (3 d)	Vomiting, poor feeding, failure to thrive and hypotonia. Died 6 m
P3	PCCA	Chile	c.229C>T (p.R77W)	c.414+5G>A (p.A138fs)	Late-onset (9 m)	Normal psychomotor development (IQ 84) Hypotonia. Alive 29 y
P4	PCCB	Chile	c.1218_1231del14ins12 (p.G407fs)	c.1218_1231del14ins12 (p.G407fs)	Early-onset (3 d)	Hypotonia. Severe psychomotor delay IQ<50. Died 2 y
P5	PCCB	Chile	c.1218_1231del14ins12 (p.G407fs)	c.1218_1231del14ins12 (p.G407fs)	Early-onset (14 d)	Severely retarded. (IQ 40); hypotonia.Gastrostomy. Alive 16 y
P6	PCCB	Brasil	c.1218_1231del14ins12 (p.G407fs)	c.1218_1231del14ins12 (p.G407fs)	Early-onset (5 d)	Hypotonia, severe psychomotor delay. Died 9 m
P7	PCCB	Chile	c.1218_1231del14ins12 (p.G407fs)	c.1298dupA (p.A434fs)	Early-onset (2 d)	Normal development (IQ 90); hypotonia. Died 8 y
P8	PCCB	Argentina	c.654+462 A>G (r.654ins72)	c.494G>C (p.R165P)	Early-onset (first days)	Several striking metabolic decompesations. Slight disability and hypotonia. Delay in sitting, standing and gait assessments at 2y. Alive 2 y 1 m
P9	PCCB	Brasil	c.990dupT (p.E331X)	c.1228C>T (p.R410W)	Early-onset (2 d)	Hypotonia, convulsions and feeding problems. Gastrostomia. Severe neurological and psychomotor delay. Leucopenia. Alive 15 y
P10	PCCB	Ecuador	c.1218_1231del14ins12 (p.G407fs)	c.493C>T (p.R165W)	Late- onset (14 m)	Moderate psychomotor delay. Alive 16 y
P11	PCCB	Chile	c. 502G>A (p.E168K)	c. 502G>A (p.E168K)	Late-onset (6 m)	Normal development (IQ 88); hypotonia. Alive 14 y.
P12	PCCB	Chile	c.1218_1231del14ins12 (p.G407fs)	c. 502G>A (p.E168K)	Late-onset (10 m)	Hypotonia; moderate psychomotor delay (IQ 67). Alive 16 y
P13	PCCB	Argentina	c.1218_1231del14ins12 (p.G407fs)	c.502G>A (p.E168K)	Late-onset (3 m)	Slight hypotonia. No growth retardation. Alive 14 y
P14	PCCB	Chile	c.1173dupT (p.V392fs)	c. 502G>A (p.E168K)	Late-onset (5 m)	Severely retarded (IQ 45); hypotonia. Growth retardation. Gastrostomy. Alive 15 y

[a] *y* Years, *m* months, *d* days

Mediterranean populations (Desviat et al. 2004; Martinez et al. 2005).

We have found five different variation changes in three unrelated PCCA-deficient patients, one of them novel, whereas in PCCB-deficient cases we have found a more homogenous mutational spectrum with two prevalent mutations (c.1218_1231del14ins12 and c.502G>A). Nine out of 14 PA patients had at least one copy of either of these

Table 2 Genotypes, clinical findings in isolated methylmalonic aciduria and methylmalonic aciduria combined with homocystinuria in Latin American patients

Patient no.	Gene[a]	Country (ethnicity)	In vivo B_{12} responsiveness	Allele 1	Allele 2	Onset (age of dignosis)[b]	Clinical findings[b]
P15[c]	MUT (*mut^0*)	Argentina	No	c.1587_1594del8 (p.A530fs)	c.1846C>T (p.R616C)	Early-onset (3 d)	No renal disease, no psychomotor delay. Alive 7 y
P16[c]	MUT (*mut^0*)	Argentina (Spanish-Italian)	No	c.572C>A (p.A191E)	c.1068G>A (p.W356X)	Early-onset (3 d)	Recurrent urinary infections. No psychomotor delay. Alive 1 y 5 m
P17[c]	MUT (*mut^0*)	Argentina	No	c.1846C>T (p.R616C)	c.1846C>T (p.R616C)	Early-onset (3 d)	Consanguinity. Polycystic kidneys, bilateral hydronephrosis. Severe psychomotor delay. Alive 3 y 4 m
P18[c]	MUT (*mut^0*)	Chile	No	c.655A>T (p.N219Y)	c.593delA (p.A197fs)	Early-onset (10 d)	Mild psychomotor delay (IQ 75). Hypotonia. Gastrostomy. Alive 2 y
P19[c]	MUT (nd)	Chile	No	c.1871A>G (p.Q624R)	c.1871A>G (p.Q624R)	Early-onset (3 d)	No consanguinity. Severe psychomotor delay. Gastrostomy. Alive 8 m
P20[d]	MUT *(mut$^-$)*	Venezuela	No	c.607G>A (p.G203R)	c.2080C>T (p.R694W)	Late-onset (24 m)	Normal psychomotor development. Alive 6 y
P21[d]	MMAA	Chile	No	c.562G>C (p.G188R)	c.562G>C (p.G188R)	Late-onset (7 m)	Consanguinity; moderate psychomotor delay, measles, IQ 76. Renal failure. Alive 10 y
P22[c]	MMAA	Chile	Yes	c.450dupG/ (p.P151fs)	c.733G>A (p.S189fs)	Late-onset 7 m	Lost for follow-up since 5y. Alive 15 y
P23[d]	MMAA	Chile	Yes	c.358C>T/ (p.Q120X)	c.812_813dupAG (p.L272fs)	Late-onset 2 m	Slight hypotonia, no renal disease. Normal neurological development (IQ 81). Alive 17 y
P24[c]	MMAA	Chile	Yes	c.594dupT/ (p.E199fs)	c.594dupT (p.E199X)	Late-onset (4 m)	Moderate psychomotor delayv(IQ 79). no renal disease. Alive 15 y
P25[c]	MMAA	Chile	Yes	c.358C>T (p.Q120X)	c.733G>A (p.S189fs)	Early-onset (6 d)	Hypotonia. Normal neurological development (IQ 87). Alive 13 y
P26[d]	MMAA	Ecuador	Yes	c.433C>T (p.R145X)	c.433C>T (p.R145X)	Early-onset (8 m)	Cortical atrophy and bilateral basal ganglia lesions on MRIPsychomotor delay
P27[c]	MMAB	Argentina	No	c.290 G>A (p.G66fs)	c.349-1 G>C (p.I117_Q118del)	Early-onset	Asymptomatic.Alive 12 y
P28[c]	MMACHC	Argentina	–	c.271dupA (p.Arg91LysfsX14)	c.271dupA (p.Arg91LysfsX14)	Early-onset (post-morten)	Progressive multisystem organ affectation, hypotonia; anaemia. Died 3 m
P29[c]	MMACHC	Argentina	–	c.271dupA (p.Arg91LysfsX14)	c.271dupA (p.Arg91LysfsX14)	Early-onset (5 d)	Megaloblastic anaemia, plaquetopenia, hypoalbuminemia. Anasarca. Tubular dysfunction. Irreversible metabolic acidosis. Died 1 m

[a] *nd* Not determined

[b] *y* Years, *m* months, *d* days

[c] Patients described in this work

[d] Patients described previously (Merinero et al. 2008)

two mutations, allowing their use as molecular diagnosis markers, eliminating the time-consuming biochemical and cellular testing currently used to assign the patients to the PCCA and PCCB groups. These two mutations might also be excellent candidates for molecular testing in the new PA patients coming from neonatal screening programmes.

The deep intronic change c.654+462 A>G in the PCCB gene found in P8 was previously identified in a Turkish patient (Rincon et al. 2007). The newly identified patient is of Italian descent and therefore we speculate that this variant change may have originated in the Mediterranean basin.

In addition to genetic counselling, one of the main goals of the genetic analysis of the affected patients around the world is to search for new therapeutic targets. It is worth noting that antisense therapy in P8 patient's cell line rescues normal splicing and functional PCC activity as previously described (Rincon et al. 2007) and suggests once more that the antisense approach might be clinically promising in inherited metabolic diseases among other genetic diseases (Gurvich et al. 2008; Lacerra et al. 2000; Pros et al. 2009; Wood et al. 2007). In both PA and MMAuria, a number of patients are carriers of this type of deep intronic changes (Rincon et al. 2007; Perez et al. 2009), and with a small number of antisense oligonucleotides, several patients may be treated.

Regarding the *mut*, *cblA*, *cblB* and *cblC* patients, the majority of the mutations identified in this work have been previously described (Acquaviva et al. 2005; Martinez et al. 2005; Worgan et al. 2006; Lerner-Ellis et al. 2006; Richard et al. 2009), and the four novel allelic variants identified are presumably disease-causing mutations due to their predicted severe effect on the corresponding protein.

Regarding MMAuria *cblA* type patients, all but one of them carry in-frame or out-of-frame PTC mutations as has been described in other mutational analyses (Dobson et al. 2002; Lerner-Ellis et al. 2004; Martinez et al. 2005). To date, several reports have described the therapeutic approach based on read-through of in-frame PTC to enable synthesis of full-length proteins (Linde and Kerem 2008). A high-throughput screen identified the drug PTC124 or Ataluren®. Recently, clinical trials with this compound have been underway for cystic fibrosis, Duchenne muscular dystrophy, and haemophilia patients (http://www.ptcbio.com). The response to PTC124 depends on the levels of nonsense transcripts (Kerem et al. 2008), so mRNA analysis in patients' cells is relevant for the identification of patients with a potential to respond to the treatment. We have described a number of *cblA* type patients in whom the PTC transcripts are stable evading the degradation by nonsense-mediated mRNA decay (Merinero et al. 2008). This finding has also been recently described in the *MMACHC* gene associated to the p.R132X mutation, and this has been related to a milder form of the disease (Lerner-Ellis et al. 2009). In any case, although MMAuria *cblA* type patients might be the best candidates to be included in a clinical trial with PTC124, further in vitro investigation in disease cellular models should be done before starting treatment.

The mutational analysis also allows the investigation of phenotype-genotype correlations in order to try to improve the prognosis. Taking into account the genotype of PCCA patients, the missense change p.R77W, a loss of function mutation with intramitochondrial disminished stability (Clavero et al. 2002), and the new splicing mutation c.414+5G>A might be mild mutations, associated to late-onset presentation and mild clinical findings. On the contrary, mutations p.P423L and p.M373K associated to early-onset symptoms are presumably severe.

Regarding PCCB-deficient patients, the early-onset presentation was associated to severe frame-shift changes. The early-onset patient P9 who presented a severe neurological and psychomotor delay is carrier of the out-of-frame mutation p.E331X mutation and the missense change p.R410W. Functional analysis of this mutant protein p.R410W showed that it had close to 12% residual activity with normal immunorreactive PCCB protein (Perez-Cerda et al. 2003), but in bacterial systems, the protein was able to fold only in permissive conditions (Chloupkova et al. 2002). Although this change might be considered as a milder one, the loss of function of folding mutations are usually associated with variable genotype–phenotype correlations (Andresen et al. 1997; Pey et al. 2003, 2007). The early-onset patient P8 is compound heterozygous for a severe deep intronic change and the missense change p.R165P which severely affects the function of the PCCB protein in a eukaryotic expression system. Another change in the same residue, p.R165W, was shown to be a severe misfolding effect (Chloupkova et al. 2002).

Contrary to neonatal cases, the late-onset PCCB patients have a more favourable outcome. All of them are alive although two of them are severely retarded (IQ <50). All late-onset patients are functionally hemizygous for the missense changes p.E168K or p.R165W, correlating with previous studies in which these mild mutations play a dominant role when associated to a severe mutation in compound heterozygous fashion (Perez-Cerda et al. 2000).

Concerning MMAuria patients, the mut^0 type exhibited the most severe form of the disease with early-onset presentation, while mut^- and *cblA* patients presented a milder form with late-onset presentation, and in general normal psychomotor development as previously reported (Horster et al. 2007, 2009; Merinero et al. 2008). It is worth noting that in our study *cblA* patients are the less severe, usually responsive to B_{12}, as has also been described (Fowler et al. 2008; Merinero et al. 2008). Only one patient

homozygous for a missense change was unresponsive to cobalamin (Merinero et al. 2008) ,and no other disease-causing mutations were found in the *MUT, MMAB* and *MMADHC* genes in this patient. This patient exhibited a poorer outcome compared to other *cblA* patients emphasizing the fact that cobalamin responsiveness is an important predictor for the outcome in MMAuria *cblA* type. In *cblB* patient P27, the genotype–phenotype correlation was not straightforward. He has two splicing mutations but currently the clinical outcome is normal. Further in vitro expression analysis of these splicing mutations will provide clues to understanding the associated phenotype. Therefore, we can conclude that the clinical outcome in MMAuria depends on the gene affected and on the mutation found in each gene.

In our cohort of Latin American PA and MMAuria patients, particularly the latter, the outcome appears to be less severe compared to other populations with a higher death rate (Dionisi-Vici et al. 2006; Merinero et al. 2008; Perez-Cerda et al. 2000). The high frequency of live patients might be due to a clinical selection due to death without accurate diagnosis of early-onset patients. Therefore, implementation of neonatal screening programs in these countries will increase the detection rate of these disorders. In addition, the presymptomatic identification of late-onset patients may improve their outcome due to early initiation of treatment.

In conclusion, this report contributes to the knowledge of the genetic basis of organic acidemias in Latin American countries with useful applications for diagnostic purposes, and also represents a scientific mainstay to research in novel therapies based on the genotype. In addition, the assignment of each patient to a specific gene defect is helpful to guide clinical decisions and predict long-term outcome.

Acknowledgements This work was supported by grants from the Comisión Interministerial de Ciencia y Tecnología (SAF2007-61350), the Fondo de Investigaciones Sanitarias (PI060512) and CIBERER (INTRA/07/720.1). An institutional grant from the Fundación Ramón Areces to the Centro de Biología Molecular Severo Ochoa is gratefully acknowledged. The CIBERER is an initiative of the ISCIII.

References

Acquaviva C, Benoist JF, Pereira S, Callebaut I, Koskas T, Porquet D, Elion J (2005) Molecular basis of methylmalonyl-CoA mutase apoenzyme defect in 40 European patients affected by mut(o) and mut- forms of methylmalonic acidemia: identification of 29 novel mutations in the MUT gene. Hum Mutat 25:167–176

Andresen BS, Bross P, Udvari S, Kirk J, Gray G, Kmoch S, Chamoles N, Knudsen I, Winter V, Wilcken B, Yokota I, Hart K, Packman S, Harpey JP, Saudubray JM, Hale DE, Bolund L, Kolvraa S, Gregersen N (1997) The molecular basis of medium-chain acyl-CoA dehydrogenase (MCAD) deficiency in compound heterozygous patients: is there correlation between genotype and phenotype? Hum Mol Genet 6:695–707

Chloupkova M, Maclean KN, Alkhateeb A, Kraus JP (2002) Propionic acidemia: analysis of mutant propionyl-CoA carboxylase enzymes expressed in Escherichia coli. Hum Mutat 19:629–640

Clavero S, Martinez MA, Perez B, Perez-Cerda C, Ugarte M, Desviat LR (2002) Functional characterization of PCCA mutations causing propionic acidemia. Biochim Biophys Acta 1588:119–125

Desviat LR, Perez B, Perez-Cerda C, Rodriguez-Pombo P, Clavero S, Ugarte M (2004) Propionic acidemia: mutation update and functional and structural effects of the variant alleles. Mol Genet Metab 83:28–37

Desviat LR, Sanchez-Alcudia R, Perez B, Perez-Cerda C, Navarrete R, Vijzelaar R, Ugarte M (2009) High frequency of large genomic deletions in the PCCA gene causing propionic acidemia. Mol Genet Metab 96:171–176

Dionisi-Vici C, Deodato F, Roschinger W, Rhead W, Wilcken B (2006) 'Classical' organic acidurias, propionic aciduria, methylmalonic aciduria and isovaleric aciduria: long-term outcome and effects of expanded newborn screening using tandem mass spectrometry. J Inherit Metab Dis 29:383–389

Dobson CM, Wai T, Leclerc D, Wilson A, Wu X, Dore C, Hudson T, Rosenblatt DS, Gravel RA (2002) Identification of the gene responsible for the cblA complementation group of vitamin B12-responsive methylmalonic acidemia based on analysis of prokaryotic gene arrangements. Proc Natl Acad Sci U S A 99:15554–15559

Fowler B, Leonard JV, Baumgartner MR (2008) Causes of and diagnostic approach to methylmalonic acidurias. J Inherit Metab Dis 31:350–360

Gurvich OL, Tuohy TM, Howard MT, Finkel RS, Medne L, Anderson CB, Weiss RB, Wilton SD, Flanigan KM (2008) DMD pseudoexon mutations: splicing efficiency, phenotype, and potential therapy. Ann Neurol 63:81–89

Horster F, Baumgartner MR, Viardot C, Suormala T, Burgard P, Fowler B, Hoffmann GF, Garbade SF, Kolker S, Baumgartner ER (2007) Long-term outcome in methylmalonic acidurias is influenced by the underlying defect (mut0, mut-, cblA, cblB). Pediatr Res 62:225–230

Horster F, Garbade SF, Zwickler T, Aydin HI, Bodamer OA, Burlina AB, Das AM, De Klerk JB, Dionisi-Vici C, Geb S, Gokcay G, Guffon N, Maier EM, Morava E, Walter JH, Schwahn B, Wijburg FA, Lindner M, Grunewald S, Baumgartner MR, Kolker S (2009) Prediction of outcome in isolated methylmalonic acidurias: combined use of clinical and biochemical parameters. J Inherit Metab Dis 32:630–639

Kerem E, Hirawat S, Armoni S, Yaakov Y, Shoseyov D, Cohen M, Nissim-Rafinia M, Blau H, Rivlin J, Aviram M, Elfring GL, Northcutt VJ, Miller LL, Kerem B, Wilschanski M (2008) Effectiveness of PTC124 treatment of cystic fibrosis caused by nonsense mutations: a prospective phase II trial. Lancet 372:719–727

Lacerra G, Sierakowska H, Carestia C, Fucharoen S, Summerton J, Weller D, Kole R (2000) Restoration of hemoglobin A synthesis in erythroid cells from peripheral blood of thalassemic patients. Proc Natl Acad Sci U S A 97:9591–9596

Lerner-Ellis JP, Dobson CM, Wai T, Watkins D, Tirone JC, Leclerc D, Dore C, Lepage P, Gravel RA, Rosenblatt DS (2004) Mutations in the MMAA gene in patients with the cblA disorder of vitamin B12 metabolism. Hum Mutat 24:509–516

Lerner-Ellis JP, Tirone JC, Pawelek PD, Dore C, Atkinson JL, Watkins D, Morel CF, Fujiwara TM, Moras E, Hosack AR, Dunbar GV, Antonicka H, Forgetta V, Dobson CM, Leclerc D, Gravel RA, Shoubridge EA, Coulton JW, Lepage P, Rommens

JM, Morgan K, Rosenblatt DS (2006) Identification of the gene responsible for methylmalonic aciduria and homocystinuria, cblC type. Nat Genet 38:93–100

Lerner-Ellis JP, Anastasio N, Liu J, Coelho D, Suormala T, Stucki M, Loewy AD, Gurd S, Grundberg E, Morel CF, Watkins D, Baumgartner MR, Pastinen T, Rosenblatt DS, Fowler B (2009) Spectrum of mutations in MMACHC, allelic expression, and evidence for genotype-phenotype correlations. Hum Mutat 30:1072–1081

Linde L, Kerem B (2008) Introducing sense into nonsense in treatments of human genetic diseases. Trends Genet 24:552–563

Martinez MA, Rincon A, Desviat LR, Merinero B, Ugarte M, Perez B (2005) Genetic analysis of three genes causing isolated methylmalonic acidemia: identification of 21 novel allelic variants. Mol Genet Metab 84:317–325

Merinero B, Perez B, Perez-Cerda C, Rincon A, Desviat LR, Martinez MA, Sala PR, Garcia MJ, Aldamiz-Echevarria L, Campos J, Cornejo V, Del Toro M, Mahfoud A, Martinez-Pardo M, Parini R, Pedron C, Pena-Quintana L, Perez M, Pourfarzam M, Ugarte M (2008) Methylmalonic acidaemia: examination of genotype and biochemical data in 32 patients belonging to mut, cblA or cblB complementation group. J Inherit Metab Dis 31:55–66

Morel CF, Lerner-Ellis JP, Rosenblatt DS (2006) Combined methylmalonic aciduria and homocystinuria (cblC): phenotype-genotype correlations and ethnic-specific observations. Mol Genet Metab 88:315–321

Nogueira C, Aiello C, Cerone R, Martins E, Caruso U, Moroni I, Rizzo C, Diogo L, Leao E, Kok F, Deodato F, Schiaffino MC, Boenzi S, Danhaive O, Barbot C, Sequeira S, Locatelli M, Santorelli FM, Uziel G, Vilarinho L, Dionisi-Vici C (2008) Spectrum of MMACHC mutations in Italian and Portuguese patients with combined methylmalonic aciduria and homocystinuria, cblC type. Mol Genet Metab 93:475–480

Perez B, Rincon A, Jorge-Finnigan A, Richard E, Merinero B, Ugarte M, Desviat LR (2009) Pseudoexon exclusion by antisense therapy in methylmalonic aciduria (MMAuria). Hum Mutat 30:1676–1682

Perez-Cerda C, Merinero B, Rodriguez-Pombo P, Perez B, Desviat LR, Muro S, Richard E, Garcia MJ, Gangoiti J, Ruiz Sala P, Sanz P, Briones P, Ribes A, Martinez-Pardo M, Campistol J, Perez M, Lama R, Murga ML, Lema-Garrett T, Verdu A, Ugarte M (2000) Potential relationship between genotype and clinical outcome in propionic acidaemia patients. Eur J Hum Genet 8:187–194

Perez-Cerda C, Clavero S, Perez B, Rodriguez-Pombo P, Desviat LR, Ugarte M (2003) Functional analysis of PCCB mutations causing propionic acidemia based on expression studies in deficient human skin fibroblasts. Biochim Biophys Acta 1638:43–49

Pey AL, Desviat LR, Gamez A, Ugarte M, Perez B (2003) Phenylketonuria: Genotype-phenotype correlations based on expression analysis of structural and functional mutations in PAH. Hum Mutat 21:370–378

Pey AL, Stricher F, Serrano L, Martinez A (2007) Predicted effects of missense mutations on native-state stability account for phenotypic outcome in phenylketonuria, a paradigm of misfolding diseases. Am J Hum Genet 81:1006–1024

Pros E, Fernandez-Rodriguez J, Canet B, Benito L, Sanchez A, Benavides A, Ramos FJ, Lopez-Ariztegui MA, Capella G, Blanco I, Serra E, Lazaro C (2009) Antisense therapeutics for neurofibromatosis type 1 caused by deep intronic mutations. Hum Mutat 30:454–462

Richard E, Jorge-Finnigan A, Garcia-Villoria J, Merinero B, Desviat LR, Gort L, Briones P, Leal F, Perez-Cerda C, Ribes A, Ugarte M, Perez B (2009) Genetic and cellular studies of oxidative stress in methylmalonic aciduria (MMA) cobalamin deficiency type C (cblC) with homocystinuria (MMACHC). Hum Mutat 30:1558–1566

Rincon A, Aguado C, Desviat LR, Sanchez-Alcudia R, Ugarte M, Perez B (2007) Propionic and Methylmalonic acidemia: antisense therapeutics for intronic variations causing aberrantly spliced messenger RNA. Am J Hum Genet 81:1262–1270

Rodriguez-Pombo P, Hoenicka J, Muro S, Perez B, Perez-Cerda C, Richard E, Desviat LR, Ugarte M (1998) Human propionyl-CoA carboxylase beta subunit gene: exon-intron definition and mutation spectrum in Spanish and Latin American propionic acidemia patients. Am J Hum Genet 63:360–369

Rosenblatt DS, Wayne AF (2001) Inherited disorders of folate and cobalamin transport amd metabolism. In: Scriver CR, Beaudet AL, Sly W, Valle D (eds) The Metabolic and Molecular Bases of Inherited Diseases, vol III. McGrall-Hill, New York, pp 3897–3933

Ugarte M, Perez-Cerda C, Rodriguez-Pombo P, Desviat LR, Perez B, Richard E, Muro S, Campeau E, Ohura T, Gravel RA (1999) Overview of mutations in the PCCA and PCCB genes causing propionic acidemia. Hum Mutat 14:275–282

Wood M, Yin H, McClorey G (2007) Modulating the expression of disease genes with RNA-based therapy. PLoS Genet 3:e109

Worgan LC, Niles K, Tirone JC, Hofmann A, Verner A, Sammak A, Kucic T, Lepage P, Rosenblatt DS (2006) Spectrum of mutations in mut methylmalonic acidemia and identification of a common Hispanic mutation and haplotype. Hum Mutat 27:31–43

Molecular Genetics and Metabolism 96 (2009) 171–176

Contents lists available at ScienceDirect

Molecular Genetics and Metabolism

journal homepage: www.elsevier.com/locate/ymgme

High frequency of large genomic deletions in the PCCA gene causing propionic acidemia

Lourdes R. Desviat [a,*], Rocío Sanchez-Alcudia [a], Belén Pérez [a], Celia Pérez-Cerdá [a], Rosa Navarrete [a], Raymon Vijzelaar [b], Magdalena Ugarte [a,*]

[a] Centro de Diagnóstico de Enfermedades Moleculares, Centro de Biología Molecular Severo Ochoa, UAM-CSIC, Departamento de Biología Molecular, Universidad Autónoma de Madrid, Centro de Investigación Biomédica en Red de Enfermedades Raras (CIBERER), ISCIII, Madrid, Spain
[b] MRC Holland, Amsterdam, The Netherlands

ARTICLE INFO

Article history:
Received 26 November 2008
Received in revised form 15 December 2008
Accepted 15 December 2008
Available online 20 January 2009

Keywords:
MLPA
Propionic acidemia
Large genomic deletions
Alu sequences
PCCA gene

ABSTRACT

Mutations in either the PCCA or PCCB genes are responsible for propionic acidemia (PA), one of the most frequent organic acidemias inherited in autosomal recessive fashion. Most of the mutations detected to date in both genes are missense. In the case of PCCA deficient patients, a high number of alleles remain uncharacterized, some of them suspected to carry an exonic deletion. We have now employed multiplex ligation probe amplification (MLPA) and long-PCR in some cases to screen for genomic rearrangements in the PCCA gene in 20 patients in whom standard mutation detection techniques had failed to complete genotype analysis. Eight different deletions were found, corresponding to a frequency of 21.3% of the total PCCA alleles genotyped at our center. Two of the exonic deletions were frequent, one involving exons 3–4 and another exon 23 although in the first case two different chromosomal breakpoints were identified. Absence of exons 3 and 4 which is also the consequence of the novel splicing mutation c.231 + 1g > c present in two patients, presumably results in an in-frame deletion covering 39 aminoacids, which was expressed in a eukaryotic system confirming its pathogenicity. This work describes for the first time the high frequency of large genomic deletions in the PCCA gene, which could be due to the characteristics of the PCCA gene structure and its abundance in intronic repetitive elements. Our data underscore the need of using gene dosage analysis to complement routine genetic analysis in PCCA patients.

Introduction

Large genomic deletions and duplications represent ~6% of the reported mutations causing human disease, according to the Human Gene Mutation database statistics (www.hgmd.cf.ac.uk). This frequency has been suggested to be probably an underestimate given that standard mutation detection methods do not include systematic searches for genomic rearrangements [2].

Propionic acidemia is one of the most common organic acidemias inherited in autosomal recessive fashion and caused by a defect of propionylCoA carboxylase (PCC, EC 6.4.1.3), involved in the metabolism of branched-chain amino acids, odd-numbered chain length fatty acids and cholesterol. The enzyme consists of two non-identical subunits, α and β, encoded by the PCCA and PCCB genes, respectively. The disease is heterogeneous in clinical manifestation but usually presents in the neonatal period with vomiting, failure to thrive, lethargy and profound metabolic acidosis and can result in neonatal death or mental retardation [13].

Currently, more than 50 different mutations, mostly missense, have been reported in the PCCA and PCCB genes [10] (http://www.uchsc.edu/cbs/pcc/pccmain.htm). To date, a highly heterogeneous mutation spectrum has been reported with no prevalent mutations in the PCCA gene, while a limited number of mutations accounts for most of the mutant alleles for the PCCB gene [10].

PA patients are routinely genotyped by sequencing cDNA followed by genomic DNA analysis to confirm the identified mutation. Still, ~20% of alleles in PCCA deficient patients have remained uncharacterized at the genomic level. In some of these cases, cDNA analysis suggested the presence of exonic deletions. As currently used PCR based diagnostic techniques do not allow detection of large genomic copy number variations we analyzed these patients with multiplex ligation probe amplification (MLPA) [19], in some cases in combination with long-range PCR. This approach revealed for the first time a large number of different large genomic deletions in the PCCA gene causing propionic acidemia.

* Corresponding authors. Fax: +34 917347797.
E-mail addresses: lruiz@cbm.uam.es (L.R. Desviat), mugarte@cbm.uam.es (M. Ugarte).

1096-7192/$ - see front matter © 2008 Elsevier Inc. All rights reserved.
doi:10.1016/j.ymgme.2008.12.009

Patients and methods

Patients and genetic analysis

A total of 20 PCCA deficient with incomplete genotype after standard cDNA or genomic DNA sequencing were included in the MLPA analysis. In positive cases (patients with deletions) available parental samples were also analyzed by MLPA. Fibroblast samples were used as source of RNA and DNA. In some cases, only DNA samples were available. Total mRNA was isolated by Tripure Isolation reagent from Roche and subsequent RT-PCR was done using primers previously described [17]. For genomic DNA analysis each exon and their flanking intronic sequences were amplified separately, using PCR primers previously described [4]. The PCR products were sequenced using BigDye Terminator v.3.1 mix (Applied Biosystems, Foster City, CA) with the same primers used for amplification, and analysis by capillary electrophoresis on an ABI Prism® 3700 Genetic Analyzer (Applied Biosystems, Foster City, CA).

MLPA analysis

Two hundred and fifty nanogram of DNA purified from fibroblasts was used as starting material with the SALSA P278 PCCA MLPA kit available from MRC Holland, Amsterdam (www.mrc-holland.com). After hybridization, ligation and amplification according to the instructions of the manufacturer, 2 μl of the PCR products were mixed with 0.2 μl of fluorogenic ROX-labeled internal size standard (LIZ-500), separated on an ABI Prism 3730 Genetic Analyzer and analyzed using the Peakscanner software (Applied Biosystems, Foster City, CA). For normalization, relative probe signals were calculated by dividing each measured peak area by the sum of all peak areas of that sample. The ratio of each relative probe signal from patients was then normalized to the mean obtained with two control samples. An exon deletion was considered when the ratio was lower than 0,7. All suspected deletions were confirmed by a second MLPA analysis and corresponding parental samples were also subjected to MLPA.

Long-range PCR

Long-range PCR was performed using AccuTaq DNA polymerase (Sigma, Missouri) following the manufacturers' recommendations. Briefly, 500 ng of genomic DNA was subjected to PCR amplification in 50 μl reaction volume containing the enzyme buffer 1X, 500 μM of dNTPs, 400 nM of each primer, 2% DMSO and 2.5 U of polymerase. The primers were designed to have Tm $\geqslant$ 70 °C to allow a two-step cycling in the PCR reaction as follows: initial denaturation of 98 °C for 30 s, 30 cycles of 94 °C for 15 s, 68 °C for 8-10 min, final extension of 68 °C for 10 min, soak at 4 °C. Primer sequences were designed based on the genomic contig NT_009952.14 after masking the intronic sequences with RepeatMasker (www.repeatmasker.org). Long-range PCR products were purified using Qiaex II Gel Extraction Kit (Qiagen, Hilden) and directly sequenced with BigDye Terminator v.3.1 mix and subsequent analysis by capillary electrophoresis on an ABI Prism® 3700 Genetic Analyzer (Applied Biosystems, Foster City, CA). In some cases, long-PCR products were cloned in pCR2.1 TOPO vector (Invitrogen, Carlsbad, CA) prior to sequencing. Genomic deletions were named according to the recommended nomenclature [12] and (http://www.genomic.unimelb.edu.au/mdi/mutnomen/).

Expression analysis

Stably transformed fibroblasts derived from a PCCA deficient cell line [5] were used for expression analysis of the T62_S100del39 mutant protein. Deletion mutation of exons 3 and 4 was introduced in the pCMVA45-12 vector coding for wild-type PCCA by PCR mutagenesis (Quickchange mutagenesis kit, Stratagene, La Jolla, CA). Transfection was achieved by lipofection using Gene Porter™ (Gene Therapy Systems, San Diego, CA) cotransfecting with the vector pCMV–PCCB encoding the PCCB subunit, to achieve maximal expression [5]. PCC activity was assayed in cells harvested 72 h after transfection by the method described in [21].

Results

Genetic analysis of PA patients

As reference laboratory our center receives samples from propionic acidemia patients worldwide to perform genetic analysis of the PCCA and PCCB genes. In the past years, more than 65 PCCA and 100 PCCB patients have been genotyped, revealing mainly missense mutations, followed by small insertions and/or deletions and splicing defects. The mutation detection rate (at the genomic DNA level) has been 99.9% for the PCCB gene but only 78% for the PCCA gene.

In some PCCA patients, cDNA analysis revealed different exon skipping events concerning exons 3 and 4, exon 23, exons 13 and 14 and exons 13–20. In two of the patients heterozygous for the exons 3–4 skipping, genomic DNA analysis revealed a novel point mutation in the 5′ donor site of intron 3 (IVS3 + 1g > c, c.231 + 1g > c) (Table 1, Fig. 3B). The mutation affects the invariant G at position +1 disrupting U1 binding and likely causing a splicing defect. Intron 3 is only 104 bp long and the splicing score of the 3′ acceptor site of exon 4 analyzed with different splice predictor programmes is very poor (0.38 according to the BDGP, http://www.fruitfly.org/seq_tools/splice.html, and 75.8 according to the Analyzer Splice Tool based on Shapiro and Senapathy [20], http://ast.bioinfo.tau.ac.il/SpliceSiteFrame.htm), which could account for the fact that both exons are skipped together in the mRNA as a consequence of the point mutation.

For the rest of the exon skipping events the genomic DNA lesion remained elusive. In homozygous patients the corresponding exons failed to amplify, suggestive of a genomic deletion. Other PCCA patients carried a missense or splicing mutation in one allele, and no other mutation was detected after sequencing cDNA or exonic fragments of genomic DNA.

MLPA analysis

MLPA analysis was undertaken to identify exonic copy number variations that remain undetected by conventional methods. A total of 20 patients were included in the analysis, some with only one characterized allele and others with a suspected deletion as described above.

In 10 patients a homozygous deletion was detected as revealed by absence of the corresponding probe signals in the MLPA assay (Fig. 1). In eight patients a heterozygous deletion was deduced after visual inspection of the electrophoregrams and quantification of the ratio of the relative exon probe signal from patients compared to control samples (Fig. 2). The results are summarized in Table 1.

Two of the deletions, exons 3–4 and exon 23 were recurrent. The first was detected by MLPA in a total of 13 alleles (5 homozygous and 3 heterozygous patients) and the second in nine alleles (4 homozygous patients and one heterozygous). The rest of the identified deletions were only found in one patient each. Overall, a total of 28 alleles in our cohort presented genomic deletions, corresponding to a frequency of 21.3% in a sample of 66 genotyped patients in our laboratory (Table 1). MLPA analysis in available

Table 1
Genomic deletions and splice mutation newly identified in the PCCA gene.

Exonic deletion	cDNA change	Predicted effect	gDNA mutation[a]	N° alleles	Origin	Relative frequency (%)[b]
Δ Exons 3–4	r.184_300del	p.T62_S100del39	c.231 + 1g > c	2	Australia, Germany	1.5
Δ Exons 3–4	r.184_300del	p.T62_S100del39	c.184-558del4779	11	Italy, Turkey, Greece, USA	8.3
Δ Exon 23	r.2041_2118del	p.V681_A706del26	c.2041-2924del3889	9	Arab countries	6.8
Δ Exons 3–4	r.184_300del	p.T62_S100del39	c.184-727del8860	2	Malaysia	1.5
Δ Exons 13–14	r.1066_1284del	p.V356_G428del73	c.1066-?_1284 + ?del	2	Lebannon	1.5
Δ Exon 1	–	–	c.1-?_105 + ?del	1	Italy	0.8
Δ Exons 17–18	r.1430_1643del	p. G477fs	c.1430-?_1643 + ?del	1	Span	0.8
Δ Exons 15–19	r.1285_1746del	p.V429_S582del154	c.1285-?_1746 + ?del	1	Germany	0.8
Δ Exons 13–20	r.1066_1845del	p.V356_Q615del260	c.1066-?_1845 + ?del	1	USA	0.8
Total genomic deletions				*28*		*21.3*

[a] According to the recommended nomenclature guidelines www.hgvs.org/mutnomen [9].
[b] Calculated relative to 132 PCCA alleles analyzed in the laboratory.

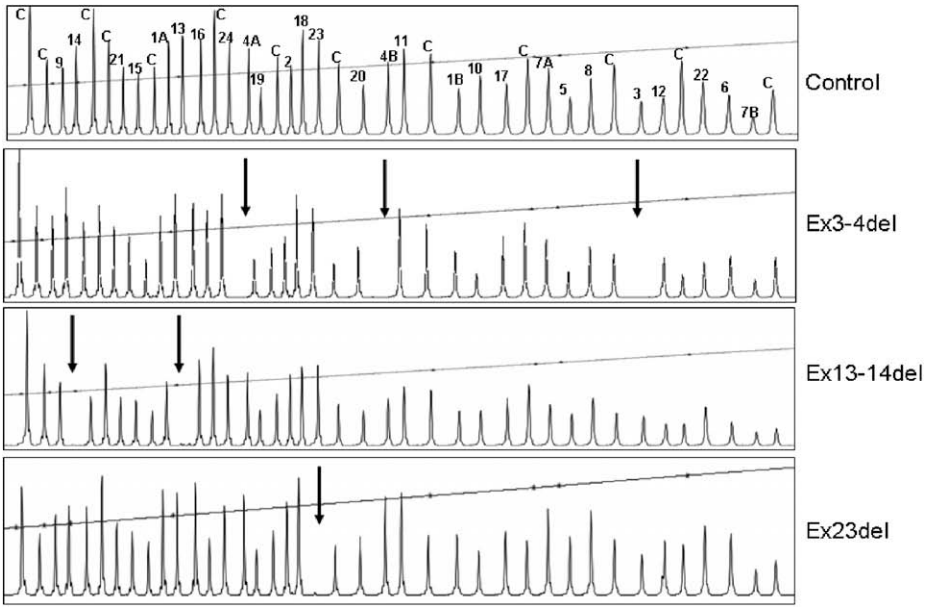

Fig. 1. Electrophoregrams obtained in MLPA analysis of samples from control and patients with homozygous deletions. Each peak represents one PCCA exon (denoted by its number) or a control probe amplification (C), recognized by a specific fragment size (*x*-axis: fragment size, *y*-axis: fluorescence intensity). The arrows point to the deleted exons as shown by absence of the corresponding peaks. Exon 4 is identified by two different probes.

parental samples confirmed the Mendelian inheritance of the deletions.

As described above, most of the deletions were also evident in cDNA analysis, verifying the results obtained from the MLPA assay. This was possible either because the patients were homozygous or because the exonic deletions were in frame, thus avoiding transcript degradation by the nonsense mediated decay (NMD) mechanism. In the patient with exons 17–18 deletion, which is out-of-frame, the transcript missing exons 17 and 18 could be detected after treatment of the fibroblasts with emetine to avoid NMD (40 μg/ml for 16 h) [3]. In the patient with deletion of exons 15–19, the primers first chosen for cDNA analysis in overlapping fragments precluded the amplification of the deletion transcript. Retrospective RT-PCR analysis with primers hybridizing to exons flanking the deletion allowed its detection.

Characterization of chromosomal breakpoints

To establish the boundaries of the two most frequent deletions long-range PCR and subsequent sequencing using a primer walking strategy was employed using DNA samples from homozygous patients with the exons 3–4 and exon 23 deletions.

Exons 3 and 4 in the PCCA gene are flanked by large introns of 8.8 Kb (intron 2) and 42.9 Kb (intron 4) (http://www.ensembl.org). Primers were designed to hybridize to introns 2 and 4 to amplify a fragment ~10 Kb long. In one patient (of Malaysian origin) a band of ~1 Kb was amplified and in the remaining patients (mostly of Mediterranean origin) a band of ~5 Kb was detected. Thus, two different deletions of estimated sizes of 9 and 5 Kb were present (Fig. 3A and C).

In the first case, chromosomal walking and sequence analysis identified a deletion of 8860 bp spanning from intron 2 to intron 4 (c.184-727del8860). Simple repeat sequence within an AluSg element was found at both sides of the deletion breakpoint suggesting Alu-mediated recombination as the origin of the deletion allele. According to the recommended nomenclature guidelines [9], the mutation was named c.184-727del8860 or g.13853044_13861904 del, in relation to the numbered nucleotides of human chromosome 13 reference sequence (NT_009952.14). In the second case, a deletion of 4779 nucleotides was identified, with a CA dinucleotide at both sides of the deletion. The deletion was named c.184-618del4779 or g.13853152_13857931del (contig NT_009952.14) (Fig. 3 A and C).

Exon 23 of the PCCA gene is flanked by introns of 12 Kb (intron 22) and 2.3 Kb (intron 23) (http://www.ensembl.org). The same

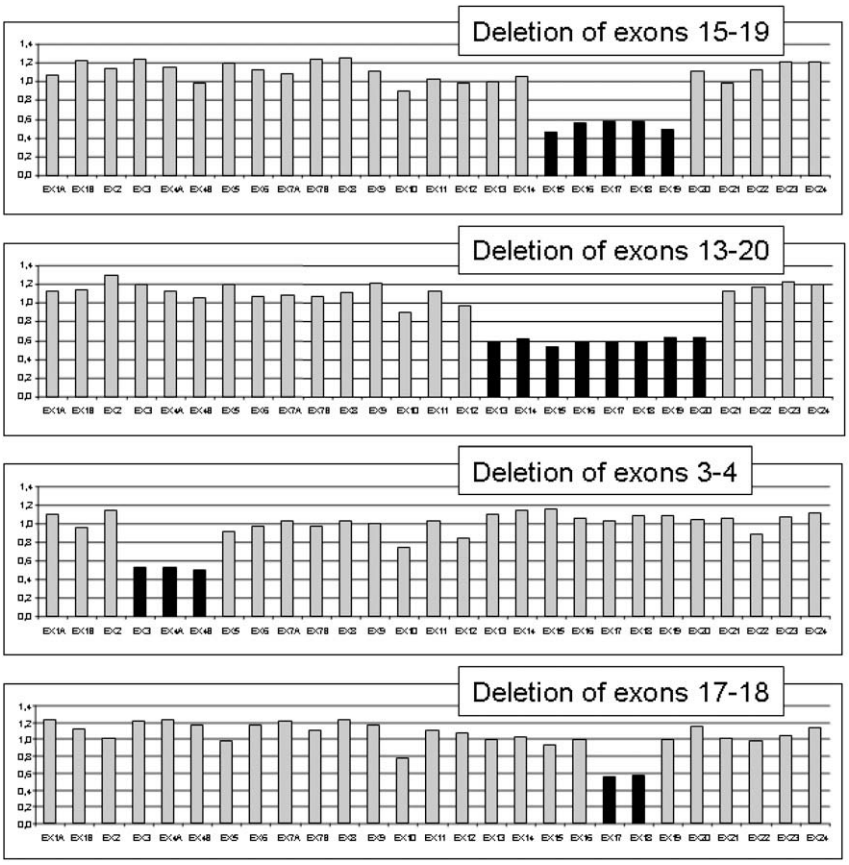

Fig. 2. Relative probe areas of the peaks corresponding to the 24 PCCA exons analyzed by MLPA of patients with different deletions in heterozygous fashion. Black bars correspond to the deleted exons, identified by a decrease of 40–55% in the normalized relative probe area levels (*y*-axis).

strategy as described above was used to identify the chromosomal breakpoints of the exon 23 deletion. Primers hybridizing to introns 22 and 23 and expected to yield a ~14 Kb PCR product resulted in a band of estimated size of 10 Kb in the homozygous patients suspected of harboring exon 23 deletion. Chromosomal walking identified a 3886 bp deletion, which was named g.436368_440254del (nucleotide numbering according to the contig NT_009952.14) or c.2119-1359del3886. In this case, the sequence GGC was found at both sides of the deletion (Fig. 3 D and E).

Functional analysis of the deletions

All the deletions presumably result in an internal in-frame deletion in the protein sequence except exons 17–18 deletion which is out-of-frame (Table 1) and deletion of exon 1 of unpredictable effect. Although in frame, the larger deletions, involving >70 amino acids presumably affect the structural and functional properties of the protein drastically. Deletion of exon 23 (26 amino acids) predictably results in a functionally null enzyme, as it involves the biotin binding site [15]. The deletion involving exons 3–4 and involving 39 amino acids is the most frequently detected and expression analysis in a eukaryotic system was performed to confirm its functional defect.

The deletion was introduced by PCR mutagenesis in the expression vector pCMVA45-12 coding for PCCA and normal and mutant constructs were transfected in a PCCA deficient cell line along with pCMV–PCCB encoding PCCB subunit of the PCC enzyme. The results demonstrate a total absence of residual activity of the protein with the 39 amino acid deletion corresponding to the exon 3–4 skipping, confirming its pathogenicity (Table 2).

Discussion

During the last few years genomic rearrangements have been described for many disease traits, with the appearance of different techniques for measuring gene dosage. In this work, MLPA was employed to screen for deletions in the PCCA gene in PA patients with no mutations in one or both alleles. This strategy has revealed an unexpected high frequency (21.3%) of deletion alleles, not recognized before. Moreover, this frequency may be considered representative of the Caucasian population, since the patients' samples were referred from laboratories located in Australia, Europe or USA. Exonic deletions may largely have escaped identification to date because the routine method for genetic diagnosis of PA patients has been to screen for mutations by PCR and sequencing. Only in homozygous patients was a deletion clearly suspected because of the failure to amplify the exons which were absent in cDNA.

In some of the heterozygous patients the deletion transcripts were not detected, either because they correspond to out-of-frame transcripts with premature stop codons which are subjected to NMD [16], or because the primers used to amplify the cDNA in overlapping fragments hybridised to deleted exons. Only in the case of exons 3–4 an additional PCR product missing exons 3 and 4 was clearly detected, although in two patients a splicing mutation (c.231 + 1g > c) was identified that accounted for the exon skipping event. MLPA and long-range PCR identified two different deletions of 8.8 and 4.7 Kb in the other alleles with the exons 3–4 deletion in cDNA. Thus, our results have uncovered three different genomic DNA lesions, one point mutation affecting splicing and two large deletions which all result in the same aberrant mRNA

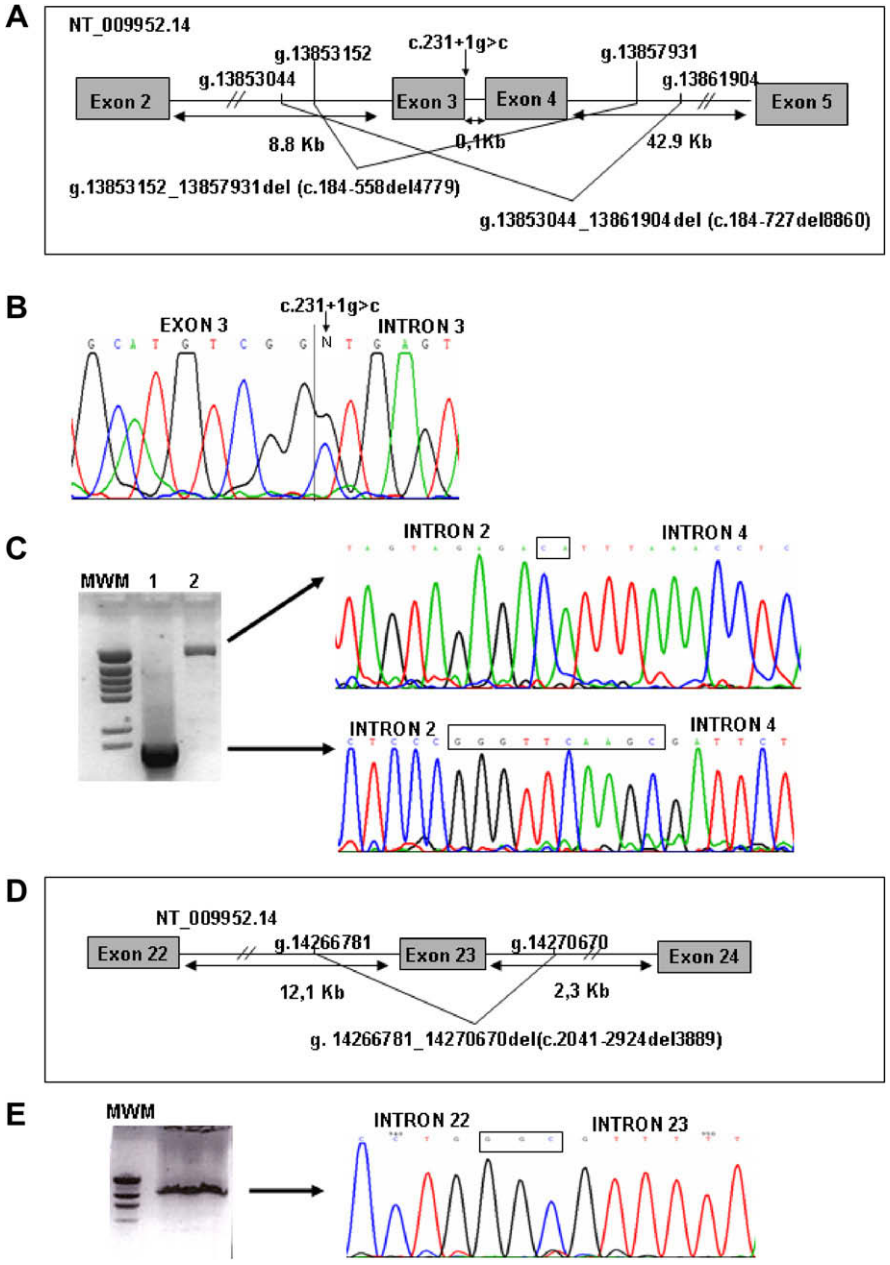

Fig. 3. Schematic figure of PCCA gene mutations involving exons 3–4 (A) and exon 23 (D) and breakpoint analysis of the deletions. In panel B the sequence of the splicing mutation IVS3 + 1g > c (c.231 + 1g > c) is shown. Panels C and E show the long-PCR products and the corresponding sequence analyzes. In panel C, lane 1 corresponds to the amplification product obtained from patients with the deletion c.184-727del8860 and lane 2 to the PCR obtained from patients with c.184-618del4779. In panel E the amplification product obtained from patients with the deletion c.2041-2924del3889 is shown.

Table 2
PCC activities in PCCA deficient fibroblasts transfected with wild-type or mutant PCCA constructs. The data show the mean ± SD from at least two independent experiments.

Transfected construct(s)	PCC activity (pmol/min/mg protein)	Relative PCC activity* (%)
pRC/CMV	110.25 ± 139	–
pCMV–PCCA + pCMV–PCCB	2475 ± 927	100
pCMV–PCCA (T62_S100del39) + pCMV–PCCB	23 ± 22	<1
Untransfected wild-type fibroblasts	1123 ± 455	–

* Residual activity relative to that obtained with cotransfection with wild-type PCCA and PCCB constructs.

missing exons 3 and 4, underscoring the need of genomic DNA analysis to characterize precisely the defect in each patient.

The 4.7 Kb deletion (c.184-618del4779) was present in 11 alleles corresponding to a frequency of 8.3% of the total PCCA alleles which makes it the most frequent mutation in our cohort of patients. Most of the patients carrying this mutant allele are of Mediterranean origin (Greek, Turkish or Italian), while exon 23 deletion is present in patients of Arab origin, probably reflecting founder effects. These results add relevant information on the genetic epidemiology of the disease and serve as basis for the implementation of a diagnostic strategy depending on the patient's ethnic or geographical background.

With this study, mutation detection rate in the PCCA gene has increased to ~98.5% in our hands. There are still ~1.5% of the alleles that remain uncharacterized corresponding in all cases to

patients with one previously identified mutation. The second allele may harbor a mutation in regulatory or, most probably, in deep intronic regions affecting the splicing process and causing pseudoexon insertion in the mRNA, as has been recognized in several diseases [11,18]. These defects escape detection as the aberrant mRNA is degraded by the NMD mechanism and intronic sequences are usually never fully sequenced.

The chromosomal breakpoints have been characterized for three of the deletions detected by MLPA analysis. In all cases, repetitive sequence elements, Alu elements or simple repeats, present at both sides of the deletions, are probably involved in the generation of the defect, as previously shown for human inherited diseases [1,6]. Repetitive sequence elements may facilitate the formation of secondary structure intermediates between DNA ends at deletion breakpoints. Regarding Alu elements, they are frequently involved in homologous unequal recombination generating human disease [7].

Recently, a ~73 Kb deletion from intron 16 to intron 19 was reported in a Saudi PA family [14]. It is tempting to speculate whether there is some feature of the genetic architecture of the PCCA gene that influences its susceptibility to deletions. At ~440 Kb, the PCCA gene is significantly larger than average, and harbors especially large introns, 10 of them greater than 20 Kb. In the DMD gene deletion hot-spots are located in large introns [8]. According to our results, in the PCCA gene there appears to be a deletion hot-spot in the region from intron 12 to intron 20 and a second minor one surrounding exons 3 and 4. Repetitive sequences constitute 45–55% of the intronic sequences involved in the deletions, with the sole exception of intron 14 (4 Kb) where no repeat sequences were identified using Repeatmasker (http://www.repeatmasker.org/). A search in the Database of Genomic Variants (http://projects.tcag.ca/variation) revealed that only one inversion and no deletions have been detected to affect the PCCA gene, indicating that rearrangements in this region are not a frequent structural variation of the human genome.

In summary, we report for the first time a high frequency of large genomic deletions affecting the PCCA gene in PA patients, which are effectively and reproducibly detected by MLPA analysis. Transcript analysis may aid in the detection or verification of the deletions, but avoiding NMD with emetine or other compounds should be employed. Alternatively, long-range PCR or real-time quantitative PCR methods [22] may be employed for confirmatory testing. Given the high frequency of PCCA gene deletions, screening for these genomic rearrangements should complement routine mutation analysis for PCCA deficient patients. Our results are of direct relevance for counseling purpose and clinical management of patients and predictive testing of relatives, allowing prenatal and carrier analysis in the affected families.

Acknowledgments

The authors thank the following doctors/physicians for sending the fibroblast samples: Burlina and Parini (Italy), Martínez-Pardo and Vilaseca (Spain), Bartholomew, Wolff and Nyhan (USA), Sewell, Holinski-Feder and Muschol (Germany), Al Sannaa (Saudi Arabia), Boneh (Australia), Ogur (Turkey), Michelakakis (Greece), Lissens (Belgium) and Melancon (Canada). The expert technical assistance of A. Sánchez and M.J. Ecay is acknowledged. This work was supported by grants PI060512 from Fondo de Investigaciones Sanitarias and SAF2007-61350 from the Comisión Interministerial de Ciencia y Tecnología. The institutional grant from Fundación Ramón Areces to the Centro de Biología Molecular Severo Ochoa is gratefully acknowledged.

References

[1] S.S. Abeysinghe, N. Chuzhanova, M. Krawczak, E.V. Ball, D.N. Cooper, Translocation and gross deletion breakpoints in human inherited disease and cancer I: nucleotide composition and recombination-associated motifs, Hum. Mutat. 22 (3) (2003) 229–244.
[2] J.A. Armour, D.E. Barton, D.J. Cockburn, G.R. Taylor, The detection of large deletions or duplications in genomic DNA, Hum. Mutat. 20 (5) (2002) 325–337.
[3] L. Brichta, L. Garbes, M. Jedrzejowska, S.N. Grellscheid, I. Holker, K. Zimmermann, B. Wirth, Nonsense-mediated messenger RNA decay of survival motor neuron 1 causes spinal muscular atrophy, Hum. Genet. 123 (2) (2008) 141–153.
[4] E. Campeau, L.R. Desviat, D. Leclerc, X. Wu, B. Perez, M. Ugarte, R.A. Gravel, Structure of the PCCA gene and distribution of mutations causing propionic acidemia, Mol. Genet. Metab. 74 (1–2) (2001) 238–247.
[5] S. Clavero, M.A. Martinez, B. Perez, C. Perez-Cerda, M. Ugarte, L.R. Desviat, Functional characterization of PCCA mutations causing propionic acidemia, Biochim. Biophys. Acta 1588 (2) (2002) 119–125.
[6] N. Chuzhanova, S.S. Abeysinghe, M. Krawczak, D.N. Cooper, Translocation and gross deletion breakpoints in human inherited disease and cancer II: potential involvement of repetitive sequence elements in secondary structure formation between DNA ends, Hum. Mutat. 22 (3) (2003) 245–251.
[7] P.L. Deininger, M.A. Batzer, Alu repeats and human disease, Mol. Genet. Metab. 67 (3) (1999) 183–193.
[8] J.T. Den Dunnen, P.M. Grootscholten, E. Bakker, L.A. Blonden, H.B. Ginjaar, M.C. Wapenaar, H.M. van Paassen, C. van Broeckhoven, P.L. Pearson, G.J. van Ommen, Topography of the Duchenne muscular dystrophy (DMD) gene: FIGE and cDNA analysis of 194 cases reveals 115 deletions and 13 duplications, Am. J. Hum. Genet. 45 (6) (1989) 835–847.
[9] J.T. den Dunnen, M.H. Paalman, Standardizing mutation nomenclature: why bother?, Hum Mutat. 22 (3) (2003) 181–182.
[10] L.R. Desviat, B. Perez, C. Perez-Cerda, P. Rodriguez-Pombo, S. Clavero, M. Ugarte, Propionic acidemia: mutation update and functional and structural effects of the variant alleles, Mol. Genet. Metab. 83 (1–2) (2004) 28–37.
[11] L. Du, J.M. Pollard, R.A. Gatti, Correction of prototypic ATM splicing mutations and aberrant ATM function with antisense morpholino oligonucleotides, Proc. Natl. Acad. Sci. USA 104 (14) (2007) 6007–6012.
[12] J.T. Dunnen, S.E. Antonarakis, Mutation nomenclature extensions and suggestions to describe complex mutations: a discussion, Hum. Mutat. 15 (1) (2000) 7–12.
[13] W.A. Fenton, R.A. Gravel, L.E. Rosenberg, Disorders of propionate and methylmalonate metabolism, in: C.R. Scriver, A.L. Beaudet, W. Sly, D. Valle (Eds.), The Metabolic and Molecular Bases of Inherited Disease, McGraw-Hill, New York, 2001, pp. 2165–2190.
[14] N. Kaya, M. Al-Owain, A. Albakheet, D. Colak, A. Al-Odaib, F. Imtiaz, S. Coskun, M. Al-Sayed, Z. Al-Hassnan, H. Al-Zaidan, B. Meyer, P. Ozand, Array comparative genomic hybridization (aCGH) reveals the largest novel deletion in PCCA found in a Saudi family with propionic acidemia, Eur. J. Med. Genet. (2008).
[15] A. Leon-del-Rio, R.A. Gravel, Sequence requirements for the biotinylation of carboxyl-terminal fragments of human propionyl-CoA carboxylase a subunit expressed in *Escherichia coli*, J. Biol. Chem. 269 (1994) 22964–22968.
[16] L.E. Maquat, Nonsense-mediated mRNA decay: splicing, translation and mRNP dynamics, Nat. Rev. Mol. Cell. Biol. 5 (2) (2004) 89–99.
[17] B. Perez, L.R. Desviat, P. Rodriguez-Pombo, S. Clavero, R. Navarrete, C. Perez-Cerda, M. Ugarte, Propionic acidemia: identification of twenty-four novel mutations in Europe and North America, Mol. Genet. Metab. 78 (1) (2003) 59–67.
[18] A. Rincon, C. Aguado, L.R. Desviat, R. Sanchez-Alcudia, M. Ugarte, B. Perez, Propionic and methylmalonic acidemia: antisense therapeutics for intronic variations causing aberrantly spliced messenger RNA, Am. J. Hum. Genet. 81 (6) (2007).
[19] L.N. Sellner, G.R. Taylor, MLPA and MAPH: new techniques for detection of gene deletions, Hum. Mutat. 23 (5) (2004) 413–419.
[20] M.B. Shapiro, P. Senapathy, RNA splice junctions of different classes of eukaryotes: sequence statistics and functional implications in gene expression, Nucleic Acids Res. 15 (17) (1987) 7155–7174.
[21] T. Suormala, H. Wick, J.P. Bonjour, E.R. Baumgartner, Rapid differential diagnosis of carboxylase deficiencies and evaluation for biotin-responsiveness in a single blood sample, Clin. Chim. Acta 145 (2) (1985) 151–162.
[22] C.P. Vaughn, E. Lyon, W.S. Samowitz, Confirmation of single exon deletions in MLH1 and MSH2 using quantitative polymerase chain reaction, J. Mol. Diagn. 10 (4) (2008) 355–360.

ARTICLE

Propionic and Methylmalonic Acidemia: Antisense Therapeutics for Intronic Variations Causing Aberrantly Spliced Messenger RNA

A. Rincón,* C. Aguado,* L. R. Desviat, R. Sánchez-Alcudia, M. Ugarte, and B. Pérez

We describe the use of antisense morpholino oligonucleotides (AMOs) to restore normal splicing caused by intronic molecular defects identified in methylmalonic acidemia (MMA) and propionic acidemia (PA). The three new point mutations described in deep intronic regions increase the splicing scores of pseudoexons or generate consensus binding motifs for splicing factors, such as SRp40, which favor the intronic inclusions in *MUT* (r.1957ins76), *PCCA* (r.1284ins84), or *PCCB* (r.654ins72) messenger RNAs (mRNAs). Experimental confirmation that these changes are pathogenic and cause the activation of the pseudoexons was obtained by use of minigenes. AMOs were targeted to the 5′ or 3′ cryptic splice sites to block access of the splicing machinery to the pseudoexonic regions in the pre-mRNA. Using this antisense therapeutics, we have obtained correctly spliced mRNA that was effectively translated, and propionyl coenzyme A (CoA) carboxylase (PCC) or methylmalonylCoA mutase (MCM) activities were rescued in patients' fibroblasts. The effect of AMOs was sequence and dose dependent. In the affected patient with *MUT* mutation, close to 100% of MCM activity, measured by incorporation of ^{14}C-propionate, was obtained after 48 h, and correctly spliced *MUT* mRNA was still detected 15 d after treatment. In the *PCCA*-mutated and *PCCB*-mutated cell lines, 100% of PCC activity was measured after 72 h of AMO delivery, and the presence of biotinylated PCCA protein was detected by western blot in treated PCCA-deficient cells. Our results demonstrate that the aberrant inclusions of the intronic sequences are disease-causing mutations in these patients. These findings provide a new therapeutic strategy in these genetic disorders, potentially applicable to a large number of cases with deep intronic changes that, at the moment, remain undetected by standard mutation-detection techniques.

In the past few years, special attention has been given in the field of genetic diseases to research on mutations affecting splicing, which generally account for 10%–30% of the total mutant alleles[1] and for which novel pharmacological and molecular therapies have begun to be tested.[2] Most of the mutations affecting splicing disrupt conserved sequences at the exon-intron junctions—namely, the 5′ donor site, the 3′ acceptor site, the polypyrimidine tract and the branch-point sequence—with different consequences (exon skipping, activation of cryptic splice sites, etc.) depending on the local sequence context.[3–5] Some mutations affect less well-conserved auxiliary splicing sequences—that is, exonic and intronic splicing enhancers or silencers—which are recognized by specific SR proteins.[6] Other types of mutations, rather than disrupting conserved splice sites, create novel ones that are erroneously used by the splicing machinery, resulting in the generation of aberrant transcripts.[4,5] These mutant-activated splice sequences generally occur deep in introns, causing the abnormal inclusion of intron sequences (pseudoexons) in the mRNA.[7,8] The true prevalence of this type of mutations is probably underestimated because few laboratories analyze intron sequences far from coding regions, and, in cDNA, the corresponding transcripts (usually with a frameshift and a premature termination codon [PTC]) are degraded by the nonsense-mediated mRNA decay (NMD) mechanism. NMD is a well-conserved mechanism that occurs naturally in cells and that actively degrades PTC-bearing transcripts, thus preventing the generation of truncated proteins that are potentially toxic to cells.[9]

Alleles with intronic mutations activating cryptic splice sites are particularly amenable to therapeutic correction if use of the aberrant splice sites can be blocked, because the wild-type splice sites remain intact, thus retaining the potential for normal splicing. In this respect, antisense oligonucleotides have been used successfully to restore normal splicing in several disease models, such as β-thalassemia/HbE disorder,[10] cystic fibrosis,[11] ocular albinism type I,[8] and ataxia telangiectasia.[12] Antisense oligonucleotides modulate the splicing pattern by steric hindrance of the recognition and binding of the splicing apparatus to the selected cryptic sequences, thus forcing the machinery to use the natural sites. This strategy has also been used in Duchenne muscular dystrophy to force the skipping of a deleterious exon containing a premature stop codon.[13]

In this work, we report the identification of three novel deep intronic mutations that lead to the insertion of a pseudoexon or cryptic exon in the mRNA of patients with methylmalonic acidemia (MMA [MIM 251000]) or pro-

From the Centro de Biología Molecular "Severo Ochoa," Consejo Superior de Investigaciones Científicas–Universitad Autónoma de Madrid, Universidad Autónoma, and Centro de Investigación Biomédica en Red de Enfermedades Raras, Madrid

Received May 24, 2007; accepted for publication August 9, 2007; electronically published October 26, 2007.

Address for correspondence and reprints: Dr. M. Ugarte, Centro de Biología Molecular "Severo Ochoa," CSIC-UAM, Facultad de Ciencias, Universidad Autónoma de Madrid, 28049, Madrid, Spain. E-mail: mugarte@cbm.uam.es

* These two authors contributed equally to this work.

Am. J. Hum. Genet. 2007;81:1262–1270. 0002-9297/2007/8106-0012$15.00
DOI: 10.1086/522376

pionic acidemia (PA [MIM 606054]). These are the two most frequent organic acidemias affecting the propionate oxidation pathway in the catabolism of several amino acids, odd-chain fatty acids, and cholesterol.[14] Both are life-threatening diseases that appear in the neonatal or infantile period and are caused by different gene defects inherited in autosomal recessive fashion and affecting the synthesis or function of two of the major enzymes of the pathway, propionyl coenzyme A (CoA) carboxylase (PCC [EC 6.4.1.3]) and methylmalonylCoA mutase (MCM [EC 5.4.99.2]), or of their coenzymes (biotin and adenosylcobalamin, respectively). Three consecutive enzymatic reactions are responsible for the conversion of proponylCoA to the succinylCoA that enters the Krebs cycle. The first reaction involves PCC that catalyzes the carboxylation of propionylCoA to D-methylmalonylCoA, which is then converted to the L form by a racemase, and, finally, the MCM enzyme catalyzes the isomerization of L-methylmalonylCoA to succinylCoA.[14]

Mutations in any of the two genes, *PCCA* or *PCCB*, which encode both subunits of the PCC enzyme, cause PA, whereas mutations in the *MUT* gene, which encodes the MCM enzyme, or in the genes *MMAA* and *MMAB* (responsible for the intramitochondrial synthesis of adenosylcobalamin) cause isolated MMA. The molecular bases of these disorders are well known, with >50 different mutations described for each of the *PCCA, PCCB,* and *MUT* genes. Missense mutations are the most frequent defects, followed by splicing mutations, which account for 15%–20% of the total alleles.[15,16]

In this work, we describe three genomic alterations—one in the *MUT* gene, one in the PCCA gene, and one in the *PCCB* gene—that are responsible for the aberrant insertion of intronic sequences in patients' mRNA. The intronic pseudoexons aberrantly inserted in the mRNA were targeted with antisense morpholino oligonucleotides (AMOs) that prevent aberrant splicing, thus generating normal mRNA, which is translated into functional protein, achieving therapeutic correction of the defect.

Material and Methods

Genetic Analysis of Fibroblast Cell Lines

The study included fibroblast cell lines from one Spanish patient with MMA described elsewhere[17] and from two patients from Turkey with PA, one PCCA deficient and the other PCCB deficient. Genetic analysis was performed using fibroblast cell lines as the source of mRNA and genomic DNA (gDNA). Total mRNA was isolated by Tripure Isolation reagent (Roche), and subsequent RT-PCR was done using primers and conditions described elsewhere.[17,18] The PCR products were sequenced with the same primers used for amplification, with BigDye Terminator v.3.1 mix and subsequent analysis by capillary electrophoresis on an ABI Prism 3700 Genetic Analyzer (Applied Biosystems). BLAST analysis was used to localize the inserted sequence. Intronic gDNA was amplified using primers located in intron 14 (5′-GTAACCCGTTTACTAGTTGCC-3′ and 5′-CACTATAACATACCTGAAGGG-3′) for the *PCCA* gene insertion, primers located in intron 5 (5′-TATCTTTCCACAGATAATGCCTC-3′) and intron 6 (5′-AAGCAAGGTTTGAGATGAATGG-3′) for the *PCCB* gene insertion, and primers located in intron 11 (5′-GGCTTCCAGCTTCATCCATG-3′ and 5′-TGGCACGTGCCTGTAGTACC-3′) for the *MUT* gene insertion. The insertions and gDNA mutations were described as recommended by the Human Genome Variation Society (HGVS). The DNA mutations are numbered on the basis of cDNA sequence and intronic positions described in Ensembl. The genomic changes were studied in 300 control alleles by restriction analysis with use of *Nla*III, *Bsa*AI, and *Bbs*I to detect the *PCCA, PCCB,* and *MUT* intronic mutations, respectively.

Splice scores of the natural and cryptic donor and acceptor sites were determined using the analysis tools from the Berkeley Drosophila Genome Project (BDGP), and prediction of the presence of exonic splice enhancer or silencer sequences was performed using ESEfinder,[6] Rescue-ESE[19] (RESCUE-ESE Web Server), and PESX[20] (PESXs Server).

Oligonucleotide Treatment and Analysis

The 25-mer AMOs were designed, synthesized, and purified by Gene Tools and were targeted to donor or acceptor cryptic splice sites in the pre-mRNA for each of the intronic inserted sequences in accordance with the manufacturer's criteria.[21] The sequence of the AMOs used is shown in figure 1. Endo-Porter (Gene Tools) was used as the delivery mechanism. For AMO treatment, 4–5 × 10^5 fibroblast cells were grown in 6-well plates, and, after overnight culture, different concentrations of AMO with 6-8 μl/ml of Endo Porter were added to the culture medium. Cells were harvested at different times, and mRNA was isolated as described above.

As we have described elsewhere,[17] the affected patient with an *MUT* mutation is compound heterozygous for the intronic insertion and a splicing mutation in the last nucleotide of exon 10 (c.1808G→A), which produces two aberrant transcripts as a result of the use of cryptic splice sites. For RT-PCR in this patient, we used a forward primer placed at the junction of exons 10 and 11 (5′-GCTATCAAGAGGGTTCATAAATT-3′) and a reverse primer located in exon 13 (5′-CTTAGAAGAAGAGATTTT-3′) to amplify only the allele corresponding to the pseudoexon insertion between exons 11 and 12. In some cases, a forward primer placed at the junction of exon 11 and inserted intronic sequence (5′-TCTTTTCCAGAGTCTCGCTCTTT-3′) was used to selectively amplify the cDNA containing the intronic insertion. For RT-PCR analysis of PCCA- and PCCB-deficient cell lines, we used primers described elsewhere.[18]

PCC activity was assayed as described elsewhere,[22] and ^{14}C propionate incorporation into acid-precipitable material was determined in intact cells grown in basal medium as propionate metabolism via MCM.[23] For the detection of biotin-bound proteins, fibroblasts were harvested by trypsinization and were freeze thawed, and protein concentration in cell extracts was determined by the Bradford assay. Equal amounts of total protein (30–50 μg) from each sample were loaded onto a denaturing 6% polyacrylamide gel. After electrophoresis, proteins were transferred to PVDF membranes (Immobilon-P [Millipore]), and the biotin-containing proteins were detected with an avidin alkaline phosphatase conjugate as described elsewhere.[24]

Minigene Construction and in Vitro Splicing Analysis

For evaluation of in vitro splicing, the pSPL3 vector (Life Technologies [Gibco BRL], kindly provided by Dr. B. Andresen) was

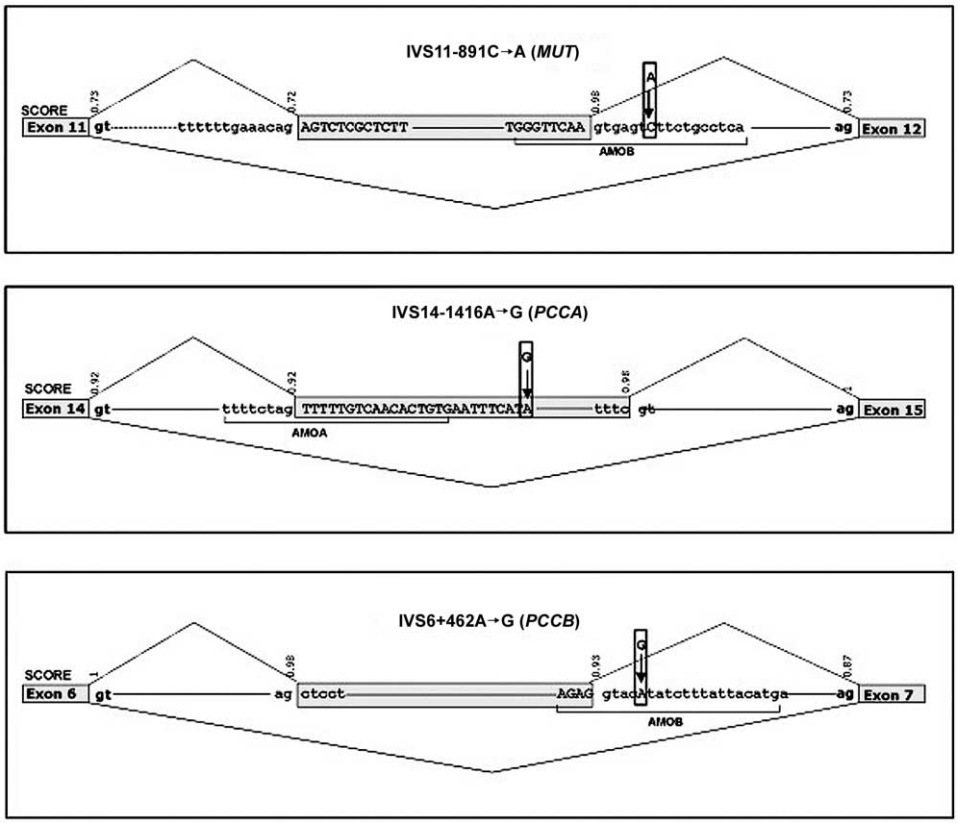

Figure 1. Schematic representation of *MUT, PCCA,* and *PCCB* regions around the pseudoexons. Exons and pseudoexons are boxed. The inserted intronic sequence is shown in uppercase letters, and the surrounding intronic sequence is in lowercase letters. The sequence of the AMO used is underlined, and splice scores calculated with the BDGP software are denoted above the corresponding 5′ and 3′ splice sites. The mutations are denoted by arrows.

used. Gene fragments corresponding to each pseudoexon and flanking regions were amplified from patients and from control DNA and were cloned into the TOPO vector (Invitrogen). For the *PCCB* minigene, the amplified fragment included exon 6. The insert was excised with *Eco*RI and subsequently was cloned into pSPL3. Clones containing the desired normal and mutant inserts in the correct orientation were identified by restriction-enzyme analysis and automated DNA sequencing. Samples of 2 μg of the wild-type or mutant minigenes were transfected into Hep3B cells by use of Jetpei (Polyplus transfections), in accordance with the manufacturer's recommendations. At 24–48 h after transfection, cells were harvested, RNA was purified, and RT-PCR analysis was performed using the pSPL3-specific primers SD6 and SA2 (Exon Trapping System [Gibco BRL]). Amplified products were separated by agarose gel electrophoresis and were further analyzed by excising the bands from the gel by means of the Qiaex Gel extraction kit (Qiagen) and subsequent direct sequencing.

Results

Genetic Analysis of Patients

The three patients with MMA and PA exhibited aberrantly spliced mRNA with an amplified band that was larger than normal after RT-PCR analysis. Direct sequencing of the products obtained by RT-PCR and subsequent BLAST search revealed that the insertions corresponded to intronic sequences flanked by cryptic 5′ and 3′ splice sites, thus resembling a pseudoexon (fig. 1). In all three patients the presence of intronic mutations presumably activates the pseudoexon (table 1), whereas the naturally used adjacent splice sites of the surrounding exons remain functional (fig. 1). These intronic variants were not present in the National Center for Biotechnology (NCBI) dbSNP, and none were found in 300 control alleles analyzed.

In the *MUT*-deficient affected patient, we had previously detected a 76-bp insertion between exons 11 and 12 (r.1957ins76) in the heterozygous state and corresponding to an exon-like region in intron 11.[17] In controls and patients with other mutations, the insertion transcript could be detected using a specific primer.[17] The patient's DNA was found to have a new C→A change in intron 11 at position +7 relative to the inserted sequence (IVS11-891C→A) (fig. 1). The scores of the 5′ and 3′ cryptic splice sites were 0.72 and 0.98, respectively, and the C→A mutation increased the 5′ cryptic splice site to 0.99. Additional *in silico* analysis revealed no significant changes in splicing regulatory sequences caused by the mutation (no exonic splicing enhancer [ESE] or exonic splicing sup-

pressor [ESS] predicted by Rescue-ESE and PESX programs and just a slight decrease in the scores for SC35, SRp40, and SRp55 by ESEfinder analysis).

In the PCCA-deficient affected patient, we have identified an 84-bp insertion between exons 14 and 15 of the *PCCA* gene (r.1284ins84) in a homozygous state. This 84-bp insertion corresponds to a pseudoexon in intron 14 and is readily detected in patients with mRNA-destabilizing mutations and even at low levels in control cell lines[25] but never in a homozygous state. No other sequence changes were detected in the amplified cDNA from the patient. The pseudoexon was amplified from gDNA of the patient and was sequenced, revealing an A→G substitution (IVS14-1416A→G) in the middle of the inserted sequence. *In silico* analysis with ESEfinder prediction software showed that the change created an SRp40 binding site and eliminated an SRp55 binding site. Rescue-ESE predicted loss of an ESE sequence and creation of two novel ones. No change was predicted by the PESX program.

In the PCCB-deficient affected patient, we have identified a new 72-bp insertion between exons 6 and 7 in the *PCCB* gene (r.654ins72) in a homozygous state, corresponding to an intron 6 region resembling an exon with 3′ and 5′ splice sites with high scores (fig. 1). Direct sequencing of the genomic region identified an A→G substitution at position +5 relative to the inserted sequence (IVS6+462A→G), increasing the cryptic 5′ donor splicing score from 0.93 to 1. Additional *in silico* analysis predicted creation of an SRp55 site (ESEfinder) and elimination of a putative silencer (PESX). Rescue-ESE predicted no changes.

Functional Analysis of the Intronic Changes

To provide evidence that the observed intronic changes are the cause of the pseudoexon inclusion in the patients' mRNA, the splicing pattern associated with these changes was further evaluated using minigenes. Minigene constructs with wild-type and mutant pseudoexons and flanking sequences were generated in the pSPL3 vector. The results of splicing analysis after transfection in Hep3B cells are shown in figure 2. The wild-type *PCCA* and *PCCB* minigene constructs showed practically total absence of pseudoexon inclusion. The *MUT* wild-type minigene produced two bands corresponding to the pseudoexon insertion and to a splicing event between the vector splice sites. The mutant constructs resulted in the pseudoexon inclusion in all cases, representing the major transcript for the *MUT* and *PCCB* minigenes and part of the transcripts for the *PCCA* minigene. Sequence analysis confirmed the identity of the transcripts in all cases. The major transcript obtained from the *PCCB* mutant minigene corresponds to the pseudoexon inclusion along with the insertion of a vector sequence caused by the cloning-derived creation of a 3′ splice acceptor site, which was chosen along with a cryptic 5′ splice site present in the vector (Exon Trapping System [Life Technologies]).

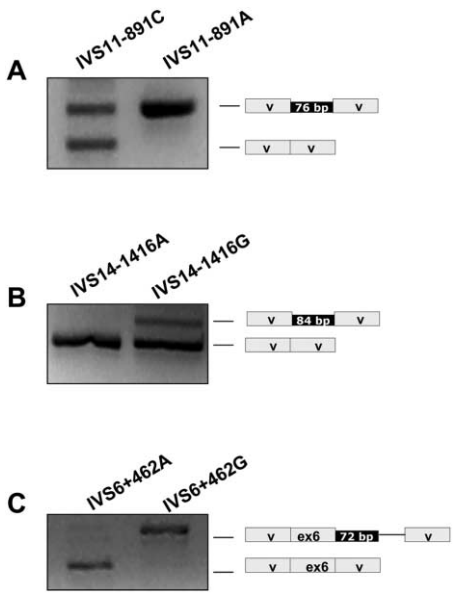

Figure 2. Splicing assay for the wild-type and mutant minigenes corresponding to the *MUT* (*A*), *PCCA* (*B*), and *PCCB* (*C*) intronic changes. The results of the RT-PCR analysis using vector-specific primers are shown along with the schematic representation of the transcripts obtained, which were characterized by sequence analysis. V = vector exonic sequences. The solid line in panel C corresponds to a cryptic exon generated during the cloning process.

Table 1. Inserted Intronic Sequences, Genomic Intronic Variations, and *in Silico* Analysis of Genomic Change

Gene (ID[a])	Origin of Inserted Sequence	mRNA Change[b]	gDNA Change[b]	*In Silico* Effect of gDNA Change[c]
MUT (4594)	Intron 11	r.1957ins76	C→A in position +7 of 5′ donor site of pseudoexon (IVS11-891C→A)	Increase in splicing score (from .98 to .99)
PCCA (5095)	Intron 14	r.1284ins84	A→G in the middle of pseudoexon (IVS14-1416A→G)	Creates SRp40 binding site and eliminates SRp55 binding site
PCCB (5096)	Intron 6	r.654ins72	A→G in position +5 of 5′ donor site of pseudoexon (IVS6+462A→G)	Increase in splicing score (from .93 to 1) in 5′ donor site of pseudoexon

[a] Gene identification (ID) numbers correspond to the NCBI Entrez Gene database.

[b] Mutation nomenclature is as recommended by HGVS. GenBank accession numbers NT_007592 (*MUT*), NM_000282.2 (*PCCA*), and NM_000532.3 (*PCCB*) were used. The genomic and transcript sequences were obtained using Ensembl.

[c] *In silico* effect analyzed by ESEfinder and BDGP.

To demonstrate that these changes are disease-causing mutations in the patients and to try to rescue *PCCA, PCCB,* and *MUT* expression in the patients' fibroblasts, we have investigated the possibility of redirecting transcript processing by modified AMOs. The AMOs used were complementary to the 5′ or 3′ cryptic splice sites of the intronic sequences inserted (fig. 1), to block access of the splicing machinery to the pre-mRNA. In all three cases, RT-PCR analysis demonstrated that the AMO used abolished the alternatively spliced transcript induced by the mutations (fig. 3).

The optimal conditions for AMO treatments were determined in each fibroblast cell line. The exclusion of intronic sequences in all cases was oligonucleotide sequence–specific, since AMO targeted to another gene had no effect on pseudoexon inclusion (data not shown). In untreated cell lines, practically no correctly spliced mRNA was detected, as shown by the lack of band comigrating with that of the control one (fig. 3). The correctly spliced fragment was generated 24 h after treatment of the cell lines with AMO complexed with peptide carrier. The products of aberrant splicing were either absent or present at much lower levels (fig. 3). The identity of the PCR products was always confirmed by sequencing.

In the *MUT*-mutated fibroblast cell line, AMO targeted to the 5′ splice site prevented the inclusion of the intronic sequence 24 h after treatment. The experiments showed dose-dependent correction of splicing (fig. 3*A*). The larger band containing the intronic insertion was detected with 10 μM AMO but not with 15 and 20 μM AMO. Using a primer located in the junction of exon 11 and the inserted pseudoexon to rescue the larger band, we observed essentially the same results (data not shown).

To test the stability of the restored, correctly spliced *MUT* mRNA, the fibroblast cell line was treated with AMO and was harvested at 1–25 d. In this experiment, the correctly spliced mRNA was still at high levels at 10 d, and trace levels of aberrantly spliced mRNA were obtained. At 15 d, similar amounts of normal and larger fragment were detected, and no normal transcript was obtained at 25 d (fig. 4).

In *PCCA*- and *PCCB*-mutated fibroblasts, we used one AMO targeted to the 3′ splice site and the 5′ splice site of the pseudoexon, respectively, and analysis was performed 72 h after AMO delivery. In *PCCA* RT-PCR analysis, low levels of the larger band with the 84-bp insertion were detected in the control sample, as has been described elsewhere.[25] In the PCCA-deficient patient, the larger band was completely absent when fibroblasts were exposed to 20 μM of AMO (fig. 3*B*). In the PCCB-deficient patient, the larger band also completely disappeared at both concentrations of AMO (fig. 3*C*).

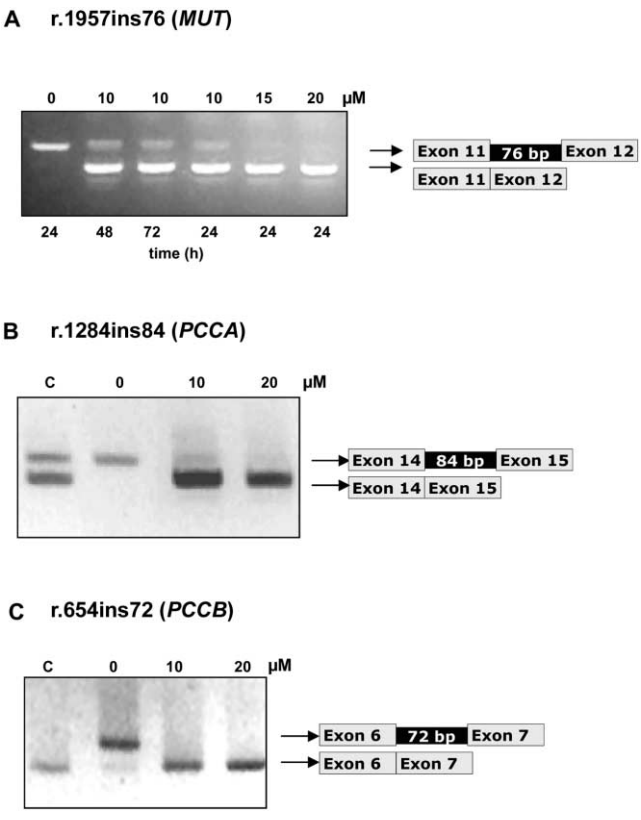

Figure 3. Correction of aberrant splicing of *MUT, PCCA,* and *PCCB* genes by AMO targeted to the pseudoexon 5′ or 3′ splice sites. *A,* RT-PCR analysis of the *MUT*-mutated cell line of total RNA extracted from untreated cells (0 μM) and treated for different times with the specified amounts of AMO targeted to the 5′ cryptic splice site. The sense primer used is located at the junction of exons 10 and 11, and the reverse primer is located in exon 13. *B,* RT-PCR analysis of the PCCA-deficient cell line untreated or treated for 72 h with 10 or 20 μM of the corresponding AMO targeted to the 3′ splice site. *C,* RT-PCR analysis of the PCCB-deficient cell line untreated or treated for 72 h with 10 or 20 μM of AMO targeted to the 5′ splice site. *Lane C,* Control cell line.

Restoration of Enzymatic Activity in MUT-, PCCA-, *and* PCCB-*Mutated Fibroblast Cell Lines*

To determine whether the RT-PCR studies correlated with restoration of activities, we measured incorporation of ^{14}C-propionate to acid-precipitable material (as determination of MCM activity) and PCC activity in *MUT*-mutated and *PCC*-deficient cell lines, respectively. PCC and MCM activities were rescued in the corresponding patients' fibroblasts 48–72 h after treatment with AMO. In the *MUT*-mutated heterozygous patient, dose-dependent activity was rescued at 48 h (fig. 5). The ^{14}C-propionate incorporation levels were close to 40% compared with control levels by use of 10 μM AMO and were close to 100% by use of 15 μM and 20 μM of AMO. In PCC-deficient cell lines, maximum activities were obtained 72 h after AMO delivery, reaching control levels of PCC activity (fig. 6).

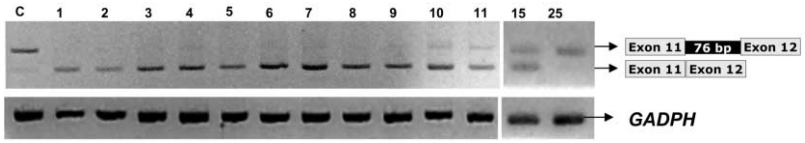

Figure 4. Time course of correctly spliced *MUT* mRNA stability in fibroblasts treated with AMO. Shown is RT-PCR analysis using primers to amplify *MUT* and *GAPDH* genes before treatment and after treatment for up to 25 d with 10 μM AMO targeted to the 5′ splice site.

No effect on MCM or PCC activities was obtained after AMO treatment in cell lines bearing different mutations and exhibiting some levels of intronic *MUT*[17] or *PCCA* gene insertions.

Restoration of Biotinylated Protein in PCCA-Mutated Fibroblast Cell Line

In the PCCA-deficient cell line, detection of biotinylated proteins was performed after treatment with the corresponding AMO. As shown in figure 7, PCCA protein, which is absent before treatment, is detected at close to normal levels 72 h after transfection with 20 μM AMO. The protein is already present 48 h after transfection (data not shown).

Discussion

In this work, we report, for the first time, the applicability of antisense therapeutics to the correction of aberrant splicing in two different organic acidemias (three gene defects), with recovery of functional protein and activity within the therapeutic range. The targeted sequences correspond to intronic sequences resembling an exon that are inserted in the mature mRNA, resulting in a PTC-bearing transcript predictably encoding a nonfunctional protein. The fact that prevention of the aberrant inclusion of the pseudoexons by use of AMO results in the recovery of enzymatic activity confirms that the insertions are the disease-causing mutations in the patients.

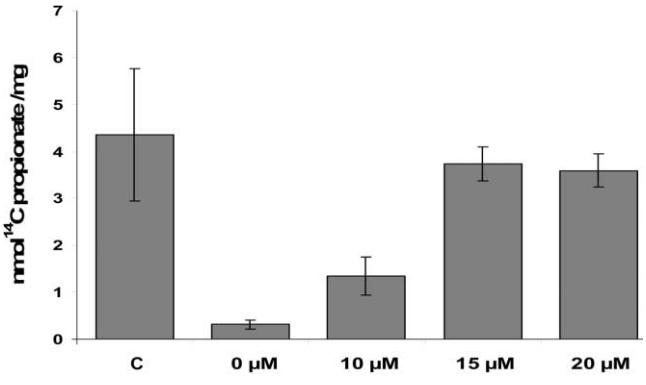

Figure 5. Functional correction of MCM activity after AMO treatment. MCM activity was measured by incorporation of [^{14}C] into trichloroacetic acid–precipitable material in the control cell line (C) and the *MUT*-mutated cell line untreated or treated with 10, 15, or 20 μM of AMO targeted to the 5′ cryptic splice site. The cells were harvested 48 h after transfection. The data show the mean ± SD from at least four independent experiments, and control data were obtained from four independent cell lines.

The *in silico* analysis of the pseudoexon 3′ and 5′ splice sites predict high scores in each case (fig. 1), thus suggesting that such sequences may be included in the mature mRNA. This prediction holds true for the *PCCA* gene insertion, which is detected with standard RT-PCR conditions at very low levels in control cell lines and at higher levels in samples from patients with frameshift or nonsense mutations that result in PTC-bearing transcripts degraded by NMD.[25] The *MUT* gene insertion can also be rescued in control cell lines by use of a specific primer, suggesting that it may be a normally rare transcript part of the "background" noise of the splicing process.[17] Potential 3′ and 5′ splice sites are highly abundant in intronic sequences, although they alone are insufficient to dictate exon recognition.[26] The fact that pseudoexon inclusion is not a frequent event during normal splicing has been attributed to defects in splicing regions, despite their apparently good consensus values, and to the enrichment in splicing silencers.[4] However, in the pseudoexons described here, a single point mutation activates the pseudoexon, thus pointing to their high resemblance to true exons. This raises the possibility that these pseudoexons might be part of a splice-controlling mechanism in which alternative splicing events can regulate gene expression by inducing the inclusion of the apparent pseudoexon and leading to NMD, as described for the tropomyosin gene.[27]

In the *MUT*-mutated and PCCB-deficient patients included in this study, a point mutation raises slightly the splicing score of the 5′ splice site of the corresponding pseudoexon, resulting in its aberrant inclusion in the mRNA. In the PCCA-deficient patient, the only change identified in the pseudoexonic region corresponds to an A→G change in the middle of the pseudoexon. Analysis with ESE prediction softwares (ESEfinder and Rescue-ESE) identified loss of an ESE and creation of novel ESE sequences, specifically a novel binding site for SRp40 (ESEfinder). This, in conjunction with the high-score cryptic 3′ and 5′ sites, most likely favors the pathogenic intronic inclusion. SRp40 knock-down experiments will also help to clarify the underlying mechanism.

In all three cases, evidence that the pseudoexon insertion is caused by the identified intronic mutations is pro-

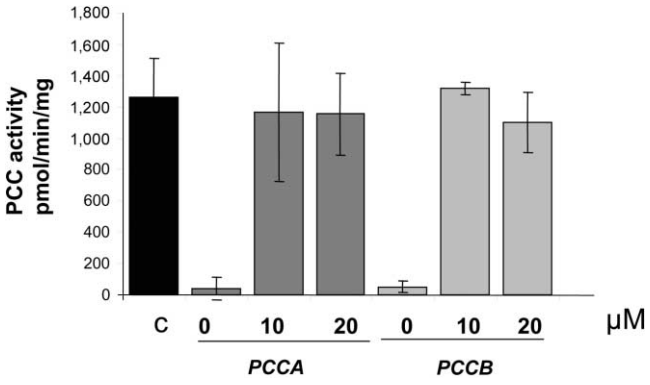

Figure 6. Functional correction of PCC activity after AMO treatment. PCC activity was measured 72 h after transfection with 0, 10, or 20 μM of the corresponding AMO in PCCA- and PCCB-deficient cell lines. The black bar corresponds to control PCC activity measured in four independent cell lines. Dark-gray bars show PCC activity in PCCA-deficient fibroblasts treated with AMO targeted to the 3′ cryptic splice site. Light-gray bars show PCC activity in PCCB-deficient fibroblasts treated with AMO targeted to the 5′ cryptic splice site. The data show the mean ± SD from at least three independent experiments.

vided by the results obtained with minigenes. The mutant constructs resulted in pseudoexon inclusion. In the *MUT* wild-type minigene, some amount of transcript with the insertion is detected, as would be expected given that it is also detectable in control cell lines. However, for *PCCA* and *PCCB* wild-type minigenes, practically no transcript with the pseudoexon insertion is detected. In the *PCCA*-mutant minigene, only part of the resulting transcripts corresponds to the insertion. This does not exactly mimic the results obtained in patients' fibroblasts, probably because of the lack of a wide-enough genomic context of the cloned pseudoexon, as has been described for exon 37 in the *NF1* gene.[4,28] A cloning-created cryptic exon derived from the vector, as occurs in the *PCCB* minigene, is a common occurrence with pSPL3,[29] but it is clear that the *PCCB* pseudoexon is included with the mutant construction but not with the wild-type one, confirming that the change leads to pseudoexon insertion.

The splicing correction by AMO was sequence specific, since control oligomers against another gene had no effect in each case. No obvious cytotoxicity was observed in the three cases. The persistence of correctly spliced *MUT* mRNA 15 d after termination of AMO delivery suggests that AMO are quite stable in the cell. In all cases, close to 100% of correctly spliced mRNA was detected after standard RT-PCR analysis, although, with a specific primer, the presence of aberrant transcript could be confirmed. This could be because the aberrant transcript is unstable as a result of the presence of PTC, and the normally spliced mRNA is amplified preferentially. In addition, the correctly spliced mRNA can be translated into significant amounts of active protein, reaching control levels, as judged by the detection of biotinylated PCCA protein in one case and enzymatic assays of all three cell lines.

All these results suggest that the antisense approach may be clinically promising for organic acidemias. Quantitative analysis of the restoration of enzymatic activity in a patient to 30%–40% of the normal level (the minimum value we obtained for the heterozygous *MUT*-mutated patient) is therapeutically significant since heterozygotes are asymptomatic. Interestingly, in both the heterozygous and homozygous patients, control activity levels can be reached with AMO treatment. This suggests that, in the treated-cell population, the amount of functional protein synthesized from the normally spliced mRNA is sufficient to correct the enzymatic defect. Studies in model animals, not feasible to date, would be highly important for discussions of the applicability of these therapies to organic acidemias. To date, treatment of PA and MMA relies on a protein-restricted diet and administration of carnitine and antibiotics, although management is sometimes poor, and long-term complications are common.[30] Our results offer a novel mutation-specific therapeutic approach for these diseases, which may be applicable to a greater number of cases than is apparent at the moment, because aberrant intronic insertions may remain undetected with standard mutation-detection techniques. In this sense, we have detected only one mutation in several patients with PA and MMA (laboratory data) who could harbor this type of mutation that results in PTC transcripts that are degraded. Treatment of cell cultures with puromycin to avoid NMD before RNA analysis may reveal additional intronic insertions.

Morpholino analogs of oligonucleotides have several characteristics that render them suitable for therapeutic applications, such as high binding specificity and stability and resistance to nucleases and to degradation by RNAseH when forming hybrids with RNA. The major issues facing clinical applications concern safe delivery and optimal dose determination for each tissue involved. Efficient and nontoxic delivery of AMO to the liver, which would be the target tissue in these diseases, is one major challenge to be overcome before the practical use of AMO in patients with organic acidemia can be envisaged. In Duchenne muscular dystrophy, antisense oligonucleotides have been

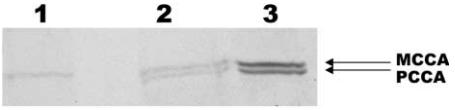

Figure 7. Recovery of biotinylated PCCA protein after AMO treatment. Biotinylated proteins were detected in total cellular extract by avidin-alkaline phospahatase assay in the PCCA-deficient cell line untreated (*lane 1*) or 72 h after treatment with the corresponding AMO (*lane 2*). *Lane 3,* Hepatoma cellular extract. Shown are the biotin-containing α-subunits of methylcrotonylCoA carboxylase (MCCA) and PCCA.

administered intravenously to patients, achieving splicing modulation to restore the coding frame for dystrophin.[31] The efficacy of antisense therapeutics for splicing correction must be determined in each disease model and for each deleterious splicing event, although the results reported to date predict a broad applicability.[7,11,12]

Acknowledgments

We thank B. Merinero and C. Perez-Cerdá, for their excellent collaboration, and Dr. Gulden Gokcay, for sending the fibroblast samples. This work was supported by grants from the Comisión Interministerial de Ciencia y Tecnología (SAF2004-06298) and Universidad Autónoma de Madrid–Comunidad Autónoma de Madrid (CCG06-UAM/BIO-0293). The institutional grant from Fundación Ramón Areces to the Centro de Biología Molecular Severo Ochoa is gratefully acknowledged.

Web Resources

Accession numbers and URLs for data presented herein are as follows:

BDGP, http://www.fruitfly.org/seq_tools/splice.html
BLAST, http://www.ncbi.nlm.nih.gov/BLAST/
Ensembl, http://www.ensembl.org/Homo_sapiens/index.html
Entrez Gene, http://www.ncbi.nlm.nih.gov/sites/entrez?db=gene
ESEfinder, http://rulai.cshl.edu/tools/ESE2/
GenBank, http://www.ncbi.nlm.nih.gov/Genbank/ (for *MUT* [accession number NT_007592], *PCCA* [accession number NM_000282.2], and *PCCB* [accession number NM_000532.3])
HGVS, http://www.hgvs.org/mutnomen/
Online Mendelian Inheritance in Man (OMIM), http://www.ncbi.nlm.nih.gov/Omim/ (for PA and MMA)
PESXs Server, http://cubweb.biology.columbia.edu/pesx/
RESCUE-ESE Web Server, http://genes.mit.edu/burgelab/rescue-ese/

References

1. Krawczak M, Ball EV, Fenton I, Stenson PD, Abeysinghe S, Thomas N, Cooper DN (2000) Human gene mutation database—a biomedical information and research resource. Hum Mutat 15:45–51
2. Tazi J, Durand S, Jeanteur P (2005) The spliceosome: a novel multi-faceted target for therapy. Trends Biochem Sci 30:469–478
3. Krawczak M, Reiss J, Cooper DN (1992) The mutational spectrum of single base-pair substitutions in mRNA splice junctions of human genes: causes and consequences. Hum Genet 90:41–54
4. Buratti E, Baralle M, Baralle FE (2006) Defective splicing, disease and therapy: searching for master checkpoints in exon definition. Nucleic Acids Res 34:3494–3510
5. Pagani F, Baralle FE (2004) Genomic variants in exons and introns: identifying the splicing spoilers. Nat Rev Genet 5: 389–396
6. Cartegni L, Chew SL, Krainer AR (2002) Listening to silence and understanding nonsense: exonic mutations that affect splicing. Nat Rev Genet 3:285–298
7. Lacerra G, Sierakowska H, Carestia C, Fucharoen S, Summerton J, Weller D, Kole R (2000) Restoration of hemoglobin A synthesis in erythroid cells from peripheral blood of thalassemic patients. Proc Natl Acad Sci USA 97:9591–9596
8. Vetrini F, Tammaro R, Bondanza S, Surace EM, Auricchio A, De Luca M, Ballabio A, Marigo V (2006) Aberrant splicing in the ocular albinism type 1 gene (*OA1/GPR143*) is corrected in vitro by morpholino antisense oligonucleotides. Hum Mutat 27:420–426
9. Maquat LE (2004) Nonsense-mediated mRNA decay: splicing, translation and mRNP dynamics. Nat Rev Mol Cell Biol 5: 89–99
10. Suwanmanee T, Sierakowska H, Fucharoen S, Kole R (2002) Repair of a splicing defect in erythroid cells from patients with beta-thalassemia/HbE disorder. Mol Ther 6:718–726
11. Friedman KJ, Kole J, Cohn JA, Knowles MR, Silverman LM, Kole R (1999) Correction of aberrant splicing of the cystic fibrosis transmembrane conductance regulator (*CFTR*) gene by antisense oligonucleotides. J Biol Chem 274:36193–36199
12. Du L, Pollard JM, Gatti RA (2007) Correction of prototypic ATM splicing mutations and aberrant ATM function with antisense morpholino oligonucleotides. Proc Natl Acad Sci USA 104:6007–6012
13. Aartsma-Rus A, Janson AA, Kaman WE, Bremmer-Bout M, den Dunnen JT, Baas F, van Ommen GJ, van Deutekom JC (2003) Therapeutic antisense-induced exon skipping in cultured muscle cells from six different DMD patients. Hum Mol Genet 12:907–914
14. Fenton WA, Gravel RA, Rosenberg LE (2001) Disorders of propionate and methylmalonate metabolism. In: Scriver CR, Beaudet AL, Sly W, Valle D (eds) The metabolic and molecular bases of inherited disease. McGraw-Hill, New York, pp 2165–2190
15. Desviat LR, Perez B, Perez-Cerda C, Rodriguez-Pombo P, Clavero S, Ugarte M (2004) Propionic acidemia: mutation update and functional and structural effects of the variant alleles. Mol Genet Metab 83:28–37
16. Worgan LC, Niles K, Tirone JC, Hofmann A, Verner A, Sammak A, Kucic T, Lepage P, Rosenblatt DS (2006) Spectrum of mutations in *mut* methylmalonic acidemia and identification of a common Hispanic mutation and haplotype. Hum Mutat 27:31–43
17. Martinez MA, Rincon A, Desviat LR, Merinero B, Ugarte M, Perez B (2005) Genetic analysis of three genes causing isolated methylmalonic acidemia: identification of 21 novel allelic variants. Mol Genet Metab 84:317–325
18. Perez B, Desviat LR, Rodriguez-Pombo P, Clavero S, Navarrete R, Perez-Cerda C, Ugarte M (2003) Propionic acidemia: identification of twenty-four novel mutations in Europe and North America. Mol Genet Metab 78:59–67
19. Fairbrother WG, Yeh RF, Sharp PA, Burge CB (2002) Predictive identification of exonic splicing enhancers in human genes. Science 297:1007–1013
20. Zhang XH, Chasin LA (2004) Computational definition of sequence motifs governing constitutive exon splicing. Genes Dev 18:1241–1250
21. Morcos PA (2007) Achieving targeted and quantifiable alteration of mRNA splicing with Morpholino oligos. Biochem Biophys Res Commun 358:521–527
22. Suormala T, Wick H, Bonjour JP, Baumgartner ER (1985) Rapid differential diagnosis of carboxylase deficiencies and evaluation for biotin-responsiveness in a single blood sample. Clin Chim Acta 145:151–162
23. Perez-Cerda C, Merinero B, Sanz P, Jimenez A, Garcia MJ,

Urbon A, Diaz Recasens J, Ramos C, Ayuso C, Ugarte M (1989) Successful first trimester diagnosis in a pregnancy at risk for propionic acidaemia. J Inherit Metab Dis Suppl 2 12:274–276
24. Clavero S, Martinez MA, Perez B, Perez-Cerda C, Ugarte M, Desviat LR (2002) Functional characterization of *PCCA* mutations causing propionic acidemia. Biochim Biophys Acta 1588:119–125
25. Campeau E, Dupuis L, Leclerc D, Gravel RA (1999) Detection of a normally rare transcript in propionic acidemia patients with mRNA destabilizing mutations in the *PCCA* gene. Hum Mol Genet 8:107–113
26. Sun H, Chasin LA (2000) Multiple splicing defects in an intronic false exon. Mol Cell Biol 20:6414–6425
27. Grellscheid SN, Smith CW (2006) An apparent pseudo-exon acts both as an alternative exon that leads to nonsense-mediated decay and as a zero-length exon. Mol Cell Biol 26: 2237–2246
28. Baralle M, Skoko N, Knezevich A, De Conti L, Motti D, Bhuvanagiri M, Baralle D, Buratti E, Baralle FE (2006) *NF1* mRNA biogenesis: effect of the genomic milieu in splicing regulation of the *NF1* exon 37 region. FEBS Lett 580:4449–4456
29. Vockley J, Rogan PK, Anderson BD, Willard J, Seelan RS, Smith DI, Liu W (2000) Exon skipping in IVD RNA processing in isovaleric acidemia caused by point mutations in the coding region of the *IVD* gene. Am J Hum Genet 66:356–367
30. Leonard JV (1995) The management and outcome of propionic and methylmalonic acidaemia. J Inherit Metab Dis 18: 430–434
31. Takeshima Y, Yagi M, Wada H, Ishibashi K, Nishiyama A, Kakumoto M, Sakaeda T, Saura R, Okumura K, Matsuo M (2006) Intravenous infusion of an antisense oligonucleotide results in exon skipping in muscle dystrophin mRNA of Duchenne muscular dystrophy. Pediatr Res 59:690–694